Czech Technical University in Prague
Faculty of Transportation Sciences
Department of Transportation Systems

New Method for Analyzing Asphalt Binders

Nová metoda pro analýzu asfaltových pojiv

by

Gabriel Skronka

A thesis submitted in partial fulfillment of
the requirements for the degree of

DOCTOR OF PHILOSOPHY (PH.D.)

Study programme: *P3710 Technology in Transportation and Telecommunications*
Field of Studies: *3708V009 Transportation Systems and Technology*

Prague, March *2021*

Thesis Supervisor:
Doc. Ing. Otakar Josef Vacín, Ph.D.
Department of Transportation Systems
Faculty of Transportation Sciences
Czech Technical University in Prague
Konviktská 20
110 00 Prague 1
Czech Republic

Thesis Co-Supervisor:
Dr. Martin Jasso
Department of Chemical and Civil Engineering
Chairholder, Bituminous Materials Chair
Schulich School of Engineering
University of Calgary
ENF 278, 2500 University Drive NW
Calgary, AB, T2N 1N4
Canada

ABSTRACT

To understand the rheological behavior of asphalt binders is a prerequisite to the appropriate designing of road constructions. The development of distresses in asphalt pavements, such as rutting, can be mitigated by using asphalt binder with rheological properties adequate to the thermal and traffic load of the pavement. To meet the requirements, new high-performance asphalt binders have been developed, usually by modifying the asphalt base with a polymer.

By means of advanced techniques, e.g., multiple stress creep recovery (MSCR) test, conducted in a dynamic shear rheometer, it is possible to determine the rutting potential of asphalt binders. This technique, however, still seems to be imprecise at currently determined shear stress levels.

This thesis aims to query the adequacy of multiple stress creep recovery test conducted at standardized shear stress levels (0.1 kPa, 3.2 kPa). For this purpose, the high temperature behavior of one base and twelve polymer modified asphalt binders is compared with the rutting potential of asphalt mixes produced from the investigated asphalt binders.

For modification a variety of polymers are used alone and in combination. Their content is adjusted to obtain modified asphalt binders with similar maximum service temperature, defined by the parameter $|G^*|/sin\delta$, as close as possible to True Grade – PG 64-yy.

The multiple stress creep recovery test is conducted on all binders at five different shear stress levels (0.1 kPa, 3.2 kPa, 6.4 kPa, 12.8 kPa, and 25.6 kPa). The rutting potential of asphalt mixes is investigated by means of Hamburg wheel-tracking test conducted at 60°C. In addition, the dynamic moduli of asphalt mixes are evaluated at different temperatures and frequencies in order to construct master curves of dynamic functions.

According to the presented research, the non-recoverable creep compliance, J_{nr}, results, measured at high shear stress levels show better correlation with the rutting potential of asphalt mixes than those measured at currently standardized shear stress levels. Furthermore, the creep compliance, J_c, results indicate even better correlation with the rut resistance of asphalt mixes and, in contrast with J_{nr}, can be better generalized to all binders, regardless of the asphalt base they are prepared from.

ABSTRAKT

Pochopení reologického chování asfaltových pojiv je důležitým předpokladem k vhodnému navrhování silničních konstrukcí. Vývoj poruch netuhých vozovek, například u tvorby trvalých deformací (vyjíždění kolejí), lze značně zpomalit vhodným výběrem konstrukčních materiálů. Z pohledu asfaltového pojiva je zvláště důležité, aby reologické vlastnosti odpovídali teplotnímu a dopravnímu zatížení vozovky. Proto za účelem splnění požadavků byla vyvinuta nová, vysoce odolná asfaltová pojiva, do které je obvykle přidáván vhodný typ a množství polymerů.

Pomocí pokročilých metodik, využívajících dynamického smykového reometru, je možné určit odolnost asfaltových pojiv proti vzniku trvalých deformací. Prozatím nejslibnější zkouška, zabývající se měřením náchylnosti asfaltových pojiv k vyjíždění kolejí, je zkouška opakovaného zatížení a odlehčení MSCR (multiple stress creep recovery). Přesto se tato zkouška při aktuálně stanovených úrovních smykového napětí stále jeví jako nepřesná.

Tento výzkum si klade za cíl zpřesnit zkoušku opakovaného zatížení a odlehčení MSCR prováděná při standardizovaných úrovních smykového napětí (0,1 kPa a 3,2 kPa). Za tímto účelem jsou zkoumány reologické vlastnosti celkem třinácti asfaltových pojiv, ze kterých dvanáct jsou polymerem modifikovaná, zatímco jedno pojivo je bez modifikace.

Množství modifikátorů a přísad je zvoleno tak, aby se výsledná pojiva ve složení co nejvíce lišila, nicméně hodnota kritické teploty po modifikaci dosahovala jednotné hodnoty 64 °C, odpovídající užitné třídě PG 64-yy.

Reologické vlastnosti asfaltových pojiv jsou stanoveny pomocí zkoušky MSCR při třech teplotách (50 °C, 60 °C, 70 °C) a při pěti různých úrovních smykového zatížení v rozmezí od 0,1 kPa do 25,6 kPa. Na asfaltových směsích, vyrobených ze zkoušených asfaltových pojiv, je provedena zkouška pojíždění kolem, jejíž výsledky jsou následně porovnány s výsledky zkoušení asfaltových pojiv. Dále, jsou sestaveny a také porovnány s vlastnostmi pojiv hlavní křivky dynamických funkcí asfaltových směsí.

Výsledky nevratné smykové poddajnosti (J_{nr}), měřené při vysokých smykových napětích, ukazují lepší korelaci s odolností asfaltových pojiv proti vzniku trvalých deformací než při standardizovaných napětích. V porovnání s J_{nr}, pomocí smykové poddajnosti (J_c) lze lépe zobecnit na všechna pojiva bez ohledu na použitých modifikátorů a základních asfaltů, a navíc ukazují lepší korelaci s odolností asfaltových směsích.

ACKNOWLEDGEMENTS

First and foremost, I would like to extend my utmost gratitude to my research supervisor, doc. Ing. Otakar J. Vacín, Ph.D., for his guidance, encouragement, mentoring, and professional support during my studies at the Czech Technical University in Prague and throughout this research.

I would also like to take this opportunity to express my gratitude to my co-supervisor, Dr. Martin Jasso, for his guidance, support, and useful advice during the last several years. His opinions and contributions are gratefully appreciated.

My sincere thanks belong also to Prof. Ludo Zanzotto for sharing his knowledge, guidance, and for giving me the opportunity and financial support to do research at the University of Calgary. His encouragement and enthusiasm have been truly inspiring.

I would also like to extend my heartfelt gratitude to Dr. Jiri Stastna and Dr. Viena Stastna whose professional advice, encouragement, immense patience, and invaluable opinion are gratefully appreciated. Their benevolence, care, sincerity, and erudition have deeply inspired me.

My special thanks are extended to Mr. Ryan Wirth and Mrs. Eva Vargova for their support and kind assistance in the laboratory.

Last, but definitely not the least, I would like to express my endless gratitude to my loved ones, especially my parents, sister, brother-in-law, grandmother, my friends, and my girlfriend. Without their love, care, and encouragement I do not think that I would be pursuing this degree.

DECLARATION

I hereby declare that the presented thesis is my own work and that I have cited all sources of information in accordance with the Guideline for adhering to ethical principles when elaborating an academic final thesis. Moreover, I state that this thesis has neither been submitted nor accepted for any other degree.

I acknowledge that my thesis is subject to the rights and obligations stipulated by the Act No. 121/2000 Coll., the Copyright Act, as amended, in particular that the Czech Technical University in Prague has the right to conclude a license agreement on the utilization of this thesis as a school work under the provisions of Article 60 (1) of the Act.

In Prague, March *2021*

.....
Ing. Gabriel Skronka

Table of Contents

LIST OF FIGURES AND ILLUSTRATIONS

LIST OF TABLES

LIST OF SYMBOLS, ABBREVIATIONS, NOMENCLATURES

Abbreviation	Definition
AASHTO	The American Association of State Highway and Transportation Officials
ADT	Average Daily Traffic
ALF	Accelerated Loading Facility
BBR	Bending Beam Rheometer
CB	Carbon Black
CRM	Crumb Rubber Modifiers
DSR	Dynamic Shear Rheometer
EAPA	European Asphalt Pavement Association
ER	Elastic Recovery
ESAL	Equivalent Single Axle Load
EVA	Ethylene-vinyl Acetate
FD	Force Ductility
FHWA	Federal Highway Administration
FLM	Fluorescence Light Microscopy
GHG	Greenhouse Gas Emission
GMA	Glycidyl Methacrylate
HDPE	High Density Polyethylene
HMA	Hot Mix Asphalt
HWTD	Hamburg Wheel-Tracking Device
HWTT	Hamburg Wheel-Tracking Test
JMF	Job Mix Formula
LDPE	Low Density Polyethylene
LVDT	Linear Variable Differential Transformer
LVE	Linear Viscoelastic (range)
MEPDG	Mechanistic-Empirical Pavement Design Guide
MF	Manufactured Fines
MFI	Melt Flow Index
MSCR	Multiple Stress Creep Recovery
NCHRP	National Cooperative Highway Research Program
NR	Natural Rubber
PAV	Pressure Aging Vessel
PE	Polyethylene
PG	Performance Grade
PMA	Polymer Modified Asphalt
PP	Polypropylene
PPA	Polyphosphoric Acid
R&B	Ring and Ball Softening Point
RCT	Repeated Creep Test
RET	Reactive Elastomeric Terpolymers

RTFO	Rolling Thin Film Oven
RTR	Recycled Tire Rubber
S	Sulphur
SARA	Saturates, Aromatics, Resins, and Asphaltenes Fractions
SBS	Poly(styrene-*b*-butadiene-*b*-styrene)
SCO	Synthetic Crude Oil
SEBS	Poly(styrene-*b*-(ethylene-*r*-butylene)-*b*-styrene)
SGC	Superpave Gyratory Compactor
SHRP	Strategic Highway Research Program
SR	Synthetic Rubber
Superpave®	Superior Performing Asphalt Pavements
TPE	Thermoplastic Elastomer
TTS	Time Temperature Superposition
VA	Vinyl Acetate
VFA	Voids Filled with Asphalt
VMA	Voids in the Mineral Aggregate
WLF	Williams-Landell-Ferry
ZSV	Zero Shear Viscosity

Symbol	**Definition**
c	Centi-
Pa	Pascal
Ps	Poise
d	Deci-
dmm	Decimillimeter (10^{-1} mm)
g	Gram
h	Hour
log	Decadic logarithm
k	Kilo-
m	Meter
m	Milli-
mol	Mole
N	Newton
ppm	Parts per million
rad	Radian
s	Second
t	Tonne (10^3 kg)
wt.%	Weight per cent

Symbol - Italic	**Definition**
a_T	Horizontal shift factor
b_T	Vertical shift factor
D_g	Glassy compliance
E	Tensile modulus

E'	Storage modulus
E''	Loss modulus
E^*	Complex modulus
$\|E^*\|$	Dynamic modulus
E_e	Equilibrium modulus
f_r	Reduced frequency
G	Shear modulus
G'	Shear storage modulus
G''	Shear loss modulus
G^*	Complex shear modulus
$G(t)$	Relaxation modulus
G_{mb}	Specific gravity
$H(\lambda)$	Continuous relaxation spectrum
I_c	Colloidal instability index
J	Shear compliance
$J'(\omega)$	Storage compliance
$J''(\omega)$	Loss compliance
$J^*(\omega)$	Complex compliance
$J(t)$	Creep compliance
J_a	Accumulated shear compliance
J_c	Creep compliance
J_e	Equilibrium compliance
J_e^0	Steady-state compliance
J_{nr}	Non-recoverable creep compliance
J_{rec}	Recovered compliance
$L(\Lambda)$	Continuous retardation spectrum
N	Number of cycles
$\%R$	Percent recovery
p	Pressure
t	Current time
t'	Past time
T_g	Glass transition temperature
T_m	Melting point
T_r, T_0	Reference temperature
t_r	Reduced time
V_a	Air voids
W	work done in cyclic stressing a material
ΔW	Energy lost through internal friction

Symbol - Greek	**Definition**
ε_0	Initial strain
ε_c	Creep end strain
ε_r	Residual strain
Λ_i	Discrete retardation time
ϕ	Phase angle

γ	Shear strain
$\dot{\gamma}$	Rate of strain
γ_e	Shear strain on the elastic element
γ_v	Shear strain on the viscous element
γ_u	Unrecovered strain
γ_0	Constant maximum strain amplitude
γ_1	Deformation at t=1 s
γ_{10}	Deformation at t=10 s
λ_i	Discrete relaxation time
τ	Shear stress
τ_0	Constant shear stress
$\dot{t}_{21}$	Time derivate of the shear stress
ε	Tensile strain
σ	Tensile stress
η	Shear viscosity
η_0	Newtonian viscosity
ξ	Time interval
ω	Angular frequency
ω_r	Reduced frequency
ρ	Density of the material
$\delta(\omega)$	Phase angle
χ_{aro}	Amount of aromatics
χ_{asph}	Amount of asphaltenes
χ_{res}	Amount of resins
χ_{sat}	Amount of the saturates

INTRODUCTION

1.1. Background

Asphalt pavements are dominating the paving industry since the beginning of the 1920s. Asphalt as a construction material is mainly used as a binder in road surfaces. It literally binds together the graded aggregate skeleton and creates a viscoelastic mixture that can be successfully utilized in flexible pavements. Besides that, the asphalt binder and aggregate skeleton asphalt mixes also contain a small amount of air, in the form of air voids. These three main components make the asphalt mix a three-phase composite. The volume and the properties of each constituent have a significant effect on the bulk properties of the asphalt mix such as the ability of the road to recover after deformation.

Due to its hardness, the aggregate skeleton provides the stable internal structure of the mix. In contrast to the aggregate, the consistency and the rheological properties of the asphalt binder are highly dependent on the ambient temperature. By using an asphalt binder adequate to the climate conditions and the traffic load, the development of permanent deformations might be prevented. Therefore, proper assessment of their rheological behavior at service temperatures can provide substantial help in designing asphalt pavements that can resist to permanent deformations.

Until the second half of the last century it has been considered that the main role of the asphalt binder in the mix is to bind the internal structure of the asphalt mix and it is the aggregate's role to resist the applied traffic load during the pavement's service time. This approach was re-evaluated when the permanently increasing level of automobilization concurrently resulted in constant deterioration of asphalt pavements.

Higher stress levels caused by higher axle loads, the increasing frequency of loadings, and the always changing temperature induce the vast majority of pavement distresses, such as rutting, fatigue and thermal cracking. It was evident that the most susceptible and temperature dependent component of the mixes, the asphalt binder, needs to be enhanced so it can endure such traffic load and environmental conditions. The demand for durable and high-quality construction materials necessitates the development of new high-performance asphalt binders, which are generally obtained by blending the base asphalt with polymer modifiers (e.g., plastomers, reactive polymers, and elastomers),

or non-polymeric additives (e.g., sulfur), or other chemical modifiers (e.g., polyphosphoric acid).

The formation of wheel paths worn into the pavement, generally known as rutting, is the most common distress occurring at high service temperatures and high traffic load. It is a permanent deformation built from accumulated irreversible deformations in all or in some of the pavement layers under repeated traffic load. Asphalt binders suitable for the environmental and traffic-induced conditions are chosen based on a set of test results. Many of the used test methods are empirical related (i.e., penetration and viscosity based specification) and are applied since the very beginning of the asphalt industry. Until the utilization of polymer modifiers, this system of asphalt binder specification worked relatively well, but the complexity and often hardly predictable nature of polymer structure in asphalt binders begged for new approaches. The development of performance related test methods provides the pavement industry with information that allows for better understanding the rheological behavior of polymer modified asphalt materials; consequently, it facilitates the selection of the construction materials to best meet the requirements of the actual highway.

Under the leadership of the American Association of State Highway and Transportation Officials (AASHTO) in 1987 a 5-year and $150 million research program, called Strategic Highway Research Program (SHRP), was conducted in order to improve the performance and durability of highways; thus to make them safer for motorists and less demanding on the environment and economy.

Based on the SHRP results, AASHTO developed the new performance grade (PG) binder specification M320 also called Superpave® (SUperior PERforming Asphalt PAVEments) that incorporated a large number of individual, mainly rheology-based test methods. With the help of the new specifications, pavement designers can choose the best performing binder tailored for specific traffic load and climate conditions. This allows the production of pavements that are more durable and resistant to rutting in extremely hot or to thermal cracking in extremely cold weather.

1.2. Statement of the problem

The Superpave® performance grade specification was developed primarily based on a study of neat asphalt binders. Consequently, many researchers proved that the new Superpave® PG specification cannot be used for full characterization of binders with

different types of polymer modifiers since it does not consider the significantly enhanced elastic properties of such binders. Therefore, many highway agencies have demanded to add supplementary tests to AASHTO M320 specification in order to confirm the presence and the volume of modifiers in the binder. These tests (e.g., elastic recovery (ER), force ductility (FD), zero shear viscosity (ZSV), tenacity, etc.), along with their specifications, are referred to as Superpave® PG "Plus" specifications. The main problem with these supplementary tests was that none of them satisfactorily expressed the field performance of binders only they signify the presence of the desired polymer in the blends. Because the presence of polymer modifiers, only further complicated the already very complex internal structure of asphalt blends, advanced techniques were needed to determine the rutting resistance of asphalt binders.

A new performance related test method was proposed, namely the repeated creep test (RCT), which was later modified by increasing the used stress levels and renamed as the multiple stress creep recovery (MSCR) test. Concurrently, a new parameter called non-recoverable creep compliance, J_{nr}, was introduced.

According to the developers, the J_{nr} rutting parameter ought to distinguish between the rutting resistance of different asphalt binders regardless of whether they are modified or not. Subsequently, the MSCR method was implemented into the Superpave® specification and successfully replaced the Superpave® PG "Plus" specifications. This method, however, still seems to be imprecise at currently determined shear stress levels, possibly because 0.1 kPa and 3.2 kPa may be lower than the stresses the pavement experiences under real traffic and weather conditions.

Therefore, the main objective of this study is to re-examine and improve the most promising asphalt binder testing method so it can better distinguish between different asphalt binders regarding their rutting resistance. As a result, the amount of time consuming and expensive asphalt mix tests can be reduced. Thus, it is necessary to understand the relationship between the properties of asphalt binders and the resistance of the mixes made of these binders.

1.3. Hypothesis

Rheological properties of different asphalt binders, including the non-recoverable creep compliance, J_{nr}, results measured at different stress levels, are compared with the actual rutting resistance of asphalt mixes. In order to estimate the rutting performance of asphalt

pavements, Hamburg wheel-tracking and dynamic modulus tests are conducted and their results compared with each other as well as with the asphalt binder rutting resistance results. The MSCR J_{nr} results evaluated at higher shear stress levels are expected to be more successful in determining the rutting resistance of different asphalt binders than the results evaluated at the currently standardized shear stress levels in Superpave® specification. The separate contribution of viscosity and elasticity to the rut resistance is also expressed from the MSCR measurements in terms of creep compliance, J_c, and recovered compliance, J_{rec}, and compared with the actual rut resistance of all binders.

1.4. Objectives

- The objective of this study is to evaluate the suitability of the multiple stress creep recovery test, that is commonly used to predict rutting resistance of asphalt binders, at standardized stress levels.
- To evaluate the effect of different types of modifiers on the binders' rheological properties and the asphalt mixes' rut resistance.
- To suggest viable changes to modify the multiple stress creep recovery test to better predict the rut resistance of asphalts binders in mixes.
- To explore the feasibility of the proposed changes.
- To develop linear viscoelastic property function master curves in order to examine the relationship between linear and non-linear properties of asphalt mixes.
- To correlate the MSCR results, measured according to the standardized and proposed changes, with the rut resistance of asphalt mixes evaluated by using Hamburg wheel-tracking device.

1.5. Organization of the Thesis

This thesis is organized into five chapters. Chapter 1 is an introduction to the problem with brief discussion of the background information on current rut resistance evaluation techniques of asphalt binders.

Chapter 2 reviews the literature available on asphalt binder types, their production and composition, the rheological background of their properties and the theory of their measurements. Furthermore, in this chapter all used modifier types and their effect on the rheological properties of asphalt binders are briefly discussed. In the second half of the chapter, the theory of the rut development, the magnitude of stresses that directly cause rutting, as well as the development of the new Superpave® rutting parameters are presented.

Chapter 3 presents the laboratory experimental program and introduces all materials and testing methods used in this study in order to evaluate the permanent deformation characteristics of thirteen different asphalt binders and their respective mixes.

Chapter 4 presents the results of asphalt and mix testing and explores ways in which the proposed testing methods could evaluate the rutting potential of asphalt binders by correlating them with asphalt mix rut resistance results.

Finally, conclusions of the research and recommendation for future work are presented in Chapter 6.

LITERATURE REVIEW

2.1. History of asphalt

Asphalt (or bitumen) as a construction material has been widely utilized by mankind since antiquity and there are evidences that its use even pre-dates recorded history [1]. In early times asphalt could be found only at natural seeps of oil, where natural liquid or gaseous hydrocarbons under low pressure slowly flowed up to the surface along with water through networks of cracks from deep underground, forming springs of hydrocarbons. Subsequently, the lighter elements vaporized, the oil thickened to viscous asphalt, or soaked into the surrounding soil, sedimental rock, or sand, and set to a hardened natural asphalt. According to Marschner *et al.* [2], early humans might have seen entrapped animals in such natural sources of asphalt and eventually learned how to turn its adhesive behavior in their favor. Because of the abundance of natural sources of asphalt in the Near East, Middle East, and today's Pakistan it was more extensively used in these areas than in any other parts of the world [3].

Several artifacts found in the El Kowm basin in Syria verifies that asphalt as an adhesive or hafting material for fixing handles of flint tools was used during the prehistoric period. Unearthed samples of such bitumen-coated stone tools have been conclusively proven to be used about 40,000 BC. In other words, asphalt as an adhesive material was used even by the Neanderthals [4]. It was later reported that several artefacts with traces of asphalt on their surface were found at the same excavation site in Syria but in lower archeological level (Hummalian level). That is, asphalt used as a hafting material to affix blade-flakes to wooden handles was prevalent at least from 180,000 BC [3].

According to the frequency of historical references to asphalt it is evident that the use of this natural material was very diverse. Every major early civilization benefited from its properties, either as a sealant, or as an adhesive, or as a filler in building construction, etc. According to Connan [1] and Connan and Deschesne [5] the most frequent use of asphalt was as mortar in building construction. This mortar generally was a mixture of bitumen (less than 30%) with mineral (clay, sand, ash, etc.) and organic materials (chopped straw, reeds). It is mentioned in the Bible that asphalt mortars were used in Babylon at the construction of the ziggurat known as the tower of Babel (Genesis 11.3) [1].

The first mention of the use of asphalt in road constructions can be linked to Babylon as well. In the late 7th century B.C., bitumen-containing mortar cemented not only the burnt bricks of the base courses, but also the meter square limestone slabs that paved the surface of ancient roads [6,7]. From antiquity to present days, asphalt continues to be successfully utilized as a waterproofing material. The most famous representative of its use as a waterproofing material in antiquity are the terraces of the Hanging Gardens of Babylon [1].

Other historical mentions of asphalt were the stories of Noah's ark (Genesis 6.14) and the tale about Moses when he was saved by his mother in a cradle on the Nile (Exodus 2.3). Both stories indicate that asphalt was commonly used as a sealing material at the beginning of written history. About 350 B.C., when the Egyptians began to run short of the resins they relied upon during the process of mummification, they figured out that asphalt could become a good substitute. Thus, asphalt blended with other aromatics (conifer resin, grease, and beeswax) became an invariable ingredient of these ointment mixtures used for embalming mummies. The very term of mummy itself possibly originates from the Persian word *mumiya*, which means bitumen or mineral pitch, more precisely: body preserved by wax or bitumen [1,8–10].

For both civilizations, the Egyptians and the Babylonians, the Dead Sea, or as the Greeks called it *Lacus Asphaltitis* (Lake Asphaltitis), was among the main sources of asphalt. Hence also the asphalt's historical names of *Jew's pitch* or *Bitumen Judaicum* (Jewish Bitumen) [1,11]. Asphalt was and still is constantly thrown out from deep seeps of the sea in a form of floating black or brownish-black resinous pebbles or blocks of various size usually swept to the shores [12].

By the second half of the 1st century B.C., when mummification was no longer fashionable, asphalt gradually lost its formal fame along with its value, thus it was more or less restricted to localities where the sources could be found. In the ensuing eras, asphalt was frequently utilized in medicine in the Middle East for various skin ailments and wounds, and against a large number of diseases [13]. The knowledge about asphalt and its healing properties primarily spread to Europe through descriptions of its medical use by Arab physicians in the 12th century. However, the negative attitude toward science that shaped medieval Europe ceased any further investigation of the potentials of asphalt and it once again became forgotten [10].

For better understanding how asphalt became one of the leading materials in paving industry, it is necessary to look into the evolution of modern road making. Before the 18th

century attempts were made to rediscover Roman road construction methods but tracks worn into the ground by thousands of passengers and their vehicles stayed the most typical roads throughout the medieval times. The rediscovery of asphalt must had waited until the early 19th century, when the industrial revolution brought along an increase in number of vehicles and an unsatisfied need for a pavement that could retrain its shape, resist to major deformation, is dustless, and waterproof while provides adequate friction and stability for traffic, generally represented by horse-drawn wagons with solid iron-tired wheels. New methods of road making had been pioneered by engineers Pierre-Marie-Jérôme Trésaguet, Thomas Telford, and John Loudon McAdam, whose techniques provided a running surface of compacted but unbound broken stone blinded with sand, dust or soil [6,14,15].

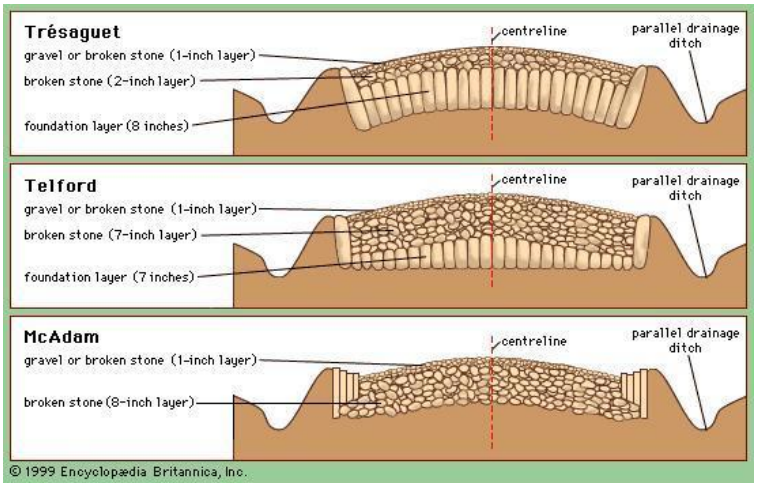

Figure 2.1 Cross sections of three 18th-century European roads, as designed by Pierre Trésaguet (top), Thomas Telford (middle), and John McAdam(bottom) [14]**.**

Although the new methods meant a great improvement in pavement construction, the surfaces of these roads were dusty in the summer, muddy in the winter, slippery, slimy, required daily maintenance, and their tenacity in urban environment was little more than marginal. From the beginning of the 19th century concurrently three promising binding materials (e.g., tar, natural asphalt, cement) seemed to be adequate for solving the problems raised by contemporary road constructions [6,14,15].

Tar can be obtained as a by-product of coal processing. As a consequence of growing demand for coal gas, a source of fuel and lightning, tar became increasingly available during the industrial revolution. In the late 1830s tar was used as a mortar for stone paving blocks, but more innovative way of its use was when it was applied as a

blinding and also as a binding material that coated individual stones, filled the open surface pores and sealed the macadam road. By adding heat tar could become less viscous, thus it could flow and slowly penetrate through the interstices between the stones of macadam courses. This technology later became known as penetration macadam [6,14,15].

Unfortunately, using tar alone appeared to be inadequate because the road surface treated with tar lacked stiffness and strength. Further development was made in 1901 when a civil engineer Edgar Purnell Hooley invented the so-called *tarmacadam* or *tarmac*. The patent for *tarmac* involved mechanical mixing of tar with aggregate prior to lay-down, and the subsequent compaction by steamroller. According to Hooley the tar should be modified by adding pitch (5.79%), Portland cement (0.41%), and resin (1.24%) [16]. The lack of durability, brittleness, and susceptibility to oxidation triggered technical improvements in tar production resulted in more enhanced and durable tars, later called road tars. Although until the second half of the 20th century tar continued to be widely used in paving industry, eventually more durable and cost-effective materials (e.g., asphalt and Portland cement) took over the market [6,14,15].

After being rediscovered in the early 18th century by a Russian-born Swiss physician and professor named d'Eyrinys, **natural asphalt** was used for various purposes (e.g., air-proofing, waterproofing, roofing, damp proofing). Asphalt as a possible paving material was first introduced at the turn of the next century in a form of mastic: a blend of tar and natural asphalt. Because of its waterproofing properties mastic was being widely used on bridge decks. In order to prevent slipperiness later sand was added to the warm mastic surface and thereafter the use of asphalt was further extended on pathways [15,17].

By the middle of the 19th century the abundance of natural asphalt throughout Western world made it available and inexpensive alternative to the other potential paving materials. The reason behind trying asphalt in paving was similar as in the case of tar: blinding the surface and binding the aggregate. In other words, it was hoped that asphalt will give strength to the construction of the pavement so it can retrain its shape and resist to major deformations, and it will prevent water from seeping into underlying structural courses. Due to its high mineral matter content (commonly pieces of limestone about 90 wt.%), natural asphalt was usually viscous enough to be mined as a solid, thus it was possible to cut it into brick-like cubes, which could be used directly on road surfaces. More common technique, however, was to grind the asphalt rock into a powder and press it into blocks. With the development of more effective field equipment and more powerful

compressing machine, and with and addition of further asphalt and heat to the powdered asphalt, so it could be pounded into cubical molds, asphalt blocks of adequate density were made. First trials with asphalt blocks were conducted in Paris (1824) and London (1838-1839), but, owing to the blocks' brittleness in winter, and softness in summer, and generally its slippery surface, none of them ended with favorable outcome for natural asphalt. Few years later, in 1854 the predecessor of compacted asphalt the first compressed powdered asphalt was built in Paris, where the grounded and heated natural asphalt was pressed, stamped, rolled and hot-ironed into macadam pavement [6,15]. After several decades of development natural asphalt did not seem to fulfill the expectations raised by dominating horse traffic in the 19th century. This changed in the beginning of the 20th century, when the rapid technical progress brought along the advent of automotive industry and also a more reliable successor of natural asphalt, the heavy end by-product of oil refining: the **refinery asphalt**. Since then, refinery asphalt continues to be one of the biggest competitors of pavement industry [15,17].

As it was implied earlier, throughout history several different names (e.g., *Jew's pitch, slime, asphalt, mineral pitch, Bitumen Judaicum, bitumen, thon*, etc.) were assigned to the same material, or more precisely, materials with analogous content. The todays common name originates in the Bible (Genesis 11.3), where the Hebrew word designating asphalt was translated as "ἄσφαλτος" (ásphaltos) in the Greek version of the Bible (*Septuagint*), and as "bitumen" in the Latin version (*Vulgate*). For many years both terms "asphalt" and "bitumen" lacked an exact definition and caused confusion when one wanted to find the correct designation. Nowadays, both these terms are used interchangeably and describe the same class of materials, however, asphalt is more frequently used in North America, while bitumen in Europe and the Eastern countries [1,8]. With the purpose of preventing any confusion, henceforth the use of term "asphalt" will be preferred in this study when referring to refined residue from the distillation process of crude oils.

2.2. Sources of asphalt

Historically, the terms bitumen and asphalt did not relate only to the above defined substances, but also encompassed naphtha, pitch, petroleum, and other mixtures of hydrocarbons regardless to their consistency [7]. Nowadays asphalt is defined by the American Society for Testing and Materials (ASTM) as *"a dark brown to black cement-*

like residuum obtained from the distillation of suitable crude oils" [18]. More general definition can be found in the current European specifications that specify asphalt (i.e., bitumen) as a *"virtually not volatile, adhesive and waterproofing material derived from crude petroleum, or present in natural asphalt, which is completely or nearly completely soluble in toluene, and very viscous or nearly solid at ambient temperatures"* [19]. In the case of paving grade asphalts the specifications determine the magnitude of solubility in 99 wt.% [20].

With regards to the origin of asphalt, it is preferable to distinguish between naturally occurring asphalt materials and manufactured or refinery asphalt materials.

2.2.1. Natural asphalt

Besides the different origin of sources, natural/native can be mainly distinguished from its manufactured relative by the presence of mineral matter that incorporated with asphalt and water creates a compound of organic and inorganic matter of variable content.

Naturally occurring deposits of asphalt with high mineral content can be found in sedimentary deposits filling pores and crevices of sand, sandstone, limestone, or argillaceous sediments. Other modes of occurrence are springs, lakes, seepages, or fissures in a vertical direction filled with hard asphalt [21].

Asphalt lakes, which are in fact springs on a very large scale, develop in places where petroleum or liquid asphalt is pushed above the surface through fissures in the rock, spread over a large area and naturally form into lakes, thus creating large deposits of the most extensively used and best-known form of natural asphalt. Seepages, on the other hand, occur where petroleum or liquid asphalt, either due to pressure of the material itself or the heat of the sun, flows out from the impregnated rock and runs towards the lower level [21].

As it was earlier discussed, natural asphalt originating from the Dead Sea found success in various types of usage through ancient times until the modern era. Dead Sea natural asphalt can be found in almost mineral-free form of asphalt blocks and pebbles seeping from above the sea level. Due to the higher gravity of the water the blocks and pebbles are constantly forced to float on the surface and are swept to the shore by winds and currents. Another occurrence of natural asphalt close to the Dead Sea is in form of asphaltic limestone, containing typically 5% asphalt [7,12].

When modern use of asphalt as a paving material evolved in Europe, two main sources provided the industry with natural asphalt: Seyssel in France and Val de Traves in Switzerland. Both deposits yielded asphaltic limestone with different asphalt content impregnating the porous mineral. The Seyssel typically contained 8% asphalt and the Val de Travers 8 to 12% asphalt [7].

Another deposit of a great importance is known as Pitch Lake (or Trinidad Lake) on the Island of Trinidad in the town of La Brea. Although vast quantities have been removed in the past, the lake with its extent that covers approximately 40 ha and is about 80 m deep still contains at least 10 million tonnes of natural asphalt what makes this natural phenomenon the largest commercially mined natural asphalt deposit in the world [21,22]. The Pitch Lake is a unique deposit yielding high-quality natural asphalt that, when freshly sampled at the center of the lake, contains 39% asphalt, 33% emulsified water and 27% mineral matter of colloidal clay [7,21,22]. At the beginning of the 20th century, due to its superior adhesive and thermoplastic properties, which are very hard to reproduce in refinery, the Trinidad Lake asphalt was widely used as a reference material for paving industry in Europe, in the US, or in China. Nowadays Trinidad Lake asphalt have found commercial application mainly as a modifier for refinery bitumen throughout the world [23–25].

Figure 2.2 Typical view of the Trinidad Lake; the asphalt surface is broken up into large folds with accumulations of rainwater in the creases, adapted from [26]

Lake Bermudez (or Lake Guanoco) in Venezuela, about 140 km west from Trinidad Lake, is another important deposit of natural asphalt. It contains high quality asphalt in

fairly pure state, consisting of 64% asphalt, 30% water, 4% insoluble organic matter and 2% dispersed mineral matter. Lake Bermudez occupies an area of about 445 ha in size what makes it the largest asphalt lake in the world, in terms of surface area. However, due to its depth that varies between 1.5 to 2 m, Lake Bermudez is smaller in volume than the Trinidad Lake [7,21].

By geochemists the term *extra heavy oil* or *bitumen* is often used interchangeably describing the same naturally occurring material of *bituminous sand*, *oil sand* or *tar sand*, although the latter is technically incorrect, since the term *tar* refers to the products of destructive distillation of various organic sources, such as coal or wood. Oil sand is a material that consists of either loose sands or partially consolidated sandstone impregnated with dense, viscous petroleum-like material, technically referred to as bitumen (or extra heavy oil). Oxidation due to water-washing and biodegradation are the main formation mechanisms of natural bitumen that converted formerly light fractions into high molecular weight components. The bitumen content of oil sands varies from zero to 22 wt.% [27–29].

Due to its high viscosity the bitumen found in oil sand deposits can be recovered only by enhanced recovery methods, such as surface mining or in situ methods (steam, solvents, thermal energy) below the surface. Compared to conventional crude oil resources, bitumen mining from oil sands require about 10 to 12% more energy during production from extraction, through upgrading/refining, until the desired end-product is made. The high rates of energy demand and the associated greenhouse gas emissions are also the cause of much controversy due to their impacts on the environment [27,30–32].

In order to avoid any confusion, it is appropriate to mention that the fundamental purpose of oil sand mining is to extract and transform upgraded diluted bitumen into usable petroleum products such as gasoline, diesel, jet fuel, kerosene, asphalt, and other hydrocarbons; while the aforementioned natural asphalts are mainly used for paving purposes. Since bitumen extracted from oil sand is not directly suitable for making asphalt pavements, other methods, like vacuum distillation and de-asphalting, must be employed, in order to separate asphalt from bitumen [32–34].

The largest bitumen deposits captured in oil sands occur in Venezuela, Orinoco Belt and Canada, Alberta, while by the end of 2018, Venezuela accounted for 17.5% and Canada for 9.7% of the world's proven oil reserves, according to BP [35]. In other words, these volumes contribute to Venezuela's total proven oil reserves being the largest in the world, before Saudi Arabia (17.2% [35]) and Canada.

2.2.2. Manufactured asphalt

At the turn of the 20th century the development of modern automobile industry required durable construction materials that were also suitable for making smooth road surfaces preferred by the new tire rubber wheels. During this period, early versions of oil refineries started to operate and yield manufactured (or refined) asphalt in large quantities that quickly became a better alternative to natural asphalt. Today, paving grade asphalts are essentially obtained by distillation of carefully selected crude oil or blend of crude oils, although modern oil refineries are based on much more enhanced technology than their forerunners.

Crude oil is a mixture of hydrocarbon compounds that display great variation in molecular weight, structure, and consequently in boiling range. Therefore, crude oil can be separated into a variety of generic fractions by distillation at different temperatures and pressure. The proportion of fractions is mainly dependent on the source of the original material, and accordingly not all crude oils contain sufficient amount of asphalt [27].

Even though crude oils consist of different hydrocarbon compounds of great variety and different molecular weight, their chemical nature can be generally classified into three groups based on the most abundant from the three main hydrocarbon groups of paraffins (alkanes or saturated linear carbon compounds), naphthenes (cycloalkanes), or aromatics present in the oil (Figure 2.3). This classification of crude is often applied also on the asphalt processed from the corresponding crude oil. Moreover, crude oils can be further divided into four groups of light, medium, heavy, and extra heavy oils, respectively, based on their specific density. Typically, light crude oils are more paraffinic, and yield higher percent of lighter fractions. On the contrary, heavy crude oils contain more naphthenes and aromatics. Extra heavy and heavy oils, as an example of Canadian and Venezuelan oil sands, tend to contain higher percent of nitrogen, oxygen, and sulfur compounds and metal contaminants than their lighter counterparts [7,36].

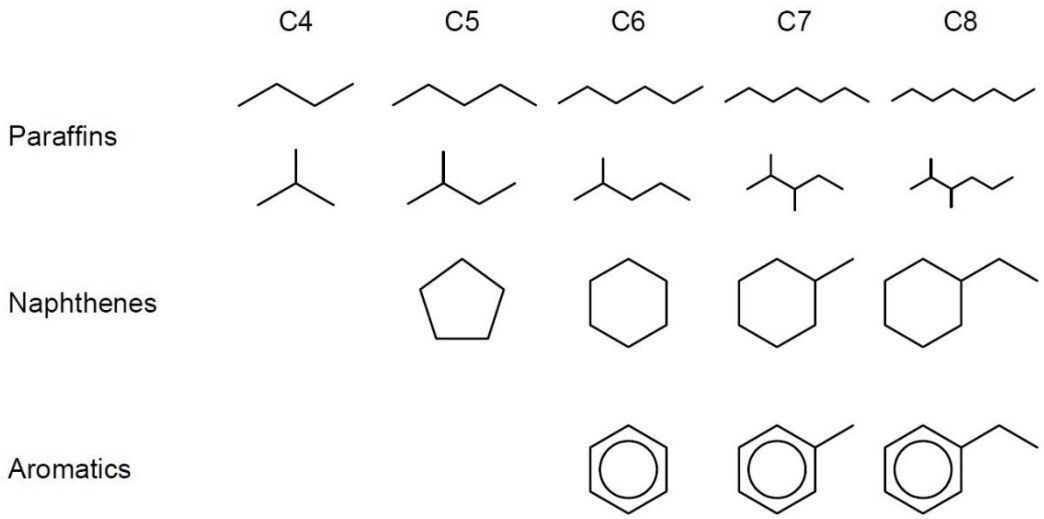

Figure 2.3 Three main groups of hydrocarbon components in crude oil

As a rule of thumb, crude oils with high percentage of low boiling components (paraffinic saturates) do not yield asphalt of sufficient amount or quality. From the known available crude oils about 10% contains enough asphaltic components (cyclic and aromatic structures) to be sufficient for asphalt production [27].

Crude oil or blends of crude oils can come either from naturally occurring crude deposits or can be extracted from oil sands. In modern refineries multiple crude oils are blended in order to produce consistent quality asphalt. Since crude oils are most often contaminated by saltwater, first they must be treated to remove the emulsion, otherwise the salt may damage the refining equipment. Only after desalting took place, the preheated crude oil may enter the fractionating columns, where the light fractions with lower boiling points (e.g., fuel gas, naphtha, kerosene, diesel, light gas oil, heavy gas oil) are separated from the crude oil by atmospheric distillation at temperatures typically between 350 and 360°C at a pressure slightly above atmospheric (1.5 bars). The liquid left at the base of the column, consisting from the highest boiling fractions, becomes the residue from the atmospheric distillation, also known as long residue. In order to achieve a residue of suitable consistency for use as an asphalt binder, further distillation must be conducted at slightly higher temperatures between 350 and 425°C but under vacuum (0.01–0.1 bars) [7,37–40].

The main reason of long residue processing at such circumstances is to prevent cracking or thermal decomposition of high molecular weight hydrocarbon compounds that would occur if the temperature would be further increased. Thus, in order to reach

the boiling point of the residue at 350–425°C the pressure must be lowered. The maximum equivalent atmospheric distillation temperature that can be achieved by vacuum distillation is between 500 and 560°C [7,37–40]. The operation conditions of vacuum distillation can be adjusted by varying the temperature and/or vacuum (pressure) inside the column to produce a vacuum residue, also known as short residue, of suitable consistency with a penetration range of 35–300 dmm. In other words, the hardness or viscosity of the residue can be also influenced by the amount of the heavy oil fractions it contains. Typically, two asphalt grades of different hardness are produced in refineries, one soft and one hard, and the intermediate grades are obtained by blending the two [7,27,38].

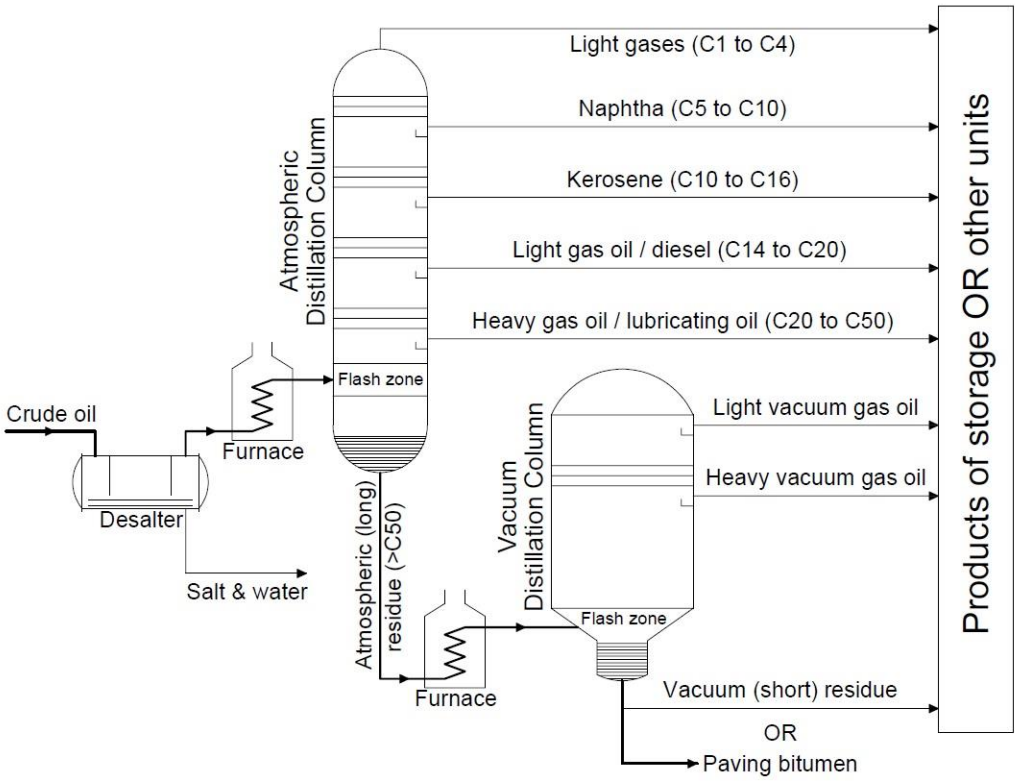

Figure 2.4 Atmospheric and vacuum distillation of crude oil

When the vacuum residue meets the required technical specification and no further processing is needed, the product can be referred to as residual asphalt or straight-run asphalt. However, not every crude oil yield asphaltic fraction of sufficient amount or quality additional steps may be required to produce paving grade asphalt binders. Several manufacturing methods (e.g., oxidation, air blowing, solvent deasphalting, thermal cracking, etc.) are available to alter the physical properties of the residue.

Air blowing or oxidation is usually applied when the high temperature performance of vacuum residue needs to be improved in order to meet the specifications. This process involves passing air through vacuum residue at elevated temperatures what causes chemical conversion of some of the relatively low molecular weight maltenes into higher molecular weight asphaltenes (see further in this chapter). During the main reaction of oxidative dehydrogenation, small amount of oxygen is being partly incorporated as labile functional group within the residue and subsequently eliminated as water. As a result of this reaction, typically, cycloalkanes (naphthene), aromatics, and polar aromatics are conversed into more aromatic, polar and complex polyaromatic compounds (Figure 2.5) [38,41]. As regards the physical properties, the main purpose of oxidation is to stiffen the vacuum residue, increase its softening point and viscosity and decrease the penetration.

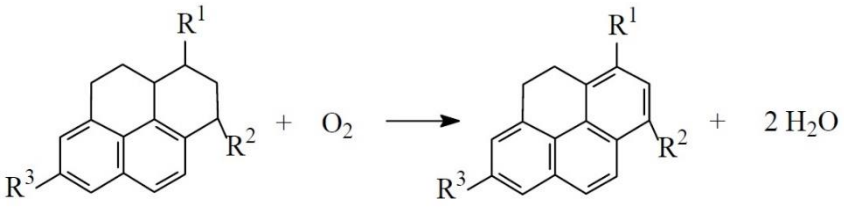

Figure 2.5 Effect of oxidation on complex polyaromatic compounds

Oxidation remained the best process to produce very hard asphalts, mostly used in the roofing industry. Despite the enhanced rheological properties and higher amount of asphaltenes, oxidized asphalts are in many cases not suitable for road application due to their substantially higher viscosity and softening point (for a given penetration value) and susceptibility to thermal cracking. However, by reducing the amount of air blowing, penetration grade asphalt can be produced, also known as semi-blown or air-rectified asphalt that have similar properties to those of straight-run asphalts [38,42].

Like crude oil, asphalt is also an extremely complex mixture of organic compounds composed of paraffinic (e.g., n-heptanes), naphthenic, and aromatic groups, respectively. Asphalt, as a residue of fractional distillation, mainly consist of hydrocarbon molecules of high molecular weight and high boiling point. The increase in boiling point is mainly caused by the higher number of carbon atoms in the substituent. Hydrocarbons with the same number of atoms may form different compounds or isomers of different shape. However, the number of isomers increase substantially with the increasing number of carbon atoms. For example, hydrocarbons with four carbon atoms (C_4 alkanes) may form

2 isomers, with 15 carbon atoms (C_{15} alkanes) 4347 isomers, and with 25 carbon atoms (C_{25} alkanes) no less than 36,797,588 different isomers. This means, that the potential number of compounds in asphalt can reach astronomical values. Furthermore, other types of compounds, such as the aromatic derivates or heteroatoms are also present in asphalt. This makes asphalt an extremely complex mixture of molecules that vary quite significantly from one asphalt to another. Therefore, the isolation of all chemically and structurally different compounds from asphalt is virtually impossible and also unnecessary task. Nonetheless, there are alternative ways to analyze asphalts and understand their properties either by elemental analysis or class fractionation [38,43].

The elemental analysis of asphalts from various sources indicates that beside the abundant organic hydrocarbon compounds they also contain small quantities of heteroatoms, mainly sulfur-, nitrogen-, and oxygen-containing compounds as well as small amounts of metal constituents. The vast majority of asphalts contain 82–88 wt.% of carbon and 8–11 wt.% of hydrogen. Therefore, neither the carbon content nor the hydrogen content is particularly instructive even though the physical properties of asphalts produced from different sources of crude processed by different technology vary substantially. Asphalts generally contain about 0–6 wt.% of sulfur, 0–1.5 wt.% of oxygen, and up to 1 wt.% of nitrogen, furthermore, traces of metals among them the most abundant are vanadium about 254 ppm, nickel about 83 ppm, or other heteroatoms if contaminated with coproduced brine salts (natrium, magnesium, calcium, and sodium chloride) [27,38,44].

Heteroatoms generally contribute to polarity within the molecules they are bonded to. Polarity can be understood as an asymmetric electron density that causes partial positive and partial negative charges of the molecule. The presence and amount of polar compounds in asphalt is very important because they tend to organize into preferred orientations and form a three-dimensional intermolecular structures that are held together by weak electrostatic and other short range forces even at intermediate temperatures, even though the rate of association may be slow. These highly organized molecules are dispersed in the surrounded non-polar continuous phase that organizes only at very low temperatures. Conversely, at higher temperatures, the associations of polar molecules decrease, and the asphalt becomes more dissociated, less viscous, and less resistant to deformation. Therefore, by increasing the amount of heteroatoms the number of polar molecules and their associations will rise too, causing that the asphalt becomes less susceptible to deformation, stiffer, and more viscous, nonetheless, also more fragile.

However, at this point it has to be pointed out that paving asphalts with relatively similar performance typically consist of different degree of polar molecule associations, resulting in that the rates and magnitudes of stiffening, even though they experienced the same oxidizing conditions, may vary substantially from one another [45].

Sulfur is generally the most present polar atom in asphalt. It appears in two main forms: aromatic rings and organic sulfides, whereas representatives of the latter group, like sulfides, thiols, and in a less extent sulfoxides, are much more susceptible to oxidation and hydrogenation, unlike aromatic rings. When oxidative conditions occur, sulfoxides can further oxidize into more polar compounds [44].

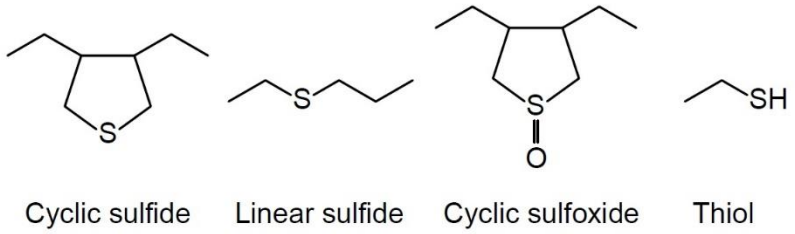

Figure 2.6 Sulfur compounds presented in asphalt

Nitrogen is present in asphalt in two main forms of compounds: nonbasic (pyrrole, carbazole and derivates) and basic (pyridine, quinoline and derivates). Both types of compounds are highly resistant to removal. Furthermore, pyridines enhance the ability of asphalt to adhere to aggregate surfaces [44].

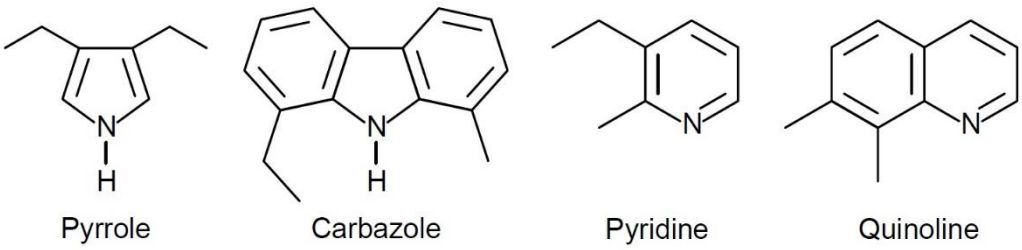

Figure 2.7 Nitrogen compounds presented in asphalt

Oxygen is present in asphalt mainly in a form of carboxylic acids, however it is also present in other forms, like phenols or ketones. The content of oxygen in asphalt is increasing as a result of oxidative aging by atmospheric oxygen that also hardens the asphalt [44,46].

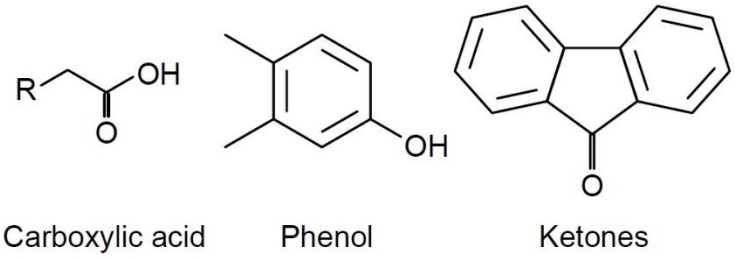

Figure 2.8 Oxygen compounds presented in asphalt

Despite the fact that the proportion of the elements in asphalts vary over fairly narrow limits their rheological properties may differ significantly. For another reason, but neither elemental analysis nor complete chemical analysis is a viable option if one is to understand the properties of asphalt. Therefore, an alternative of the two is to separate the constituent molecules into various fractions depending on their size and solubility in polar, aromatic, or non-polar solvents. Common practice is to divide asphalt into two main fractions called asphaltenes and maltenes, where maltenes are usually further subdivided into three increasingly polar fractions of saturates, aromatics, and resins (Figure 2.9). Thus, the composition of asphalts is usually given in terms of the relative quantity of these four fractions and named SARA after the first letters of each fractions.

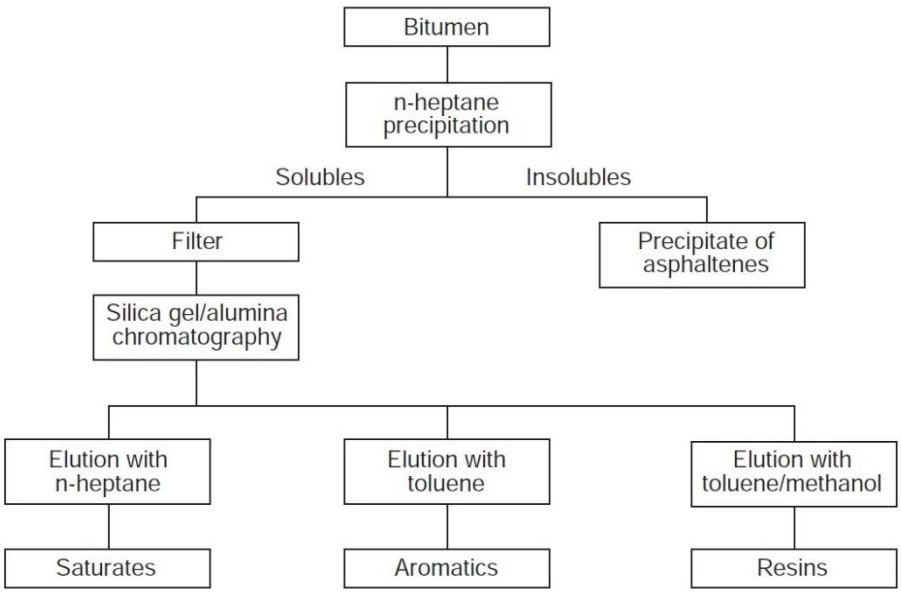

Figure 2.9 Schematic of the separation of asphalt into its various fractions: saturates, aromatics, resins, and asphaltenes (SARA) – chromatographic method [38]

There are several standard methods available for separation of asphalt into the four fractions. Even though the solvents and experimental set-up may differ, traditionally the asphaltenes, as the most polar of all four fractions, are first separated from the asphalt using n-heptane (alternatively n-pentane) precipitation. In order to define the relative quantity of saturates, resins, and aromatics (Figure 2.10) in the n-heptane-soluble portion (maltenes), elution-adsorption liquid chromatography on active alumina is employed as the absorbent with solvents of increasing polarity and aromaticity [43,47–50].

Saturates are slightly colored or colorless liquid of a medium viscosity at room temperature with a glass transition temperature around –70°C. It mainly consists of non-polar straight and branched-chain aliphatic hydrocarbons and very few polar or aromatic molecules with only traces of heteroatoms [38]. Usually, in paving grade asphalts the amount of saturates is ranging about 5–15 wt.%. Their molecular weight is the lowest of all four fractions that varies between 470 and 880 g/mol [7,51,52].

The most abundant fractions in asphalt are aromatics and resins, both typically in amounts of 30–45 wt.%. When isolated, aromatics at room temperature form a yellow to red liquid of high viscosity with a glass transition temperature about –20°C, which is about the glass transition temperature of the parent asphalt. Their molecular weight varies between 570 and 980 g/mol. Typically, they consist of slightly aliphatic carbon skeleton with lightly condensed aromatic rings [7,36,38,51].

When isolated, resins form a dark brown to black heavy liquid at room temperature that is fluid when heated and brittle when cold, although it is not clear yet whether they exhibit a glass transition. Resins, also called polar aromatics, contain a small amount of heteroatoms, that contribute to their polar nature. Compared to asphaltenes, resins are found to have lower molecular weight ranging between 780–1400 g/mol, and a less complex aromatic structure. Generally, they are a transition from oils to asphaltenes, and thus, play an important role in stabilizing the asphaltenes [7,36,38].

Asphaltenes, the n-heptane insoluble fraction of asphalt, form a black or dark brown powder at room temperature. Their molecular weight is the highest of all four fractions ranging between 800–3500 g/mol. Asphaltenes consist of highly condensed fused aromatics rings with pending aliphatic chains forming almost planar molecules. Due to the presence of heteroatoms, including metals such as nickel and vanadium, they contain more polar groups of a great complexity. Thanks to the presence of polar groups, asphaltenes greatly influence the adhesion of asphalt onto mineral aggregates [53,54]. The asphaltene content in paving grade asphalts are ranging between 5–20 wt.% and are

considered to have significant effect on the rheological properties of the parent asphalt by increasing its hardness and viscosity [7,38].

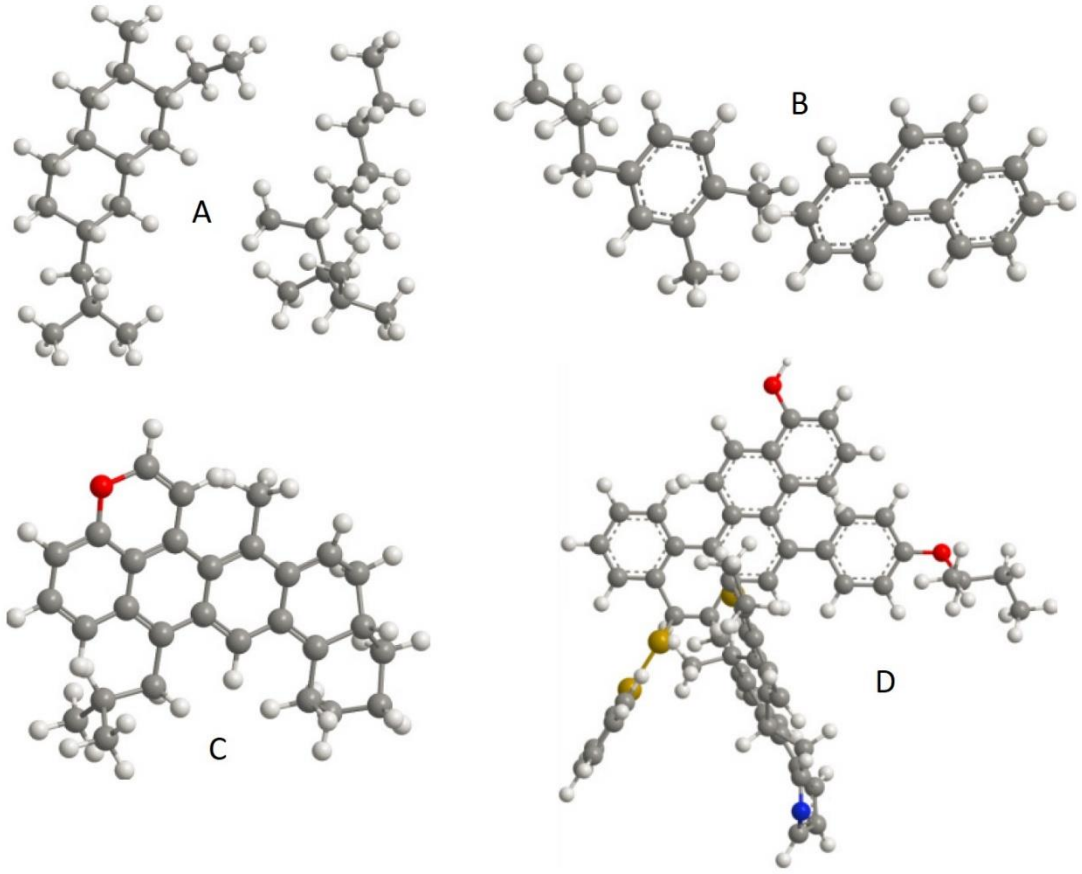

Figure 2.10 Fractional composition of bitumen expressed by molecular structure: A – saturates; B – aromatics; C – resins; D – asphaltenes, adapted from [36]

2.3. The colloidal structure of asphalt

At the beginning of the 20th century early studies of Rosinger and Nellensteyn described the asphaltenes as structures very close to free carbon that form a colloidal suspension within the oily maltene phase. This was further developed and a colloidal structure of asphalt was proposed with asphaltenes being present in the form of micelles [55,56].

Generally, by exposing asphaltenes to solvents (in the case of asphalt: maltenes) they start to associate what leads to the formation of aggregates – micelles (Figure 2.11). The size of the micelle is dependent on the temperature, on the nature of the solvent, on the content of asphaltenes and on the average molar mass [7,57]. Away from the center of the micelle there is a gradual transition to less polar aromatic resins. Furthermore, these

layers are extending outwards into the less aromatic, oily dispersive medium, while the semi-solid resins thought to act as peptizing agent (i.e., surfactants) and are responsible for the formation of colloidal suspensions. Thus, micelle consist of an asphaltene center that adsorb high molar mass resins which surround the micelles. The micelles disperse in the less aromatic and saturate components and forms the stable colloidal system [38,43,58,59].

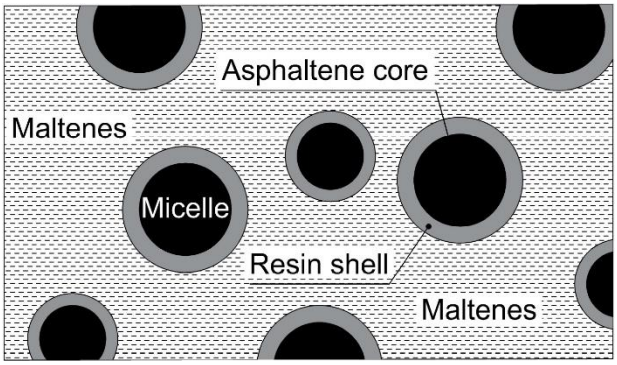

Figure 2.11 Simplified scheme of the colloidal structure of bitumen

Owing to their repulsive forces it is believed that resins prevent the flocculation of the associated asphaltene structure, thus are responsible for the stability of the micelles and keep them in suspension [58,60]. To describe the stability of asphalt Gaestel *et al.* [61] introduced the colloidal instability index I_c as a ratio of the sum of the amounts of asphaltenes and saturates to the sum of the amount surfactants (i.e., resins and aromatics)

$$I_c = \frac{\chi_{asph} + \chi_{sat}}{\chi_{aro} + \chi_{res}} \tag{2.1}$$

where χ_i is the weight content of the generic family (i = asphaltenes, resins, aromatics, or saturates). The lower colloidal instability index means that the asphaltenes are more peptized (i.e., dispersed) by the resins in the oil based medium. The value of I_c typically ranges from 0.5 to 2.7 for paving grade asphalts, while the higher value usually indicates more oxidized asphalts [57,58,62,63].

A rather rheological approach was introduced by Pfeiffer *et al.* [64] that distinguished between sol asphalts that exhibited Newtonian behavior and gel asphalts with strong non-Newtonian behavior, typical for oxidized asphalts (more about Newtonian behavior in Chapter 2.5.2). However, the majority of paving grade asphalts exhibit an intermediate (i.e., sol-gel) behavior, indicating the presence of both types of chemical structure.

In structural terms, the difference between sol and gel types is considered to be dependent on the content of asphaltene molecules and their interactions within the maltene phase. While the sol type is thought to occur when the asphaltene micelles are fully dispersed and gel type when fully interconnected (Figure 2.12). As a consequence, oxidized asphalts typically have stronger elasticity than straight-run asphalts and higher colloidal instability index. This interpretation corresponds with the fact that when compared with softer asphalt, originating from the same crude, harder asphalts contain more asphaltenes and less aromatics but almost unchanged amount of resins. This indicates that colloidal changes gradually occur by transformation of aromatics to resins, and resins to asphaltenes [64].

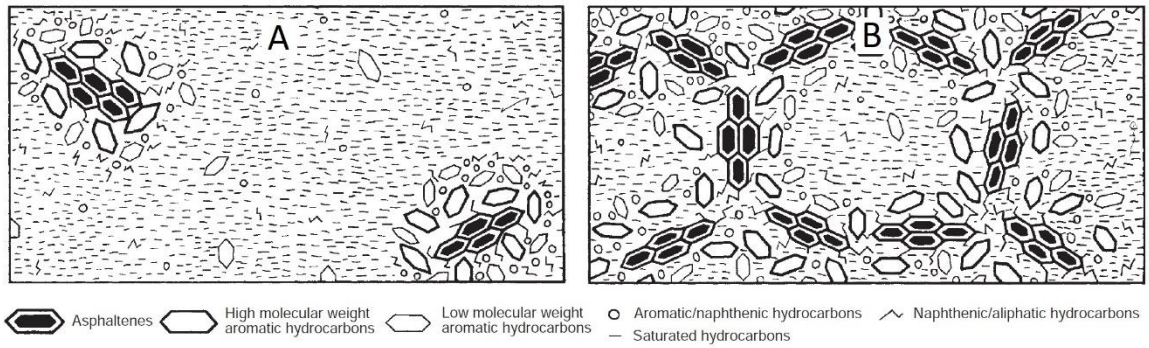

Figure 2.12 Schematic representation of sol type (A) and gel type (B) asphalt, adapted from [38]

There is still considerable conjecture about whether the micelle in asphalt is composed only of asphaltene molecules, or it is composed of asphaltene and resin molecules [43,64]. Consequently, Yen and Dickie [65] proposed a more precise model of the internal structure of asphaltenes, known as Yen model. This model suggested that asphaltenes are polycondensated multi-polymers with different repeating blocks and miscellaneous interactions inside the structure, forming micelle by association with maltenes. On the basis of X-Ray diffraction it was suggested that the cluster of planar polyaromatic hydrocarbon asphaltenes associate through π-π bonding form graphite-like stacks (maximum of 5 to 6 layers) that are surrounded by aliphatic chains and form what is known as the "island" structure [7,38,43,65], as it is depicted by Rogel in Figure 2.13.

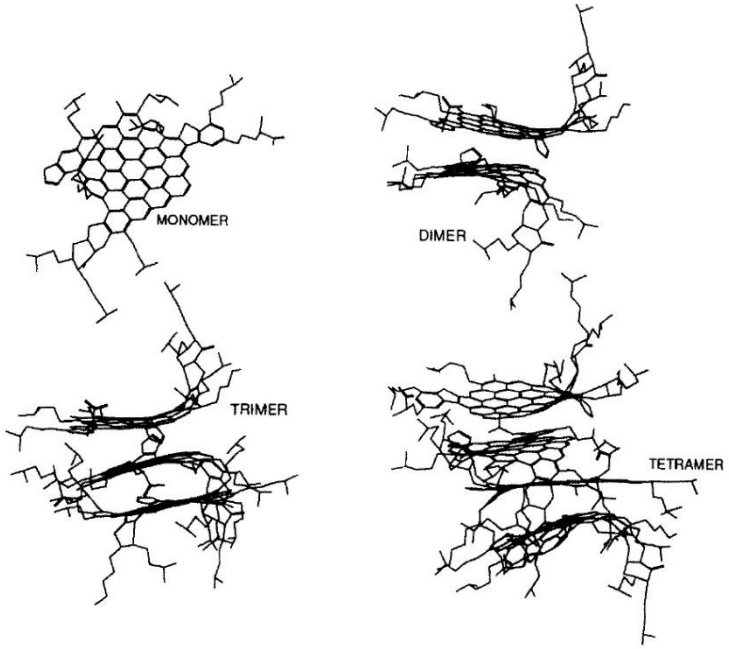

Figure 2.13 Optimized structures of asphaltene molecule and its aggregates, adapted from [66]

Even though by implementing the colloidal hypothesis many experimental results can be successfully interpreted, other studies, mainly conducted by Strategic Highway Research Program (SHRP), consider asphalt as a simple homogeneous fluid. Their hypothesis is based on the rheological properties of asphalts and consider asphalt as a simple homogenous fluid [67]. Another SHRP model suggest that asphalt is a mixture of strong and weak bases, strong and weak acids, neutral compounds, and amphoteric compounds, while the latter are a combination of base and acid within the same molecule. Several methods were introduced that allow to separate asphalt components into fractions according to their acidity [68,69].

As already stated above, the performance of asphalt is affected by the types of compounds it contains and their proportion, nonetheless, at the present no precise relationship has been established between the two. Furthermore, studies show that depending on the type of the used solvent or the chosen technique of investigation of internal structure, different results are obtained. Therefore, complete understanding of the internal structure still does not exist and hence in order to better understand the influence of asphalt components on its properties further research will be needed.

2.4. Polymer modified asphalt

Since the end of World War II, the number of vehicles per citizen has greatly increased as well as their speed and load. In addition, most roads were subjected to an overloading that was not considered during the design process and caused increase in demand on maintenance, faster deterioration, and, consequently, increase in costs. Therefore, in order to extend the life of pavements and to satisfy the present and also future demand on pavement resistance to deformation and other stress related failures the performance of conventional asphalt binders needed to be improved. This situation led to development of new, modified, better performing asphalt binders that are more resistant to deformation and also to temperature changes.

During its service time, several types of failures may reduce the quality and performance of asphalt pavement, among which rutting, fatigue cracking and thermal cracking represent the three main distress modes. It is important to mention that all the pavement distresses listed above may also be the result of badly designed asphalt mix (i.e., aggregate job mix formula, air void content, asphalt content, etc.) [70].

Rutting is a longitudinal vertical deformation of a pavement surface in a wheel path constituted of irreversible (permanent) deformations that accumulated in all or in some of the pavement layers under repeated traffic load, forming lane grooves worn into the pavement. It occurs at high service temperatures typical for the months of hot weather or in regions with hot climates when the viscosity of the asphalt binder in the pavement decrease. More about rutting in Chapter 2.6 [71].

Figure 2.14 Rutting of the asphalt pavement, adapted from [72]

Fatigue cracking is also a traffic induced distress that typically occurs as a result of the application of a stress-relaxation cycles associated with vehicle passage at intermediate temperatures on aged asphalt pavements. Under repeated load the pavement flexes and a tensile strain is induced in the base layer. Therefore, after several years fatigue cracks evolve at the underside of the asphalt base and propagate upwards until they reach the surface of the pavement where they form into localized interconnecting cracking in the surface layer. Since the cracking pattern resembles the scales on the back of a crocodile the name of alligator or crocodile cracking is also widely used [38,73].

Figure 2.15 Fatigue (crocodile/alligator) cracking of the asphalt pavement [74]

The last form of the main three distresses of asphalt pavements is **thermal cracking**. It is related to periodic seasonal and day-night thermal variations and is typical for extremely cold climate. At low temperatures, close to glassy state, the asphalt binder becomes too stiff and lose the ability to withstand and dissipate the stresses caused by the contraction of the mix. Thermal cracking appears in a form of traverse cracks that propagate through the asphalt layers to the full depth of the pavement. In order to endure these thermally induced stresses, the relaxation characteristics of the mix must be adequate to the rate of contraction governed by the coefficient of thermal expansion of the pavement. Depending on the used materials and the temperature, thermal cracking can appear either suddenly, or may develop at a slower rate, taking several seasons to propagate through the asphalt layers [38,75].

Figure 2.16 Thermal cracking of the asphalt pavement [76]

In order to enhance their engineering properties, and therefore avoid the development of the potential pavement distresses, asphalt binders are frequently modified by variety of materials. According to the definition adopted, modified asphalts are those asphalts whose properties have been changed by the use of a chemical agent. When added to the asphalt base, this agent alters its chemical structure and/or physical and mechanical properties. The resulting materials are either manufactured in a plant which is distant from the worksite or by a special mobile unit immediately before mixing [77].

Air-blowing may also be considered as a modification that helps to enhance the high temperature performance of soft asphalt binders. It was early observed that not only oxygen could react with asphalt, but other compounds too, such as sulfur or various acids (e.g., sulfuric, acid sludge, fatty acids) [78]. Furthermore, asphalt modification with these compounds proved to be much less complicated, when compared to air-blowing, since no specific production units were required, only a normal storage tank, an agitator, and a heater. Nonetheless, these early compounds were later replaced by other, more promising additives, among which polymer modifiers became the most popular [7,38].

During modification, polymers or other additives are incorporated in asphalt by mechanical mixing or chemical reaction. For paving purposes generally one or more polymers are blended with the asphalt, while the polymer dosage is usually in the range of 1 to 7 wt.% with respect to the asphalt and the needed performance grade. When the modification is successful, the resulting material should gain some improved properties, such as higher stiffness at high temperatures, higher cracking resistance at low temperatures, better moisture resistance or longer fatigue life, etc. Polymer modification

can also bring other advantages, such as reduction of the thickness of pavement, improved resistance to abrasion as well as to oxidation and aging [70].

However, not all polymers can be used as asphalt modifier, since some of the binder's properties (e.g., high temperature viscosity) should not be altered significantly, so that the existing pavement building processes and apparatus can still be used. Nonetheless, polymers suitable for modification primarily have to be compatible with the asphalt base, then resistant to thermal degradation during mixing, as well as during application or storage. In addition, the polarity of asphalt and polymer molecules should be similar, since molecular polarity of two materials affects their solubility in a way that only materials with similar level of polarity have a tendency of being miscible and therefore compatible with each other [70,79].

As it was discussed earlier in Chapter 2.3, it is difficult to determine the real internal structure of neat asphalt which is by the addition of polymer modifier further complicated. In most cases, the asphalt-polymer interactions are just of physical kind and the final morphology of the mixture can be defined according to two limiting cases of perfect and totally absent solubility of the polymer in the asphalt. In the first case, the polymeric macromolecules would be completely dispersed in the base asphalt resulting monophasic structure of the asphalt-polymer blend with perfect storage stability. However, in this case, the added polymer would probably lose its ability to form glassy domains as well as its desired rheological properties derived from its intermolecular entanglements. In the second case, even if assuming that the melted polymer was appropriately dispersed in the asphalt base, separation will occur. The separation is controlled by Stokes sedimentation rate, meaning that the rate of sedimentation depends on the size of particles and difference in density of these particles and the asphalt [80].

Therefore, the main goal is to obtain an intermediate biphasic condition in which a polymer-rich phase and an asphaltene-rich phase coexist in a micro-scale metastable equilibrium. In other words, the polymer modifier should be solvated to such extent at which its "polymer-like" properties at service temperatures sustain, therefore, partially miscible polymers are preferred. Nonetheless, the difference in density between the two phases will always result separation, with the polymer-rich phase creaming to the top and the asphaltene-rich phase precipitating. Its extent should be reduced as much as it is possible, because once the polymer-rich phase macroscopically segregates in storage tank, it may damage the pumping apparatus and in addition the desired enhancements of neat asphalt through modification would be completely lost. Thus, separation, and more

precisely the rate of separation is of great importance and is basically limited by the maximum storage time at high temperatures and therefore reduced viscosity [7,70,77].

When the polymer is compatible with the asphalt base it most probably interacts with the maltenes and gets swollen by them while forming a relatively stable network. Due to swelling, the polymer-rich phase occupies a volumetric fraction far greater than that of the polymer mass in the blend, which is usually between 3 and 7 wt.%. The interaction between the lighter asphalt components and the polymer leads to a local solvent extraction which also alters the original colloidal equilibrium. Furthermore, when the polymer content in asphalt reaches a certain amount (depending on the polymer/asphalt couple, this concentration varies widely between 4 and 10 wt.%), phase inversion occurs, with asphaltene-rich phase dispersed in polymer-rich matrix. In this case the rheological properties of the blend will unambiguously resemble those of the polymer. Nevertheless, the ideal microstructure is when the polymer modified asphalt (PMA) is composed of two interlocked continuous phases which also determines the optimum content of the polymer modifier. The PMA usually shows better overall performance, storage stability and cost-effectiveness when these conditions are met [80–82].

From the economic viewpoint, the modification also has to be cost-effective, meaning that it is not always better to achieve higher performance for the pavement. The high cost of polymers compared to asphalt makes the commercial use of modified asphalt only attractive if by using PMA the overall expenses, incurring during service time, will be reduced. Therefore, prior to the designing process, the needed degree of performance for the road should be always considered.

According to the latest data released by the European Asphalt Pavement Association (EAPA) in 2018, the PMB consumption in most of the European countries was usually less than 20% of the total asphalt consumption. This percentage in the Czech Republic was 27% from the total of 420,000 tonnes during the year 2018 [83].

Although a wide array of polymers has been used as modifiers in asphalt industry, according to the chemical structure and properties they can be divided into three main groups of thermoplastic elastomers, plastomers, and reactive polymers. Another group of materials widely used for asphalt modification, but due to their substantially different mechanism of modification should be mentioned as a separate category, are crumb rubber modifiers (CRM). Generally, elastomers enhance the strength and elasticity of asphalt base, while plastomers and reactive polymers improve their load resistance and rigidity. In contrast with most of the polymer modifiers, reactive polymers contain functional

groups and are believed to chemically react with some components of the asphalt. More detailed analysis of these polymer modifiers follows in the next chapters.

2.4.1. Thermoplastic elastomers

Thermoplastic elastomers (TPE) are a group of copolymers (i.e., their polymer chain is derived from more than one species of monomer) that incorporate, both thermoplastic and elastomeric properties. TPEs have properties at their service temperature similar to those of vulcanized rubber but can be processed and reprocessed at elevated temperatures as the thermoplastic polymers. Unlike vulcanized rubber, TPEs soften on heating and harden on cooling resulting in that their use during manufacture is relatively easy. The number of possible thermal cycles depends only on the resistance of the polymer to oxidation. This characteristic behavior is without doubt their major advantage because it makes these materials well suited, both technically and economically, to continuous manufacturing. Due to their elastic properties, TPEs can resist permanent deformation mainly because after stretching to moderate strains they are able to recover their original shape once the load is removed [84,85].

In contrast with other types of copolymers, such as random copolymers, which are a random mixture of monomers, block copolymers are made by sequential addition of monomers (Figure 2.17). In the most cases TPEs are diblock copolymers with one plastomeric (rigid) and one elastomeric block or they are triblock copolymers with plastomeric blocks at each end of the elastomeric block. In pure block copolymers, the plastomeric block do not contain any structural unit of the elastomeric block, and vice versa [84,85].

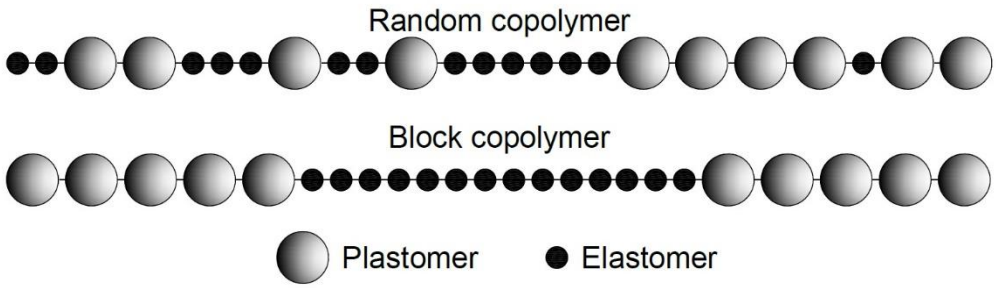

Figure 2.17 Difference between the polymer structures of random and block copolymer

One of the main differences between vulcanized rubber and TPE lies in the different characteristics of the network nodes. The network in vulcanized rubbers is formed by chemical reaction during which the polymer chains are linked together by strong covalent bonds with help of crosslinking agents. In the case of TPE networks, thermoplastic blocks self-agglomerate to glassy or crystalline hard domains that are formed by weak interactions and function as physical crosslinks (nodes) that interconnect the soft elastomeric domain in a three-dimensional network (Figure 2.18). While chemical crosslinks are stable, both mechanically and thermally, physical crosslinks are reversible and can be reformed by heat. Therefore, TPEs exhibit a much wider range of properties, and they can be easily molded and recycled only by addition of heat [84,85].

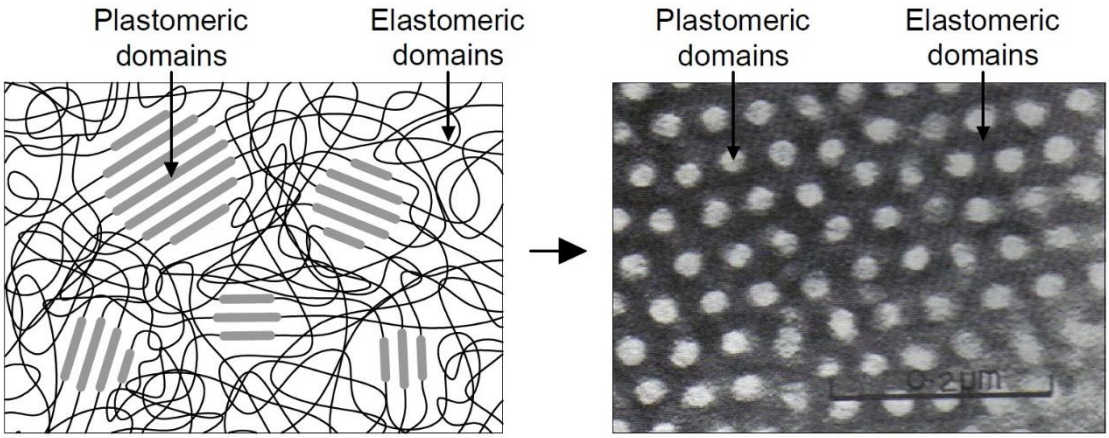

Figure 2.18 Schematic microstructure of a TPE (left) and an image of the microstructure of styrene-*b*-butadiene-*b*-styrene (SBS) triblock copolymer under microscope (right, adapted from [86]**)**

The plastomeric domains are known to be incompatible with the elastomeric macromolecules, so they form an immiscible two-phase system, where the plastomeric rigid node-like domains are dispersed in a continuous elastomeric phase. Due to the fact that the domains of hard phase can also act in the role of filler, TPEs may become stiffer if the nodes are especially large, causing and improvement in mechanical properties at high deformations. On the other hand, too large nodes may have a negative impact on elasticity at low temperatures [84].

The two immiscible phases retain many of the properties of the respective homopolymers which are in some extent combined in TPEs. For instance, TPEs may exhibit two glass transition temperatures (softening point, T_g, or melting points, T_m),

unlike random copolymers, which exhibit a single intermediate T_g or T_m. As a result of this, under the glass transition of both phases TPEs are hard and rigid materials, while above glass transition temperature of one of the two phases (in this case the elastic phase) TPEs become elastic and behave as vulcanized rubber. This means, that at ambient temperatures the hard phase stays rigid and strong and the elastomeric phase becomes elastic and can be easily extended. When the TPE is further heated, the hard domains soften resulting in network weakening until the material becomes sufficiently soft to flow. At this temperature the polymer can be processed by commercial technology available in polymeric industry. Although the ability of being processable above certain temperatures is considered as a benefit, it is also a detriment, since it limits the temperature range over which the TPEs can be used as an elastomeric material. The temperature use window of different TPEs is illustrated in Figure 2.19 where the values of T_g of the soft phase and the T_g or T_m of the hard phase is determined from the temperature dependence of tensile modulus, E, for each polymer [86].

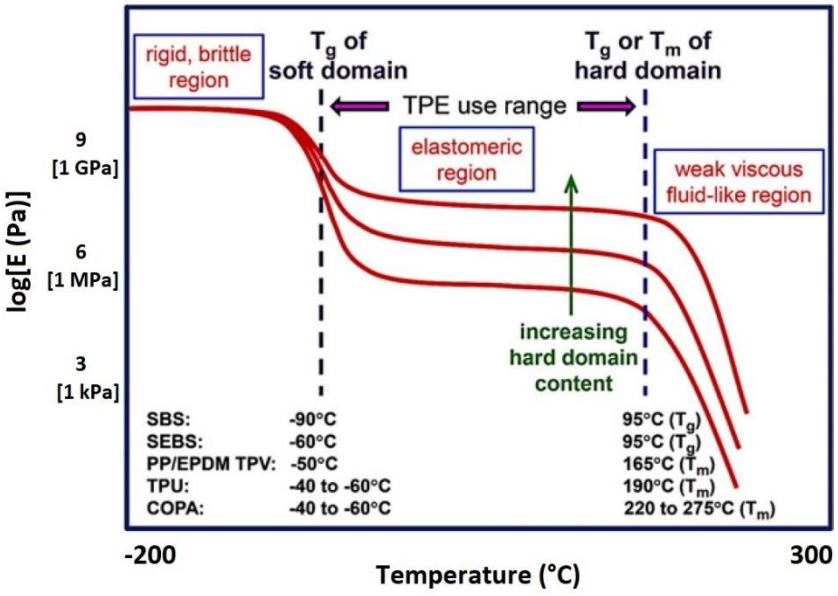

Figure 2.19 Schematic illustration of the temperature dependence of tensile modulus, E, for different TPEs, adapted from [86]

When these materials are cooled again, the hard domains self-assemble into small crystalline or glassy domains while recovering the original internal three-dimensional structure of the material along with its mechanical properties (strength, elasticity, toughness) [86,87].

Due to the two-phase nature of TPEs it is also apparent that their properties depend not only on the properties of each respective homopolymers but also on relative amount of these two phases. Generally, with an increasing content of hard phase the material will change its rheological properties from elastic to hard, rigid plastic. This is illustrated in Figure 2.20 (also in Figure 2.19) where the tensile curves (stress/strain) of **poly(styrene-*b*-butadiene-*b*-styrene) (SBS)** triblock copolymer of different hard phase (styrene) content are plotted [86,87].

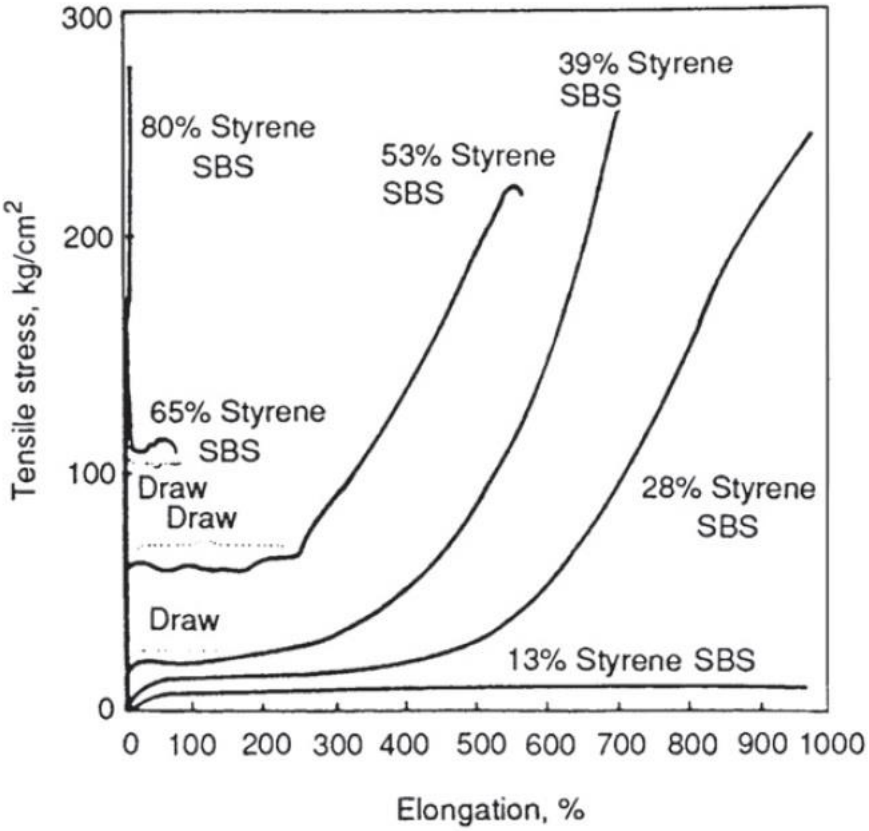

Figure 2.20 Tensile properties of SBS of different styrene content, adapted from [86]

To date, multi-block copolymers of diene (butadiene, isoprene) and styrene constitute the most frequently used and the oldest category of thermoplastic elastomers used for asphalt modification, among which the aforementioned SBS is the most successful one. SBS is a triblock copolymer with plastomeric styrene blocks at each end of the elastomeric butadiene block (Figure 2.21).

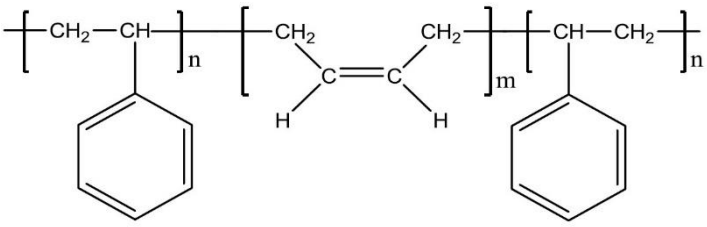

Figure 2.21 Chemical formula of the styrene-*b*-butadiene-*b*-styrene (SBS) triblock copolymer

Due to their thermoplastic nature (solubility parameters similar to the components present in asphalt, T_g of plastic and elastomeric phase close to 95°C, and -90°C, respectively) blending SBS block copolymers with asphalt is extremely easy and effective. When SBS is blended with asphalt, the elastic asphalt-compatible polybutadiene (PB) midblock becomes swollen by absorption of maltenes while forming a polymeric 3-D network structure having properties comparable to those of vulcanized rubber with the polystyrene (PS) endblocks acting as physical crosslinks. Such a swollen network of maltene extended SBS is illustrated in Figure 2.22. In this system the intrinsic 3-D network of SBS triblock is maintained whereas the volume of the polymer increases up to ten times of its initial volume, preferentially as a result of its similar solubility parameter to the low condensation aromatics of maltenes [88].

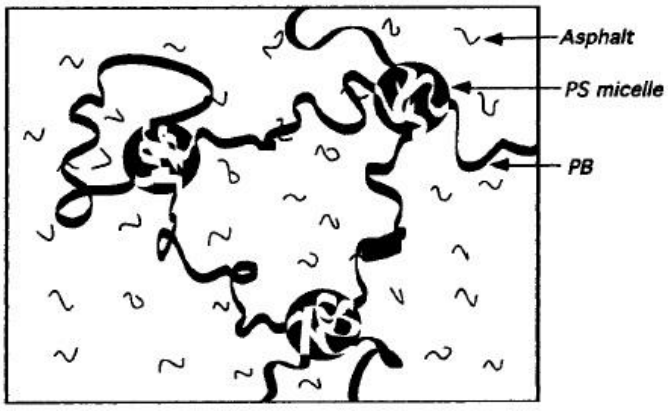

Figure 2.22 Schematic illustration of a network in the asphalt/SBS blend where the polystyrene endblocks form into spherical micelles which are interconnected by the swollen polybutadiene midblocks, adapted from [89]

The resulting material can be described as a two-phase system of SBS-rich phase, extended by a portion of maltenes, and the rest of maltenes with all the asphaltenes. The creation of the polymeric 3-D network in the asphalt/SBS blend is of high importance, since this structure is whereby the elastomeric properties of SBS take effect in the pavement [89–92].

Although depending on many factors (e.g., polystyrene content, asphalt/polymer compatibility, etc.), it can be generally said that the critical concentration at which phase inversion occurs is around 6 to 10 wt.% of SBS in the asphalt/SBS blend. In Figure 2.23 SBS-modified 50/70 Pen grade asphalt with increasing polymer concentration observed by fluorescence light microscopy (FLM) is illustrated. The lightly toned regions are assigned to polymer-rich phase, whereas the asphaltene-rich phase appears dark. When the concentration of SBS is below 10 wt.% (Figure 2.23A and Figure 2.23B) the polymer-rich phase is present in a form of discrete macrodomains dispersed in the continuous asphaltene-rich matrix. However, near the phase inversion at critical level of polymer concentration about 10 wt.% of SBS a co-continuous morphology of modified asphalt is found where both the polymer-rich and the asphaltene-rich phases are simultaneously present and form an interlocked continuous phase (Figure 2.23C). Above this concentration complete continuity inversion happens in which, despite of the significantly lower content of polymer compared to asphalt, the polymer-rich phase becomes the continuous matrix (Figure 2.23D) [77,89].

Once the SBS-rich phase is formed, the rubbery supporting network passes its elastic properties to the asphalt base resulting in improvement in its viscoelastic properties over a larger temperature use window. For example, when compared to neat binders, SBS-modified asphalt binders indicate increased complex modulus and viscosity, improved elastic response at intermediate temperatures, and lower creep stiffness at low temperatures resulting in significantly better resistance to rutting and thermal cracking [81,93]. A typical neat asphalt may perform well at temperatures between 10 to 50°C. However, the same asphalt modified by SBS may display good results at much broader temperature range between –20 to 76°C [90].

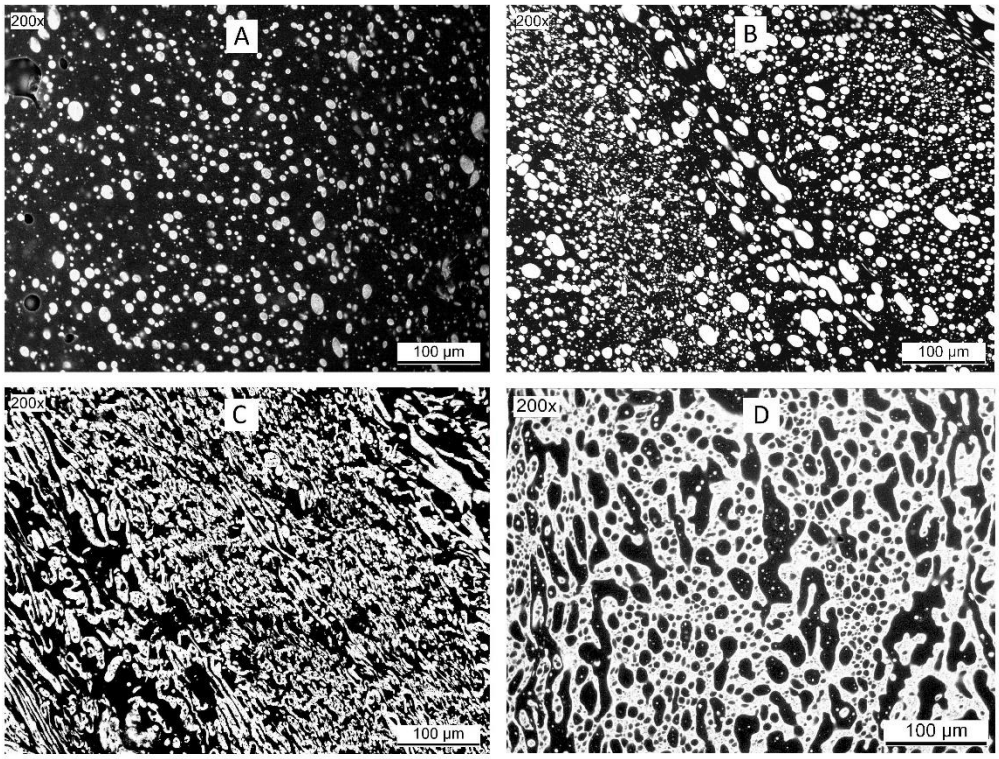

Figure 2.23 Microstructure of the asphalt/SBS blends containing SBS (30% styrene content) concentration of (A) 4%, (B) 8%, (C) 10%, (D) 12% examined by fluorescence light microscopy (FLM), magnification 200x

The essential difference between SBS-modified and neat asphalt is illustrated in Figure 2.24. If existed, ideal asphalt material, meant for road constructions (dotted line), would preserve its consistency throughout the whole service temperature range but become processable (i.e., less viscous) at high temperatures. However, the consistency of "real" neat asphalt decreases almost linearly as the temperature rises. Although such material is easy to process at laying temperatures, its properties can be inadequate at service temperatures, since it becomes too soft at intermediate temperatures and too brittle at low temperatures. As for SBS-modified asphalt, the consistency-temperature curve closely approaches that of the ideal behavior by combining satisfactory processability at higher temperatures with smaller variations in performance at service temperatures [77].

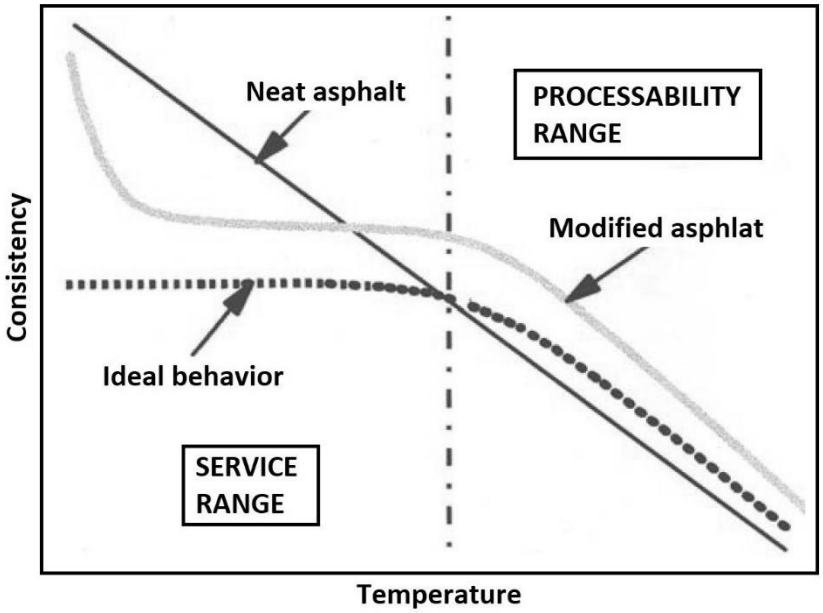

Figure 2.24 Schematic diagram depicting the effect of TPEs on the consistency of neat asphalt at different temperatures, adapted from [77]

An extensive literature on asphalt modification with styrenic thermoplastic block copolymers is available, among which studies of Becker et al. [82], Airey [94–96], Fawcett and McNally [97,98], Polacco et al. [99,100], Elseifi et al. [101], Lu and Isacsson [102], Wloczysiak et al. [103,104], Chen et al. [105], and Lundström and Isacsson [106] worth mentioning.

One of the main disadvantages of SBS polymer is the presence of unsaturated double bonds in polybutadiene blocks that makes it unstable and sensitive to heat, oxidation and ultraviolet, particularly under mechanical stress. The problem of unsaturated double bonds can be partially eliminated by hydrogenation of SBS (chemical saturation). Hydrogenated materials, such as styrene-*b*-(ethylene-*r*-butylene)-*b*-styrene triblock copolymers (SEBS) are highly resistant to thermo-oxidative degradation. However, as the double bonds disappear, the copolymer becomes less polar, resulting in worse compatibility, faster phase separation, and therefore higher storage instability. Compared to SBS, other problems with SEBS are the higher cost involved by the hydrogenation process and the reduced elastic properties, which further limits its application as a bitumen modifier [70,93].

2.4.2. Plastomers

The second group of polymers widely used for asphalt modification are plastomers. Some of the disadvantages of TPEs, such as the above-mentioned high cost and sensitivity to oxidation, can be partially eliminated by using plastomers, which are available in large quantities with different mechanical properties and at low cost. Generally, plastomers contribute to the high rigidity and resistance to deformation by forming tough 3-D network in the asphalt [38,70].

Most of the currently used plastomers for asphalt modification, including polyethylene (PE), polypropylene (PP), and their copolymers, belong to thermoplastic polyolefins. Polyethylene and polypropylene with their share of about 58% of the total plastic market are the most mass-produced polymers [107]. Due to the abundance of these materials mainly in a form of polymer waste that accounts for more than one million tonnes per year, also makes their use a sustainable solution, both environmentally and economically [108–113].

The production of **polyethylene** is based on polymerization of ethylene, a gaseous hydrocarbon obtained from atmospheric distillation of crude oil, hence their very simple structure (Figure 2.25). Because of their symmetric molecular structure, they tend to crystallize, therefore polyethylene are semi-crystalline materials with excellent chemical resistance, and good fatigue and wear resistance. Since the crystalline domains are generally more densely packed than the amorphous domains, the density of the polymer is closely related to its degree of crystallinity, which in turn depends on the degree of branching of the polymer chains. Hence, the less the polymer chains are branched, the higher the crystallinity of the polyethylene. Higher crystallinity contributes to hardness, stiffness, chemical and thermal stability, tensile strength, whereas the amorphous portions provide certain elasticity and ductility to the material above glass transition temperature [114].

Several types of polyethylene can be produced with different structure and therefore with different properties. According to their density and structure (branching) polyethylene compounds are divided into two main types of low density polyethylene (LDPE) and high density polyethylene (HDPE), illustrated in Figure 2.25. Both compounds have very different physical properties. While LDPE compounds have lower melting point (typically between 105 to 115°C), high degree of short- and long-chain branching, higher ductility, and better elasticity, HDPE compounds have higher melting

point (typically between 125 to 132°C), tensile strength and low extent of branching, allowing the mostly linear molecules pack together and form the crystal structure [114–116].

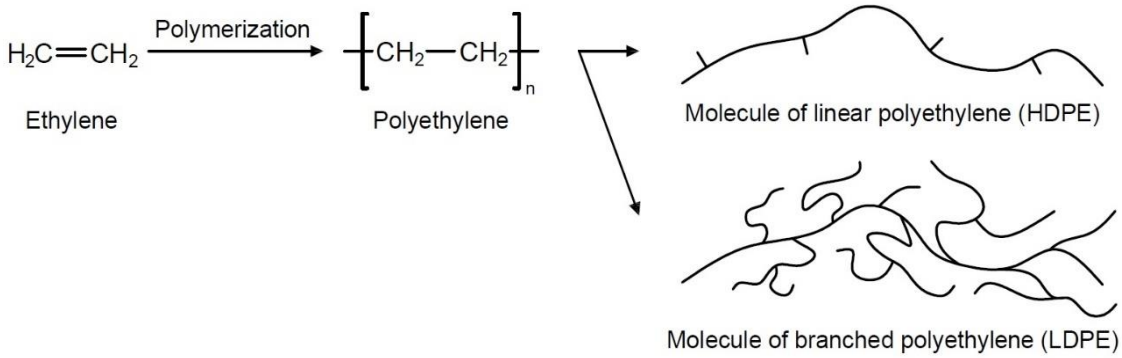

Figure 2.25 Formation of polyethylene from ethylene via polymerization process and its basic types

The second most widely used polyolefin is **polypropylene**. Polypropylene is prepared by polymerizing propylene, another gaseous byproduct of atmospheric distillation of crude oil. Depending on the type of catalyst during polymerization that affect the orientation of the pendant methyl groups attached to the alternate carbon atoms, the polypropylene can be divided into: isotactic, syndiotactic, or atactic (Figure 2.26). Due to the regular, repeating arrangement, isotactic and syndiotactic polypropylene have a high degree of crystallinity.

As far as the degree of crystallinity is concerned, the same applies to the polypropylene as to polyethylene: the higher crystallinity results in better chemical resistance and better mechanical properties such as hardness, stiffness and tensile strength. However, in the case of polypropylene, crystalline and amorphous regions differ only slightly in their density. Due to the presence of the tertiary hydrogen on the carbon atom bonded to the pendant methyl group, polypropylene is more susceptible to oxidation than polyethylene. The melting point of polypropylene varies with the degree of crystallinity. Therefore, perfectly isotactic polypropylene has the highest melting point of about 171°C. Syndiotactic polypropylene with a degree of crystallinity of 30% has a melting point of about 130°C [114,117].

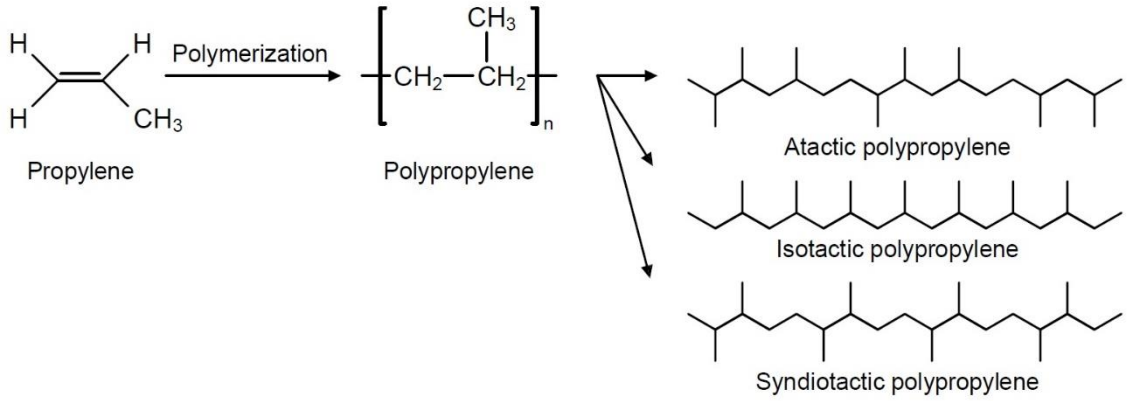

Figure 2.26 Formation of polypropylene from propylene via polymerization process and its basic types

Similar to TPEs, when polyolefins are introduced into asphalt, they become swollen by the light aromatic components from the parent asphalt and a biphasic structure is formed with a polyolefin phase dispersed in an asphalt matrix. Their degree of swelling is usually smaller than those of SBS [118,119], however, similar ones were also reported [120]. Nonetheless, at certain concentration, about 5 to 30 wt.% of polyolefins, phase inversion occurs [118,120,121]. In order to improve the properties of asphalt to some extent, the creation of polymeric 3-D structure in a form of co-continuous morphology of polymer-rich and asphaltene-rich domains is desired for polyolefin modified asphalt. Nevertheless, the presence of weakly bonded polymer-rich domains forming a physical network within the asphaltene-rich continuous phase even at lower polymer content, when the "rigid" polyethylene domains are interconnected through weak polymer chain bridges of different length and strength, was also reported [121].

The addition of polyolefins into asphalt is known to enhance its stiffness, viscosity, fatigue resistance, resistance to deformation, and provide better adhesion between the asphalt and the aggregate. On the other hand, polyolefins fail to significantly improve the elasticity of asphalt [113,115,121–125].

The biggest disadvantage of polyethylene and polypropylene is their non-polar nature, which is the result of the absence of polar atoms (e.g., oxygen, nitrogen) in the polymer. This negatively affects the compatibility of polyolefins with asphalt; hence causes separation of the polymer from the asphalt during hot storage. In addition to this, the regular and long chains of polyolefin materials tend to pack together and crystallize,

which could also lead to separation that further destabilizes the asphalt. This can be partially overcome by choosing the most compatible polymer according to their melt flow index (MFI). It was reported that plastomers with higher MFI (i.e., the higher the MFI, the lower the viscosity) are more compatible with asphalts and indicate better low-temperature performance. However, they enhance to a lesser extent the high-temperature performance of the asphalt. Nevertheless, even by choosing the most compatible polyolefin, separation will occur. Therefore, in the case of polypropylene and polyethylene, storage stability remains the most significant problem to be solved [126,127].

In order to overcome the shortcomings attributed to the non-polar nature of polyolefins, they are frequently modified by polar groups. Good example of such polyethylene based copolymer often used for asphalt modification is **ethylene-vinyl acetate (EVA)**. Ethylene-vinyl acetate is a random copolymer obtained by polymerization of ethylene and a comonomer of vinyl acetate (VA) (Figure 2.27). The insertion of VA is meant to increase the compatibility of polymer with asphalt by increasing the polarity of the polymer chain and reducing its crystallization ability, since it disrupts the closely packed crystalline microstructure of the ethylene-rich segments. This alteration generally results in that EVA copolymers indicate low crystallinity, when compared to polyolefins. Nevertheless, the degree of crystallinity, along with their other properties, are highly dependent on the proportion of the comonomer. In fact, EVA with low content of polar acetate group has similar properties as LDPE. Due to the presence of two monomers in EVA, they tend to form an immiscible two-phase system, similar to that of SBS, with a stiff polyethylene-rich crystalline phase and a rubbery vinyl acetate-rich amorphous phase [70,128,129].

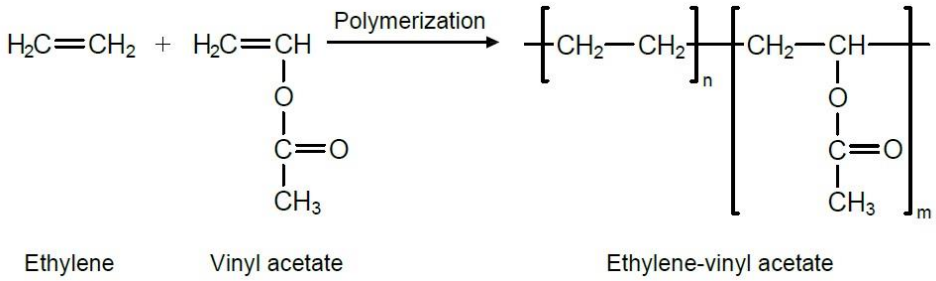

Figure 2.27 Formation of ethylene-vinyl acetate via polymerization process

After EVA copolymers are added into asphalt, similar processes take place as in the case of thermoplastic elastomers, namely, the polymer (more precisely the elastic, asphalt-compatible polar vinyl acetate-rich phase) gets swollen by the light components of the asphalt while forming a relatively stable polymeric 3-D network. Only in this network nodes are formed by crystallization of the ethylene-rich segments in the chains which are interconnected by the elastic acetate-rich segments. Since for asphalt modification neither too low nor too high degree of crystallization is desired, the content of vinyl acetate must be chosen carefully. Too high content of vinyl acetate leads to low crystallinity; therefore, the polymer network becomes easy to disrupt once the few crystallites are disturbed by the insertion of asphalt molecules. On the other hand, when the amount of vinyl acetate in EVA is too low, a reduction of the amorphous phase and a formation of large rigid crystalline PE-rich domains takes place. This directly results in that the polymer loses its flexibility, polarity, swelling ability, and as a consequence of these, its compatibility with the asphalt. In addition, crystallinity has a major effect on the polymers' melting points. The optimal content of vinyl acetate in EVA copolymers, used for asphalt modification, should be in the range from 18 to 28 wt.%. EVA copolymers containing such amount of VA have a melting point about 85 and 69°C, respectively. One of the most interesting features of EVA can be related to its relatively low melting point, namely that above this temperature separation of polymer from the asphalt takes place, leading to a sudden drop in the viscosity and in other rheological properties of the blend. This process is reversible and once the temperature decreases below melting point association and subsequent recrystallization occur [70,128,129].

From the morphological viewpoint, with increasing EVA concentration in the asphalt/polymer blend a gradual change in the two-phase microstructure can be observed. At low EVA concentration, the polymer-rich phase is dispersed in the continuous asphaltene-rich phase. As the EVA concentration increases, at certain point both phases become continuous. At higher concentrations phase inversion occurs and the polymer-rich phase becomes continuous [92,130]. If two interlocked continuous phases form in the asphalt/polymer blend, the properties of modified asphalt could be enhanced to a large extent.

In addition to vinyl acetate content, EVA copolymers are classified according to their melt flow index (MFI). A strong relationship was found between the MFI of EVA copolymers and some of the respective modified binders' properties (e.g., viscosity, stiffness, hardness, and elasticity) at medium-high temperatures (30–75°C). However, in

contrast with PE and PP, no relationship was reported between MFI and the asphalt/polymer morphology expressed in terms of size and distribution of the polymer-rich phases [129].

A great number of researches claim, that the introduction of EVA into asphalt improves its temperature susceptibility and increases its stiffness, therefore it becomes more resistant to permanent deformations [129–136]. Nevertheless, similarly to other plastomers, EVA fails to significantly improve the elasticity of the asphalt binder, and have a tendency to separate from the asphalt [137], although recently, Bulatović *et al.* [138] reported satisfactory hot storage stability results up until 5 wt.% of EVA (Elvax 265, containing 28 wt.% of VA with a MFI of 6 g/10 min). Furthermore, the glass transition temperature of EVA is in the range of that of the asphalt binders' T_g, resulting in that it is not able to improve their low-temperature properties [93].

The abundance of waste plastomers and their ability to enhance certain high- and medium-high temperature properties of asphalt make them cost-effective alternative to more expensive modifiers. Nevertheless, because of their unresolved problems related to low-temperature characteristics and to hot storage stability, more promising polymeric and non-polymeric materials were preferred within the framework of this dissertation.

2.4.3. Reactive elastomeric terpolymer

As it was already mentioned in Chapter 2.4.2, PE-based copolymers, which indicate higher polarity and compatibility with asphalt, can be prepared by addition of polar comonomers to the PE polymer backbone. In the case of EVA, the comonomer is inert with respect to the asphalt, and only increases the polarity of the polymer without being chemically reactive with the asphalt. Another approach is to use functional groups as a comonomer that can bond with the asphalt compounds (supposedly with the asphaltenes) and concurrently is able to enhance the asphalt performance and increase the polymer/asphalt compatibility. As a third option are **reactive elastomeric terpolymers** (also called reactive ethylene terpolymers) **(RET)** which contain both reactive and non-reactive polar groups [70,139].

Examples include ethylene-based copolymers, commercialized as random terpolymers of ethylene, glycidyl methacrylate (GMA) and an ester group, usually methyl, ethyl, or butyl acrylate (Figure 2.28). The epoxy ring of GMA is thought to be able to chemically bond with asphalt and the acrylic ester improves the polymer polarity and

thermal stability, while the main chain provides the flexibility of the macromolecule. Thanks to the presence of the reactive epoxy group in the polymer RETs are often used as compatibilizers for various polymeric blends and act as a crosslinking agents. This is precisely the feature that can be useful for asphalt modification. Therefore, RETs can be used either as asphalt modifiers or as a chemical "bridge" between asphalt and other conventional polymers [139,140].

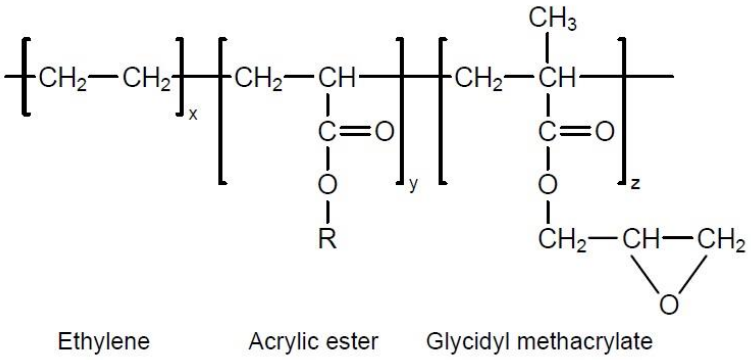

Figure 2.28 Schematic structure of random ethylene terpolymer (RET)

Unfortunately, due to the extremely complex chemical nature of asphalt, it is difficult to determine the character and the real number of chemical bonds formed in the asphalt/RET blend. Nevertheless, it is assumed that during mixing at high temperatures the curing (crosslinking) of the epoxy group is catalyzed by heat resulting in the opening of the epoxy ring. According to the manufacturers, this opened epoxy ring then most likely reacts with the carboxyl groups present in asphaltenes (Figure 2.29), thus forming an ester link between asphalt and polymer. However, other reactions are also possible between the GMA group and the functional groups present in asphalt. Moreover, intermolecular crosslinking between RET molecules can also take place and could lead to the formation of a polymer network not necessarily involving asphalt molecules [139,141].

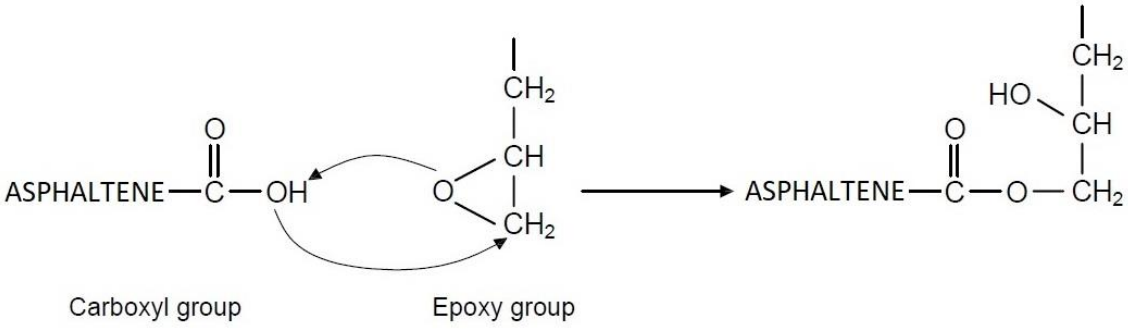

Figure 2.29 The crosslinking reaction of RET with carboxyl group in asphaltene

After mixing with asphalt, in order to complete as many reactions as possible, curing at storage temperature is suggested. Once the reactions are complete, these bonds, and also the highly polar nature of RET, prevent the asphalt/RET blend from phase separation and improve storage stability. Nonetheless, asphalt modification by RET polymers has its limitations. For example, the polymer amount, the curing and mixing time and temperature, must be chosen very carefully because a higher amount (usually more than 2–2.5 wt.%) of RET may cause chemical gelation of the asphalt, a formation of an insoluble, infusible (thermoset) material.

The performance of RET-modified asphalt binders can be significantly enhanced by an addition of polyphosphoric acid (PPA) which has found its success in reducing the risk of gel occurrence [141,142].

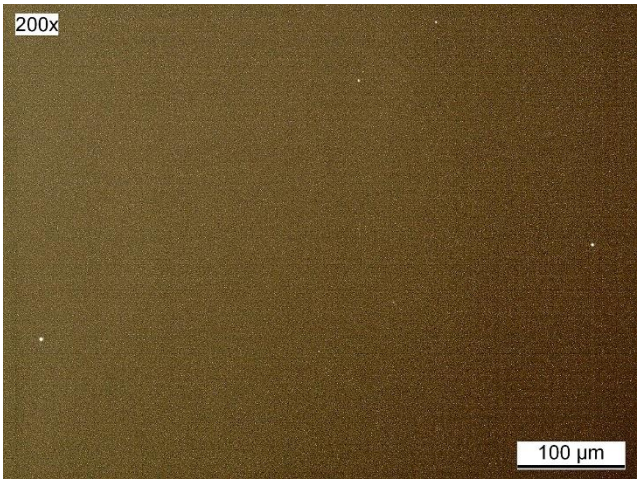

Figure 2.30 Homogenous morphology of 60/70 Pen grade asphalt modified with 2.5 wt.% RET examined by fluorescence light microscopy (FLM), magnification 200x

It was reported in numerous studies that the addition of RET into asphalt results in increase in stiffness and elasticity, and it positively affects the binder's ageing resistance. In addition, the use of RETs lead to a significant improvement in rutting resistance. Generally, RETs tend to increase the high temperature performance without harming the low temperature performances of the asphalt [141–147].

2.4.4. Crumb rubber modifier

The idea of harvesting the flexible nature of recycled tire rubber (RTR) in asphalt pavements is almost as old as the use of vacuum-distilled asphalts for the same purpose and dates back to the beginning of the 20th century. However, the first viable technologies came to light only in the early 1960's. Since then, numerous studies and practical experience revealed that the addition of RTR into asphalt increases the lifespan of the asphalt pavement by increasing its resistance to rutting, to reflective cracking, and fatigue cracking. In addition it can reduce traffic noise, design thickness and life-cycle costs [148–153].

Due to the thermoset (i.e., infusible, insoluble) nature of rubber in tires, first they have to be processed by means of mechanical shredding or chipping. Once the steel and fabric components are removed, the reclaimed rubber is further grinded until the size of the grains are small enough, ranging from about 0.5 to 5 mm, which is more suitable for asphalt modification. Crumb rubber modifier (CRM) is the common name of these size-reduced rubber particles utilized for asphalt modification.

Different types of grinding methods produce rubber particles with different surficial character, which can substantially affect the resulting properties of the CRM-modified asphalt (also called rubberized asphalt). Generally, two main grinding methods are used to reduce RTR: cryogenic and ambient types. In the case of cryogenic grinding the RTR is frozen until it becomes brittle, then shattered with a hammer mill. Ambient grinding is conducted at or above room temperature and is performed by means of rotating blades and knives. Consequently, the shape of the ambient tire powder particles is coarser and more irregular with relatively large surface areas, while the cryogenic tire powder particles possess regular shape with a small surface area (Figure 2.31). When compared to ambient tire powder, cryogenic rubber particles with smooth surface showed reduced reaction with the asphalt; therefore, the use of CRM from cryogenic grinding in asphalt mixtures is not recommended [154–156].

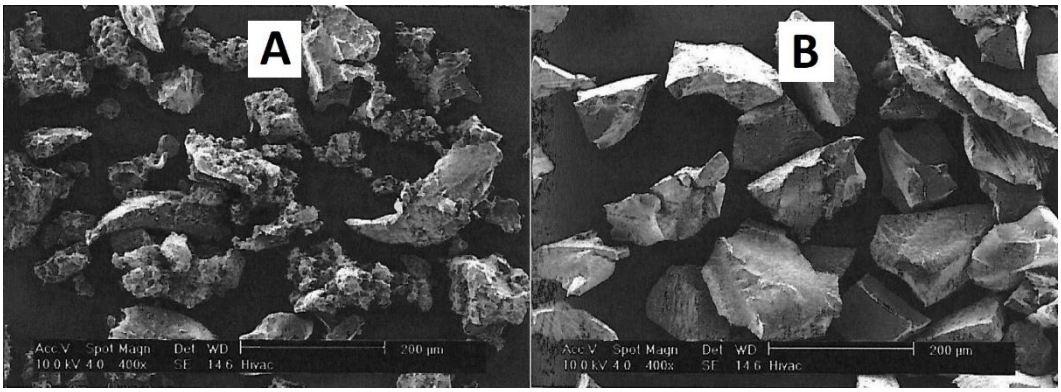

Figure 2.31 Ambient (A) and cryogenic (B) rubber crumbs examined by scanning electron microscopy (SEM), magnification 400x, adapted from [148]

Before the 1960's, rubberized asphalt pavements were often produced by addition of a small quantity of ground rubber of large size (6.3–9.5 mm) to the mineral aggregate mixture where it complemented or replaced part of the job mix formula (JMF). Then, the more successful technology of thoroughly mixing CRM with asphalt for a relatively short period of 45 to 60 min was introduced. The former technology is known as "dry process", while the latter as "wet process". Nonetheless, mainly because of the weak interfacial adhesion between the CRM and asphalt mixture, the dry process has not been widely adopted [157].

During wet process the maltene phase of the asphalt swell the rubber particles over a gradient distribution (i.e., the outer sphere of the rubber particle is more swollen than the inner sphere). Simultaneously, chemical degradation of tire rubber takes place that includes the scission of S-S, C-S and C-C bonds. Therefore, if the temperature is high or the time is long enough, devulcanization and depolymerization will occur. As a result of scission of crosslinked and main chain bonds, partial dissolution of the rubber in the asphalt occurs. Depending on the amount of CRM, the level of swelling, degradation and dissolution, the resulting binder indicate increased viscosity and elasticity. The whole process of swelling and degradation depends on many factors, such as: temperature, time of mixing, particle size, source of CRM, amount of CRM, source of asphalt, processing method, etc. Nevertheless, until crosslinked rubber particles are present in asphalt, the prevention of their separation at high temperature remains a problem that limits the widespread usage of CRM in pavements. However, recent studies have shown that the storage stability of CRM-modified asphalt can be improved by adding substances to attain chemically stabilized blends [158–160], or by mixing it with low percentage of

conventional polymers, with compatibilizer, with sulfur, or with hydrogen peroxide pre-treated CRM particles [148].

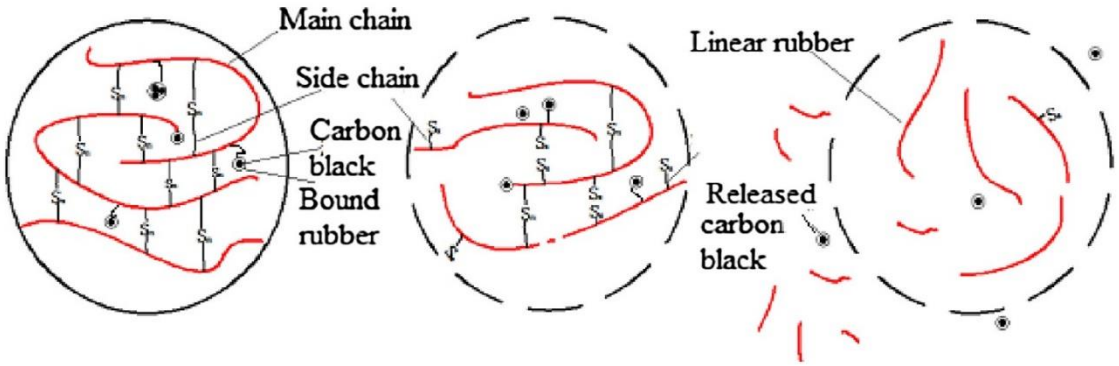

Figure 2.32 Schematic of swelling and degradation of the rubber network, adopted from [157]

The original wet process relies on swelling the rubber particles with the oily fractions of asphalt. Over the interaction period limited in 45 to 60 min the CRM and asphalt are thoroughly mixed together at elevated temperatures between 190 to 218°C. Additionally, at the end of the process the CRM-modified asphalt should maintain or exceed a minimum value of rotational viscosity threshold of 1500 cPs (1.5 Pa.s) at temperature 177°C (or 190°C) in order to achieve the ability that allows great film thickness (better chip retention) in paving mixes without excessive drain down or bleeding. The purpose of this process is to maximize the swelling of the rubber particles, while minimizing their devulcanization and depolymerization which would cause dispersion of the rubber into the asphalt; hence the limited time and temperature values. As a result of swelling, reduction of the oily fraction occurs while the size of the rubber particles increases, and their consistency softens [161]. The reduction of the inter-particle distance allows the formation of gel structures that provide significantly improved engineering properties, such as increased viscosity, elasticity, resistance to permanent deformation and fatigue with little effect on low temperature properties [148].

Cracking resistance at low and intermediate temperatures is one of the biggest advantages of CRM modification. Moreover, CRM-modified asphalts also indicate an outstanding aging resistance during service time [162–164]. However, due to the lack of the reinforcing polymer network, the rutting resistance of CRM-modified asphalt is not as high as it is in the case of typical polymer modified asphalts. Besides that, in CRM-

modified asphalt polymer contacting network is formed by the swelling of rubber. In order to overcome this problem, more often conventional polymer modifiers (e.g., SBS, PE, etc.) are added to the CRM-modified asphalt. These composite-modified asphalts indicate an improved resistance to permanent deformation or rutting along with better hot storage stability [165,166].

As an alternative to all the technologies mentioned above, another form of the wet process has been introduced in the USA that significantly enhance the hot storage stability of CRM-modified asphalt blends. In this process CRM and asphalt are blended at elevated temperatures (between 200 to 300°C) and at high shear stresses in the order of few thousands RPM. In contrast to the ordinary wet process, the goal of this technology is to replace the characteristic swelling by devulcanization/depolymerization and leave the CRM being digested into the asphalt, resulting in a smooth, homogenous product. However, the depolymerization and the subsequent release of rubber components into the asphalt cause a decrease in stiffness, viscosity, and elasticity of the CRM/asphalt blend; thus, the effect of the modification is significantly reduced. Nonetheless, this process allows the addition of more CRM to the blend (~25 wt.% or even more ~30 wt.% [167]) than in the original wet process (≤10 wt.%), although careful selection of the blend components is prerequisite for high level of solubilization of the CRM within the bitumen matrix (explained below). Depending on the presence of stabilizing additives in the blend (e.g., calcium hydroxide), similar concentrations of CRM (i.e., 5–25 wt.%) are recommended in the Czech standards as well, while the mixing temperature usually ranges between 170 to 185°C [168,169].

CRM is a complex mixture of different materials, mainly consisting of natural rubber (NR) and synthetic rubber (SR), which are crosslinked with sulfurs and reinforced with carbon black (CB) or silica. Depending on the source of the RTR, the content of these materials varies from CRM to CRM. While truck tire rubbers mainly consist of NR, which are more prone to degradation, passenger tire rubbers primarily consist of synthetic rubbers (e.g., butadiene rubber (BR), styrene butadiene rubber (SBR)). It was shown that at high shearing NR starts to degrade at 180°C, whereas the degradation rate of SR sharply increases only at 240°C [170]. Therefore, CRM produced from passenger car tire rubbers indicate lower susceptibility to high temperatures and to degradation [157,171].

Furthermore, the swelling/degradation rate and ratio depend on the size of the CRM particles as well, as on the composition of the base asphalt. The added rubber can dissolve more in asphalt binders with lower viscosity (higher aromatic content). It was also shown

that finer rubber particles swell and dissolve faster. Small particles also positively influence the hot storage stability of the CRM-modified asphalt. Nevertheless, coarse particles are more prone to form an elastic skeleton in the mixture that can provide better elasticity to the resulting pavement, although these materials require an accurate blend design and continuous agitation during hot storage to prevent the RTR particles from separation (Figure 2.33) [172].

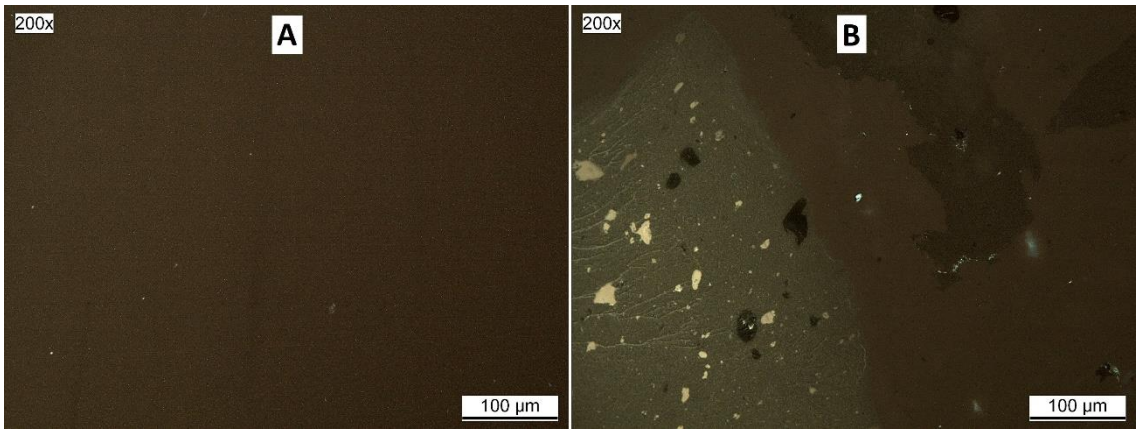

Figure 2.33 Phase separation of 60/70 Pen grade asphalt base modified with 20-mesh (0.841 mm) CRM during hot storage (A) – TOP, (B) – BOTTOM, examined by fluorescence light microscopy (FLM), magnification 200x

2.4.5. Other chemical modifiers

The use of **polyphosphoric acid (PPA)** as an asphalt modifier was first reported in the USA at the beginning of the 1970s [173]. The primary objective of adding PPA to asphalt was to increase the viscosity of asphalt without significantly altering its penetration in order to provide a paving asphalt binder with improved temperature susceptibility characteristics [174].

PPA is a liquid mineral polymer with high viscosity at ambient temperatures. There are two commercial methods for preparation of PPA and both use phosphoric acid (H_3PO_4), also known as orthophosphoric or monophosphoric acid, as a basic compound for the synthesis. The pure compound of orthophosphoric acid is a colorless solid, however, it is normally encountered as an aqueous solution, which is a colorless, odorless, and non-volatile syrupy liquid, with maximum water concentration of 85–90%.

According to the first method, phosphoric acid is dehydrated at high temperatures while two or more phosphoric acid molecules join into large molecules and convert into

pyrophosphoric ($H_4P_2O_7$), triphosphoric ($H_5P_3O_{10}$), tetraphosphoric acid ($H_6P_4O_{13}$), etc. leading to the final stage of condensation and formation of PPA with general formula $H_{n+2}P_nO_{3n+1}$. When using the second method, phosphorus pentoxide (P_2O_5) dispersed in H_3PO_4 is heated in order to yield PPA. The dispersion method usually produces highly polymerized products with more than 10 repeat units, whereas the dehydration method tends to produce PPA with short chains [175].

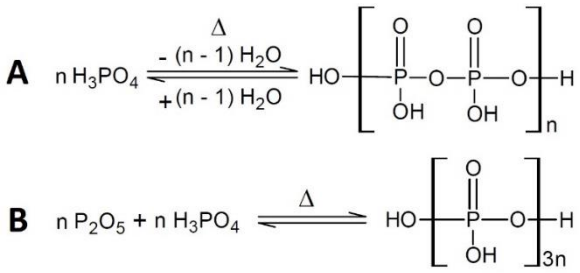

Figure 2.34 Production of PPA using the dehydration (A) and dispersion (B) method (*n* is an integer), adopted from [175]

The number of repeat units in the PPA chain varies from one molecule to another within the end-product. For example, it was shown that 100% phosphoric acid is a mixture of orthophosphoric (H_3PO_4) and pyrophosphoric acid ($H_4P_2O_7$) in a ration 1:9. As a result, PPA grades can be characterized by the distribution of their chain lengths present in the substance. Figure 2.35 presents the distribution of chain lengths for three common commercial grades used for asphalt modification. Typically, PPAs with higher grade are more viscous, which can be explained by the chain entanglements caused by the elongation of the molecular chains [175].

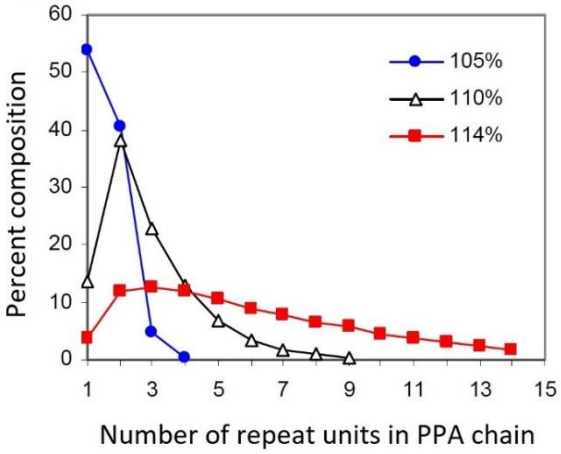

Figure 2.35 Distribution of chain lengths in three PPA grades, adopted from [175]

Generally, polyphosphoric acids are widely used in organic chemistry as a reagent for numerous organic synthesis. It is precisely this reactive nature that has triggered the idea of introducing PPA into asphalt. Furthermore, the fact that is does not contain any free water also makes it suitable for asphalt modification. Prior to this, phosphorous compounds (P_2O_5 and H_3PO_4) and PPA were in asphalt industry utilized as catalysts in the production of air blown asphalts, whereas PPA has been used for this purpose ever since [176].

Although it is generally recognized that PPA reacts with asphalt, due to the extreme complexity of asphalt the exact nature of the reactions is not completely understood. As it was discussed in Chapter 2.3, asphaltenes consist of complex polyaromatic compounds aggregated together showing a lamellar structure. The degree of association is controlled by the polarity of each components through weak hydrogen bonding. It has been suggested that PPA acts through the neutralization of polar interactions between the stacked asphaltene molecules, resulting in their de-agglomeration. The reduction of micellar aggregate size directly cause an increase in the surface to volume ratio that alters the original colloidal equilibrium which in turn increases the viscosity of asphalt by tilting the colloidal balance towards the gel character [7,141,175,177]. However, this theory does not justify the decrease in saturates, which is also a characteristic accompanying phenomenon of PPA-modification. Therefore, other modification mechanisms have been proposed, which also take into account the probable effect of PPA-modification on the lower weight components present in asphalt: co-polymerization of saturates, alkyl aromatization of the saturates, crosslinking of neighboring asphalt segments, formation of ionic clusters, cyclisation of alkyl-aromatics, generic reaction with asphaltenes, etc [174]. Regardless of the reaction mechanism, PPA-modification alters the solvation of the asphaltenes and increase their effective volume, causing an increase in viscosity. Its effect is somehow comparable to those obtained with air-blowing, except that the resulting material lacks the fragility problem of air-blown asphalts [7,141].

Modification of asphalt with PPA leads to higher softening point, increase in viscosity, and a slight increase or no change in penetration. In terms of rheology the addition of PPA to asphalts does not provide any elastic properties to the blend, but it enhances the high-temperature performance of the asphalt without significantly affecting the low-temperature performance. Moreover, studies have shown that PPA can be used as a partial substitute of the polymer to obtain PMAs with the same performance grade only at lower polymer content [149,177–180].

Among the broad range of polymer modifiers, PPA proved to be beneficial in combination with SBS, reactive ethylene terpolymers (e.g., Elvaloy™), and even with CRM. When PPA is added to SBS-modified asphalts it increases their high-temperature performance while concurrently improves their mixing and compaction characteristics [179–181]. With reactive ethylene terpolymers (RET), it most probably catalyzes the reactivity of the glycidyl methacrylate groups and reduces the reaction time from one day to hours. Furthermore, RET combined with PPA indicate substantially better high-temperature performance than alone [180–182]. Although the addition of PPA to CRM-modified asphalt does not seem solve the storage stability problems typical for these blends, it can improve their mixing and compaction characteristics while increasing their high-temperature performance [38,157,183,184].

Due to its positive effect on the properties of asphalt, **sulfur** was found to be successful in asphalt modification. The most common allotrope of sulfur form cyclic octatomic molecules with a chemical formula of S_8. Elemental sulfur at ambient temperatures forms a bright yellow, somewhat transparent crystal. Above its melting point (~115°C) sulfur becomes a viscous liquid of red color, containing polymerized molecules of S_8. Above its boiling point (~444°C) a complete depolymerization of macromolecules occurs, which is accompanied by a decrease in viscosity of the resulting liquid [141].

Sulfur remained the most widely used vulcanizing agent of unsaturated rubbers since its capability of interaction with C=C double bonds was discovered at end of 19th century. This ability proved to be useful in improving the storage stability of natural and synthetic rubber-modified asphalt. Nevertheless, the positive effects of sulfur on the asphalt binders' properties was well known even before the appearance of the first synthetic polymers. Therefore, a distinction should be made between sulfur extended asphalt binders (sulfur used as an independent modifier) and polymer modified binders in which sulfur has a role of a crosslinking agent [141].

The addition of sulfur as an independent modifier into asphalt is generally considered since the beginning of the 20th century. The primary objective of the use of sulfur in asphalt was to increase their ductility. Nowadays, asphalt binders containing large quantities of added sulfur (≥20 wt.%) are commonly known as "sulfur extended asphalts". Part of the added sulfur dissolves and chemically reacts with asphalt, modifying the asphalt properties by lowering the viscosity and increasing the ductility. However,

above a certain concentration the remaining part of the sulfur crystallizes and acts as a structuring agent (Figure 2.36) in asphalt when the mixture cools [38,141].

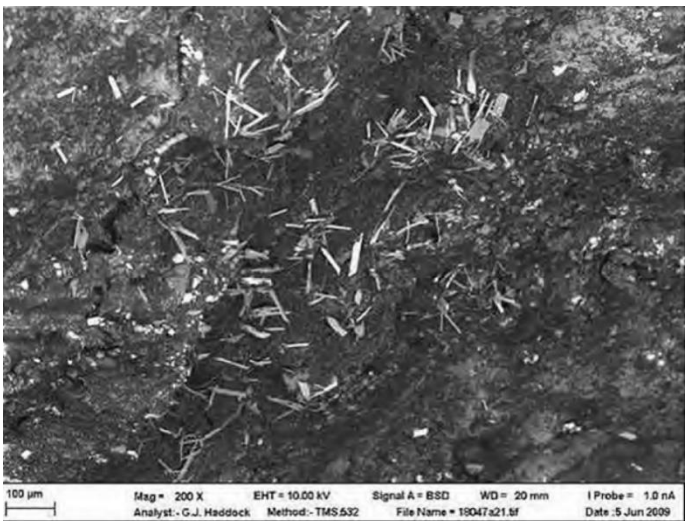

Figure 2.36 Sulfur-modified asphalt with crystallized sulfur structures examined by scanning electron microscopy (SEM), magnification 200x, adopted from [38]

According to the mixing temperatures, sulfur reacts differently with the asphalt components. For example, hydrogenation may occur at mixing temperatures lower than 140°C which may result in a formation of poisonous and flammable gases (e.g., hydrogen sulfide). However, at much higher temperatures the formation of C-S bonds within aromatic and naphthenic components may unfavorably alter the colloidal structure of the blend. Therefore, the optimum content of sulfur is thought to be in the range from 20 to 30 wt.% and the blending/mixing temperatures not higher than 150°C [38,141].

Although sulfur-modified asphalts indicate better mechanical properties and, when compared to conventional asphalts, are generally more workable during paving (lower compaction temperatures), the evolution of hazardous gases during mixing, or in case the asphalt is exposed to naked flame, remain an unresolved problem [38].

Sulfur vulcanization is a chemical process that plays a key role in converting the plastic blend of natural or synthetic rubber into the final elastic product of various hardness, elasticity, and mechanical durability. It was shown that similar crosslinking process takes place in polymer modified asphalt when sulfur is added into the blend. It is believed that sulfur is able to form crosslinking bridges between polymer chains and couple polymer and asphalt through sulfide and/or polysulfide bonds [185]. These chemical crosslinks are much stronger than the physical ones (e.g., the self-agglomerate

crystalline hard domains of PS blocks in SBS copolymers) resulting in that they are more successful in stabilizing the 3-D polymer network in the asphalt matrix even at high temperatures. The network stabilizing along with the coupling between polymer and asphalt prevent the polymer phase from separation while increasing the hot storage stability of the blend.

From all the unsaturated polymer modifiers SBS proved to be a good candidate for sulfur vulcanization. The addition of sulfur in order to vulcanize asphalt blends containing dispersed particles of unsaturated SBS not only stabilized the 3-D polymer network but also improved the PMBs elasticity, resistance to permanent deformations, and other thermo-rheological properties [79,185–187].

Nonetheless, sulfur should be added only after the polymer has attained good dispersion and swelling because it would otherwise freeze the morphology at an earlier stage, resulting in a useless material. Even though, vulcanized SBS-modified asphalt showed exceptional thermo-rheological properties, they indicate higher susceptibility to oxidative ageing and poor recyclability. Furthermore, due to the abstraction of hydrogen atoms in both asphalt and polymer modifiers, undesired formation of hydrogen sulfide may occur [188,189].

2.5. Rheological aspect

Due to the complex internal structure of asphalts that varies quite significantly from one asphalt to another, which is further complicated by the introduction of polymer modifiers, one may find it difficult to predict their future behavior in pavements only by evaluating their chemical and internal structure. In addition, the service behavior of asphalt pavements is closely linked to the mechanical properties of the asphalt binder they contain. Therefore, in order to understand the behavior of asphalt pavements during their service time the determination of the thermo-mechanical properties of their respective asphalt binder under different traffic-related stresses at wide range of temperatures is of great importance.

Asphalt binders beneath their glass transition temperature, T_g, (about –20°C), tend to behave like an elastic solid, while at elevated temperatures like Newtonian fluid (usually above 60°C, for modified asphalts even higher). In between the two extremes, they behave as viscoelastic materials. Moreover, their consistency and mechanical properties in this viscoelastic range vary not only with changing temperatures, but also

with changing stress rates and levels. Rheology, as a study of the flow and deformation of time-temperature dependent materials under the influence of stresses proved to be a useful tool in their characterization. The rheological behavior of materials can be regarded as being between two extremes: ideal elastic behavior and ideal viscous behavior. A short overview and background of the rheological theories is given in this chapter.

2.5.1. Elasticity

Generally, in rheology, the properties of materials are described by the relations between the stress and deformation tensors or their time derivates. In this brief overview the tensorial character of the time-dependent shear strain, $\gamma_{12}(t)$, and shear stress, $\tau_{12}(t)$, are disregarded and simply called strain, γ, and stress, τ.

If the material shows an ideal elastic behavior, during deformation it accumulates the energy of loading in the form of elastic energy which can be completely recovered once the loading force is removed and the material regained its undeformed state. This is an ideal behavior without any energy dissipation and the magnitude of the stress is always directly proportional to strain but independent of the rate of strain. Such material is called "ideal elastic solid" and described for the uniaxial stress by the Hooke's law

$$\sigma = E\varepsilon \tag{2.2}$$

where σ is the tensile stress and ε is the tensile strain. The constant of proportionality E is called Young's modulus. However, the rheological properties of asphalt binders are often defined by their mechanical performance under shearing, the deformation of a solid when it experiences a force parallel to one of its surfaces while its opposite face experiences an opposing force (such as friction). Consequently, Hooke's law in the case of simple shear can be written as follows

$$\tau = G\gamma \tag{2.3}$$

where τ is the shear stress, γ is the shear strain and G is the shear modulus of rigidity [190].

Another way to describe elastic behavior is to specify the strain that results from the application of specific stress. In the case of ideal elastic solid, the strains appear at the moment the stress is applied, without any time delay, therefore the strain can be written as

$$\gamma = J\tau \tag{2.4}$$

where J is the shear compliance. Therefore, the following simplified relation applies to an ideal elastic solid that follows Hooke's law

$$J = 1/G \tag{2.5}$$

Within the framework of rheology mechanical models are put to use in order to describe the behavior of different materials. In these mechanical models, the ideal elastic deformation is represented by the Hookean spring which is characterized by the proportionality constant of shear modulus, G. The ideal response of such material is plotted in Figure 2.37.

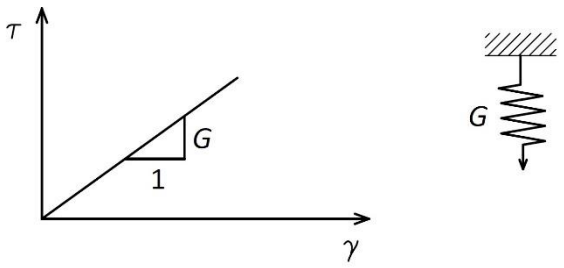

Figure 2.37 Diagrammatic representation of a Hookean material and its ideal response to shear strain

2.5.2. Viscosity

Viscosity of a material is a measure of its resistance to continuous deformation. In accordance with Newton's law, an ideal viscous material can be defined as a material in which stress is directly proportional to the rate of strain (i.e., change in strain) but independent of the strain itself. Thus, the following equation can be written

$$\tau = \eta\dot{\gamma} = \eta\frac{d\gamma}{dt} \tag{2.6}$$

where τ is the shear stress, η is the shear viscosity and $\dot{\gamma}$ the shear rate. Materials following this law are called "Newtonian fluids" [190]. The viscosity of Newtonian fluids is constant, and its value does not change with changing rate or magnitude of strain. They do not exhibit any preferred shape and all the energy invested in the deformation process is completely dissipated in the form of heat. The simple mechanical analogue of the Newtonian fluid is a dashpot, which is characterized by the proportionality constant of viscosity, η. The ideal response of a completely viscous material is plotted in Figure 2.38.

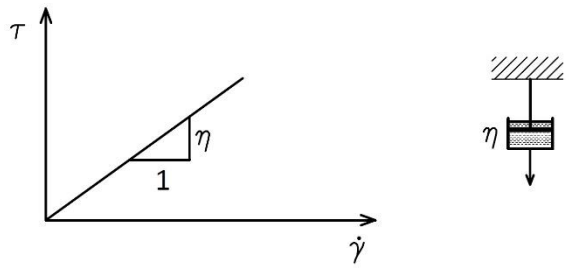

Figure 2.38 Diagrammatic representation of a Newtonian fluid and its ideal response to constant shear rate

However, many materials are non-Newtonian, and exhibit different shear dependent viscosity under various shear rates. They can be classified in several ways, depending on how they deviate from ideal behavior. Some of these deviations are illustrated in Figure 2.39.

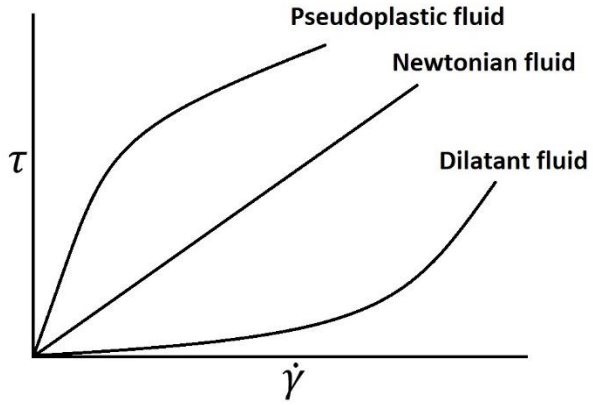

Figure 2.39 Newtonian and non-Newtonian behavior of materials

Pseudoplastic fluids get thinner as the shear rates increase (shear-thinning), dilatant fluids increase their viscosity as shear rates increase (shear-thickening). The rheological behavior of asphalt binders can change from pseudoplastic to Newtonian and to dilatant as the shear stress is increased, as it is illustrated in Figure 2.40. Nonetheless, conventional rheological tests are usually not conducted throughout a sufficiently wide range of shear rate to identify these kinds of changes in rheological behavior [191].

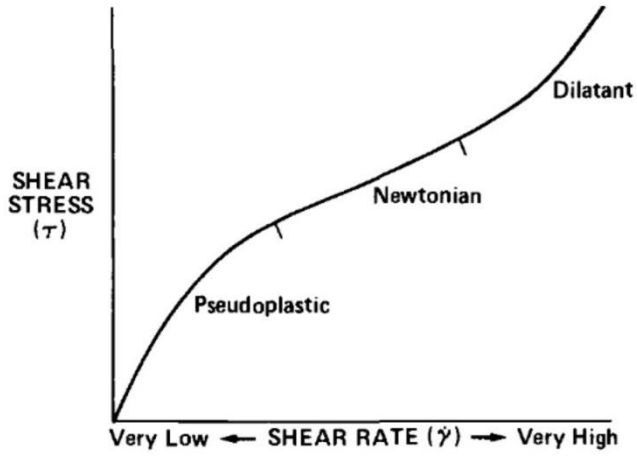

Figure 2.40 Hypothetical behavioral changes of asphalt binders, adapted from [191]

2.5.3. Viscoelasticity – Basic mechanical models

The categories of Hookean solid and Newtonian fluid are rather idealizations, even though it can be assumed, that the behavior of many solids approaches Hooke's law for a certain magnitude of strain, and the behavior of many liquids approaches Newton's law at certain rates of strain. Nonetheless, real materials, under real conditions simultaneously exhibit both viscous and elastic behavior, i.e., viscoelastic behavior. Therefore, in the case of viscoelastic materials the mechanical energy that results in generated deformation is partially stored and partially dissipated in a form of heat [190].

Viscoelastic materials can be represented by the combination of the two basic mechanical elements of elastic spring and viscous dashpot either in parallel or in series (Figure 2.41). The overall system of these one-dimensional mechanical models behaves analogously to the real material.

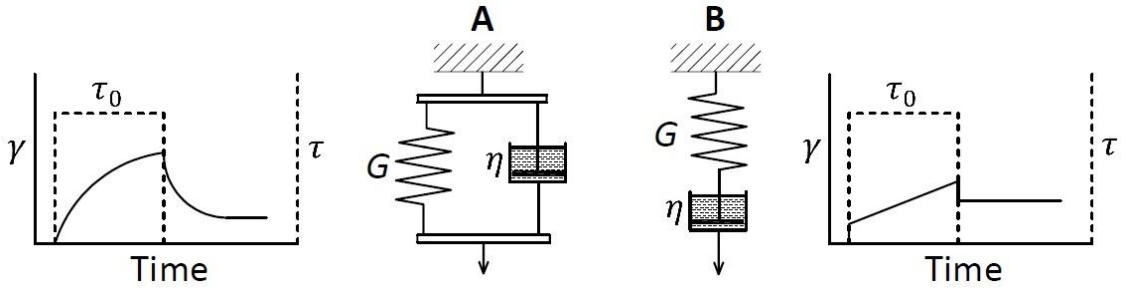

Figure 2.41 The simplest linear viscoelastic models and their creep behavior under constant shear stress τ_0: Voigt-Kelvin unit (A) and Maxwell unit (B)

The combination of the two basic elements in parallel, called the **Voigt-Kelvin model** or simply **Voigt model** (Figure 2.41A), results in the simplest representation of a viscoelastic solid (see Chapter 2.5.6). It is an important building block in other, more complex models where it is referred to as *Voigt unit*. According to this model, equilibrium requires that the extension (strain) in the spring is equal to the extension in the dashpot, therefore the total stress is equal to the sum of the stresses in each element. Thus, the resulting balance equation for the stress is as follows

$$\tau = \tau_e + \tau_v \tag{2.7}$$

where τ is the total shear stress, τ_e is the elastic shear stress (spring) and τ_v is the viscous shear stress (dashpot). By using Equation (2.3) and Equation (2.6) we get

$$\tau = G\gamma + \eta\dot{\gamma} = G\gamma + \eta\frac{d\gamma}{dt} \tag{2.8}$$

It is easy to see, that after sudden application of the shear stress, the dashpot will retard the growth of the strain until the whole system reaches the maximum strain given by the spring, τ/G, hence its viscoelastic solid behavior.

The next simple one-dimensional mechanical model of viscoelastic materials is when two single elastic and viscous element are connected in series. This model is the simplest representation of a viscoelastic liquid (see Chapter 2.5.6), and it is called **Maxwell model** (Figure 2.41B). Analogously to the Voigt model, the stress in the spring is equal to the stress in the dashpot, and the total extension (strain) is equal to the sum of the strains in each element. Therefore, the resulting balance equation for the strains is as follows

$$\gamma = \gamma_e + \gamma_v \tag{2.9}$$

where γ is the total shear strain, γ_e is the shear strain on the elastic element (spring) and γ_v is the shear strain on the viscous element (dashpot). To eliminate γ_e and γ_v Equation (2.9) needs to be differentiated. Thus, for the rate of strain can be written

$$\dot{\gamma} = \dot{\gamma}_e + \dot{\gamma}_v \tag{2.10}$$

By substituting Equation (2.6) and the time derivate of Equation (2.3) and knowing that $\tau = \tau_e = \tau_v$ we get

$$\dot{\gamma} = \frac{\dot{\tau}_e}{G} + \frac{\tau_v}{\eta} = \frac{\dot{\tau}}{G} + \frac{\tau}{\eta} \tag{2.11}$$

Similar to the Voigt model, the Maxwell model does not, by itself, satisfactorily represent viscoelastic behavior, but it serves as an important building block in more complex models where it is generally called *Maxwell unit*.

A viscoelastic material shows both retardation of strain (i.e., creep), and relaxation of stress depending on the type of excitation. The two phenomena are simply dual expression of the fact that the intermolecular configurations require time to rearrange. Creep deformation takes place, when sudden stress is applied on the tested material, while relaxation occurs when sudden strain is applied on the relaxed material (more about creep experiment in Chapter 2.5.6) [190].

Voigt unit is capable of expressing strain retardation, but it cannot express stress relaxation, and the opposite is true for the Maxwell unit. In more complex models the introduction of *relaxation time*, λ, for Maxwell units and *retardation time*, Λ, for Voigt units gives us another useful tool for better understanding the behavior of the viscoelastic materials.

In the following section the differences between retardation time and relaxation time will be explained briefly on two experiments:
Retardation time, Λ – excitation of the Voigt unit by sudden constant stress
Relaxation time, λ – excitation of the Maxwell unit by sudden constant strain

Solving the first order non-homogenous differential Equation (2.11) with the initial condition $\gamma(0) = 0$ gives

$$\gamma(t) = \frac{\tau_0}{G}\left(1 - e^{-\left(\frac{G}{\eta}\right)t}\right) \tag{2.12}$$

where the parameter η/G is called the *retardation time*, Λ, of the material and is a measure of the time taken for creep strain to accumulate. In other words, it is the time required for the Voigt unit to deform to ~63% (or $1 - 1/e$) of its total deformation. Therefore, the shorter the retardation time, the more rapid the creep straining is [192,193]. For the strain as a function of any given loading time when a constant stress of magnitude, τ_0, is imposed, we get

$$\gamma(t) = \frac{\tau_0}{G}\left(1 - e^{-\frac{t}{\Lambda}}\right) \tag{2.13}$$

and for the creep compliance function, where $J(t) = \gamma(t)/\tau_0$ from Equation (2.4) and Equation (2.5), we get

$$J(t) = \frac{1}{G}\left(1 - e^{-\frac{t}{\Lambda}}\right) = J\left(1 - e^{-\frac{t}{\Lambda}}\right) \tag{2.14}$$

From Equation (2.13) is apparent that if $t \to \infty$ the maximum strain is $\gamma_{max} = \tau_0/G$. Therefore

$$\gamma(t) = \gamma_{max}\left(1 - e^{-\frac{t}{\Lambda}}\right) \tag{2.15}$$

According to the Equation (2.15) the strain, developed in a Voigt unit upon application of a constant stress, reaches its final value only at infinite time (Figure 2.42A). For an ideal elastic material retardation time is zero $\Lambda \to 0$, i.e., no retardation is present in the system and the strain approaches its maximum immediately.

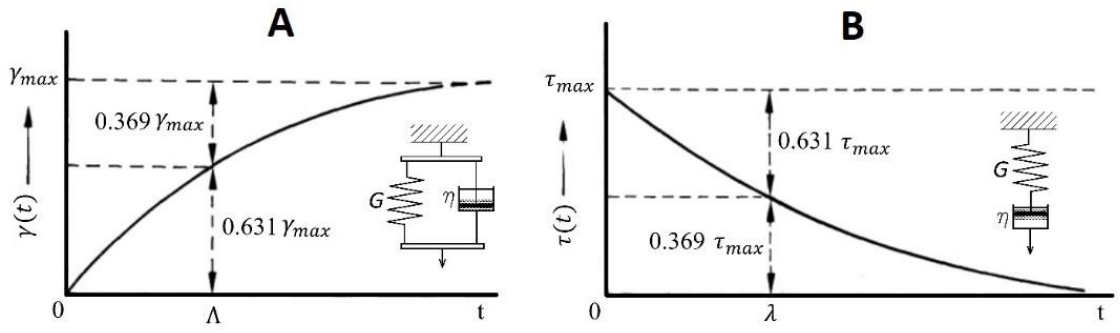

Figure 2.42 Strain response to step stress (A) and stress response to step strain (B)

Turning now to the Maxwell unit, the relaxation time is also given as

$$\lambda = \eta/G \tag{2.16}$$

Without going into the details, the function of stress in a Maxwell unit upon imposition of a constant strain of magnitude γ_0 can be expressed by solving Equation (2.11) and by substituting Equation (2.16) we get

$$\tau(t) = \gamma_0 G e^{-\frac{t}{\lambda}} \tag{2.17}$$

From Equation (2.17) is apparent that the stress induced in a Maxwell unit upon application of constant strain relaxes with time, and at loading times sufficiently long $t \to \infty$ the stress will reach zero (Figure 2.42B). In other words, when the Maxwell unit is subjected to a strain γ_0, the spring will stretch immediately, while the dashpot will take time to react by relaxing the stress in the unit. In an ideal elastic material $\lambda \to \infty$ the stress

would stay constant, i.e., the stress would take an infinite time to relax. With the initial (maximum) value of stress $\tau_{max} = \gamma_0 G$ at $t = 0$ the Equation (2.17) is therefore:

$$\tau(t) = \tau_{max} e^{-\frac{t}{\lambda}} \tag{2.18}$$

2.5.4. Advanced mechanical models

As it was stated in Chapter 2.5.3 the Voigt and Maxwell units cannot represent viscoelastic materials adequately and both are limited to express either stress relaxation (Maxwell unit) or strain retardation (Voigt unit). The addition of two or more Voigt units in parallel would not change the nature of the model's behavior, only alter its parameters. The same applies to the Maxwell units, only in series. Therefore, Maxwell units are always in parallel with each other, or with an isolated spring or dashpot, while the Voigt units are always in series with each other, or with an isolated spring or dashpot [194].

Even though the combination of these basic units is only limited by their position relative to each other, Roscoe [195] showed that all models, irrespective of their complexity, can be reduced to two canonical forms.

By adding a finite but large number, N, or an infinite number of Maxwell elements in parallel we obtain the **generalized Maxwell model** shown in Figure 2.43. The generalized Maxwell model sufficiently represents the linear viscoelastic behavior of a viscoelastic liquid. In order to obtain a model that also represents viscoelastic solid an extra isolated spring must be added in parallel to the model [194,196].

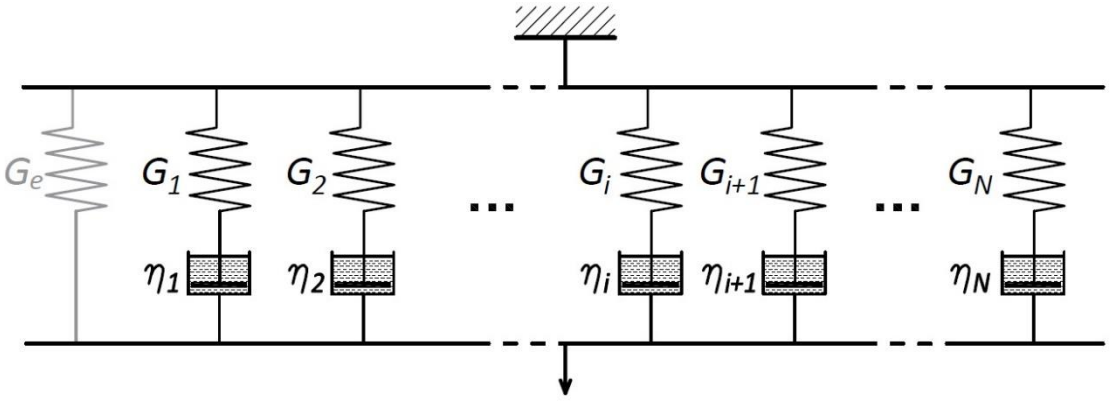

Figure 2.43 Generalized Maxwell model

Each dashpot element is assigned a viscosity, η_i, and each spring element is assigned a shear modulus contribution, G_i, i.e., there are N pairs of material constants.

When the generalized Maxwell model is subjected to shear relaxation experiment, as it is depicted in Figure 2.42B, the force on each unit relaxes exponentially in accordance with Equation (2.17) for each ith pair. Thus, in simple shear the relaxation modulus for the whole model is

$$G(t) = \frac{\tau(t)}{\gamma_0} = G_e + \sum_{i=1}^{N} G_i e^{-\frac{t}{\lambda_i}} \tag{2.19}$$

where the relaxation times, λ_i, are defined as η_i/G_i. For viscoelastic solid a further Maxwell unit with an infinite relaxation time ($\lambda_i \to \infty, \eta_i \to \infty$) and with a corresponding relaxation modulus, G_e, needs to be added. The set of N pairs $\{G_i, \lambda_i\}_{i=1,2,\dots,N}$ is called the discrete relaxation spectrum of the material [194,196].

The mechanical analogue for the **generalized Voigt model** can be obtained (Figure 2.44) by the addition of finite number, N, or an infinite number of Voigt units in series. When the generalized Voigt model is subjected to constant load, analogously to creep experiment, illustrated in Figure 2.42A, the strains developed on each ith unit accumulate; thus in accordance with the Equations(2.12),(2.13), and (2.14) the shear creep compliance of generalized Voigt model for a viscoelastic liquid is as follows

$$J(t) = \sum_{i=1}^{N} J_i \left(1 - e^{-\frac{t}{\Lambda_i}}\right) + \frac{t}{\eta_0} \tag{2.20}$$

where retardation times, Λ_i, are defined as η_i/G_i. If one is to describe a viscoelastic solid the term t/η_0 can be omitted. The set of N pairs $\{G_i, \Lambda_i\}_{i=1,2,\dots,N}$ is called the discrete retardation spectrum of the material constants [194,196].

If the number of elements is increased without limit (i.e., $N \to \infty$) continuous functions, called the continuous relaxation or retardation spectrum (not part of the thesis), can be obtained.

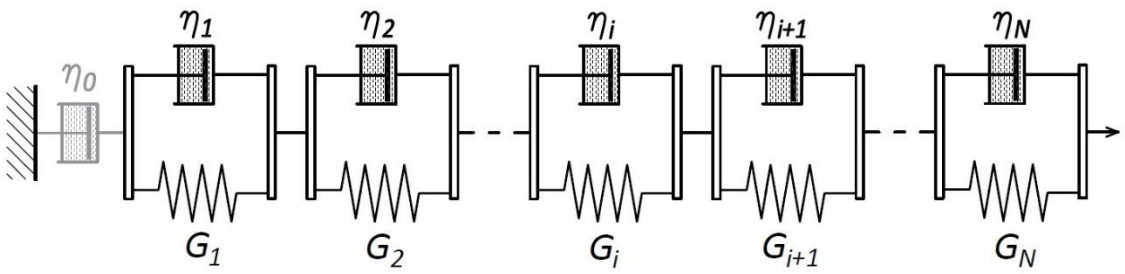

Figure 2.44 Generalized Voigt model

2.5.5. Linear viscoelasticity

Since viscoelastic materials indicate different stress-strain relationship at different rates of straining, it can be concluded that their mechanical properties depend on time, i.e., on the speed of deformation. Consequently, the relations between stress and strain or rate of strain of viscoelastic materials cannot be expressed by material constants as in the case of ideally elastic or ideally viscous materials, and their behavior is rather characterized by time-dependent material functions. There are many books and papers on the basic linear viscoelasticity. One of the best is the classic book by Ferry [196] that was used as the theoretical basis in this thesis.

Generally, the linear viscoelastic behavior is observed when the deformation is sufficiently small and slow. In other words, when both strain and rate of strain are infinitesimal then the time-dependent stress-strain relations are linear [194]. An additional condition of the theory of linear viscoelasticity is that the present state of a material depends on the history of deformation or stressing. According to the Boltzmann superposition principle the effects of mechanical history are linearly additive, where the stress is described as a function of rate of strain history or alternatively the strain is described as a function of the history of rate of change of stress [196].

The following linear constitutive equation represents the mathematical form of the superposition principle

$$\tau_{21}(t) = \int_{-\infty}^{t} G(t - t')\, \dot{\gamma}_{21}(t')dt' \tag{2.21}$$

and can be read as: the shear stress at present time, t, under an arbitrary shear strain rate history is a linear superposition (integral sum) of all rates of shear strain, $\dot{\gamma}_{21} = \partial\gamma_{21}/\partial t'$, applied at previous times, t', multiplied by the values of a characteristic material function, called the relaxation modulus, $G(t)$, corresponding to the time intervals $(t - t')$ which have elapsed since the start of deformation, t', up to the current time, t [196].

An alternative constitutive equation can be written for strain as a function of the history of the time derivate of the stress

$$\gamma_{21}(t) = \int_{-\infty}^{t} J(t - t')\, \dot{\tau}_{21}(t')dt' \tag{2.22}$$

where $\dot{\tau}_{21} = \partial\tau_{21}/\partial t'$ and $J(t)$ is called the shear (creep) compliance [196].

Lot of information can be obtained about the materials from the measurements of linear viscoelastic properties which may help to understand the nature and the rates of

configurational rearrangements, and the interaction of the macromolecules present in modified asphalt and most importantly in polymer modified asphalt [196].

2.5.6. Time-dependent linear viscoelastic material functions

There are several ways to measure linear viscoelastic response. One of the simplest is the **creep testing** (Figure 2.45), briefly discussed in Chapter 2.5.3. In this experiment a sudden shear stress is applied within a very short period before t_0 and then maintained constant. The resulting strain can be expressed from Equation (2.22) as

$$\gamma(t) = \tau J(t) \tag{2.23}$$

As it was described in Equation (2.5) the shear compliance of an ideally elastic solid is equal to reciprocal modulus ($J = 1/G$). However, it must be noted that this simplified relation does not apply to viscoelastic materials (i.e., $J(t) \neq 1/G(t)$). Even though the creep compliance, $J(t)$, can be transformed to the relaxation modulus, $G(t)$, much simpler relationship can be achieved with dynamic experiments, described later in this chapter.

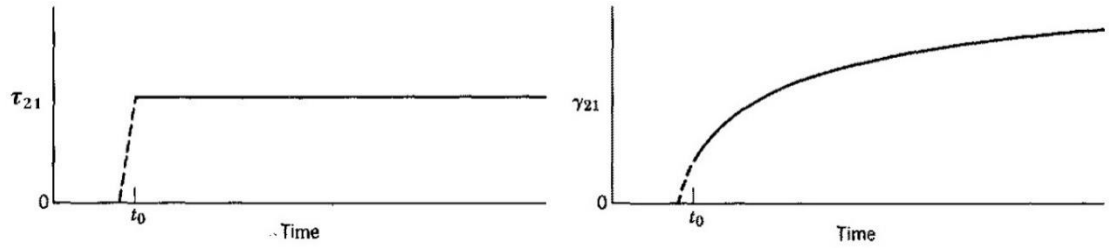

Figure 2.45 Time profile of shear creep experiment, adopted from [196]

An extension of creep testing is when the tested material is excited by a constant stress that is held for a certain length of time then removed and let the material recover its initial state. As it was described in Chapter 2.5.5 the effects of mechanical history are linearly additive. For example, in creep experiment with a sequence of small changes in stress, τ_i, acting at time, u_i, the resulting strain, $\gamma(t)$, would be as follows [196]

$$\gamma(t) = \sum_{u_i=-\infty}^{u_i=t} \tau_i J(t - u_i) \tag{2.24}$$

It is possible to distinguish between materials, which under constant stress after certain length of time eventually reach an equilibrium deformation in creep, $\gamma(\infty) \equiv \lim_{t\to\infty} \gamma(t) = \tau_0 J_e$, characterized by an equilibrium compliance, J_e, or materials,

that lack the constant equilibrium compliance and deform until the cession of the stress. The former materials are called *viscoelastic solids*, while the latter *viscoelastic liquids*. The creep and recovery experiment for viscoelastic solid is schematically illustrated in Figure 2.46 [194,196].

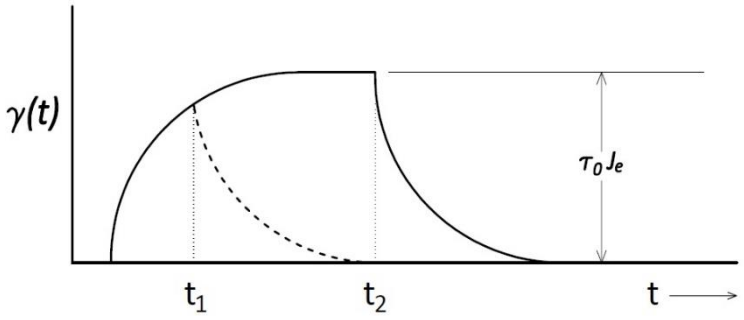

Figure 2.46 Schematic time profile of the shear creep and shear recovery performed on a viscoelastic solid, adopted from [196]

Asphalt binders at intermediate temperatures are generally considered as viscoelastic liquids with no equilibrium compliance, J_e, but they have a steady-state compliance, J_e^0. Typically, when viscoelastic liquids are exposed to constant stress the rate of strain decreases until it approaches a limiting value, and a situation of steady flow is eventually attained, governed by a Newtonian viscosity, η_0. This can be interpreted on the mechanical model in Figure 2.43 as the sum of all the viscosity values of the dashpots. When the stress is removed, in the case of viscoelastic solid, the deformation and the compliance function decrease until the material regains its original shape. In the case of viscoelastic liquid, the elastic part of the deformation recovers, while the strain, resulted from the viscous flow, becomes permanent. The shear creep followed by creep recovery of such material is illustrated in Figure 2.47 [194,196].

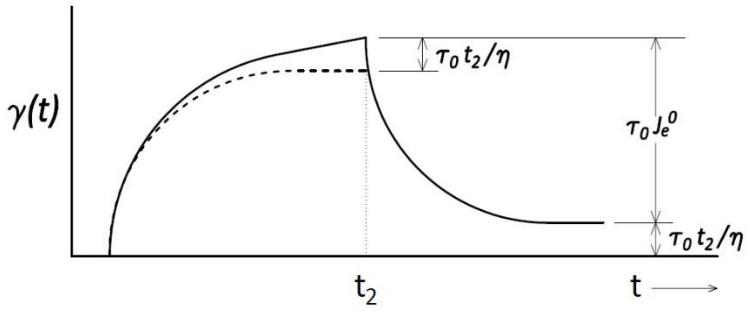

Figure 2.47 Schematic time profile of the shear creep and shear recovery performed on a viscoelastic liquid, adopted from [196]

The creep is the sum of the deformation approaching a constant value defined as $J_e^0\tau_0$, plus the deformation, $\tau_0 t/\eta_0$, resulting from the viscous flow. Therefore, the steady-state compliance can be interpreted as a measure of the elastic deformation during steady flow. The creep strain after a long time, but before the stress was removed, is given by

$$\gamma(t) = \tau_0(J_e^0 + t/\eta_0) \tag{2.25}$$

and by using the Equation (2.24) the strain during the recovery is given as a sum of the strain developed during creep and the subsequent recovery is then

$$\gamma(t) = \tau_0[J_e^0 + t/\eta_0 - J(t - t_2)] \tag{2.26}$$

Note that the removal of stress (according to the superposition principle) is equivalent to applying an additional stress, $-\tau_0$, with the same magnitude only in the opposite direction [194,196].

Another important method is the **periodic or dynamic experiment**, which is, together with stress relaxation (not presented) and creep experiment, the most frequently used experiment for viscoelastic materials. However, non-periodic experiments usually provide reliable results for "long" loading times of the order of seconds, periodic testing gives an opportunity to determine the response of materials to loads of very short duration. Nonetheless, there is an overlapping region between the two types of experiment, where both can be successfully used [192].

Dynamic experiments use a very small-amplitude oscillating shear stress (or strain) as an input to the material and the resulting oscillatory shear strain (or stress) is monitored. The tested material is excited with a periodic input, usually with a sinusoidal alteration at a frequency f expressed in (Hz), or in the case of angular frequency ω in (rad/s). The above non-periodic experiments at time t are qualitatively equivalent with their periodic counterparts at time $\omega = 1/t$. If the sinusoidal input alternation has sufficiently small amplitude then the viscoelastic behavior of the test material is linear, the resulting output will also alternate sinusoidally at the same frequency but will be out of phase with the input by a phase angle, δ, as it is illustrated in Figure 2.48.

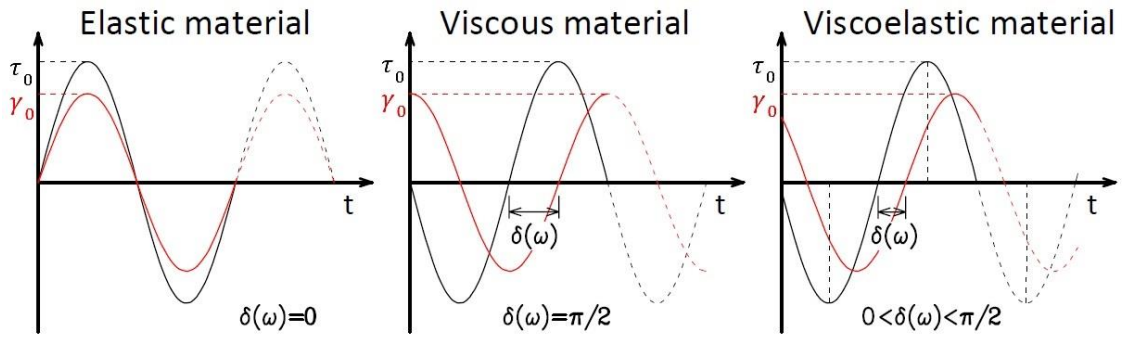

Figure 2.48 Time profile of a simple shear experiment with sinusoidally varying shear loading

The sinusoidal strain can be represented as

$$\gamma(t) = \gamma_0 \sin \omega t \tag{2.27}$$

where the γ_0 is the constant (maximum) strain amplitude and ω is the angular frequency $[\omega] = \text{rad/s}$. The rate of strain therefore

$$\dot{\gamma}(t) = \omega\gamma_0 \cos \omega t \tag{2.28}$$

and by substituting $s = t - t'$ in Equation (2.21)

$$\tau(t) = \int_0^\infty G(s)\, \omega\gamma_0 \cos[\omega(t-s)]ds \tag{2.29}$$

After expanding the $cos[\omega(t-s)]$ in the Equation (2.29) the shear can be written as

$$\tau = \gamma_0(G' \sin \omega t + G'' \cos \omega t) \tag{2.30}$$

where the term of $G'(\omega)$ is the shear storage modulus (elastic component) and $G''(\omega)$ is the shear loss modulus (viscous component) [196].

From Equations (2.27) and (2.30) it is apparent that $G'(\omega)$ is in phase with the input strain, γ, while $G''(\omega)$ is $\pi/2$ out of phase. If the phase angle, $\delta(\omega)$, is zero, the stress output is completely in phase with the strain input and the material can be considered as an ideally elastic. Whereas, if the phase angle, $\delta(\omega)$, is $\pi/2$, it is completely out of phase and the tested material is completely viscous. As it was already stated, viscoelastic materials have both viscous and elastic behavior, therefore, their phase angle is between $0 < \delta(\omega) < \pi/2$ [197].

Assuming, that the resulting stress is of the form

$$\tau(t) = \tau_0 \sin(\omega t + \delta) \tag{2.31}$$

and by using trigonometric formula, we get

$$\tau(t) = \tau_0 \cos\delta \sin\omega t + \tau_0 \cos\omega t \sin\delta \tag{2.32}$$

The comparison of Equations (2.30) and (2.32) shows that

$$G' = (\tau_0/\gamma_0)\cos\delta \tag{2.33}$$

$$G'' = (\tau_0/\gamma_0)\sin\delta \tag{2.34}$$

$$G''/G' = \tan\delta \tag{2.35}$$

From Equations (2.33) to (2.35) it is apparent, that every dynamic measurement at a given frequency simultaneously yields two independent quantities of G' and G'' and the ratio, $\tan\delta$, between them. It is usually convenient to express stress as a complex quantity and then introduce the complex (or dynamic) modulus G^*

$$\tau^*/\gamma^* = G^* = G' + iG'' \tag{2.36}$$

$$(\tau_0/\gamma_0) = |G^*| = \sqrt{G'^2 + G''^2} \tag{2.37}$$

The relation between G^*, G', G'', and $\tan\delta$ can be also illustrated by a vector diagram Figure 2.49. The length of each vector represents the value of the corresponding parameter, while G^* is the vector sum of the two moduli, G' and G''. The storage modulus, G', is related to the energy stored as potential energy and its release in the periodic deformation, while the loss modulus, G'', is associated with the dissipated energy (as heat) when the materials are deformed. The loss $\tan\delta$ is the internal friction or damping of the material, and it can be interpreted as the ratio of energy dissipated per cycle to the maximum potential energy stored during cycle [198].

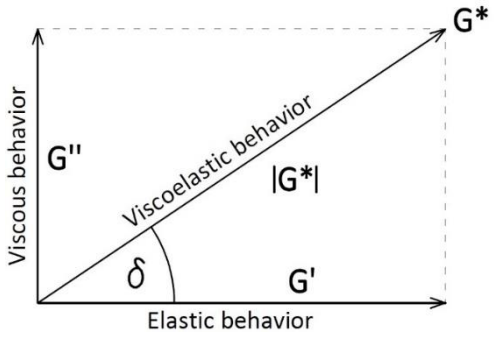

Figure 2.49 Relationship between viscous, elastic, and complex modulus

The data from these dynamic measurements can also be expressed in terms of a complex compliance

$$\gamma^*/\tau^* = J^* = 1/G^* = J' - iJ'' \tag{2.38}$$

where J' is the storage compliance, defined as the ratio of the strain in the phase with the stress to the stress, while J'' is the loss compliance, defined as the ratio of the strain $\pi/2$ out of phase with the stress to the stress. Note that even though the relation between the complex compliance, J^*, and complex modulus, G^*, (Equation (2.38)) is reciprocally related, their components are not [196]. The relationship between the individual components are given by the following equations:

$$J' = \frac{G'}{(G'^2 + G''^2)} \tag{2.39}$$

$$J'' = \frac{G''}{(G'^2 + G''^2)} \tag{2.40}$$

$$G' = \frac{J'}{(J'^2 + J''^2)} \tag{2.41}$$

$$G'' = \frac{J''}{(J'^2 + J''^2)} \tag{2.42}$$

2.5.7. Time-temperature superposition

In linear viscoelastic (LVE) region asphalt binder can be described as thermodynamically simple material, meaning that tests performed at high temperatures for a short time (high frequency) are equivalent to tests at low temperatures for a long time (low frequency). In other words, asphalt binders indicate equivalent rheological behavior at high temperature over short time period than at lower temperature but longer time duration.

This phenomenon can be successfully used to conduct either hardly feasible short-time experiments or those that would take too long. Therefore, with help of a method, called time-temperature superposition, it is possible to describe the behavior of a viscoelastic material on a substantially wider time/frequency range only by conducting measurements at different temperatures. Subsequently, with help of these experimental data obtained at different time/frequencies and temperatures a single master curve can be obtained that can significantly extend the effective time and frequency scale and provide us with very useful information about the inner structure of the material.

As an example, when a dynamic test is repeated at varying temperatures, the data can be shifted in order to create a single master curve that allows to determine the time dependence of the viscoelastic functions on the widest possible time/frequency interval.

In the viscoelastic region of a material at very low frequencies typically the viscous behavior of asphalt materials dominate, while with increasing frequency, the elastic behavior become more and more dominant. Therefore, the storage modulus G' increases until it reaches the glassy modulus G_g.

If the generalized Maxwell model (see Chapter 2.5.4) is used to represent the relaxation modulus of dynamic data, the resulting functions can be described by discrete relaxation (Maxwell) spectra $\{G_i, \lambda_i\}_{i=1,2,\dots,N}$ extracted from $G'(\omega)$ and $G''(\omega)$ and vice versa [199].

By substituting this discrete spectrum (Equation (2.19)) in the constitutive equation (Equation (2.21)) the dynamic moduli (i.e., $G'(\omega)$ and $G''(\omega)$) can be written as

$$G'(\omega) = G_e + \sum_{i=1}^{N} \frac{G_i(\omega\lambda_i)^2}{1 + (\omega\lambda_i)^2} \tag{2.43}$$

$$G''(\omega) = \sum_{i=1}^{N} \frac{G_i(\omega\lambda_i)}{1 + (\omega\lambda_i)^2} \tag{2.44}$$

where $i = 1,2,\dots,N$. Once the relaxation spectrum is determined, the other linear viscoelastic functions can be calculated [194,196].

In accordance with the generalized Maxwell model and by means of the Rouse theory [200] the effect of the change in temperature from T_0 to T will shift the material's experimental results (e.g., $G'(\omega)$, $G''(\omega)$,…) in a way as it changes the relaxation times of the respective mechanical model as follows

$$\lambda_i(T) = a_T \lambda_i(T_0) \tag{2.45}$$

where T_0 (sometimes denoted as T_r) is the reference temperature, T is the original temperature at which the measurement was conducted, and a_T is the horizontal shift factor on the abscissa ω which is a function of both T_0 and T. The changes in the magnitude of material functions are also defined by the Rouse theory. For example, for elastic moduli of the generalized Maxwell model, G_i, the theory predicts

$$G_i(t) = G_i(T_0)\frac{T\rho}{T_0\rho_0} = \frac{G_i(T_0)}{b_T} \tag{2.46}$$

where ρ is the density of the material at temperature T, and the expression of $b_T = T_0\rho_0/T\rho$ is the vertical shift factor on the ordinate for $G'(\omega)$, $G''(\omega)$. Based on the Equation (2.19) the following can be written

$$G(t,T) = \frac{1}{b_T}\sum_{i=1}^{N} G_i(T_0)e^{-\frac{t}{\lambda_i(T_0)a_T}} \tag{2.47}$$

For the creation of master curves the reduced moduli, G_r, the reduced time, t_r and the reduced frequency, ω_r(or f_r), are defined as follows

$$G_r(t) = G(t,T)\frac{T_0\rho_0}{T\rho} \tag{2.48}$$

$$t_r = \frac{t}{a_T} \tag{2.49}$$

$$\omega_r = \omega a_T \text{ or } f_r = f a_T \tag{2.50}$$

And for the master curve of the relaxation modulus at reference temperature T_0 from the values of G at several experimental temperatures for a thermodynamically simple material as

$$G_r(t_r) = \sum_{i=1}^{N} G_i(T_0)e^{-\frac{t_r}{\lambda_i(T_0)}} \tag{2.51}$$

If the curves of the relaxation modulus from experimental data at different temperatures are plotted against time, the function a_T is obtained as the magnitude of the horizontal shift necessary to superpose the data obtained at temperature T_i to reference curve (at T_0). The temperature dependency of the horizontal shift factor, a_T, can be described reasonably well by the Williams–Landel–Ferry (WFL) equation

$$\log(a_T) = \frac{-A(T-T_0)}{B+(T-T_0)} \tag{2.52}$$

where A and B are constants [200].

2.6. Rutting in Asphalt Pavements

Rutting is a major distress in flexible pavements and is defined as a longitudinal vertical depression of the pavement surface in a wheel path of roadways. Rutting contributes to poor ride quality and driving hazard manifested by increased potential of structural

failure, hydroplaning and consequently steering difficulty. Therefore, to obtain rut resistant pavements is one of the main objectives of the paving industry.

Rutting in flexible pavements develops gradually in wheel paths with increasing number of traffic load repetition that directly results in the incremental accumulation of small permanent deformations in all or in some of the pavement layers. It is often followed in its later stage by lateral movement of the hot mix asphalt (HMA) material underneath the wheel path caused by shear deformation that contributes to the creation of upheaval zones on the sides of the wheel paths [201]. The total measured rutting is then the sum of the settlement in the center and the "height" of the heave.

Generally, three types of rut can develop in asphalt concrete pavements as it is depicted in Figure 2.50. The first, called wear rutting, is the result of gradual loss of coated aggregate particles from the pavement surface and its root cause can be found either in environmental or traffic influences (e.g., abrasives, studded tires). Although the majority of rutting occurs in the top 75–150 mm of the pavement, deformations may occur also in different pavement structural layers resulting in the second type of rutting, called structural rutting. It is a result of repeated traffic load that vertically deforms not only the surface layers of the pavement, but also its sublayers. The third type of rutting, called instability rutting, is a result of either the use of poor binding material or an inadequate design of the HMA layer which, therefore, cannot resist the stresses imposed upon the pavement. The absence of sufficiently stiff HMA in the surface layers, that can also resist to flexural stresses at the bottom of the layer, results in lateral displacement of material within the layer that occurs beneath the wheel path. The total rutting is the combination of all the above mentioned permanent deformations accumulated in all layers in the pavement structure [202].

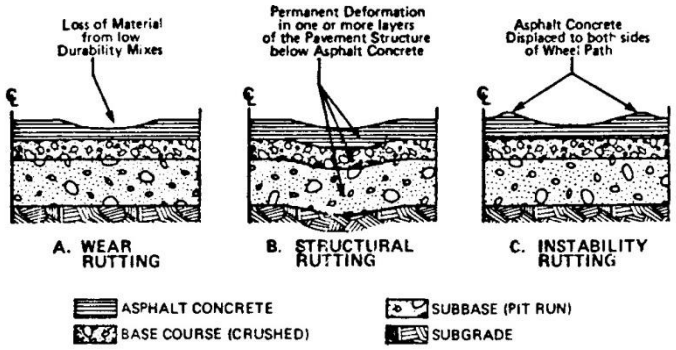

Figure 2.50 Description of rutting types, adapted from [202]

The development of rutting is a result of two main mechanisms: densification (decrease in volume, increase in density) and shear deformation (no volume change). Densification primarily happens at the beginning of the pavement's service life, usually within the first year, and it develops underneath the wheel path with no significant upheaval along its sides. During this process the HMA layers become load-compacted and stiffened due to the rearrangements of the aggregate particles and expelling of air voids. After the densification is complete, further deformations occur resulting in volume decrease of material beneath the wheel path which approximately equals to the volume increase in the adjacent upheaval zones along the sides. Studies have shown that the primary rutting mechanism causing such material displacement (without change in volume) is shear deformation [203]. In the final stage, called tertiary flow, when enough distortion has occurred, the rate of deformations rapidly increases resulting in noticeable damage due to the combined effects of moisture susceptibility and rutting [204].

Therefore, the development of rutting can be divided into three stages, namely primary, secondary, and tertiary rutting (Figure 2.51). The primary stage is characterized by an initial high rate of rutting (compaction) which decreases with the growing number of wheel passes. The secondary stage is characterized by a low nearly constant rate of rutting, predominately the result of shear deformation. Finally the tertiary stage, which is characterized by a high rate of distortion that eventually culminates in shear failure.

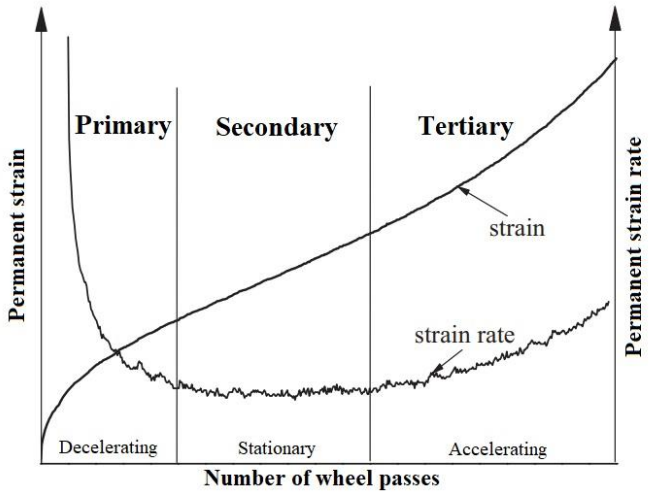

Figure 2.51 Three stage of rutting of asphalt mixture, adapted from [205]

The susceptibility of asphalt pavements to rutting is influenced by many parameters such as aggregate characteristics (e.g., surface texture, gradation, shape, size, etc.), binder

properties (e.g., stiffness, elasticity, viscosity, etc.), mixture volumetric properties (e.g., binder content, air void content, etc.), and environmental or operating conditions [204]. As such, asphalt in HMAs is not only a binder that holds together the aggregate skeleton, but also a viscoelastic material, characterized by a certain level of rigidity, that has a load carrying role in the asphalt mix. Therefore, they have a critical role against rutting in flexible pavements and their resistance to permanent deformation is highly dependent on temperature, stress level, loading time, etc.

Three basic types of models aim to predict the progression of rutting depth in the pavement: empirical models, mechanistic-empirical models, and mechanistic models. Empirical models are derived from laboratory or field test data by regression equations fitted to the observed data, such as physical mix related properties, loading and weather conditions. Empirical laboratory models are often based on the result of either static or dynamic creep tests, or from dynamic triaxial test, while empirical field models are typically derived by means of statistical analysis. Empirical models aim to estimate the future performance of the asphalt mixture based solely on the recorded deformation history as a mere extrapolation [206].

Mechanistic-empirical models are derived from a combination of characteristic material data obtained from laboratory or field tests and an appropriate mechanical analysis of the future pavement (i.e., often using elastic or viscoelastic layered theory).

Fully mechanistic models are derived from structural mechanical analysis of the pavement. Based on mechanistic hypothesized rutting mechanism, complex constitutive models are constructed to evaluate stresses, strains, magnitudes of permanent deformations, cracking and other distresses [206].

2.7. Finding an effective tool for rutting susceptibility estimation of asphalt binders

Recognizing the limitations of the traditional penetration-viscosity-based asphalt binder characterization procedure in 1987, the Federal Highway Administration (FHWA) of the United States initiated a nationwide research program called the Strategic Highway Research Program (SHRP). The output of this program was the creation of Superpave® (SUperior PERforming Asphalt PAVEment) specifications and test methods for asphalt binders and asphalt mixes, collectively called the Superpave® pavement design system.

To minimize the development of distresses (e.g., low temperature cracking, fatigue cracking, rutting) the new specification addressed the asphalt binder rheological performance at high and low temperatures by introducing specific criteria that must be met. In 1993 the performance grade (PG) binder specifications were adopted by The American Association of State Highway and Transportation Officials (AASHTO) and were introduced as AASHTO M320 (formerly designated as AASHTO MP1) [207]. Superpave® provided a useful method for evaluating and understanding the mechanism of rutting and introduced a tool, the dynamic shear rheometer (DSR) [208], to perform the measurement of the respective binder characterizations.

2.7.1. Superpave®-specified rutting parameter

Due to their viscous nature, asphalt binders flow and dissipate energy through frictional losses. The dissipated energy can be determined at a certain loading frequency and temperature by means of dynamic measurements conducted on DSR. Anderson *et al.* [68] assumed that rutting is caused by the total dissipated energy from the stress/strain curve. In other words, the more energy is dissipated, the greater permanent deformation accumulates over time.

The total work done in cyclic stressing a material (per unit volume) is given by

$$W = \int \tau d\gamma \tag{2.53}$$

and the energy lost through internal friction and heat is as follows

$$\Delta W = \int_{t_1}^{t_1+T} \tau d\gamma = \int_{t_1}^{t_1+T} \tau \frac{d\gamma}{dt} dt \tag{2.54}$$

where t_1 is some starting time and T is the period of oscillation, $T = 2\pi/\omega$. Substituting in Equations (2.28) and (2.31) for strain and stress and for $t_1 = 0$ the energy loss per cycle is given by

$$\Delta W_i = \pi \tau_0^2 J'' \tag{2.55}$$

where ΔW_i is the total energy dissipated at the ith cycle, τ_0 the maximum shear stress applied and J'' is the loss compliance. Further substitution of Equations (2.34) and (2.37) into Equation (2.40) and the result into Equation (2.55) gives

$$\Delta W_i = \pi \tau_0^2 \frac{|G^*| \sin \delta}{|G^*|^2} = \pi \tau_0^2 \frac{\sin \delta}{|G^*|} = \pi \tau_0^2 \frac{1}{\frac{|G^*|}{\sin \delta}} \tag{2.56}$$

where $|G^*|$ is the magnitude of the shear complex modulus and δ is the phase angle, while the inverse of the loss compliance, $1/J'' = |G^*|/\sin\delta$, was introduced as the rutting parameter. From the Equation (2.56) it is evident that the larger the rutting parameter, $|G^*|/\sin\delta$, the less energy is dissipated with each loading cycle, indicating more stiff and elastic binder which is less prone to permanent deformation or rutting (for $\delta = 0$ the $\Delta W_i = 0$). Consequently, in Superpave® specification the rutting parameter, $|G^*|/\sin\delta$, is used in the high temperature performance grading of a binder as an indicator of rutting resistance [192,196].

Despite the fact that the Superpave® specified performance grading system is a significant improvement to the earlier grading systems it still was primarily based on the study of neat asphalt binders refined from crude oil with no polymer additives. However, as already mentioned, polymer modified binders at their service temperatures behave as a non-Newtonian fluid and exhibit non-linear reaction to stress and strain loads on a much higher level than neat binders do. Moreover, under a very low stress and strain levels, as it is in the case of the linear measurements during the evaluation of the rutting parameter, it is unlikely that the polymer network in the binder would be activated.

Consequently, the new specification was yet again not able to express the effect of polymers in the binder. The polymer chains, however, can significantly rearrange with increasing stress and strain levels. Therefore, after many years of application, the rutting parameter, $|G^*|/\sin\delta$, measured by DSR was found to be inadequate in describing the rutting performance of certain binders, particularly, the polymer modified ones [209–211].

Subsequently, the National Cooperative Highway Research Program (NCHRP) Project 9-10, "Superpave® Protocols for Modified Binders", was initiated to determine the suitability of the new specification protocols for modified binders. The NCHRP Project 9-10 eventually concluded that the Superpave® performance grade specifications could not be used for full characterization of binders with different types of polymers [212].

Therefore, many state agencies have introduced additional tests to characterize polymer modified binders, called Superpave® PG "Plus" specifications. Nevertheless, the PG "Plus" tests (e.g., elastic recovery, tenacity, force ductility) were not able to indicate the field performance of asphalt binders only the presence of the modifier in the blend. Moreover, they were time consuming and expensive as they required special equipment [213].

2.7.2. Repeated creep test

Several different rheological properties were explored and proposed to replace the existing Superpave® rutting parameter, $|G^*|/\sin\delta$. The repeated creep test (RCT) was one of the outputs of the NCHRP Project 9-10 [212]. It was introduced as a testing protocol for obtaining a new high temperature binder specification parameter that indicate better correlation with mixture rutting properties. The project hypothesized that repeated loading is a factor to which a modified binder responds differently than neat binder and also better represents the cyclic nature of traffic loading [212,213].

In accordance with the testing protocol a constant shear stress is applied to a sample of asphalt binder for 1 s loading time followed by a 9 s unloading time when the stress is removed. The test is then repeated for a given number of cycles. The recommended test protocol is to use a shear stress in a range of 30 Pa to 300 Pa for 50 or 100 cycles [212].

The RCT test allowed to estimate the propensity to accumulation of permanent strain of binders that is believed to be the main cause of the development of permanent deformations in asphalt mixes. Since the four-element Burgers model (i.e., a Voigt unit and a Maxwell unit in series) proved to be a good representation of the asphalt binder behavior it was employed to fit the data obtained from RCT test. The Burgers model components and the division of the response into the components of the elastic, delayed-elastic, and viscous response for each cycle is illustrated in Figure 2.52. In accordance with the Burgers model the time-dependent shear strain $\gamma(t)$ is expressed as follows

$$\gamma(t) = \gamma_1 + \gamma_2 + \gamma_3 = \frac{\tau_0}{G_0} + \frac{\tau_0}{G_1}\left(1 - e^{-\frac{G_1}{\eta_1}t}\right) + \frac{\tau_0}{\eta_0}t \tag{2.57}$$

where γ_1 is the elastic strain, γ_2 is the delayed-elastic strain, γ_3 is the viscous (permanent) strain, τ_0 is the constant shear stress, G_0 is the spring constant of Maxwell unit, G_1 is the spring constant of Voigt unit, η_1 is dashpot constant of Voigt unit, and η_0 is the dashpot constant of Maxwell unit. Dividing Equation (2.57) by the constant shear stress, τ_0, the creep compliance, $J(t)$, can be divided into the following components

$$J(t) = J_e + J_{de}(t) + J_v(t) \tag{2.58}$$

where J_e is the elastic, J_{de} is the delayed-elastic, and J_v is the viscous component. Based on this separation of creep response the viscous component was chosen for the use as an indicator of the contribution of binders to rutting resistance. However, for practical reasons, instead of using J_v, which has a unit of 1/Pa, the inverse of viscous creep compliance $G_v = 1/J_v = \eta_0/t$ was used and defined as the viscous component of the

creep stiffness. Equation (2.57) implies that the accumulated permanent deformation, γ_3, is a function of viscosity, load, and loading time. Therefore at an appropriately chosen testing stress, τ_0, and time of loading, t, the viscous component of the stiffness, G_v, more precisely the viscosity, η_0, could be directly related to the propensity to accumulation of permanent strain of binders and their contribution to resistance of mixture rutting.

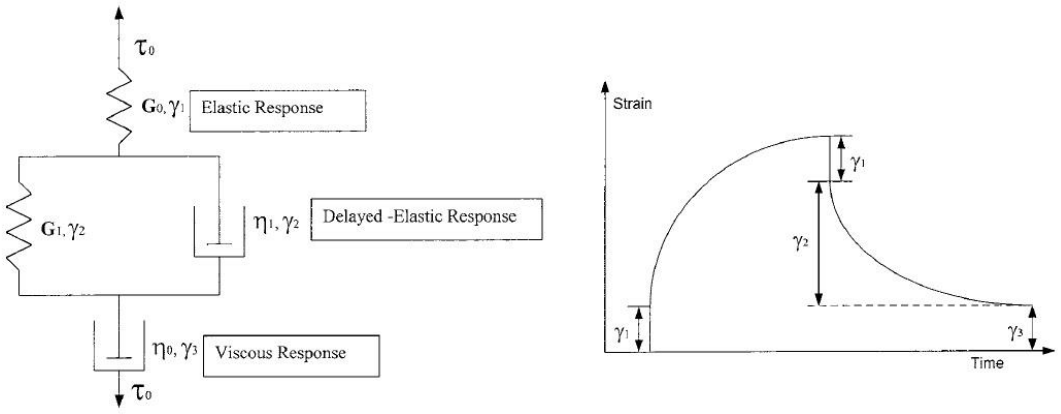

Figure 2.52 Burgers model and its response, adopted from [212]

Compared to the rutting parameter, $|G^*|/\sin\delta$, the creep stiffness, G_v, evaluated by the repeated creep testing protocol, better estimated the propensity of binders to rutting. Nevertheless, stresses and strains in the mixes can be significantly higher than the linear limit for the asphalt binder; thus, testing at low stress levels might be still misleading when characterizing the rutting resistance of an asphalt binder [214].

Shenoy [215] developed a rheological parameter with an attempt to improve the Superpave® rutting parameter, $|G^*|/\sin\delta$. He proposed to use the percent un-recovered strain, γ_{unr}, (permanent deformation) to characterize the susceptibility of asphalt binders to rutting by means of dynamic oscillatory measurements. According to his theory, the un-recovered strain, γ_{unr}, that occurs during the repeated creep test can be calculated directly from dynamic measurements. Shenoy suggested that the un-recovered strain, γ_{unr}, should be expressed as a function of complex modulus, $|G^*|$, and phase angle, δ, as follows

$$\gamma_{unr} = \frac{100\tau_0}{|G^*|}\left(1 - \frac{1}{\tan\delta \sin\delta}\right) \tag{2.59}$$

In order to minimize the un-recovered strain, the following term in Equation (2.60), which is the inverse of the non-recoverable compliance, $\gamma_{unr}/100\tau_0$, needs to be maximized

$$\left(\frac{|G^*|}{1-\frac{1}{\tan\delta\sin\delta}}\right) \tag{2.60}$$

The term proposed by Shenoy (Equation (2.60)) was meant as a refinement to the Superpave® rutting parameter of $|G^*|/\sin\delta$. The drawback of this parameter is that it is not valid at phase angles below 52°, therefore its use is restricted to only limited temperature ranges for every asphalt–mixture set, since in the case of mixtures the phase angles are more likely to be below 52° at conventional testing temperature ranges [215].

2.7.3. Multiple stress creep recovery test

Asphalt binders that indicate similar behavior in the linear viscoelastic region can exhibit substantially different behavior under high strains and stresses within the non-linear region. Experimental studies showed that the strain levels experienced by the asphalt binder in the mixture is high enough (an average of 7.8 times and the maximum of 510 times the bulk strain of the mixture) to merit the measurement of the non-linear viscoelasticity of binders [216–219]. The non-linear behavior of hot mix asphalt (HMA) can be caused by the rotation and slippage of aggregates and the localized high strains in the binder phase [217]. However, all the methods described in previous chapters are based on linear viscoelastic theory. Furthermore, their inability to predict rutting resistance of modified asphalts was shown by many researchers [212,220,221]. Therefore, in order to characterize the resistance of asphalt binders to permanent deformation, higher stress and strain levels should be used during testing which are more similar to those experienced in the asphalt mixtures.

D'Angelo *et al.* [220] improved the repeated creep test (RCT) and recommended to use multiple stress levels of 0.025, 0.050, 0.1, 0.2, 0.4, 0.8, 1.6, 3.2, 6.4, 12.8, and 25.6 kPa at 10 cycles for each stress level and renamed the test as multiple stress creep recovery (MSCR) test. Similarly to RCT, the stress is applied for one second followed by a nine seconds recovery within each cycle.

The MSCR test is started at the lowest stress level and increased to the next stress level at the end of every tenth cycle with no time lag between the cycles. The average un-recovered strain, γ_u, for the ten creep and recovery cycles is then divided by the applied stress for those cycles yielding the parameter what is referred to as the non-recoverable creep compliance, J_{nr}. The lower the value of the asphalt binder's non-recoverable creep

compliance is, the more resistant to rutting the asphalt mixture is (more about J_{nr} in Chapter 3.4.3).

Based on the J_{nr} result for many neat asphalt binders, over a wide range of stress, D'Angelo *et al.* [220] suggested to use only two stress levels of 0.1 and 3.2 kPa for testing at their performance grade temperature because the results indicated that these materials tend to behave in a linear fashion typically up to 3.2 kPa stress level (in Figure 2.53, neat binders are the PG 58-28 and the PG 64-22). Nonetheless, in the case of polymer modified asphalt binders the linearity can be noticeably altered even at lower stress levels. In Figure 2.53 the most noticeable example of such asphalt binder is the SBS and SBR-modified [209].

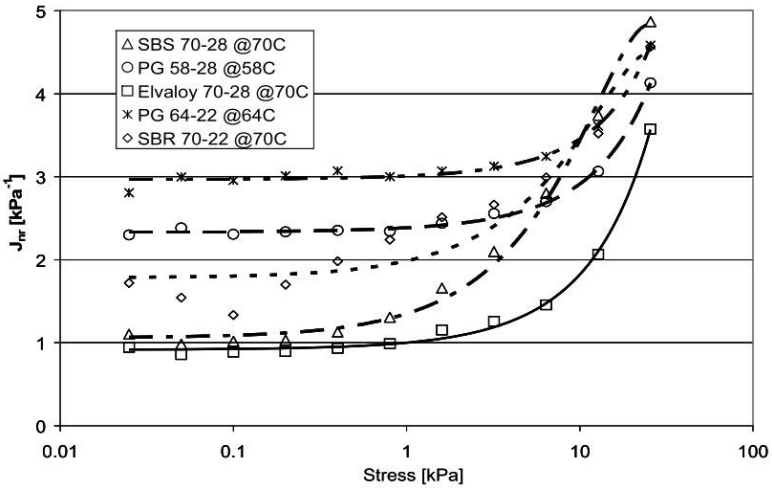

Figure 2.53 Non-recoverable creep compliance, J_{nr}, results of two neat binders and three polymer modified binders at their respective PG temperature, adopted from [209]

Hamburg rut testing at three different temperatures was conducted on asphalt mixes that contained asphalt binders of different low temperature PG gradation (PG 58-28, PG 58-34, PG 58-40) from which the PG 58-28 was neat binder, and the other two were crosslinked SBS-modified binders, all obtained from MnRoad study [222]. The Hamburg testing was done using a 703 N load on a solid steel wheel with average reported contact stress of 105 psi (~724 kPa) in a temperature range of 58 to 70°C. The Hamburg rut results when correlated to the non-recoverable creep compliance, J_{nr}, evaluated at 12.8 kPa and at respective temperatures, indicated substantially better correlation (R^2=0.93) than the SHRP binder criteria of $|G^*|/\sin\delta$ (R^2=0.65) [223].

The ability of the non-recoverable creep compliance, J_{nr}, to predict rutting resistance was also verified on asphalt binders used within the study conducted at the Federal Highway Administration's (FHWA) Accelerated Loading Facility (ALF) [224]. ALF is a full scale accelerated loading facility where asphalt mix test sections can be loaded with standard or specially designed wheel configurations and loads. The ALF machines have frames 29 m long with rails to direct rolling wheels. Each ALF machine was capable of applying an average of 35,000 wheel passes per week by using a half-axle load ranging from 33 to 84 kN [224–226].

In 2002 twelve hot mix test sections were constructed for the evaluation of various polymer modified (SBS, CRM, Elvaloy™), air-blown and neat asphalts. Construction of the test lanes was performed with standard HMA production and paving equipment to simulate real world conditions as close as it is possible. The 14 m long test sections were then heated to 64°C and trafficked with super-single (425/65R22.5 wide base) tire that was subjected to 45 kN load and run at 19 km/h. In order to accelerate the accumulation of permanent deformations in the section the loading was one directional without transverse wander [224–226].

Eventually, the SHRP binder criteria of $|G^*|/\sin\delta$ and the non-recoverable creep compliance, J_{nr}, measured at 64°C were compared to the rutting that accumulated during the ALF testing. Due to the high loads on the tire (approximately 4.5 t for a single wheel, while in the Czech Republic the maximum load is 5.0 t for one wheel) and the slow speed of the wheel, ALF can be considered as a very high stress accelerated loading facility, therefore, the J_{nr} of these binders was evaluated at the highest stress level of 25.6 kPa. The correlation of the SHRP criteria $|G^*|/\sin\delta$ to rutting indicated very poor results (R^2=0.22). Much better correlation was observed between the non-recoverable creep compliance, J_{nr}, and the ALF rutting results (R^2=0.82). The ALF rutting experiment also emphasized the need to evaluate the stress sensitivity of the binders to determine high temperature rutting properties especially of polymer modified binders, since some of the binders (i.e., SBS-modified very soft base asphalt) that under low shear testing appeared to be the most rut resistant indicated much worse resistance to rutting under high shear or heavy loading. These studies reported that reducing J_{nr} by half typically reduces rutting also by half [223].

Asphalt binders from the I-55 Mississippi field study [227] were also tested in order to verify the new J_{nr} rutting parameter. It was a field trial of eight polymer modified asphalt binders (mainly SB, SBS, CRM-modified) that started in 1996 and the

performance of the test sections (0.8 km long) made from these binders were monitored for six years. The test sections experienced typical highway traffic with a mix of loadings and variable temperatures. The average daily traffic (ADT) for the test section was estimated to be 25,000 with 28% trucks, and the 20 year design equivalent single axle loads (ESAL) were 19 million [223].

The J_{nr} rutting parameter evaluated at 3.2 kPa shear stress level indicated the best correlation with the rutting results of the I-55 Mississippi field study. Similarly as in previous cases, the non-recoverable creep compliance, J_{nr}, indicated substantially better correlation (R^2=0.75) even with the actual traffic-induced rutting results than the SHRP binder criteria of $|G^*|/\sin\delta$ (R^2=0.32) [223].

Another research that evaluated a wide variety of straight-run, polymer modified, and other modified binders [228] reported relatively good correlation between the J_{nr} rutting parameter and Hamburg rut results. During the MSCR measurements, 0.4 kPa and 15.0 kPa shear stress was applied on the asphalt binder samples. The HWTT mixture results showed better correlation with the J_{nr} rutting parameter measured at the higher stress level of 15.0 kPa (R^2=0.82) than at the lower stress level (R^2=0.74). Similarly to the MnRoad study, Hamburg device with steel wheel, 703 N test load, and 52 passes per minute was used for mixture testing.

According to D'Angelo *et al.* [220], due to the very high loads and constant high temperature, the ALF test cannot successfully simulate the real rutting conditions. Consequently, despite the good correlation between the J_{nr} rutting parameter measured at 25.6 kPa and the ALF rutting results, the application of this high pressure during MSCR testing was waived. Furthermore, even though the results of Hamburg test correlated well with the rutting parameter of J_{nr} measured at 12.8 kPa (MnRoad study), due to the steel wheel-induced high loads and slow speed at a high constant temperature, the Hamburg rutting test was also considered to exaggerate the rutting conditions when compared to the I-55 Mississippi field study [220].

The results clearly showed that the newly introduced MSCR test results are considerably more successful in predicting the rutting resistance than the Superpave® $|G^*|/\sin\delta$ binder criteria at high PG temperatures. Subsequently, MSCR test method was proposed as a replacement of the PG "Plus" tests and introduced in AASHTO TP70 [229,230]. The most recent version of this test procedure is described in AASHTO T350, which was also adopted in 2015 by the European Committee for Standardization (CEN) and introduced in the European standard of EN 16659 [231]. Based on the conclusions of

the I-55 Mississippi field study and based on the observations that the J_{nr} results of neat binders indicated linear behavior up to 3.2 kPa shear stress level [220], the recommendation of D'Angelo *et al.* [220], that only two stress levels of 0.1 and 3.2 kPa should be used, was accepted and implemented in the standards. However, as it was mentioned earlier, the same linear fashion does not hold true for polymer modified asphalts binders [209]. Therefore, from this point of view, the importance of the limiting value of 3.2 kPa shear stress level can be queried.

Other researches also reported good correlation between the J_{nr} results measured at higher than 3.2 kPa shear stress levels and the rutting resistance of the asphalt mixes [232,233].

2.8. Stresses present in the pavement versus in the Hamburg wheel-tracking test specimen

In order to optimize the complexity of modeling the pavement-tire contact pressure it is usually simplistically equated to tire inflation pressure uniformly distributed over a circular contact area. In fact, pavement-tire contact is not circular and contact pressure is neither uniform nor the same as tire inflation pressure and is significantly dependent on the load magnitude, tire inflation pressure, tire structure, tire tread, vehicle speed, temperature, driving conditions (e.g., accelerating, steady rolling, braking), etc.

During the movement of the tire, the stresses transmitted to the pavement vary and are expected to be maximized at the center of the tire, and minimized at its edges. However, experimental measurements conducted by De Beer *et al.* [234,235] have demonstrated that the non-uniform tire-pavement contact pressure distribution is more complicated. In addition, the actual tire-pavement contact pressure is three-dimensional (3-D) and consist of both vertical part and horizontal (lateral and longitudinal) components (Figure 2.54), although in magnitude the two horizontal contact shear stresses are much smaller than the vertical stress.

The distribution of lateral (or transverse) contact stresses at right angles to the direction of the moving tire, plotted in Figure 2.54B and Figure 2.54E, clearly indicate inward shear towards the tire center. These stresses are in balance, with zero stress in the wheel center, therefore, the resultant force is zero. Nevertheless, the lateral contact stress contributes to the tensile stress outside the tire edge. As a result of this the pavement

surface is simultaneously experiencing tensile stresses that tend to pull the HMA from the center of the tire and compression caused by vertical stresses [234].

The lowest of the three contact stresses, called longitudinal contact stress, is the one that exerts its effect in the direction of the tire travel (Figure 2.54C and Figure 2.54F). It normally results in two or three peaks and is highly dependent on the rolling resistance between the tire and the pavement, and on the traction, braking or acceleration. Similarly to the lateral stress, longitudinal stress is also in balance with zero value of stress at the wheel center [234].

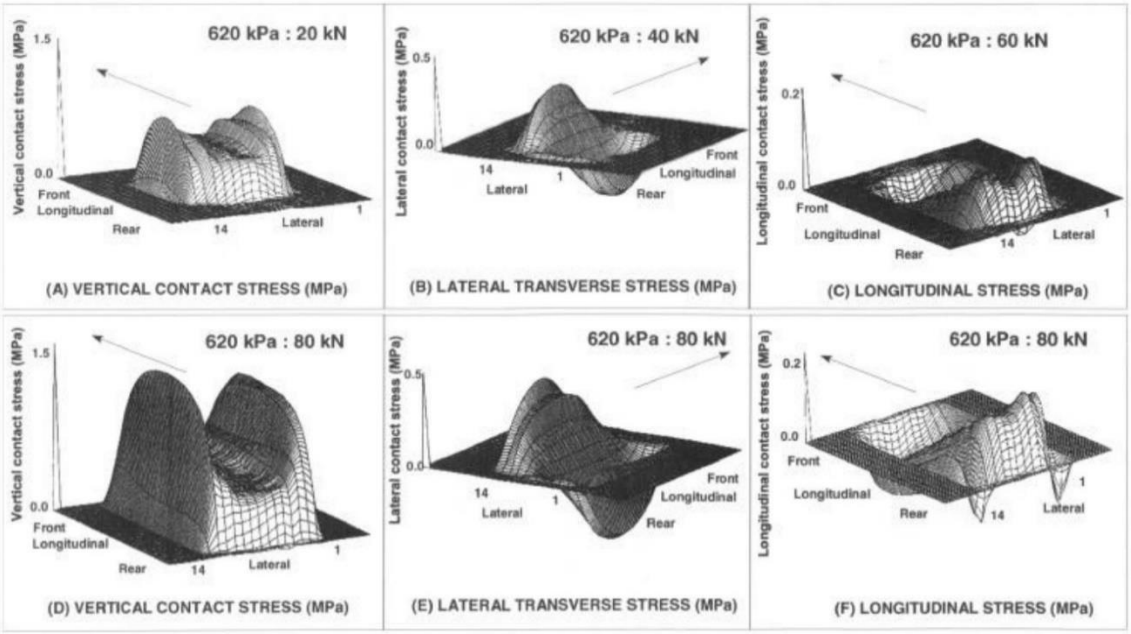

Figure 2.54 Actual non-uniform contact stress distributions measured for a slow moving (~1.2 km/h) free rolling smooth single truck tire (11.00 x 20 14 ply bias/cross-ply), adapted from [234]

Tielking and Roberts [236] showed that non-uniform contact pressures cause higher pavement strains than uniform contact pressures. Their results also showed that the non-uniformity of tire loading and the magnitude of contact pressure have a significant effect on the strain distributions in HMA layers.

An increase in the tire inflation pressure reduces the tire-pavement contact area resulting in an increase in the tire-pavement contact stress which may cause more damage to the pavement. Studies by De Beer *et al.* [234] and Yoo *et al.* [237] showed that the three main factors influencing the tire contact area is determined by the tire tread shape, the inflation pressure and the axle load. The distribution shapes for the over- and under-

inflation tire pressure was represented by El-Kholy and Galal [238] by utilizing finite element method. In the case of over-inflation, the stress distribution along the tire width was simplified to a second-order parabolic shape with its peak value at the center of the contact area, while in the case of under-inflation (or overload), the contact stress distribution was expressed by two intersected second-order parabolic shapes with two peak values. Figure 2.55 illustrates the distribution of the simulated non-uniform contact stress used and developed by El-Kholy and Galal [238] for both over- and under-inflation pressure. These simplifications were fairly near to the experimental results presented by De Beer *et al.* [234,235,239]. The effects on the actual pavement of over- and under-inflation pressure is also evident from Figure 2.55 [239]. Since tire loading is transmitted to the pavement surface through the tread ribs, more complex traffic loading models represent the contact area by a series of rectangular treads, while including the three-dimensional (3-D) complex state of stresses [240–242].

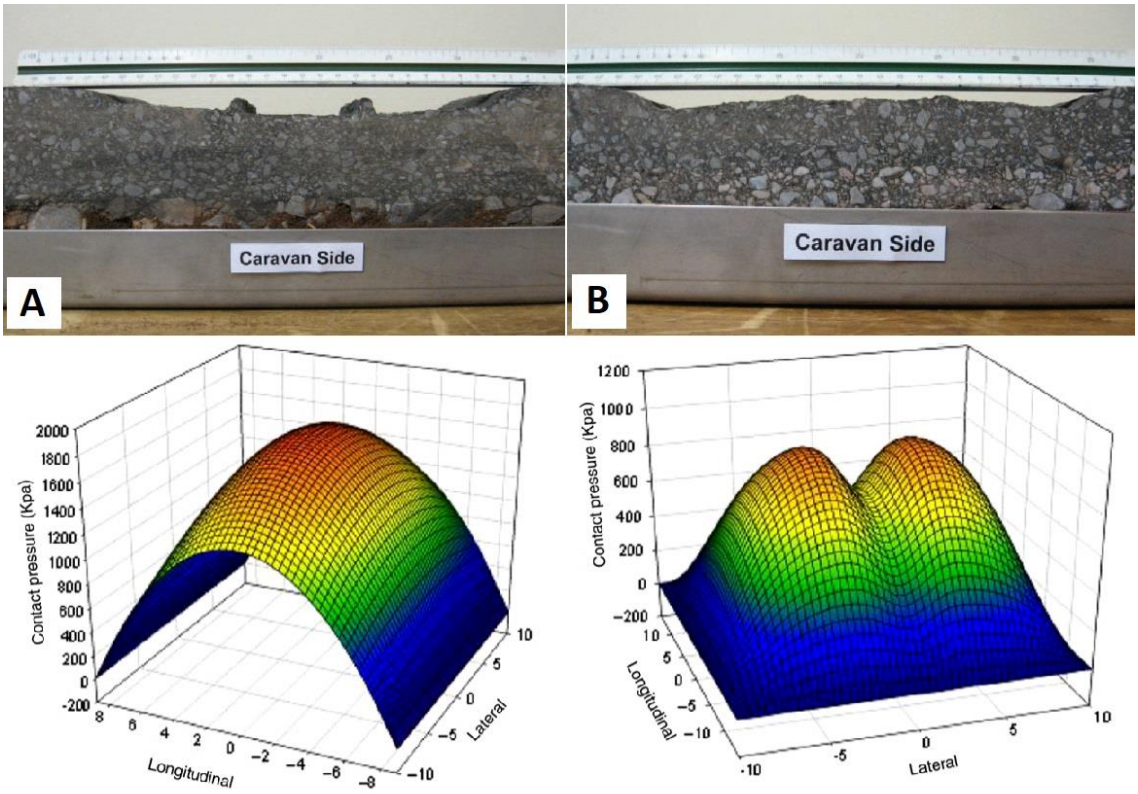

Figure 2.55 Non-uniform contact stress distribution and their effect on the pavement for over- (A) and under-inflation (B) pressure of 793 kPa and 483 kPa, respectively, with 28 kN load, adopted from [238,239]

In Figure 2.56 the vertical contact stress distribution at different inflation pressures (horizontal axis ranging from 520 to 800 kPa) and tire loads (vertical scale ranging from 15 to 50 kN) are presented on an example of slow moving (~1.2 km/h) single radial tire type 11xR22.5 with grooves. The experimental measurements clearly show the changes in the contact stress pattern from a relatively light load, where the maximum stress is toward the tire center (typical bell shape), to the typical dual bell, or m-shape, where the load is carried mostly by the tire sidewalls, showing the highest contact stresses at the tire edges. According to Beer *et al.* [239] the average inflation pressures (cold) of heavy vehicle tires are currently approaching an average of 800 kPa, with maximum pressures exceeding 1,000 kPa. In Figure 2.56 the measurements indicate that the contact stresses at ideal tire load of 20 kN and inflation pressure of 720 kPa may reach 900 kPa, while at even higher tire loads these pressures may exceed 1,000 kPa.

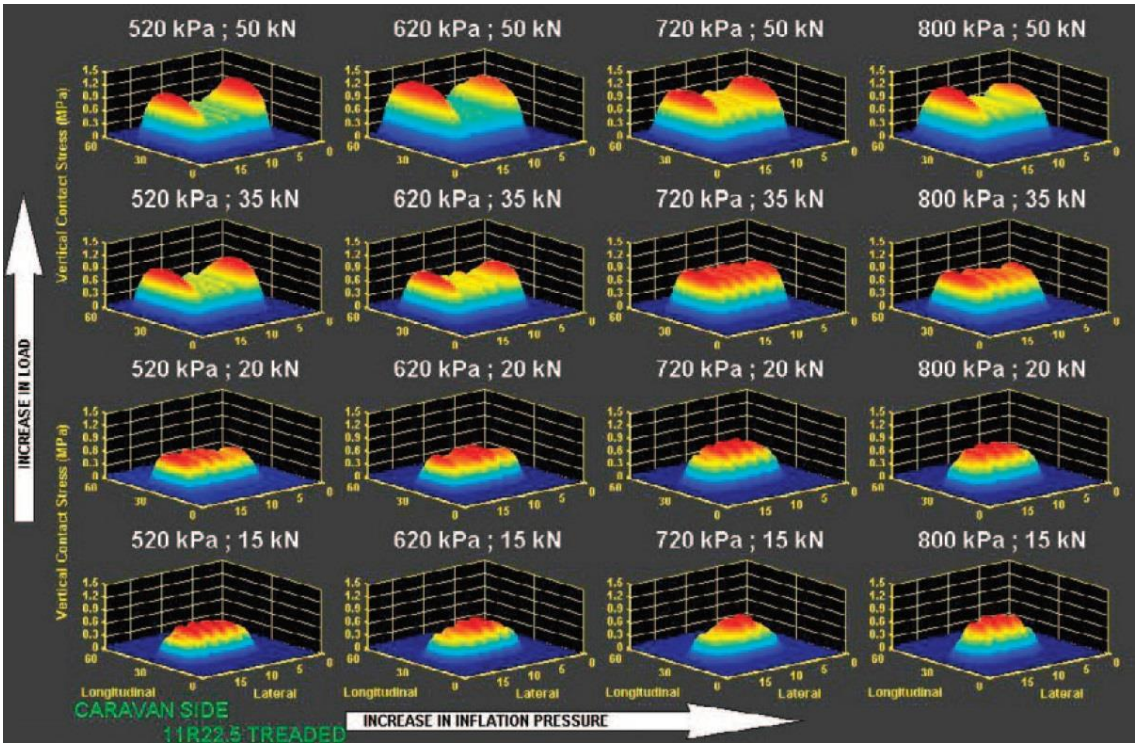

Figure 2.56 Graphic illustrations of the tire load vs. inflation pressure relationship on the vertical contact stress distribution of a slow moving single radial tire type 11xR22.5 with tread, adopted from [239]

Zak and Vavricka [243] analyzed the vertical contact stress distribution of a Hamburg wheel-tracking device built by ConTech (Dubi, Czech Republic) which was equipped with solid rubber tires (rubber hoop glued to a steel wheel core). The equipment was capable of testing a pair of samples simultaneously. The rubber wheels had a diameter

of 203 mm, a width of 50 mm, and oscillated at 50 times per minute. Each rubber wheel applied a load of 700 N on the measured contact area 22 mm long and 50 mm wide (1100 mm^2). The value of the uniformly distributed contact pressure corresponding to these quantities was therefore ~636 kPa. In contrast, by utilizing 3-D finite element modeling the study reported a parabolic-like distribution of vertical contact stress between the rubber wheel and the surface of the sample with a maximum value of ~1000 kPa in the center of the contact area (Figure 2.57A). Compared to the measurements of Beer *et al.* [239] similar maximum vertical contact pressures can be measured at the combination of 20 kN tire load and 800 kPa tire inflation pressure, illustrated in Figure 2.57B.

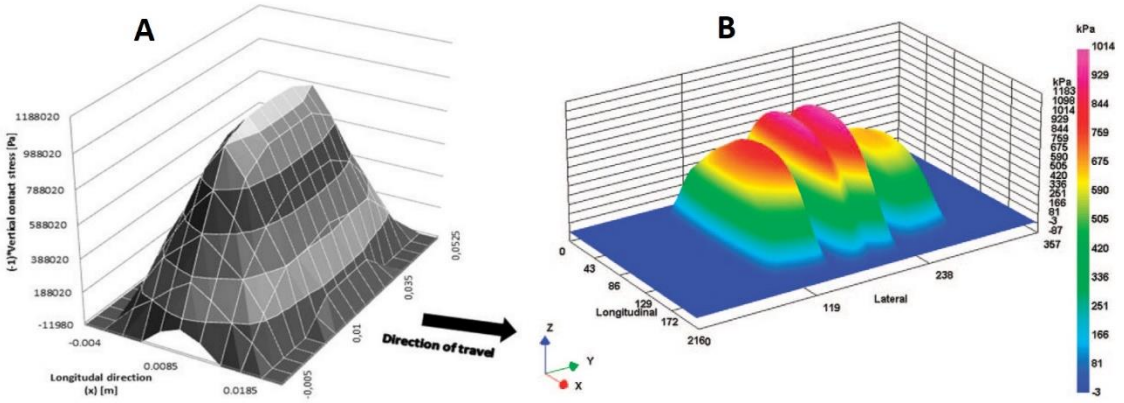

Figure 2.57 Vertical contact stress between the asphalt mix sample and the Hamburg wheel-tracking device (A), and the vertical contact stress distribution of a single tire (11xR22.5), tire loading of 20 kN and inflation pressure 800 kPa (B), adopted from [235,243]

The Hamburg wheel-tracking device, used by D'Angelo [223] for asphalt binder testing (MnRoad study), was equipped with steel wheels. The wheels of such device had a diameter of 203 mm and a width of 47 mm. Each steel wheel weighed 158 lbs. (~702.819 N), resulting in an average contact stress (uniform distribution) between the HMA sample and the steel wheel of 105 psi (~723.95 kPa), both values reported by the manufacturer [244]. The corresponding steel wheel/HMA sample contact area was therefore 970.8 mm^2 (20.7 mm long and 47 mm wide).

Due to the substantially lower hardness of the rubber hoop, used by Zak and Vavricka [243], compared to the steel wheel one would assume even higher differences between the two contact areas (970.8 mm^2 vs 1100 mm^2). Tsai *et al.* [245] determined the width and length of the contact area of the steel wheel apparatus to be 47 mm

and 11.8 mm (554.6 mm^2), respectively. Such significant decrease in contact area, compared to those reported by the manufacturers (970.8 vs 554.6 mm^2), results in substantially higher vertical contact stress (uniformly distributed) about 1267 kPa, and even higher peak contact stress if non-uniformly distributed.

Therefore, it can be concluded, that the average vertical contact stress, induced by the steel wheel of the Hamburg device used by D'Angelo [223] in MnRoad study, were considerably higher than those reported by Zak and Vavricka [243] for Hamburg device equipped with rubber hoop.

Wasage *et al.* [229] reported good correlation (R^2=0.98) between the Hamburg rutting results of two asphalt binders and the J_{nr} results measured at 12.8 kPa shear stress level. The apparatus used in the study was also equipped with solid rubber tires and was built by the same manufacturer as the one used by Zak and Vavricka [243]. Both, the mixture and the respective binder results, were evaluated at three different temperatures of 40, 50, and 60°C. In accordance with AASHTO T324 the applied load was set to 705 N, and the average (uniform) contact stress given by the manufacturer was 730 kPa [244]. The rubber wheels had a diameter of 203 mm, a width of 47 mm and the device operated at 52 wheel passes per minute. The contact area, expressed from the magnitude of tire load and vertical contact stress, were therefore about 20.5 mm long and 47 mm wide (~966 mm^2). However, considering the measurements conducted by Zak and Vavricka, the actual contact area between the HMA and the rubber hoop was closer to 1034 mm^2 (22 mm x 47 mm) what would have resulted in an average uniform contact pressure of 681 kPa.

In summary, Hamburg wheel-tracking devices equipped with steel wheel, apply to the HMA samples on average 1267 kPa contact pressure (uniform), while Hamburg devices of identical dimensions with rubber wheel between 681 and 730 kPa. Since the strain/stress distributions are very sensitive to the contact pressure magnitude and non-uniformity of the wheel loading, the steel wheel-induced non-uniform contact stresses may in fact exaggerate the rutting susceptibility of the tested binders [237].

Nonetheless, when the tire inflation pressures and tire loads of heavy trucks are compared to an ideal tire inflation (~234 kPa) and average wheel load (~4.0 kN) of midsize passenger cars the substantially higher contribution of heavy trucks to the development of permanent deformations become evident and beyond question. The traffic composition of highways in the Czech Republic consists of 73.3% passenger cars plus motorcycles and 26.7% heavy trucks [246]. Therefore, the evaluation of rutting resistance

should be rather based on the effects of heavy trucks. From this perspective, the vertical contact stress ranging between 630 and 730 kPa with ~1000 kPa peak value of non-uniformly distributed contact stress applied on the HMA sample by the Hamburg wheel-tracking device equipped with rubber hoop can be considered optimal.

MATERIALS AND METHODS

Both asphalt binder and asphalt mixture testing are part of the experimental program of the dissertation. In the following chapter, base asphalt binders and polymer modifiers used for asphalt modification are described along with the production of asphalt mixes and their characteristics. Furthermore, the testing protocols employed on both asphalt binders and mixes are briefly discussed along with the suggested changes of the multiple stress creep recovery (MSCR) test protocol.

3.1. Materials

Three conventional asphalts, a commercial product of Husky Energy, prepared by vacuum distillation of the same crude oil to 80/100, 200/300 and 300/400 Pen grade, were used in this dissertation. Note that the penetration grades of the vacuum residues are in accordance with the now withdrawn Canadian federal conventional asphalt specification (CAN/CGSB-16.3-M19 Asphalt Cement For Road Purposes) that was replaced by Superpave® performance grading, and it is used only for informational purposes.

The two softer vacuum residues were used as a base for modification by different polymers and their combinations, producing twelve PMAs, while the 80/100 Pen grade straight-run asphalt was investigated without any modification.

The most important physical and empirical properties and the Superpave® classification of the three base asphalts are presented in Table 3.1, Table 3.2, and Table 3.3, respectively.

Table 3.1 Properties of the 80/100 Pen grade base asphalt

	Unit	Base asphalt 80/100 Pen grade
Original binder		
Penetration (100g/5s), 25°C	[dmm]	91
Softening point	[°C]	46.5
Viscosity @135°C	[mPa·s]	437
Dynamic Shear $\lvert G^* \rvert / \sin \delta$=1.00 kPa @ Temperature	[°C]	64.8
RTFO Residue		
Mass Loss	[%]	–0.47
Dynamic Shear $\lvert G^* \rvert / \sin \delta$=2.20 kPa @ Temperature	[°C]	64.8
MSCR $J_{nr,3.2kPa}$ @64°C	[1/kPa]	4.39
MSCR %R @3.2 kPa @564°C	[%]	–0.1
PAV Residue		
Dynamic Shear $\lvert G^* \rvert \sin \delta$=5000 kPa @ Temperature	[°C]	19.8
Creep stiffness @60s	[MPa]	260
m-value @60s	[-]	0.323
@ Temperature	[°C]	–17
Superpave Performance Grade		PG 64-22
True Performance Grade		PG 64-27
Performance Grade by MSCR @64°C		PG 64S-27

Table 3.2 Properties of the 200/300 Pen grade base asphalt

	Unit	Base asphalt 200/300 Pen grade
Original binder		
Penetration (100g/5s), 25°C	[dmm]	234
Softening point	[°C]	37.8
Viscosity @135°C	[mPa·s]	223
Dynamic Shear $\lvert G^* \rvert / \sin \delta$=1.00 kPa @ Temperature	[°C]	54.4
RTFO Residue		
Mass Loss	[%]	–0.85
Dynamic Shear $\lvert G^* \rvert / \sin \delta$=2.20 kPa @ Temperature	[°C]	55.7
MSCR $J_{nr,3.2kPa}$ @52°C	[1/kPa]	2.91
MSCR %R @3.2 kPa @52°C	[%]	1.40
PAV Residue		
Dynamic Shear $\lvert G^* \rvert \sin \delta$=5000 kPa @ Temperature	[°C]	7.4
Creep stiffness @60s	[MPa]	278
m-value @60s	[-]	0.341
@ Temperature	[°C]	–25
Superpave Performance Grade		PG 52-34
True Performance Grade		PG 52-35
Performance Grade by MSCR @64°C		PG 52S-35

Table 3.3 Properties of the 300/400 Pen grade base asphalt

	Unit	Base asphalt 300/400 Pen grade
Original binder		
Penetration (100g/5s), 25°C	[dmm]	358
Softening point	[°C]	
Viscosity @135°C	[mPa·s]	166.5
Dynamic Shear $\|G^*\|/\sin\delta$=1.00 kPa @ Temperature	[°C]	49.7
RTFO Residue		
Mass Loss	[%]	–0.91
Dynamic Shear $\|G^*\|/\sin\delta$=2.20 kPa @ Temperature	[°C]	50.3
MSCR $J_{nr,3.2kPa}$ @46°C	[1/kPa]	2.46
MSCR %R @3.2 kPa @46°C	[%]	
PAV Residue		
Dynamic Shear $\|G^*\| \sin\delta$=5000 kPa @ Temperature	[°C]	6.6
Creep stiffness @60s	[MPa]	266
m-value @60s	[-]	0.324
@ Temperature	[°C]	–28
Superpave Performance Grade		PG 46-37
True Performance Grade		PG 49-38
Performance Grade by MSCR @64°C		PG 46S-37

In total six different modifiers and additives were used in order to alter the physical properties of the 200/300 and the 300/400 Pen grade base asphalts. Their content and combination was chosen and adjusted in a way that the Superpave® performance grade temperature of the modified blends before and after RTFO short-term aging was similar to true performance grade – PG 64-yy. The target PG grade was chosen based on the PG gradation of 80/100 Pen grade straight-run asphalt.

From the group of reactive elastomeric terpolymers (RET), Elvaloy™ 5160 (Figure 3.1), and Elvaloy™ EP1170 (commercially not available) were chosen for modification. Both polymers are produced by DOW Company (formerly by DuPont Company) and can be characterized as ethylene-based RETs with different content of glycidyl methacrylate (GMA), thus with different reactivity. The characteristics of these materials are presented in Table 3.4 and Table 3.5.

Elvaloy™ 5160 was used either alone or in combination with other polymers, while Elvaloy™ EP1170 was combined only with polyphosphoric acid (PPA).

Table 3.4 The physical properties of Elvaloy™ 5160 [247]

Characteristics		**Elvaloy™ 5160**
Property	Unit	Value
Vinyl acetate (min)	[%]	20
Glycidyl methacrylate (min)	[%]	5
Density @20°C	[g/cm^{3}]	0.95
Physical form	-	Pellet
Melt index @190°C/2.16 kg	[g/10 min]	12
Melting point	[°C]	80
Freezing point	[°C]	55
Maximum processing temperature	[°C]	220

Table 3.5 The physical properties of Elvaloy™ EP1170

Characteristics		**Elvaloy™ EP1170**
Property	Unit	Value
Vinyl acetate (min)	[%]	NA
Glycidyl methacrylate (min)	[%]	>5
Density @20°C	[g/cm^{3}]	NA
Physical form @25°C	-	Pellet
Melt index @190°C/2.16 kg	[g/10 min]	NA
Melting point	[°C]	NA
Freezing point	[°C]	NA
Maximum processing temperature	[°C]	NA

Figure 3.1 Free-flowing pellets of Elvaloy™ 5160 before low shear mixing with asphalt base

Because of its good results with asphalt and possible reaction with RET polymers, polyphosphoric acid (PPA) grade 115% H_3PO_4 (phosphoric acid), the product of Innophos Inc. (US), was used either alone or in combination with RET polymers to modify asphalt binders.

Table 3.6 The properties of polyphosphoric acid, PPA 115 [248]

Characteristics		**PPA 115**
Property	Unit	Value
P_2O_5 content	[%]	82.5–83.5
Density @20°C	[g/cm^3]	2.03–2.06
Melting point	[°C]	<0.1
Boiling point	[°C]	540
Physical state @25°C	-	Thick Liquid
Arsenic	[ppm]	<85
Ortho	[%]	4–6
Pyro	[%]	14–18
Tri	[%]	15–19
Tetra	[%]	15–19
Higher	[%]	40–50

Another polymer used for modification was SBS D1101 produced by Kraton Performance Polymers Inc. SBS D1101 is characterized as a medium molar mass linear block copolymer of styrene and butadiene with content of styrene of 31 wt.%. SBS is also used either alone or in combination with other polymers and/or additives in order to achieve the desired maximum service temperature of 64°C. The basic properties of SBS D1101 are shown in Table 3.7.

Table 3.7 The properties of thermoplastic elastomer Kraton® D1101 [249]

Characteristics		**Kraton® D1101**
Property	Unit	Value
Volatile matter (max)	[%]	0.7
Block Styrene (min)	[%]	29–33
Total styrene	[%]	31
Physical form @25°C	-	Pellet
Specific gravity	[g/cm^3]	0.94
Melt index @200°C/5 kg	[g/10 min]	<1
Hardness	°Shore A	69
300% Modulus	[MPa]	2.76
Elongation	[%]	880

Figure 3.2 Free-flowing pellets of SBS modifier before high shear mixing

One of the additives used in combination with SBS D1101 is technical sulfur, which was chosen as crosslinking agent. Furthermore, vacuum gas oil (VGO) was also used, which is usually added to asphalt binders to improve their low temperature characteristics. The basic properties of technical sulfur and VGO can be seen in Table 3.8 and Table 3.9, respectively.

Table 3.8 The properties of crosslinking agent, sulfur

Characteristics		**Sulfur**
Property	Unit	Value
Density @20°C	[g/cm^3]	2.07
Melting point	[°C]	113
Boiling point	[°C]	445
Physical state/form @25°C	-	Crystal/Powder
Solubility in CS_2	(%)	95.5–96.5

Table 3.9 The properties of vacuum gas oil

Characteristics		**VGO**
Property	Unit	Value
Boiling point	[°C]	327
Flash point	[°C]	179
Relative density @4°C	[-]	0.935
Physical state @25°C	-	Light liquid
Hydrogen sulfide (H_2S) content	[ppm] max	1

Another modifier used in combination with the above described modifiers/additives was the 30-40-mesh crumb rubber modifier (CRM), a commercial product of Recovery Technologies Inc. (Canada), made from vulcanized rubber reclaimed from old scrap tires.

Table 3.10 The properties of crumb rubber modifier

Characteristics		**CRM**
Property	Unit	Value
Mesh	-	30–40
Maximum particle size	[μm]	600
Type	-	Ambient
Total rubber hydrocarbon (NR&SR)	[%]	50
Carbon black	[%]	32
THF extractable	[%]	11
Ash	[%]	4

Figure 3.3 Crumb rubber modifier (30-40-mesh) reclaimed from old scrap tires

3.2. Preparation of asphalt blends

Out of the three straight-run asphalts the 80/100 Pen grade asphalt was tested without any modification, while the two less viscous binders, the 200/300 and 300/400 Pen grade asphalts, were blended with modifiers and/or additives. Depending on the types of modifiers different mixing protocols were used. The composition of all blends is summarized at the end of this chapter in Table 3.11.

3.2.1. Modification of asphalt by Elvaloy™ 5160

The modification protocol in the case of asphalt/Elvaloy™ 5160 was as follows: polymer was slowly added into the molten asphalt and stirred for seven hours. As a representative of RET modifiers, Elvaloy™ 5160 is also characterized as a polymer in which the curing takes place under the influence of either pressure, catalyst or added heat. Therefore, due to the reactive nature of Elvaloy™ 5160, the prepared blend was cured in the oven for an additional twenty-four hours at curing temperature before testing.

If the concentration of RET polymers exceed a limiting value, which is dependent on the properties of the polymer as well as on the chemical and physical structure of the asphalt base, the creation of an infusible and impermeable product of gel takes place. This results in the deterioration of some properties of the asphalt blend, such as pumping ability, mixing with aggregates etc. In order to avoid the risk of chemical gelation, the content of Elvaloy™ 5160 was fixed at 2.5 wt.%. The blending and curing times were adopted from the industry.

3.2.2. Modification of asphalt by Elvaloy™ 5160 and PPA 115, and by Elvaloy™ EP1170 and PPA 115

The modification protocol of asphalt blends with Elvaloy™ 5160/PPA 115, and Elvaloy™ EP1170/PPA 115 was as follows: in both cases the RET polymers were added to the molten 200/300 Pen grade asphalt and blended for six hours. Subsequently, PPA 115 was added to the blend and it was further mixed for one hour. Both blends were cured in the oven for an additional twenty-four hours at curing temperature before testing and mixing with aggregates. The blending and curing times were adopted from the industry. The concentration of RET and PPA was in both cases fixed at 2.0 wt.% and 0.2 wt.%, respectively.

3.2.3. Modification of asphalt by PPA 115

The preparation of asphalt blend modified only by PPA 115 was done by blending PPA 115 with the molten 200/300 Pen grade asphalt for an hour. Samples were prepared immediately after blending and then either tested, or cooled down to ambient temperature in accordance with the used testing protocols. The optimal concentration of PPA 115 was found to be 1.2 wt.%.

3.2.4. Modification of asphalt by SBS D1101

The modification protocol of asphalt blend with SBS D1101 was as follows: polymer was added to the molten 200/300 Pen grade asphalt and mixed with high shear mixer until no separate parts of polymer were observed. The optimal polymer concentration was found to be 3.3 wt.%, which corresponded to asphalt/SBS D1101 blend with dispersed polymer phase. Samples were prepared immediately after blending and then either tested, or cooled down to ambient temperature in accordance with the used testing protocols.

3.2.5. Modification of asphalt by SBS D1101 and Elvaloy™ 5160

The modification protocol of asphalt blend with SBS D1101 and Elvaloy™ 5160 was as follows: SBS D1101 was added to the molten 200/300 Pen grade asphalt and mixed with high shear mixer until no separate parts of polymer were observed up until one hour. Subsequently, Elvaloy™ 5160 was added to the blend and stirred using a low shear mixer for another five hours. The prepared blend was cured in the oven for an additional twenty-four hours at curing temperature before being tested and mixed with aggregates. The optimal SBS D1101 and Elvaloy™ 5160 concentration was found to be 2.0 wt.% and 1.0 wt.%, respectively.

Figure 3.4 Low (left) and high shear (right) mixers used in the study

3.2.6. Modification of asphalt by SBS D1101, Elvaloy™ 5160 and PPA 115

The modification protocol of asphalt/SBS D1101/Elvaloy™ 5160/PPA blend started with addition of SBS D1101 to the molten 200/300 Pen grade asphalt and mixed with high shear mixer until no separate parts of polymer were observed up until one hour. Subsequently, Elvaloy™ 5160 was added to the blend and stirred using a low shear mixer for another four hours then PPA 115 was added and the blend was further mixed for one hour. The optimal SBS D1101, Elvaloy™ 5160, and PPA 115 concentration was found to be 1 wt.%, 1 wt.%, and 0.2 wt.%, respectively.

3.2.7. Modification of asphalts by SBS D1101 crosslinked with sulfur

In order to produce an asphalt blend with 3-D polymer network by adding crosslinking agent, 200/300 Pen grade and 300/400 Pen grade asphalts were modified by SBS D1101/sulfur as follows: polymer was added to the molten asphalts and mixed with high shear mixer until no separate parts of polymer were observed up until one hour. Subsequently, sulfur was added to the blend and stirred using a low shear mixer for another two hours. In order to complete the vulcanization process, the prepared blend was stored in heated oven for an additional twenty-four hours before being tested and mixed with aggregates. While the concentration of sulfur was in both cases fixed at 0.12 wt.%,

the SBS content in the case of 200/300 Pen grade and 300/400 Pen grade asphalt was set at 2.7 wt.% and 3.5 wt.%, respectively.

3.2.8. Modification of VGO added asphalt by SBS D1101 crosslinked with sulfur

The modification protocol in the case of asphalt/VGO /SBS D1101/sulfur was as follows: vacuum gas oil was added to the molten 300/400 Pen grade asphalt and heated together until the blending temperature was reached. Then the polymer was added to the molten VGO/asphalt blend and mixed with high shear mixer until no separate parts of polymer were observed up until two hours. Subsequently, sulfur was added to the blend and stirred using a low shear mixer for another two hours. In order to complete the vulcanization process the prepared blend was stored in heated oven for an additional twenty-four hours before being tested and mixed with aggregates. The concentration of SBS D1101, VGO, and sulfur was determined at 4.3 wt.%, 5 wt.%, and 0.12 wt.%, respectively.

3.2.9. Addition of CRM to asphalt modified by Elvaloy™ 5160 and PPA 115, and by SBS D1101 crosslinked with sulfur

Two asphalt blends were modified by 30-40-mesh crumb rubber modifier. In the case of asphalt/Elvaloy™ 5160/PPA/CRM blend, the modification protocol was as follows: first the RET polymer was added to the molten 200/300 Pen grade asphalt and mixed for three hours then the PPA 115 was added and the blend was mixed for an additional one hour. Subsequently, the crumb rubber was added, and the blend was stirred for another two hours. The optimal concentration of RET, PPA, and CRM was determined at 1 wt.%, 0.2 wt.%, and 2 wt.%, respectively.

In the case of asphalt/SBS/sulfur/CRM blend the modification protocol was as follows: SBS D1101 was added to the molten 200/300 Pen grade asphalts and mixed using a high shear mixer until no separate parts of polymer were observed up until one hour. Subsequently, sulfur was added to the blend and stirred using a low shear mixer for another two hours. Then the CRM was added and mixed with the blend for an additional two hours. The optimal concentration of SBS, sulfur, and CRM was determined at 1 wt.%, 0.12 wt.%, and 3 wt.%, respectively.

In both cases, samples were prepared immediately after blending and then either tested, or cooled down to ambient temperature in accordance with the used testing protocols.

Table 3.11 Composition of all asphalt blends

Base Binder	Sample ID/ Polymer Type Designation	Elvaloy 5160 wt.%	Elvaloy EP1170 wt.%	PPA 115 wt.%	SBS D1101 wt.%	Sulfur wt.%	VGO wt.%	CRM wt.%
80/100	None	100.00						
200/300	RET+PPA	2.00		0.20				
	SBS+S				2.70	0.12		
	RET	2.50						
	RET+SBS	1.00			2.00			
	SBS				3.30			
	PPA			1.20				
	RET+PPA+CRM	1.00		0.20				2.00
	SBS+RET+PPA	1.00		0.20	1.00			
	SBS+S+CRM				1.00	0.12		3.00
	RET(EP)+PPA		2.00	0.20				
300/400	SBS+S				3.50	0.12		
	SBS+S+VGO				4.30	0.12	5.00	

3.3. Preparation of asphalt mixes

Preparation of the hot mix asphalt samples was conducted according to the Superpave mix design method AASHTO R35-12 [250]. Prior to binder mixing with aggregate, the desired combined gradation of the aggregate skeleton was designed, which consisted of five different mineral aggregate stockpiles produced by Lafarge North America Inc. (Calgary, Alberta): 16 mm, 12.5 mm, 5 mm, manufactured fines (MF), and washed MF and no intermixtures were added.

Dense-graded (also called well-graded) HMA was chosen for testing, as this mix is generally the most suitable for all pavement layers and all traffic conditions. The combined gradation had a nominal maximum aggregate size of 12.5 mm, which conformed to the minimum and maximum gradation requirements specified in AASHTO M323-12 [251].

Table 3.12 Aggregate gradation of stockpiles blended to produce combined gradation of dense-graded HMA with 12.5 mm nominal size

Sieve size (mm)	Mineral aggregate stockpile gradation (% passing)					12.5 mm[1] Combined gradation
	16 mm	12.5 mm	5mm	MF	Washed MF	
19.0	100.0	100.0	100.0	100.0	100.0	100.0
16.0	95.7	100.0	100.0	100.0	100.0	99.6
12.5	40.7	97.4	100.0	100.0	100.0	93.4
9.5	8.5	69.0	100.0	100.0	100.0	82.8
4.75	1.2	4.0	67.5	93.2	88.7	58.0
1.18	0.7	1.7	4.2	43.7	37.1	24.3
0.60	0.7	1.6	3.6	31.1	24.8	17.1
0.30	0.7	1.5	3.0	21.9	14.6	11.5
0.15	0.6	1.3	2.3	15.1	7.1	7.4
0.075	0.6	1.1	1.6	11.0	4.9	5.4

MF Manufactured fines
[1] Nominal size

The combined gradation, the minimum and maximum gradation requirements for dense-graded mix, and the proportion of each type of aggregate in the combined gradation are presented in Figure 3.5.

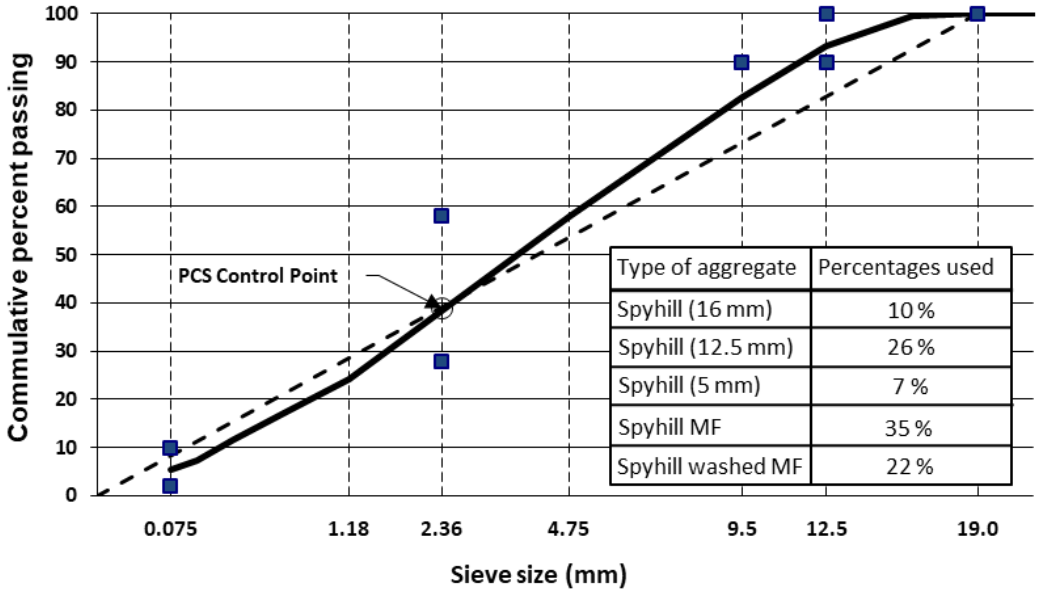

Figure 3.5 The combined gradation plotted on 0.45 power chart

When preparing the asphalt mixes, the same job mix formula (JMF) was used for each HMA with asphalt content of 5.9 wt.% to ensure that the only difference between the mixes was the type of the asphalt binder. Furthermore, the asphalt mixes were compacted to the same gradation with the same air void content of 6%.

The same mixture conditioning procedure was carried out in accordance with AASHTO R30 [252]. This procedure is meant to represent the short-term aging of asphalt mixes and mimic the oxidation and asphalt absorption into the aggregates that would occur for a typical dense-graded HMA during mixing and construction. During short-term aging procedure the loose mix was spread out at an even thickness and heated in a forced-draft oven for four hours at 135 ± 3°C. The mixture was stirred in every 60 ± 5 min to maintain uniform conditioning.

Figure 3.6 Hot mix asphalt mixer

3.4. Test methods – asphalt binders

Within the scope of this study, both conventional (empirical) and physical properties of binders are evaluated. In the following chapter, the testing protocols are briefly discussed.

3.4.1. Empirical test methods – asphalt binders

Penetration test without doubt is one of the oldest empirical test methods used for characterizing the asphalt binders' consistency. The main advantage of this test is its simplicity and that it could easily characterize the measure of hardness or consistency of the asphalt binders. However, with the advent of modified asphalts, the simplicity of the test also became its main drawback since it could not express the elasticity of the material.

Asphalt sample was heated until molten, then poured into the steel container to a depth of at least 10 mm in excess of the expected penetration. The sample was then protected from dust and allowed to cool at a temperature between 15 to 30°C for one hour. Along with the transfer dish, it was then transferred in the water bath at 25 ± 0.1°C, in which the temperature of water and asphalt sample was maintained at 25 ± 0.1°C for 60 minutes. The needle was adjusted until it made a contact with the surface of the sample. Testing was conducted at temperature 25 ± 0.1°C. Through the needle, 100 g weight was applied for five seconds. At least three readings were made at three points on the surface of the sample not less than 10 mm apart and not less than 10 mm from the side of the dish. Between each testing the needles were changed and the results were expressed as the vertical distance in one tenth of a millimeter or in decimillimeters (1 dmm = 0.1 mm).

Figure 3.7 Penetrometer and the penetration needles

Ring and ball method was used to determine the softening point of asphalt binders. The softening point of asphalt is the temperature at which the substance attained a particular degree of softening. The test consisted of two brass ring and two steel balls. The softening point is the temperature at which the standard steel balls pass through the samples of asphalt in a mold and fall through a height of 25 mm, while heated in water or glycerin at controlled rate.

Asphalt sample was heated until molten, then poured into the ring mold. After cooling for thirty minutes on ambient temperature, the material was levelled in the ring by removing the excess material with a warmed, sharp knife. Water bath was filled with distilled water to a height of 50 mm above the upper surface of the rings. The starting temperature was 5 ± 1°C at which the samples were kept for fifteen minutes.

The normalized steel balls (3.5 g, ⌀ 9.5 mm) were then placed on the bitumen film, and the temperature of the water heated at a uniform rate of 5 ± 0.5°C per minute. As the temperature increased, the bituminous material softened and the steel balls sank through the rings until they touched the bottom plate. At the point when both balls reached the bottom plate the temperatures were recorded, and the average of the two readings was reported as the softening point.

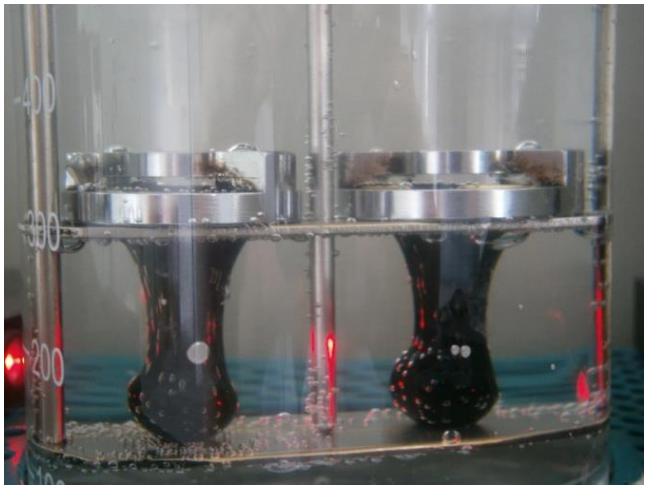

Figure 3.8 Ring an ball apparatus

By many manufacturers, the **elastic recovery** was used to confirm whether a sufficient type or amount of modifiers was added to the asphalt base to provide significant elastomeric characteristics. The test was widely used as PG "Plus" test, an additional test to the Superpave® performance grade specification.

As per EN 13398, the elastic recovery of an asphalt binder was measured by the recoverable strain determined after severing the elongated briquet specimens of the material of the form shown in Figure 3.9. The specimens were pulled to a specified distance, at a specified speed and at a specified temperature.

After the elastic recovery molds were assembled, they were greased and placed on top of an also greased tile. The heated asphalt sample was poured into the molds and left to cool for sixty minutes at ambient temperature. Then the excess asphalt was trimmed using a hot knife and placed into the water bath for 90 ± 10 min that was maintained at 25.0 ± 0.5°C. After the side pieces of the molds were detached, the rings at each end of the molds were attached to the hooks of the testing device. Once the test was started, the samples were stretched at a uniform speed (50.0 ± 2.5 mm/min) to an elongation

of 200 ± 1 mm. As soon as the 200 mm of elongation was reached, the test specimens were cut into two halves at the midpoint within ten seconds using the scissors. The specimen was then left in the testing machine in an undisturbed condition at 25.0 ± 0.5°C for 30 ± 1 min. The total length of the specimen with the severed ends just touching each other was measured and the elastic recovery was reported as a percentage to which the asphalt sample recovered its original length.

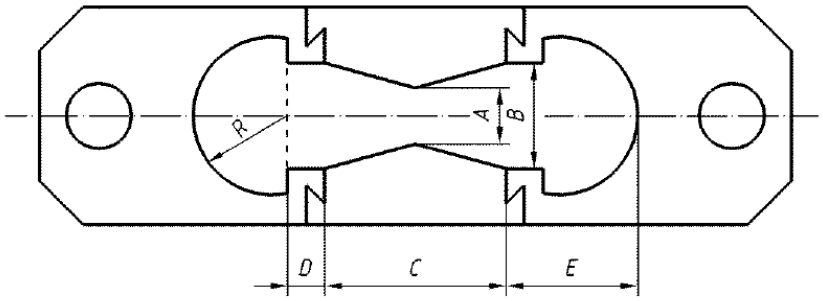

Figure 3.9 Mold for making briquette specimen

3.4.2. Superpave® asphalt binder specification

In order to address the processability (pumpability, mixability, workability) of asphalt binders at manufacturing and construction temperatures, their **viscosity** is determined using rotational viscosimeter. Since, usually both temperatures are fairly similar, regardless of the environment, the temperature specified in the Superpave® PG grade asphalt binder specification was set at 135°C.

The molten sample of 10.3 ± 0.1 g was poured into the preheated sample chamber, which was then placed into the preheated environmental chamber (Thermosel) unit of the Brookfield viscosimeter DV-II+ Pro equipped with spindle SC4-27. The preheated spindle was carefully lowered into the sample, which was then maintained at 135°C for approximately thirty minutes and was allowed to equilibrate at test temperature for further ten minutes. Viscosity was reported as the average of three readings given in millipascal-seconds [mPa·s]. According to the specification AASHTO T316-13 [253], the maximum viscosity at 135°C must not exceed 3000 mPa·s in order to ensure the processability of the asphalt and asphalt mixes.

Figure 3.10 Rotational viscosimeter

The effects of manufacturing and placement of asphalt pavements was simulated with help of artificial short-term aging of blends in the **rolling thin film oven (RTFO)** in accordance with the standard AASHTO T240-13 [254]. One of the main goals of the Superpave® PG binder specification is to perform physical properties testing on binders that were exposed to similar effects as those experienced during manufacture and placement, so that their properties are as close as possible to their field performance.

During manufacture (mixing) and construction processes asphalt binders lose some of their light oily fractions (i.e., volatiles) resulting in an increase in their viscosity. Therefore, as a second purpose of RTFO is to provide a quantitative measure of the volatiles lost during the aging process. However, the mass of some binders may also increase due to oxidative products formed during the test.

Two hours prior to testing the oven was preheated until the temperature stabilized at 163 ± 1°C with. Heated sample of asphalt binder (in eight bottles of approximately 35 ± 0.5 g each) was poured into a bottle. Immediately after pouring, each bottle was turned on their side without rotating and placed on a cooling rack for at least 60 min but no more than 180 min before start. Once the bottles were placed in the RTFO oven carousel it was rotated at 15 ± 0.2 r/min for 85 min (Note: EN 12607 specifies 75 min) while the temperature of the oven was maintained at 163°C and the airflow into the bottles

at 4000 ± 300 ml/min. According to AASHTO T240-13 a mass loss for any grade must not be higher than 1.0 wt.%.

Figure 3.11 Rolling thin film oven (RTFO) with bottles in the carousel

During their service time asphalt pavements become prone to low temperature related distresses (e.g., thermal and fatigue cracking). In order to address these types of distresses, Superpave® PG binder specification require to test long-term aged asphalt binders at intermediate and cold temperatures. Therefore, accelerated aging of asphalt binder using a **pressurized aging vessel (PAV)** was used in accordance with AASHOT R28-12 [255] to simulate in-service aging over a seven to ten-year period in a pavement.

PAV test was conducted on RTFO-aged residues placed in two stainless steel pans of 50 ± 1 g each and aged at the specified aging temperature for twenty hours in a vessel pressurized with air to 300 psi (2.07 MPa). The ageing temperature was selected according to the grade of the asphalt blend. After performing accelerated oxidative aging, the asphalt blend residue was degassed in a vacuum oven before being used for further analysis.

Dynamic mechanical analysis of asphalt binders using a dynamic shear rheometer (DSR) was conducted according to AASHTO T315-12 [256]. As described in Chapter 2.7.1, SHRP in Superpave® PG binder specification introduced two important material properties to determine in small amplitude oscillations over a range of

temperatures: the complex modulus, $|G^*|$, and the phase angle, δ. These two properties were measured at high and intermediate temperatures and at constant frequency of 10 rad/s (1.59 Hz) using the Kinexus Pro+ rheometer (Figure 3.12).

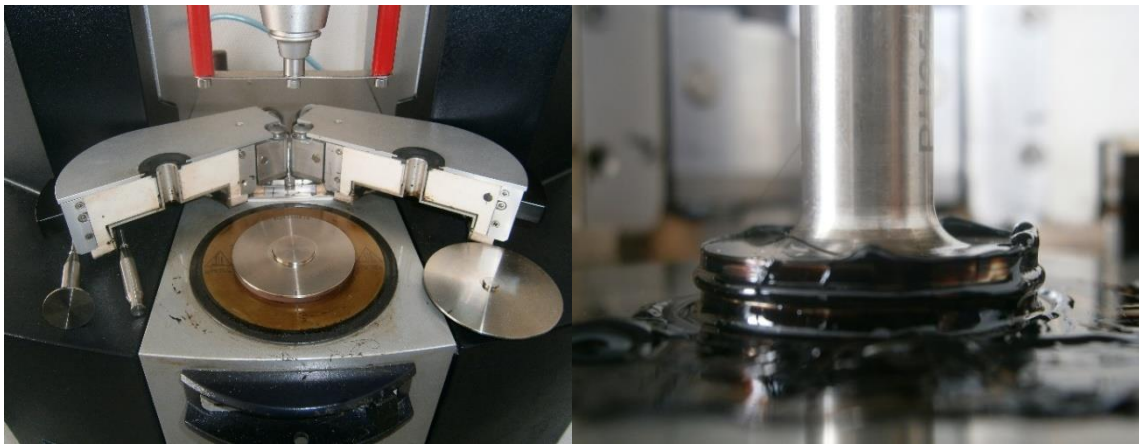

Figure 3.12 Dynamic shear rheometer (left) and a sample sandwiched between the two plates (right)

Complex modulus or shear modulus, $|G^*|$, is defined as the ratio of the resulting stress to the applied strain. By applying sinusoidal loading by the DSR, the resulting stress and strain vary periodically. Phase angle, δ, expressed in degrees, is defined as the phase shift between the applied strain and stress response of the material (Figure 2.48 and Figure 2.49). Usually, the magnitude of both properties are calculated by the DSR.

A small sample of asphalt binder was sandwiched between the two plates (plate-plate geometry) of the DSR. Unaged asphalt binders and RTFO residues were tested using plates 25 mm in diameter and 1 mm gap between the two plates. For testing PAV residues at intermediate temperatures 8 mm geometry was used with 2 mm gap. The calculation of complex modulus, $|G^*|$, and phase angle, δ, was automatically processed by software (rSpace) as well as the different service temperatures (i.e., maximum service temperature of unaged and RTFO-aged samples, and intermediate service temperature of PAV-aged samples). The tested blends had to meet the specification requirements described in AASHTO T315-12 (Table 3.13). The Superpave® rutting parameter, $|G^*|/\sin\delta$, related to the rutting resistance of asphalt blends, estimated the maximum service temperature, while the parameter, $|G^*| \cdot \sin\delta$, related to fatigue cracking, estimated the intermediate service temperatures.

Table 3.13 Requirement according to AASHTO Superpave® PG specification

Asphalt binder	DSR geometry (mm)	Angular frequency (rad/s)	Shear strain (%)	AASHTO requirement
Original	25	10	12	$\lvert G^* \rvert / \sin\delta \geq 1.0$ kPa
RTFO-aged	25	10	10	$\lvert G^* \rvert / \sin\delta \geq 2.2$ kPa
PAV-aged	8	10	1.0	$\lvert G^* \rvert \cdot \sin\delta \leq 5.0$ MPa

Usually, at low temperatures, asphalt binders harden to such an extent that their properties cannot be measured with sufficient accuracy by DSR. As a solution **bending beam rheometer (BBR)** was introduced to evaluate low temperature properties of binders (e.g., stiffness and the ability to relax stresses) from their tensile creep characteristics in accordance with AASHTO T313-12 [257]. At low temperatures, when HMA pavements contract and build up internal stresses it is essential to relax these stresses, otherwise the pavement may crack. Therefore asphalt binders that are not too stiff and are able to adapt to these stress changes without cracking are desirable.

PAV residues of the binders were used to prepare rectangular beam samples with dimensions of 125 x 12.5 x 6.25 mm. The tested beams were then cooled and conditioned at test temperature for 60 ± 2 min in a liquid bath. A constant load (980 ± 50 mN) was applied to the simply-supported asphalt beams at mid span for 240 s. The resulting deflection was monitored with time. By using beam theory, the creep stiffness, S, of the asphalt beam sample was calculated and, along with the slope, m, of the stiffness curve, $\log S$ - $\log t$, used as the low temperature characteristics of the blends. The calculations were automatically made by the BBR software.

Although originally the occurrence of thermal cracking was associated with the creep stiffness after two hours of loading, by using time-temperature superposition, an equal creep stiffness could be obtained after one minute loading, only at 10°C higher temperature than the temperature of interest. Therefore, both the creep stiffness and the slope of stiffness at sixty seconds on log-log plot of $S(t)$ was chosen as a specification parameter to determine the minimum service temperature of binders. The parameters of PAV-aged asphalt binders, required by the specification, were $S_{\max}(60)$ = 300 MPa, $m_{min}(60)$ = 0.3.

3.4.3. Multiple stress creep recovery test – asphalt binders

The Kinexus Pro+ rheometer (DSR) was utilized in this study to perform multiple stress creep recovery (MSCR) test, which evaluated the following non-dynamic values of the RTFO residue at two stress levels: non-recoverable creep compliance ($J_{nr,0.1}$, $J_{nr,3.2}$), average percent recovery ($\%R_{0.1}$, $\%R_{3.2}$), and percent difference between non-recoverable creep compliance at 0.1 kPa and at 3.2 kPa ($J_{nr,diff}$).

As described in AASHTO T350-14 [258], the MSCR test was performed on a 1 mm-high cylindrical asphalt sample sandwiched between two 25 mm-diameter parallel plates in a DSR. During the MSCR test a constant shear load was applied to the sample for 1 s, followed by 9 s recovery at zero load. Thus, one cycle could be divided into two distinguishable phases of creep and recovery. Two shear stress levels of 0.1 kPa and 3.2 kPa were applied successively, and a total of ten cycles were conducted for each stress level with no time lag between the two different loading levels at temperatures 58°C and 64°C.

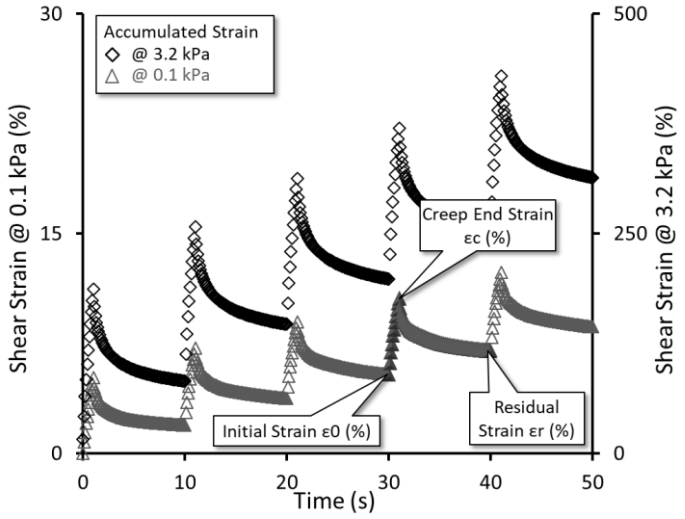

Figure 3.13 Typical five cycles of the multiple stress creep recovery testing of asphalt binders at standard stress levels

Five sequential cycles at two applied shear stress levels of the MSCR test are presented in Figure 3.13. During the measurement the resulting shear strain is monitored. A cycle is characterized by three main turning points between each phase and the corresponding strain values, namely: initial strain, ε_0, creep end strain, ε_c, and residual strain, ε_r, respectively. The initial strain is the shear deformation at the beginning of the

creep portion of each cycle, while creep end strain stands for the strain value at the end of the creep portion. Residual strain is then the shear deformation at the end of the recovery portion. In Figure 3.14 the three most important strain responses to shear stress (e.g., creep strain, recovered strain, non-recovered strain) are depicted in a plot of a typical cycle of creep and recovery test.

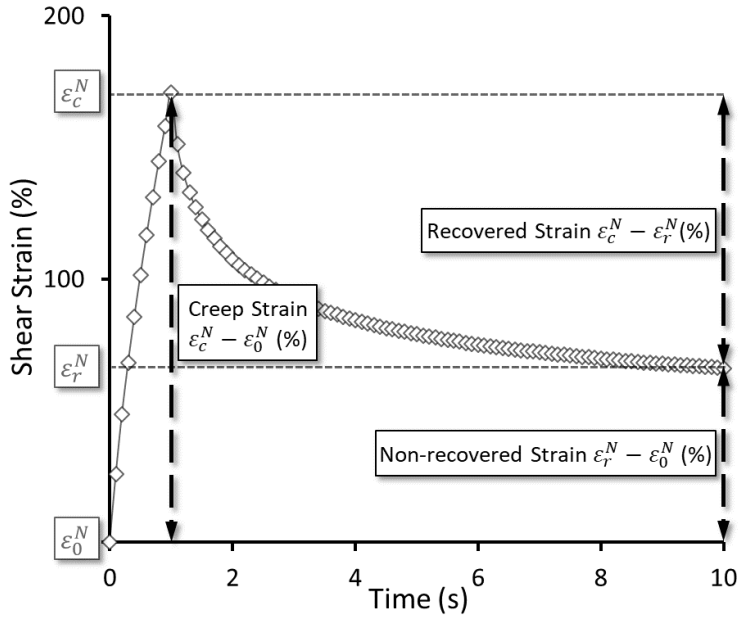

Figure 3.14 Typical cycle of the MSCR testing of asphalt binders

The non-recovered strain is the adjusted strain value at the end of the tenth second (the end of the recovery phase) of each Nth cycle given by Equation (3.1):

$$\varepsilon_{10}^N = (\varepsilon_r^N - \varepsilon_0^N) \tag{3.1}$$

The non-recoverable creep compliance, $J_{nr}(\sigma, N)$, value for one cycle is calculated in accordance with the Equation (3.2), where the non-recovered strain is divided by the applied shear stress (σ, kPa)

$$J_{nr}(\sigma, N) = \frac{\varepsilon_r^N - \varepsilon_0^N}{\sigma} = \frac{\varepsilon_{10}^N}{\sigma} \tag{3.2}$$

After ten successive cycles conducted at each applied shear stress levels the average non-recoverable creep compliance, $J_{nr}(\sigma)$, is determined in accordance with Equation (3.3):

$$J_{nr}(\sigma) = \frac{\sum_{N=1}^{10} J_{nr}(\sigma, N)}{10} \tag{3.3}$$

As described in Chapter 2.7.3, the polymer chain in polymer modified asphalt blends may substantially rearrange when the applied stress level is increased, resulting in non-linear strain response. According to AASHTO M332, the percent increase in J_{nr} of a binder due to the increased stress levels from 0.1 to 3.2 kPa must be less than or equal to 75% of the J_{nr} at 0.1 kPa. This limiting value should ensure that the tested binder will not be overly stress-sensitive to unexpected heavy loads at high service temperatures [213].

$$J_{nr,diff} = \frac{J_{nr,3.2\ kPa} - J_{nr,0.1\ kPa}}{J_{nr,0.1kPa}} * 100 \leq 75\% \tag{3.4}$$

As described earlier, D'Angelo *et al.* [209] proved that J_{nr} can be more successful in determining the rut resistance of asphalt binders than Superpave® PG "Plus" tests or even the SHRP binder criteria of $|G^*|/\sin\delta$. However, J_{nr} alone cannot sufficiently identify the presence of an elastomeric polymer in the asphalt, since even very stiff air-blown binders exhibit extremely low J_{nr} values, despite having minimal flexibility. In order to replace the empirical elastic recovery tests, that were used by many agencies to confirm the presence and the volume of modifiers in the binder, percent recovery ($\%R$) was introduced. It is the average value of the proportion of recovered strain to creep strain (Equation (3.5) and (3.6)).

$$\%R(\sigma, N) = \frac{\varepsilon_1^N - \varepsilon_{10}^N}{\varepsilon_1^N} * 100 \tag{3.5}$$

$$\%R(\sigma) = \frac{\sum_{N=1}^{10} \%R(\sigma, N)}{10} \tag{3.6}$$

where

$$\varepsilon_1^N = (\varepsilon_c^N - \varepsilon_0^N) \tag{3.7}$$

which is the adjusted strain value at the end of the creep portion (i.e., after 1.0 s) of each cycle.

Percent recovery provides significant information about the presence of elastomeric polymers in the binder or about how successful their reaction was with the asphalt base. In combination with J_{nr}, $\%R$ can determine if the binder's elastic response is primarily from the polymer network present in the blend and not from the stiffening of the asphalt base. A specification limit was established based on a power function presented in Equation (3.8).

$$\%R = 29.371 \cdot J_{nr,3.2\ kPa}{}^{-0.2633} \quad (3.8)$$

Only the binders above the MSCR specification line are considered being sufficiently modified with an acceptable elastomeric polymer.

It is important to note that the MSCR specification line stops at 2.0 kPa^{-1}, since the main goal of its use is to assure that very stiff binders with no polymer will not be classified as elastomeric and assure that the polymer modified binders have well developed polymer networks [259]. Therefore, $J_{nr,3.2\ kPa}$ values greater than 2.0 kPa^{-1} are not required to have any minimum value of $\%R$.

Based on the J_{nr} results measured at PG maximum service temperature and at 3.2 kPa stress level MSCR allows to categorize asphalt binders into four different grades, each of which corresponds to a specific traffic intensity. Asphalt binders from each group should be sufficiently rut resistant in order to withstand the corresponding traffic loading ranked from standard to extreme. In accordance with AASHTO M332-14 [260], $J_{nr,3.2\ kPa}$ results of asphalt binders ranging from 4.5–2 kPa^{-1}, 2–1 kPa^{-1}, 1–0.5 kPa^{-1} and less than 0.5 kPa^{-1} correspond to standard traffic (S) (<10 million ESALs traffic and >70 km/h load rate), high traffic (H) (10–30 million ESALs traffic or 20–70 km/h load rate), very high traffic (V) (>30 million ESALs traffic or <20 km/h load rate) and extremely high traffic (E) (for >30 million ESALs traffic and <20 km/h load rate), respectively.

3.5. Test methods – Asphalt mixes

3.5.1. Hamburg wheel-tracking test

Although full-scale track tests would be desirable, they are time consuming and costly to construct. Therefore, laboratory size wheel tracking tests, which are a much cheaper alternative to full-scale track tests, became widely used by researchers and highway agencies as a tool for prediction of the rutting potential of HMA pavements. Furthermore, the efficiency of laboratory size wheel tracking tests is beyond question, since it can be completed within couple of days, even if sample preparation is included.

The test successfully simulates the actual stress conditions occurring in the pavement, although its purpose is still limited to the ranking of materials rather than predicting the actual rutting depths in the field. Nonetheless, the relationship between

the performance of asphalt mixes in the wheel tracking test and their behavior on site was confirmed by many researchers [261–263].

The Hamburg wheel-tracking test (HWTT) was conducted in accordance with EN 12697-22+A1 to determine the rutting resistance of the produced asphalt mixes [264]. At least two slab specimens with dimensions of 320 x 260 x 50 mm were prepared from each asphalt mix using hydraulic segment compactor. After their volumetric characteristics were determined, the slab specimens were trimmed and fixed in steel molds of the Hamburg wheel-tracking device (HWTD). The slab specimens were conditioned at constant temperature of 60°C controlled by hot air for twelve hours before testing.

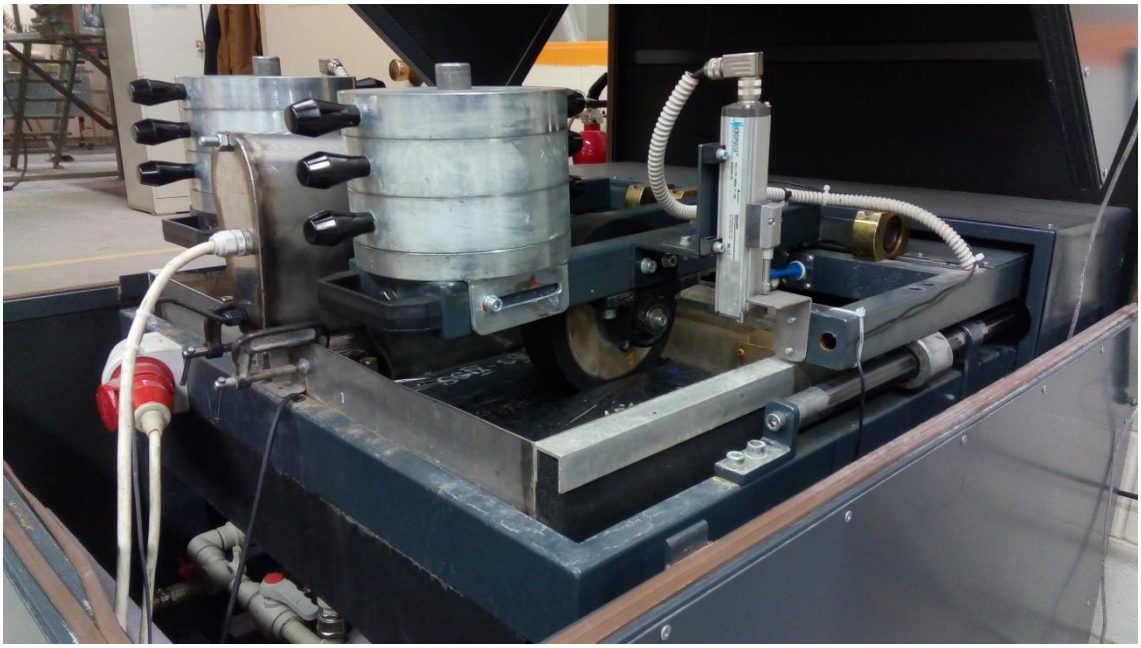

Figure 3.15 Hamburg wheel-tracking device after testing

A wheel with a 20 x 47 mm solid rubber hoop and an outside diameter of 203 mm was reciprocated continuously on the surface of each specimen with 52 wheel passes per minute. The rubber hoop applied a 705 ± 4.5 N load on a 22 x 47 mm contact area of each HMA slab.

The rut depth was measured by a linear variable displacement transducer (LVDT) located in the middle of the specimens at different increments. The wheel continued to reciprocate either until 10,000 cycles (20,000 passes) were completed or until the impression reached a depth of 20 mm.

The depth of the impression and the ambient temperature in the cabinet were recorded by an internal data acquisition and control system. The rut depth results were reported as the average value of two tested specimens.

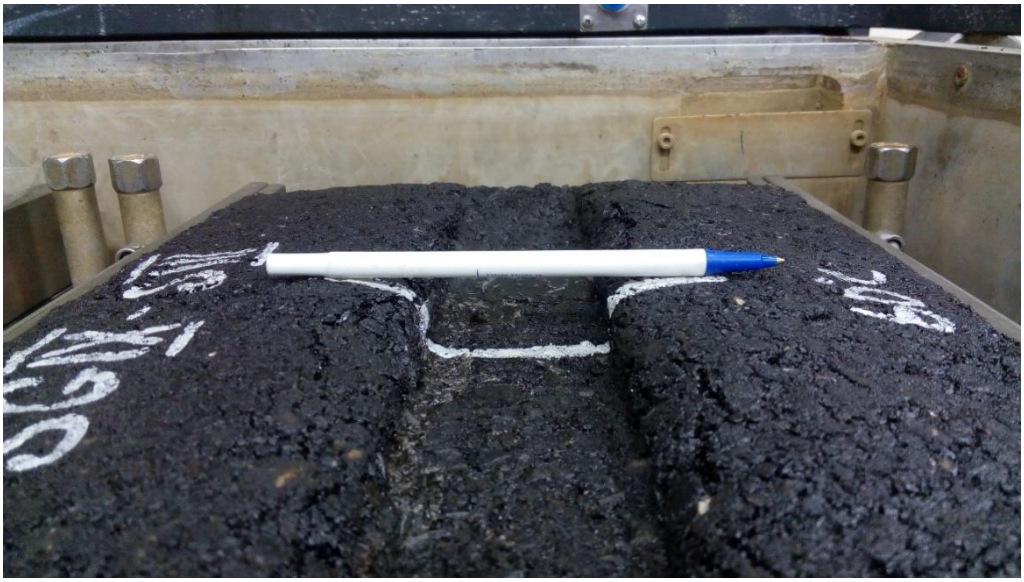

Figure 3.16 Hamburg slab specimen after 10,000 cycles of wheel tracking device at 60°C (HMA with PPA-modified binder)

3.5.2. Dynamic modulus test – Asphalt mixes

The linear viscoelastic (LVE) properties of asphalt mixes could be described by their complex modulus, E^*, evaluated over a wide frequency domain. Based on the result of Projects 9-19 and 9-29 [265] conducted by the National Cooperative Highway Research Program (NCHRP), the dynamic modulus test has been selected to be implemented in the new Superpave® volumetric mix design introduced by SHRP. The key objective of the NCHRP project was to develop simple performance tests (SPT) for permanent deformation and fatigue cracking to be incorporated in the Superpave® volumetric mix design method, because it was based only surrogate properties of the mixes to control their performance properties [265]. The NCHRP projects concluded that SPT could be used to evaluate the performance potentials of asphalt mixes and, therefore, dynamic modulus, $|E^*|$, became a key material property in asphalt mix design. The parameter of $|E^*|/\sin\phi$ was proposed to indicate permanent deformation (rutting), where the ϕ was the phase angle, representing the time lag between the applied load and the strain response. Despite the fact that SPT was developed and models have been designed to predict the stress-strain response and the performance of the mixes (rutting, fatigue

cracking, thermal cracking), eventually the system was found to be too difficult and time consuming for mix design and quality control.

Nevertheless, the dynamic modulus, $|E^*|$, in the form of a master curve has been selected to characterize the temperature and loading rate (frequency) dependency of stress-strain behavior of HMAs in the new AASHTO 2002 "Guide of Design of New Rehabilitated Pavement Structures", or "Mechanistic-Empirical Pavement Design Guide (MEPDG)", as it has later became known .

Dynamic modulus test was conducted in servo-hydraulic-controlled universal testing machine (IPC Global UTM-100) with 100 kN capacity in order to obtain the rheological parameters and develop master curves of asphalt mixes. The test was conducted in accordance with AASHTO T342-11 [266].

Cylindrical specimens 150 mm in diameter and 170 mm high were prepared by using Superpave gyratory compactor (SGC) (AASHTO T312-09). After the compacted samples were cored (diameter of 100 mm), sawed and grinded (height 150 ± 2.5 mm), their material properties were determined. Three specimens were tested for each asphalt binder and the average values were reported. Three axial LVDTs with gauge lengths of 70 mm were mounted to the specimen at 120° around the diameter to read the deformation. Before starting the test a contact load equal to 5% of the dynamic load was applied to the specimen.

Figure 3.17 Dynamic modulus test specimen (left), LVDTs mounted to the specimen (right)

The dynamic modulus test was conducted in stress-control within the LVE range. For this reason and in order to avoid damage, controlled sinusoidal vertical compressing stress wave was applied to the specimen to produce total axial strain amplitude between 50 and 150 micro strain. The displacement was measured at constant temperature and frequency. The cylindrical specimens were placed into an environmental chamber and maintained at a set of testing temperatures ranging from –15 to 60°C incremented by 15°C. Note that in order to cover a wider temperature range that included 60°C, the temperature set in this test differed from that specified in the standard. Six testing frequencies of 25, 10, 5, 1, 0.5, and 0.1 Hz, respectively were used at each temperature. Testing was performed in an unconfined compression mode from high to low frequency and from low to high temperature. After each frequency, at least five minute rest period was allowed for the sample to recover.

For each asphalt mix sample at every temperature-frequency combination the applied stress and the axial strain response were recorded and used to calculate the magnitude of dynamic modulus, $|E^*|$, and the phase angel, ϕ, related to the time lag, Δt, between the stress input and strain response at the corresponding frequency, f. The magnitude of dynamic modulus was calculated by dividing the steady state stress amplitude by the strain amplitude, analogously to Equation (2.37), as follows:

$$|E^*| = \frac{\sigma_0}{\varepsilon_0} \tag{3.9}$$

where σ_0 was the axial steady (compressive) stress, and ε_0 was the axial (compressive) strain. Based on the phase angle and dynamic modulus, the axial storage and loss moduli were calculated as:

$$E' = |E^*| \cos\phi \tag{3.10}$$

$$E'' = |E^*| \sin\phi \tag{3.11}$$

where E' was the storage modulus and E'' was the loss modulus, while

$$E^* = E' + iE'' \tag{3.12}$$

The loss tangent defined the ratio of the lost and stored energy in a cyclic deformation:

$$\tan\phi = \frac{E''}{E'} \tag{3.13}$$

Asphalt mixes within the LVE range are known to be thermodynamically simple materials, therefore, from the experimental data obtained at different smaller frequency windows and at several constant temperatures a single master curve could be obtained

that could significantly extend the effective time and frequency scale of the measurement. This can be achieved via the time-temperature superposition principle, which allows for the construction of the master curves of E', E'', and the loss tangent $\tan\phi$ by shifting the measured functions taken at different temperatures [194,196]. The method of constructing the master curves was analogous to that described in Chapter 2.5.7. To create a master curve, the reduced frequency, f_r, was defined in accordance with Equation (2.50), while the temperature dependency of the horizontal shift factor, a_T, according to the Williams–Landel–Ferry (WLF) relation described in Equation (2.52) [196].

With the help of IRIS software [267] the discrete relaxation spectrum $\{E_i, \lambda_i\}_{i=1,2,\ldots,N}$ and the retardation spectrum $\{D_i, \Lambda_i\}_{i=1,2,\ldots,N}$ was obtained by fitting the master curves of storage, E', and loss, E'', moduli in accordance with the following expressions, analogous to Equations (2.43) and (2.44):

$$E'(\omega) = E_e + \sum_{i=1}^{N} \frac{E_i(\omega\lambda_i)^2}{1+(\omega\lambda_i)^2} \tag{3.14}$$

$$E''(\omega) = \sum_{i=1}^{N} \frac{E_i(\omega\lambda_i)}{1+(\omega\lambda_i)^2} \tag{3.15}$$

where E_e was the equilibrium modulus representing viscoelastic solid that in the case of the tested HMAs equaled zero.

3.6. Experimental program – Suggested changes in MSCR asphalt binder testing

In this study, five stress levels were applied in the MSCR test: two standard levels of 0.1 and 3.2 kPa, and three additional stress levels of 6.4, 12.8, and 25.6 kPa. The goal was to evaluate the MSCR rutting potential of the asphalt binders at different shear stress levels, and to compare the results with the actual rutting results of the mixes determined by HWTT and dynamic modulus, $|E^*|$, measurements.

The evaluation of MSCR results was conducted in a similar manner for all binders. Prior to binder testing, RTFO short-term ageing was conducted on all binders, in accordance with AASHTO T240-13. The first ten cycles of MSCR were conducted at 0.1 kPa shear stress. At the end of the recovery portion of the 10th cycle at the shear stress level of 0.1 kPa, with no time lag between the cycles, either 3.2, 6.4, 12.8, or 25.6 kPa of shear stress was successively applied to the same specimen for another ten

cycles. New samples were used for each increasing stress level. The result was four new sets that were tested at one temperature for one asphalt binder (0.1 and 3.2 kPa; 0.1 and 6.4 kPa, 0.1 and 12.8 kPa, 0.1 and 25.6 kPa).

All studied binders were tested at three different testing temperatures of 50, 60, and 70°C. The lowest temperature (50°C) was reasonably lower than the binders' maximum service temperature, making it possible to investigate the binders' elastic properties and the influence of those properties on rutting resistance. The next temperature (60°C), was relatively close to the binders' maximum service temperatures but still below it. This temperature was selected to ensure that all the binders were conditioned at a lower temperature than their critical temperature. The third temperature (70°C) was above the binders' maximum critical temperature.

RESULTS AND DISCUSSION

Depending on the country, asphalt binder specifications are either based on empirical test results, physical test results, or both combined. In the following chapter the results of the most relevant EN standard tests and functional PG tests, widely used to characterize asphalt binders and therefore determine their resistance to rutting, are presented. Subsequently, MSCR test results, evaluated in accordance with the proposed changes, are discussed and then compared to the actual rutting resistance of asphalt mixtures determined by means of Hamburg test and dynamic modulus test result.

4.1. Asphalt binder results

4.1.1. Conventional binder testing results

According to the European standards, asphalt binders are fundamentally characterized by their penetration value, R&B softening point, and their resistance to hardening (or RTFO short-term aging) at 163°C, expressed in changes of penetration and softening point. Some of the basic empirical properties of the tested asphalt binders are shown in Table 4.1. According to ČSN EN 14023 most of the modified binders would be classified as PMB 120/200-40, which is also the softest asphalt binder gradation according to the classifications used in the Czech Republic. Modified binders with such consistency are used in countries with much colder climate, for example Canada, where also all the vacuum residues used in this dissertation were produced.

It should be emphasized that the goal of this study is not to design asphalts blends with properties that meet all the requirements defined in the specifications. The aim is rather to investigate different modified and non-modified asphalts on an as wide scale as possible to determine whether the MSCR binder test yields better correlations with rutting potential of hot mix asphalts at higher shear stresses than at the standardized stress levels.

The multiple stress creep recovery test was originally developed in order to eliminate the shortcomings of the $|G^*|/\sin\delta$ rutting parameter, namely, that the Superpave® performance grade specification could not be used for full characterization of binders with different types of polymer modifiers since it did not take into account the significantly enhanced elastic properties of such binders. Therefore, it failed to adequately predict the resistance to rutting of polymer modified asphalt binders.

For this reason, within the scope of this study, sufficiently soft binders were chosen for modification that allowed the use of polymer modifiers in relatively high concentration. This helped to determine the ability of MSCR test to differentiate between the rutting resistance of asphalt binders (blended with different types of polymer modifiers) at different temperatures.

When compared to the properties of their asphalt bases, the most significant decrease in penetration occurred in the case of SBS, SBS+S, and SBS+RET+PPA-modified 200/300 Pen grade and in the case of SBS-S-modified 300/400 Pen grade asphalt base (Table 4.1). Nevertheless, the 80/100 Pen grade asphalt showed the lowest penetration resulting in that it was the "hardest" of all the tested binders.

From the viewpoint of the softening point (ring and ball method) the crosslinked SBS-modified binders and RET-modified binders showed the highest values, indicating either the presence of the elastic polymer network or the successful RET/asphaltene reaction within the blends. In terms of change in softening point the crosslinked SBS-modified binders proved to be the least susceptible to RTFO short-term aging. Contrarily, the 80/100 Pen grade straight-run asphalt and the PPA-modified asphalt showed the highest susceptibility to short-term aging.

In the case of crosslinked SBS-modified asphalt blends the exceptionally high elastic recovery results successfully revealed the presence of the elastic polymer network in the blend. Worth mentioning that the elastic recovery results showed relatively high values of elasticity in the case of RET, RET+PPA, and RET(EP)+PPA-modified binders as well. On the other hand, as expected the 80/100 Pen grade straight-run asphalt along with the PPA-modified blend indicated low elasticity.

Based on these empirical results, both the crosslinked SBS-modified and RET-modified binders were expected to be the most rut resistant, while due to their low elasticity and relatively low softening point the 80/100 Pen grade binder and PPA-modified binder the least resistant to deformation.

Table 4.1 Basic empirical properties of asphalt binders in accordance with the European standards (bolded values did not meet the requirements defined in national standard specifications ČSN EN 14023 and ČSN EN 12591)

		Empirical Test Results (penetration grading)					
Base Binder	Polymer Type Designation	Un-aged Pen[a] at 25°C (dmm)	Un-aged R&B[b] (°C)	RTFO-aged R&B[b,c] (°C)	Increase in Soft. Point (°C)	Retained Pen (%)	Elastic recovery[d] at 25°C (%)
80/100	None	91	46.5	56.0	**12.6**	58	10.0
200/300	RET+PPA	149	51.9	60.6	**8.7**	**59**	78.0
	SBS+S	146	55.3	57.6	2.3	61	92.5
	RET	172	53.1	60.2	7.1	**56**	69.0
	RET+SBS	149	46.4	57.0	**10.6**	**57**	53.5
	SBS	141	44.9	55.7	**10.8**	**58**	45.0
	PPA	151	46.4	59.0	**12.6**	**56**	31.0
	RET+PPA+CRM	150	45.3	50.8	5.5	**59**	52.5
	SBS+RET+PPA	146	46.5	55.5	**9.0**	**57**	61.5
	SBS+S+CRM	156	43.4	54.0	**10.6**	**53**	57.0
	RET(EP)+PPA	156	51.3	60.6	**9.3**	**59**	67.0
300/400	SBS+S	169	62.4	62.7	0.3	62	94.5
	SBS+S+VGO	205	65.1	65.1	0.0	**59**	99.5

[a] EN 1426 Determination of the Needle Penetration
[b] EN 1427 Determination of the Softening Point, Ring and Ball Method
[c] EN 12607-1 Determination of the Resistance to Hardening, RTFO Method
[d] EN 13398 Determination of the Elastic Recovery of Modified Bitumen

4.1.2. Superpave® PG grading of asphalt binders

Even though, the unaged binders blended from the 300/400 Pen grade asphalt base showed higher service temperatures than the required 64°C, the objective that similar maximum service temperatures (PG 64-yy) of asphalt binders ought to be reached with or without modification was satisfied once they all experienced RTFO short-term aging. The resulting performance continuous grade of these asphalt binders lied between 62.9 and 66.9°C.

The maximum, intermediate, and minimum service temperatures of all binders before and after they experienced RTFO short- and PAV long-term ageing along with mass loss and viscosity results are summarized in Table 4.2.

It is worth mentioning that the formula with added VGO had the highest decrease in maximum service temperature and the highest value of mass loss after RTFO aging and was therefore according to the Superpave® binder specification the most sensitive to aging. Moreover, its mass loss value did not meet the requirements of being less than 1% defined in AASHTO M320 [207].

Asphalt blends prepared from the 200/300 Pen grade asphalt base (PG 52-35) gained on average two grades (+12°C) higher service temperature while their minimum

service temperature was only slightly altered and only in the case of PPA-modified asphalt enhanced. As for the asphalt blends prepared from 300/400 Pen grade asphalt base (PG 50-37) the maximum service temperature in both cases was increased more than three grades (18°C), while due to the added VGO the minimum service temperature was decreased almost one grade lower (–5°C) in the case of SBS+S+VGO, and only –1°C in the case of SBS+S-modified binder.

Asphalt binders with relatively high concentration of RET (e.g., RET+PPA, RET, RET(EP)+PPA) and the 300/400 Pen grade blends with crosslinked SBS indicated the highest increase in viscosity, while the PPA-modified binder the lowest.

Table 4.2 Basic physical properties required for Superpave® PG grading (bolded results did not meet the specification)

		Superpave® Test Results (performance grading verification)[a]					
Base Binder	Polymer Type Designation	Un-aged Max. Service Temp.[b] (°C)	RTFO-aged Max. Service Temp.[c] (°C)	PAV-aged Inter. Service Temp.[d] (°C)	BBR Min. Service Temp.[e] (°C)	Mass Loss[f] (%)	Viscosity[g] at 135°C (mPa·s)
80/100	None	64.8	64.8	19.8	-17	-0.47	437.0
200/300	RET+PPA	65.5	65.9	10.9	-24	-0.71	785.8
	SBS+S	65.6	64.0	10.8	-25	-0.82	571.0
	RET	62.7	62.9	11.1	-24	-0.68	710.8
	RET+SBS	63.5	64.4	11.7	-23	-0.71	617.9
	SBS	63.7	63.9	13.4	-23	-0.70	593.9
	PPA	64.4	64.0	10.9	-26	-0.83	409.9
	RET+PPA+CRM	64.0	64.6	11.6	-25	-0.97	445.9
	SBS+RET+PPA	64.0	64.8	11.4	-24	-0.75	569.9
	SBS+S+CRM	63.5	66.9	12.7	-25	-0.78	421.0
	RET(EP)+PPA	64.5	64.7	10.6	-25	-0.82	623.9
300/400	SBS+S	70.0	64.4	7.0	-28	-0.93	630.0
	SBS+S+VGO	72.7	64.3	2.3	-32	**-1.90**	620.0

[a] AASHTO M320 Standard Specification for Performance-Graded Asphalt Binder
[b] AASHTO T315 Un-aged Binder Performance Criterion: $|G^*|/\sin\delta \geq 1.00$kPa
[c] AASHTO T315 RTFO-aged Binder Performance Criterion: $|G^*|/\sin\delta \geq 2.20$kPa
[d] AASHTO T315 PAV-aged Binder Performance Criterion: $|G^*|\sin\delta \leq 5000$ kPa
[e] AASHTO T313 PAV-aged Binder Performance Criterion: m-value ≥ 0.300, S ≤ 300 MPa
[f] AASHTO T240 RTFO Method, Mass Change (loss or gain) Shall Be Less Than 1.00%
[g] AASHTO T316 Un-aged Binder Viscosity Criterion: $\eta \leq 3$ Pa.s

According to the PG specification from all the tested binders the 300/400 Pen grade blends proved to possess the widest service temperature range (Figure 4.1) what made them the most promising at both temperature extremes.

From the viewpoint of rutting potential, the similar maximum service temperatures indicated similar rutting resistance, and only the viscosity differences measured at 135°C allowed to distinguish between the binders' rutting potential. From this perspective PPA,

SBS+S+CRM, RET+PPA+CRM-modified, and the 80/100 Pen grade straight-run asphalt binders were most likely susceptible to rutting. Nonetheless, viscosity measured at 135°C cannot imply the binders' resistance to rutting at much lower service temperatures and, due to the studied binders intentionally similar maximum service temperatures, neither the $|G^*|/\sin\delta$ SHRP binder criteria [212].

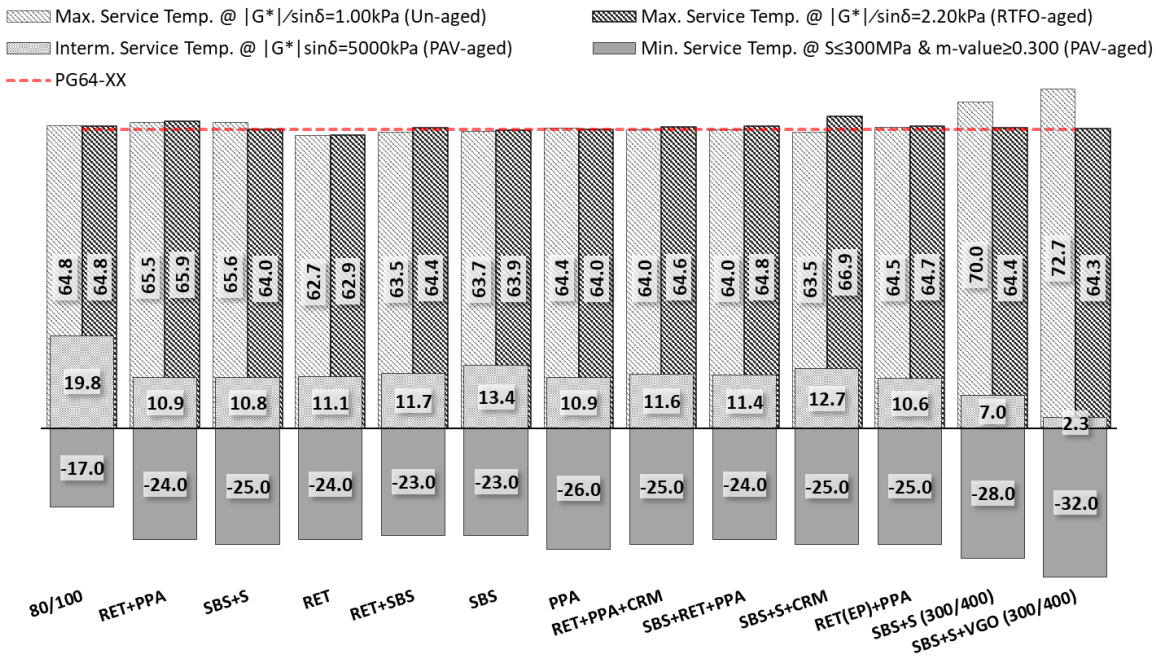

Figure 4.1 The results of minimum, intermediate, and maximum service temperatures of the prepared asphalt blends

Regardless of the relatively small differences between the maximum service temperatures of the used asphalt blends they would be either categorized as PG 58-yy or PG 64-yy. Therefore, MSCR test at standard shear stress levels of 0.1 and 3.2 kPa was conducted at both 58 and 64°C temperatures.

The MSCR test results measured at 58°C are presented in Table 4.3. The non-recoverable creep compliance (J_{nr}) at 0.1 kPa indicated that the most susceptible asphalt to rutting were the 80/100 Pen grade straight-run and the SBS-modified asphalt. The most resistant were the blends prepared from 300/400 Pen grade asphalt. Since the MSCR test considers both the viscous (i.e., hardness) and also the elastic properties of the tested binders, the substantially better results of these asphalts were unambiguously due to their outstanding elastic properties. From the 200/300 Pen grade blends RET+PPA and SBS+S-modified asphalt binders showed noticeably good results. The percent

recovery ($\%R$) results also confirmed that the reason behind the outstanding performance of the above-mentioned asphalt blends was mainly due to their gained elasticity.

The MSCR test conducted at 3.2 kPa showed similar results as at 0.1 kPa with the 80/100 Pen grade straight-run asphalt being the most susceptible to rutting (the highest J_{nr} and the lowest $\%R$ results) while the 300/400 Pen grade blends the most resistant (the lowest J_{nr} and the highest $\%R$ results) followed by RET+PPA and SBS+S-modified 200/300 Pen grade asphalts.

According to their stress sensitivity results, the SBS+S+VGO-modified 300/400 Pen grade blend, along with the SBS+S+CRM-modified and the PPA-modified 200/300 Pen grade blends proved to be the most sensible to changes in stress. From the three stress sensitive binders only the PPA-modified blend passed the criterion of $J_{nr,diff} \leq 75\%$ at 58°C defined by AASHTO M332 [260].

Table 4.3 MSCR test results measured at 58°C (bolded results did not meet the specification)

Base Binder	Polymer Type Designation	Superpave® Test Results (MSCR grading verification)[a,b,f]					
		$J_{nr,0.1kPa}$[c] (kPa^{-1})	$J_{nr,3.2kPa}$[c] (kPa^{-1})	$J_{nr,diff}$[d] (%)	$\%R_{0.1kPa}$ (%)	$\%R_{3.2kPa}$[e] (%)	$\%R_{diff}$ (%)
80/100	None	1.617	1.850	14.4	5.5	1.8	67.3
200/300	RET+PPA	0.438	0.553	26.1	66.9	61.0	8.8
	SBS+S	0.537	0.773	44.0	67.5	58.4	13.5
	RET	0.944	1.309	38.6	49.2	36.5	25.8
	RET+SBS	1.050	1.434	36.6	34.2	21.1	38.3
	SBS	1.216	1.521	25.1	23.4	14.3	38.9
	PPA	0.832	1.437	72.7	37.9	7.8	79.4
	RET+PPA+CRM	1.015	1.504	48.2	39.1	22.3	43.0
	SBS+RET+PPA	0.868	1.226	41.2	43.3	23.7	45.3
	SBS+S+CRM	0.798	1.451	**81.8**	41.0	12.8	68.8
	RET+PPA	0.707	0.930	31.6	50.6	39.7	0.0
300/400	SBS+S	0.211	0.283	34.4	84.4	81.7	3.2
	SBS+S+VGO	0.074	0.149	**101.3**	93.4	89.6	4.1

[a] AASHTO T320 Standard Specification for Performance-Graded Asphalt Binder
[b] AASHTO M332 Standard Specification for Performance-Graded Asphalt Binder Using MSCR Test
[c] AASHTO M332 RTFO-aged Binder Performance Criterion: $J_{nr,3.2kPa} \leq 4.5 kPa^{-1}$
[d] AASHTO M332 RTFO-aged Binder Stress Sensitivity Criterion: $J_{nr,diff} \leq 75\%$
[e] AASHTO M332 RTFO-aged Binder Elasticity Indicator in case $0.10 \leq J_{nr} \leq 2.00\ kPa^{-1}$ (not required)
[f] AASHTO T240 RTFO Method

The MSCR test results measured at 64°C are presented in Table 4.4. Identically to the MSCR results measured at 58°C, 80/100 Pen grade straight-run asphalt and the SBS-modified blend were the least resistant to rutting at 64°C and at 0.1 kPa, while the most resistant were the 300/400 Pen grade asphalt blends. However, due to their stress sensitivity and low elasticity, the PPA-modified binder, along with the 80/100 Pen grade and SBS-modified binders, proved to be the least rut resistant at 3.2 kPa.

On the other hand, in addition to the 300/400 Pen grade blends, the RET+PPA-modified 200/300 Pen grade blend exhibited very promising J_{nr} and $\%R$ results. Nonetheless, the crosslinked 300/400 Pen grade blends showed significantly higher stress susceptibility at 64°C than the RET+PPA-modified 200/300 Pen grade blend.

Table 4.4 MSCR test results measured at 64°C (bolded results did not meet the specification)

		Superpave® Test Results (MSCR grading verification)[a,b,f]					
Base Binder	Polymer Type Designation	$J_{nr,0.1kPa}$[c] (kPa^{-1})	$J_{nr,3.2kPa}$[c] (kPa^{-1})	$J_{nr,diff}$[d] (%)	$\%R_{0.1kPa}$[e] (%)	$\%R_{3.2kPa}$[e] (%)	$\%R_{diff}$ (%)
80/100	None	3.810	4.390	15.2	2.7	-0.1	103.7
200/300	RET+PPA	0.993	1.292	30.2	57.7	48.4	16.1
	SBS+S	1.327	2.396	**80.6**	56.3	34.0	39.6
	RET	2.004	2.933	46.4	39.8	24.5	38.4
	RET+SBS	2.378	3.446	44.9	26.5	11.0	58.5
	SBS	3.235	4.315	33.4	18.8	6.3	66.5
	PPA	2.367	4.487	**89.6**	27.6	2.5	90.9
	RET+PPA+CRM	2.405	3.790	57.6	28.5	11.0	61.4
	SBS+RET+PPA	2.019	3.156	56.3	32.7	11.7	64.2
	SBS+S+CRM	1.803	3.511	**94.7**	33.1	5.4	83.7
	RET(EP)+PPA	1.586	2.211	39.4	25.8	39.4	52.7
300/400	SBS+S	0.582	1.107	**90.2**	76.0	60.5	20.4
	SBS+S+VGO	0.438	0.961	**119.6**	83.9	69.2	17.5

[a] AASHTO T320 Standard Specification for Performance-Graded Asphalt Binder
[b] AASHTO M332 Standard Specification for Performance-Graded Asphalt Binder Using MSCR Test
[c] AASHTO M332 RTFO-aged Binder Performance Criterion: $J_{nr,3.2kPa} \leq 4.5 kPa^{-1}$
[d] AASHTO M332 RTFO-aged Binder Stress Sensitivity Criterion: $J_{nr,diff} \leq 75\%$
[e] AASHTO M332 RTFO-aged Binder Elasticity Indicator in case $0.10 \leq J_{nr} \leq 2.00\ kPa^{-1}$ (not required)
[f] AASHTO T240 RTFO Method

At 3.2 kPa stress level and at 64°C the 80/100 Pen grade straight-run asphalt displayed negative $\%R$ value as can be seen in Table 4.4. This phenomenon, reported by many researchers [135,268–270], was due to the fact that the used rheometer was not able to respond and unload stress as quickly (instantaneously) as it was required in MSCR test. This usually occurs at the combination of adequately high temperatures, high stress levels and low modification level, when even modified asphalts show negligible elasticity.

Under such conditions and due to the delayed response of the DSR during stress unloading, a small strain increase occurred even after the first second of the cycle (i.e., during recovery phase), shown in Figure 4.2. Per definition, $\%R$ is the proportion of recovered strain to creep strain (Figure 3.14), as described in Equation (3.5), while the value of recovered strain is the difference of the strain at the end of creep phase (creep end strain, ε_c^N) and the strain at the end of recovery phase (residual strain, ε_r^N). Therefore, mathematically even the slightest increase during recovery phase ($\sum_{N=1}^{10}(\varepsilon_c^N - \varepsilon_r^N)/10 < 0$, when $\varepsilon_r^N > \varepsilon_c^N$) gave negative value for the total $\%R$, if it was

not followed by sufficiently large recovered strain during the last nine seconds of the cycle. These negative values usually indicated low elasticity and the $\%R$ values could be considered as tending to zero. Nonetheless, in this study their actual measured negative values are presented.

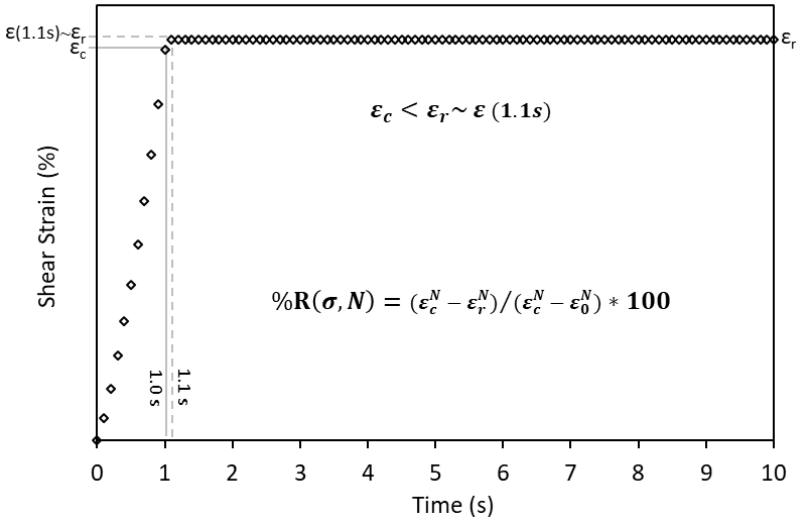

Figure 4.2 Strain increase after creep phase as the result of the incapability of the DSR rheometer to quickly unload stress

According to the MSCR grading system (AASHTO M332) from all the tested binders only the two 300/400 Pen grade blends met the criterion for extremely heavy grade at 58°C testing temperature, indicating that both binders would be able to sustain extreme traffic conditions at 58°C service temperature, with SBS+S+VGO-modified binder being the most rut resistant (Figure 4.3). From the 200/300 Pen grade blends the RET+PPA, SBS+S and the RET(EP)+PPA-modified asphalts met the criterion for very heavy grade while the $J_{nr,3.2kPa}$ values of the remaining binders fell between 1.0 and 2.0 kPa^{-1}, classifying them as heavy grade binders.

Most of the binders were classified as standard or heavy grade binders at 64°C, which in most cases meant at least one grade decrease in MSCR classification. The only binder classified as very heavy grade was the SBS+S+VGO-modified 300/400 Pen grade blend. Two binders classified as heavy grade binders were the SBS+S-modified 300/400 Pen grade asphalt and the RET+PPA-modified 200/300 Pen grade asphalt. None of the binders failed the maximum MSCR criterion of 4.5 kPa^{-1}, although

the 80/100 Pen grade straight-run, the SBS and the PPA-modified 200/300 Pen grade blends' results fell very close to the limiting value at 64°C.

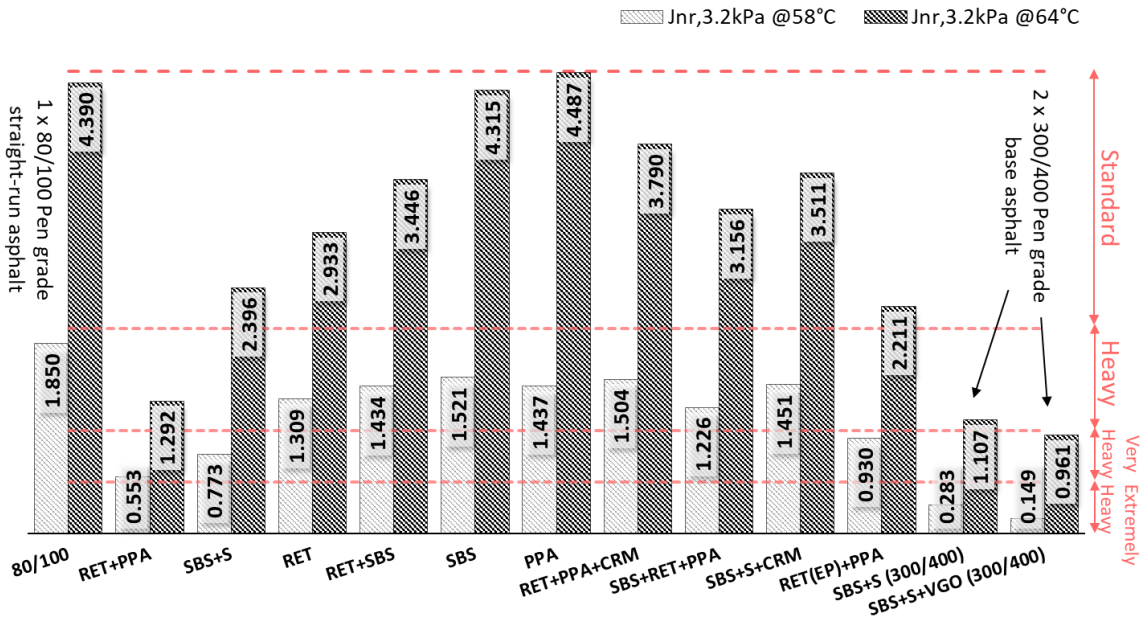

Figure 4.3 MSCR grading, non-recoverable creep compliance, J_{nr}, measured at 3.2 kPa and at temperatures 58 and 64°C

Even though with the exception of 80/100 Pen grade straight-run asphalt, all binders were polymer modified, half of them fell below the MSCR %R specification line at 58°C (Figure 4.4), indicating insufficient or low level of modification, as described in Chapter 3.4.3. Binders that met the specification limit at 58°C were the SBS+S+VGO and the SBS+S-modified 300/400 Pen grade blends and the RET+PPA, SBS+S, RET(EP)+PPA, RET-modified 200/300 Pen grade blends.

Only three binders indicated sufficient level of modification at 64°C, namely the two 300/400 Pen grade blends and the RET+PPA-modified 200/300 Pen grade. The rest of the tested binders were observed to have their $J_{nr,3.2kPa}$ values greater than 2.0 kPa^{-1}, and therefore these binders were not required to have any minimum value of %R.

Even though their $J_{nr,3.2kPa}$ was greater than the 2.0 kPa^{-1} limiting value the elasticity of SBS+S and RET(EP)+PPA-modified 200/300 Pen grade blends also worth mentioning (see Table 4.3 and Table 4.4.).

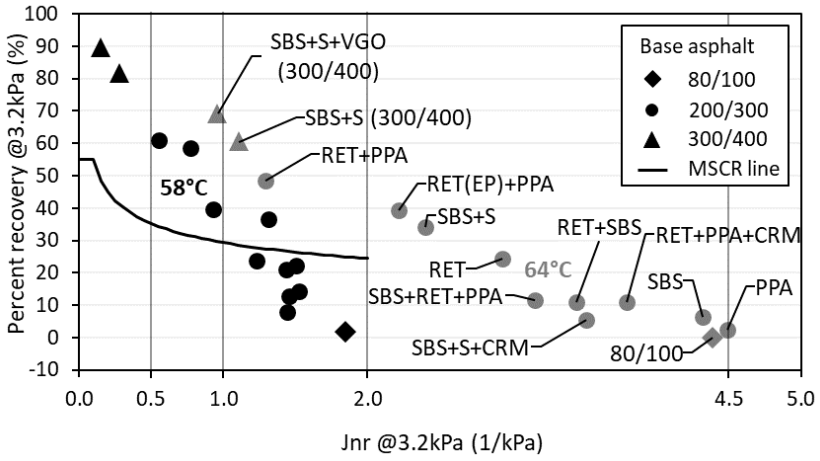

Figure 4.4 MSCR %*R* vs. J_{nr} at 3.2 kPa and at temperatures 58 and 64°C

The performance grade (PG), true performance grade, and the PG specified by MSCR results at 58 and 64°C of the studied binders are presented in Table 4.5. Since the true performance grade of the binders was close to PG 64-yy, more precisely lied between PG 62-yy and PG 65-yy, 64°C was chosen for MSCR grading temperature. According to this classification, as already mentioned above, the SBS+S+VGO, SBS+S-modified 300/400 Pen grade blends and the RET+PPA-modified 200/300 Pen grade blend seemed to be the most rut resistant of all the tested binders at 64°C.

Table 4.5 Superpave® performance grade, true performance grade, and performance grade by MSCR at 58 and 64°C

		Superpave® Performance Grading[a,b]			
Base Binder	Polymer Type Designation	Performance Grade	True Performance Grade	Performance Grade by MSCR at 58°C	Performance Grade by MSCR at 64°C
80/100	None	PG 64-22	**PG 64-27**	PG 58H-27	**PG 64S-27**
200/300	RET+PPA	PG 64-34	**PG 65-34**	PG 58V-34	**PG 64H-34**
	SBS+S	PG 64-34	**PG 64-35**	PG 58V-35	**PG 64S-35**
	RET	PG 58-34	**PG 62-34**	PG 58H-34	**PG 64S-34**
	RET+SBS	PG 58-28	**PG 63-33**	PG 58H-33	**PG 64S-33**
	SBS	PG 58-28	**PG 63-33**	PG 58H-33	**PG 64S-33**
	PPA	PG 64-34	**PG 64-36**	PG 58H-36	**PG 64S-36**
	RET+PPA+CRM	PG 64-34	**PG 64-35**	PG 58H-35	**PG 64S-35**
	SBS+RET+PPA	PG 64-34	**PG 64-34**	PG 58H-34	**PG 64S-34**
	SBS+S+CRM	PG 58-34	**PG 63-35**	PG 58H-35	**PG 64S-35**
	RET+PPA	PG 64-34	**PG 64-35**	PG 58V-35	**PG 64S-35**
300/400	SBS+S	PG 64-34	**PG 64-38**	PG 58E-38	**PG 64H-38**
	SBS+S+VGO	PG 64-40	**PG 64-42**	PG 58E-42	**PG 64V-42**

[a] AASHTO T320 Standard Specification for Performance-Graded Asphalt Binder
[b] AASHTO M332 Standard Specification for Performance-Graded Asphalt Binder Using MSCR Test

4.1.3. Accumulated creep compliance results at five shear stress levels

To investigate the feasibility of using high shear stress levels in the MSCR test, it was necessary to assess the MSCR results for each binder at different temperatures and stress levels. The accumulated creep compliance, J_a, (Equation (2.23)) of all binders evaluated at 50, 60 and 70°C testing temperature and at five shear stress levels (i.e., 0.1, 3.2, 6.4, 12.8, 25.6 kPa) are presented in this chapter. All results were measured according to the testing protocol described in Chapter 3.6.

Even though the 80/100 Pen grade straight-run asphalt indicated the highest resistance to shear loading at 50°C (during creep phase), due to its negligible recovery it was ranked among the four least rut resistant binders at all stress levels (Figure 4.5). However, at temperatures higher than the R&B softening point of the RTFO-aged binder (i.e., 60 and 70°C) its stiffness became comparable to the polymer modified binders' (Figure 4.6 and Figure 4.7).

Another binder worth mentioning was the PPA-modified blend which sensitivity to the change in stress levels was the most obvious of all tested binders (see also Figure A.7). While at standard stress levels its results indicated better or slightly better rut resistance with greater recovery than the 80/100 Pen grade asphalt, or even the SBS and SBS+S+CRM-modified binders, at higher stress levels, starting with 6.4 kPa, it became the least resistant binder to deformation from all the tested binders. Its unambiguous sensitivity to the increase in shear stress level was due to the fact that PPA only alters the colloidal structure of the asphalt base without forming any kind of polymer network within the binder. Therefore, the enhanced elastic properties of the PPA-modified blend were the result of stiffening of the vacuum base. Nevertheless, it proved to be considerably susceptible to both stress and temperature. Hence, such binders may deteriorate during service time much faster than it could be predicted from the results given by the MSCR test conducted at standard shear stress levels.

Even though, the SBS+S and the SBS+S+VGO-modified 300/400 Pen grade blends were the most rut resistant at the combination of 50°C and all the applied shear stresses, under critical conditions, such as the combination of 70°C and stress levels higher than or equal to 6.4 kPa, RET+PPA-modified binder proved to be the most resistant to rutting.

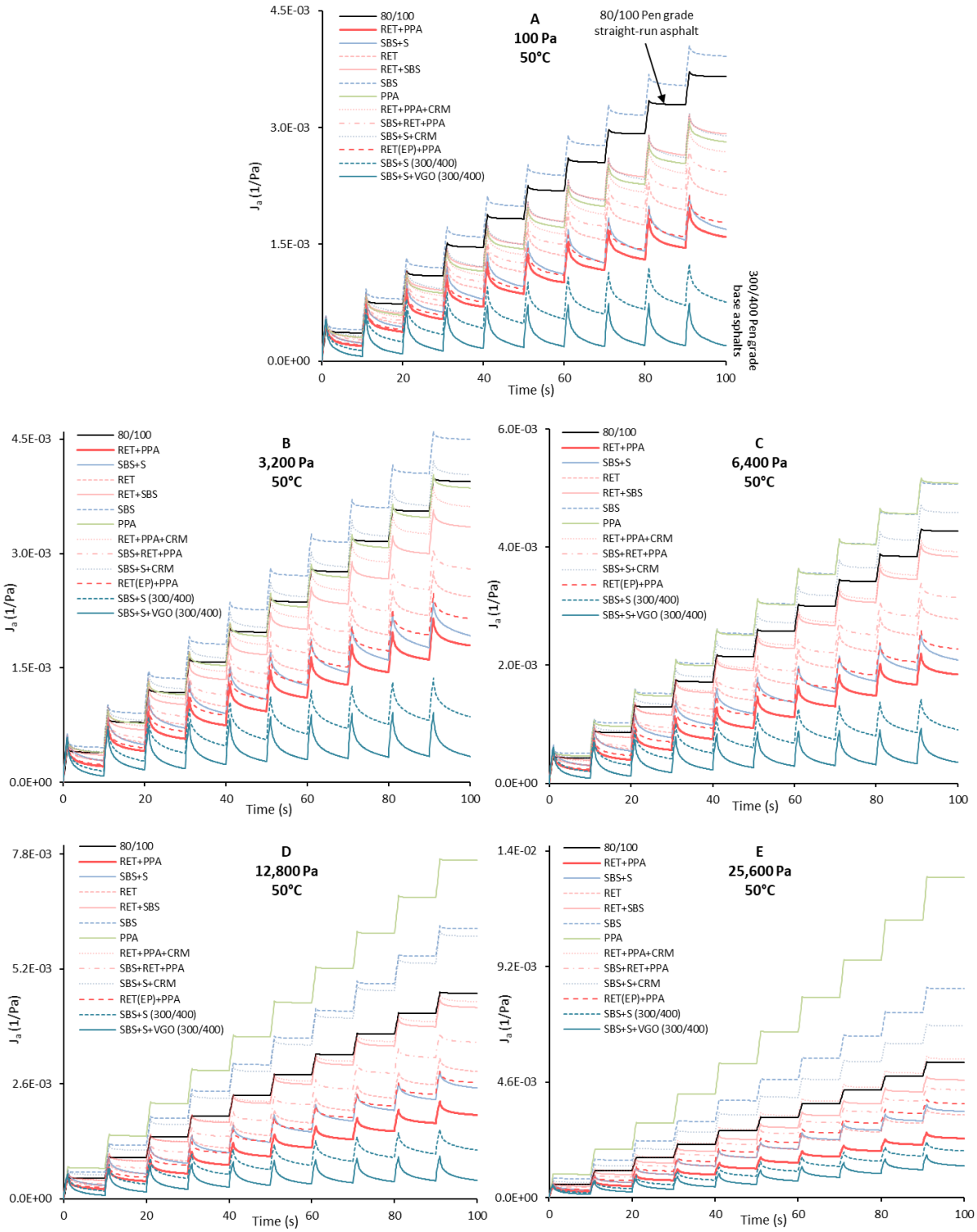

Figure 4.5 Plot of the accumulated creep compliance, J_a, results of all binders at five shear stress levels ranging from 100 to 25,600 Pa, test conducted at 50°C

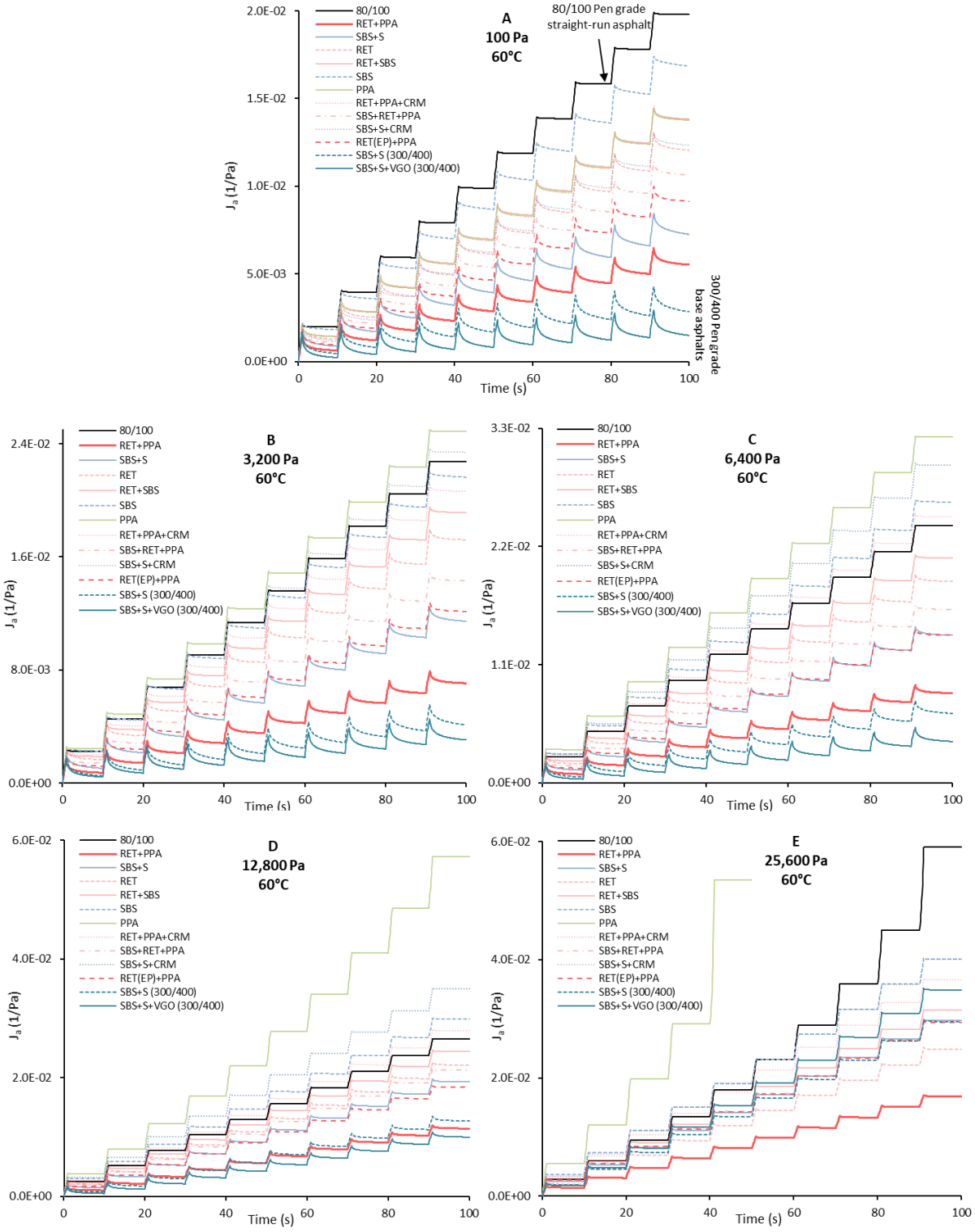

Figure 4.6 Plot of the accumulated creep compliance, J_a, results of all binders at five shear stress levels ranging from 100 to 25,600 Pa, test conducted at 60°C

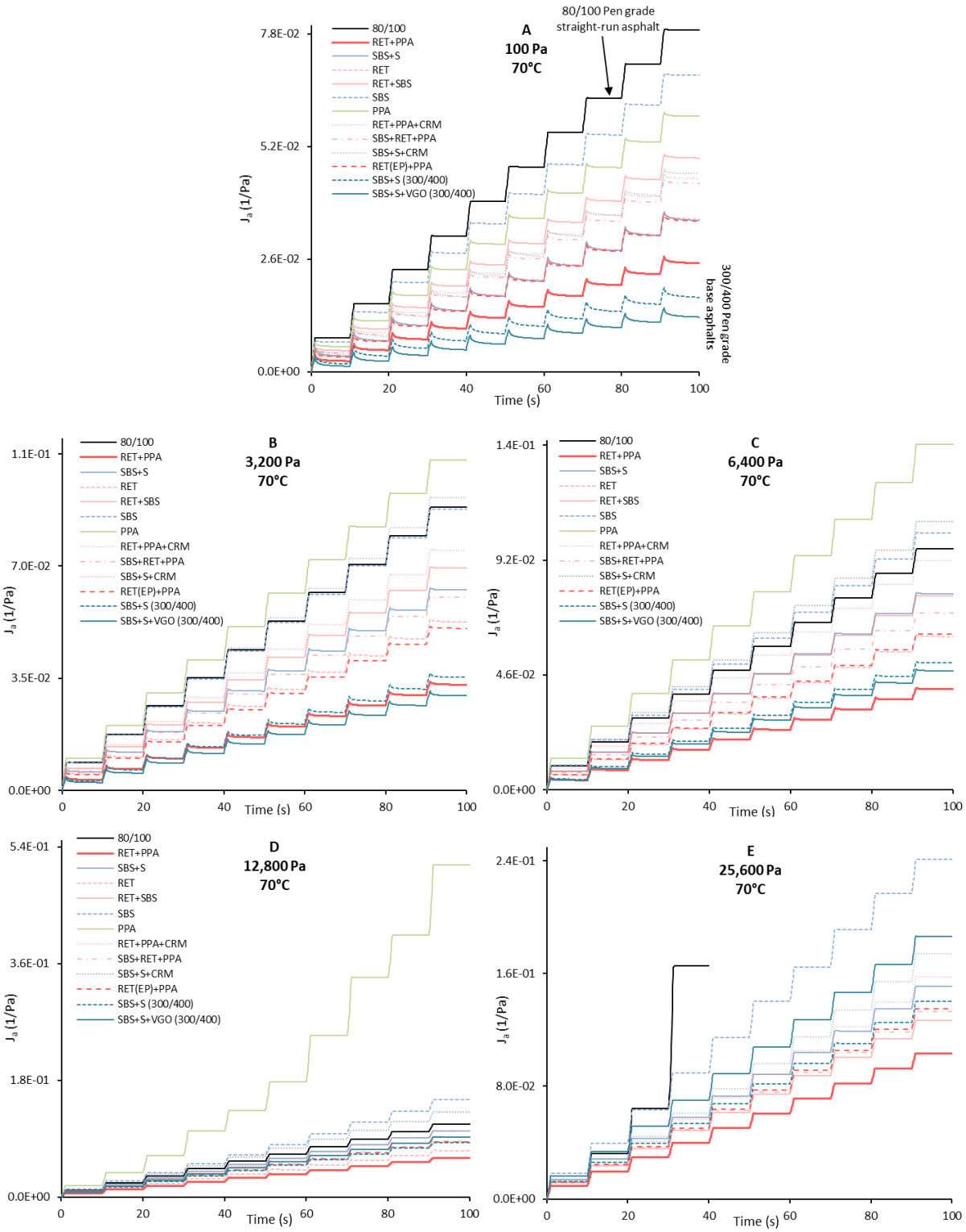

Figure 4.7 Plot of the accumulated creep compliance, J_a, results of all binders at five shear stress levels ranging from 100 to 25,600 Pa, test conducted at 70°C

The non-recoverable creep compliance, J_{nr}, results of six selected binders at each MSCR cycle (i.e., each cycle out of the ten at the same shear stress level) are plotted in Figure 4.8, Figure 4.9, and Figure 4.10.

Often only with a slight difference most of the binders yielded similar compliance results within the same set of ten cycles at any repeating cycle. However, depending on the testing temperature and the tested binder, at 12.8 and 25.6 kPa the difference between the J_{nr} results of each cycle became more prominent than at lower stress levels. Although differences between the cycles were reported by other researchers [46] the magnitude of these differences queried the repeatability and thus the accuracy of the MSCR test at the combination of too high stresses and high testing temperatures.

In Figure 4.8 the J_{nr} results of the two most susceptible binders (i.e., 80/100 and PPA) are presented at different shear stress levels.

In the case of PPA-modified binder the combination of 50°C and 25.6 kPa shear stress was critical that resulted in increasing J_{nr} values with every successive cycle, indicating material fatigue. Similar increasing J_{nr} values could be observed at 60 and 70°C testing temperature and 12.8 kPa shear stress level. Moreover, the application of 25.6 kPa shear stress level at 60 and 70°C resulted in complete damage of the samples (Figure 4.8B-B and B-C).

As for the 80/100 Pen grade asphalt, only the highest stress level proved to be critical at testing temperatures higher than its RTFO-aged R&B softening point (i.e., 60 and 70°C). Nonetheless, at 70°C and at 25.6 kPa stress level the 80/100 Pen grade asphalt sample was completely damaged after four cycles (Figure 4.8A-C).

The polymer modified asphalt blends containing a stable polymer network, such as the crosslinked SBS+S+VGO (300/400), or the RET+PPA-modified 200/300 Pen grade asphalt base (most probably chemically crosslinked with asphaltenes), indicated very low and slightly unstable J_{nr} values at 50°C. This changed at 60 and 70°C where most of the measurements became more consistent. It is worth mentioning that at most of the stress levels the first several cycles yielded noticeably different results from the remaining ones, i.e., the J_{nr} values changed with increasing number of creep and recovery cycles. This was due to the reorganization and stretching of the tangled large molecular chains in the case of crosslinked SBS+S, while in the case of RET+PPA-modified blend it was due to the reorientation of polymer network which was chemically bonded with asphaltenes. The fact that at high temperatures and high shear stress levels the RET+PPA-modified asphalt blend was the most resistant to deformation also supported the theory of the

creation of covalent bonds between Elvaloy™ 5160 and the asphaltene components. Nonetheless, averaging the response for 10 cycles at each stress level can lead to misleading values. Therefore, in order to reach more "stable" MSCR results higher number of cycles would be needed, mainly in the case of crosslinked polymer modified asphalt blends. Or as it was suggested by other researchers, only the second half of the cycles should be considered at each stress level [233].

The difference between the crosslinked SBS+S and dispersed SBS is evident from Figure 4.10. Due to its crosslinked polymer network the SBS+S-modified binder initially indicated slightly inconsistent J_{nr} values, similar to those of the RET+PPA and SBS+S+VGO-modified asphalt blends. The SBS-modified binder containing dispersed polymer phase, resembled the results of the 80/100 Pen grade straight-run and the PPA-modified binders, with 12.8 kPa being the highest shear stress level that resulted in relatively stable results through the whole temperature range.

Based on these results it could be concluded that the highest testing temperature to apply 25.6 kPa shear stress level without completely damaging the samples of such "soft" and non-crosslinked binders during testing was 50°C, while at 60°C it was 12.8 kPa, and 6.4 kPa at 70°C (see also Figure A.7 and Figure A.8 in Appendix-A).

In terms of stability the J_{nr} results during MSCR testing in the case of the remaining seven blends (not presented) were comparable either to the RET+PPA and SBS+S-modified binders (e.g., RET, RET+SBS, RET+PPA+CRM, SBS+RET+PPA, SBS+S+CRM, RET(EP)+PPA) or to the SBS+S+VGO-modified 300/400 Pen grade blend (SBS+S-modified 300/400 Pen grade blend). In addition, all of these remaining binders withstood the highest stress level of 25.6 kPa even at the highest testing temperature of 70°C.

The results of European comparative tests have also shown that the repeatability and reproducibility of the MSCR test depend not only on the temperature at which the test was performed, but also on the level of the shear stress used [271]. According to the research that included MSCR results of a total of forty-nine asphalt laboratories, the measurements performed at lower temperatures (in the case of the study it was 60°C) showed reproducible results at 6.4 kPa shear stress level (the highest stress level used in the study). However, at 70°C the reproducibility decreased considerably at all studied shear stress levels. Therefore, lower temperatures are desired to conduct MSCR test at high shear stresses.

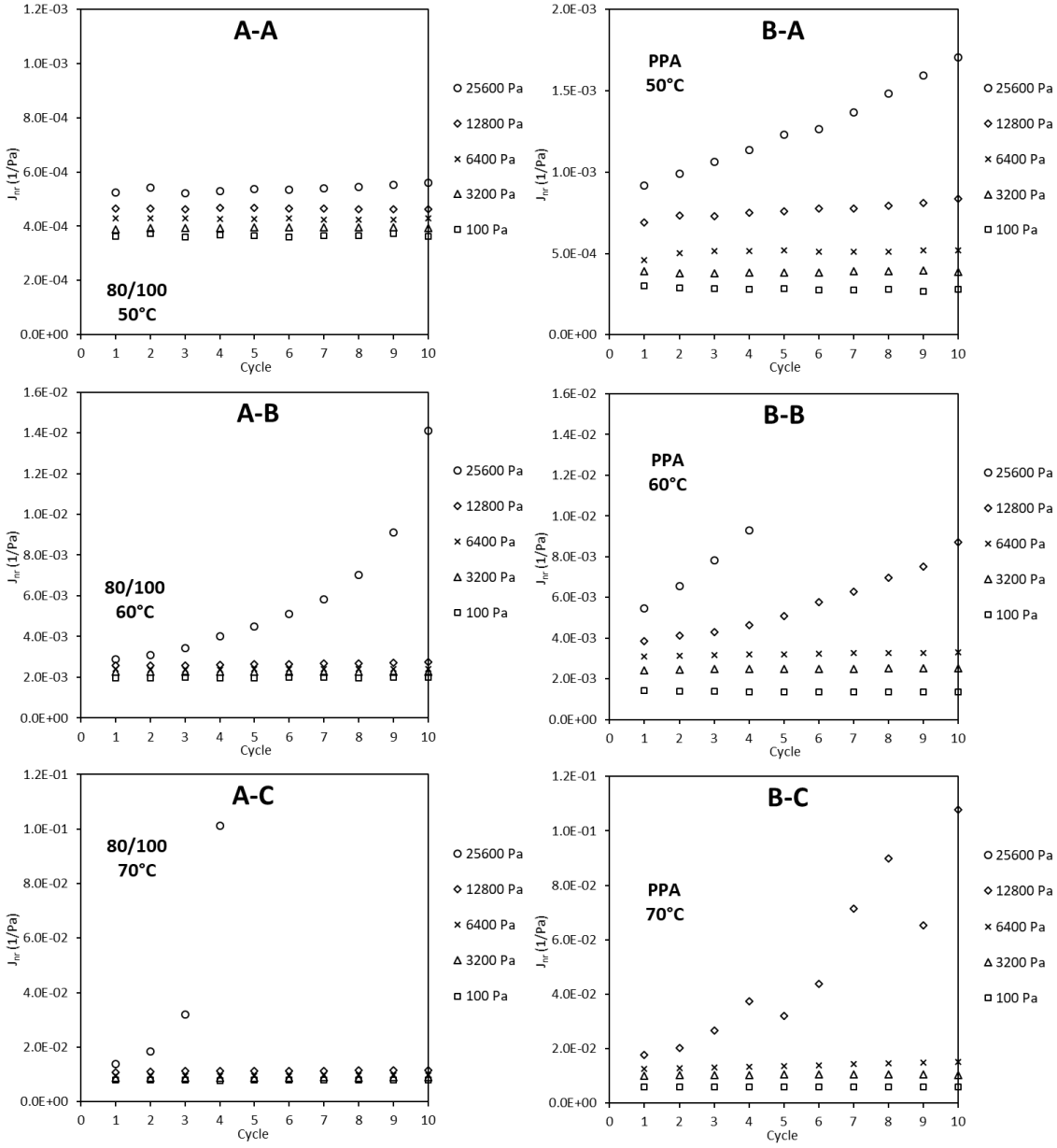

Figure 4.8 Non-recoverable creep compliance of 80/100 Pen grade straight-run asphalt (left, A-) and PPA-modified 200/300 Pen grade blend (right, B-) at 50°C (-A), 60°C (-B), and 70°C (-C) at each MSCR cycle

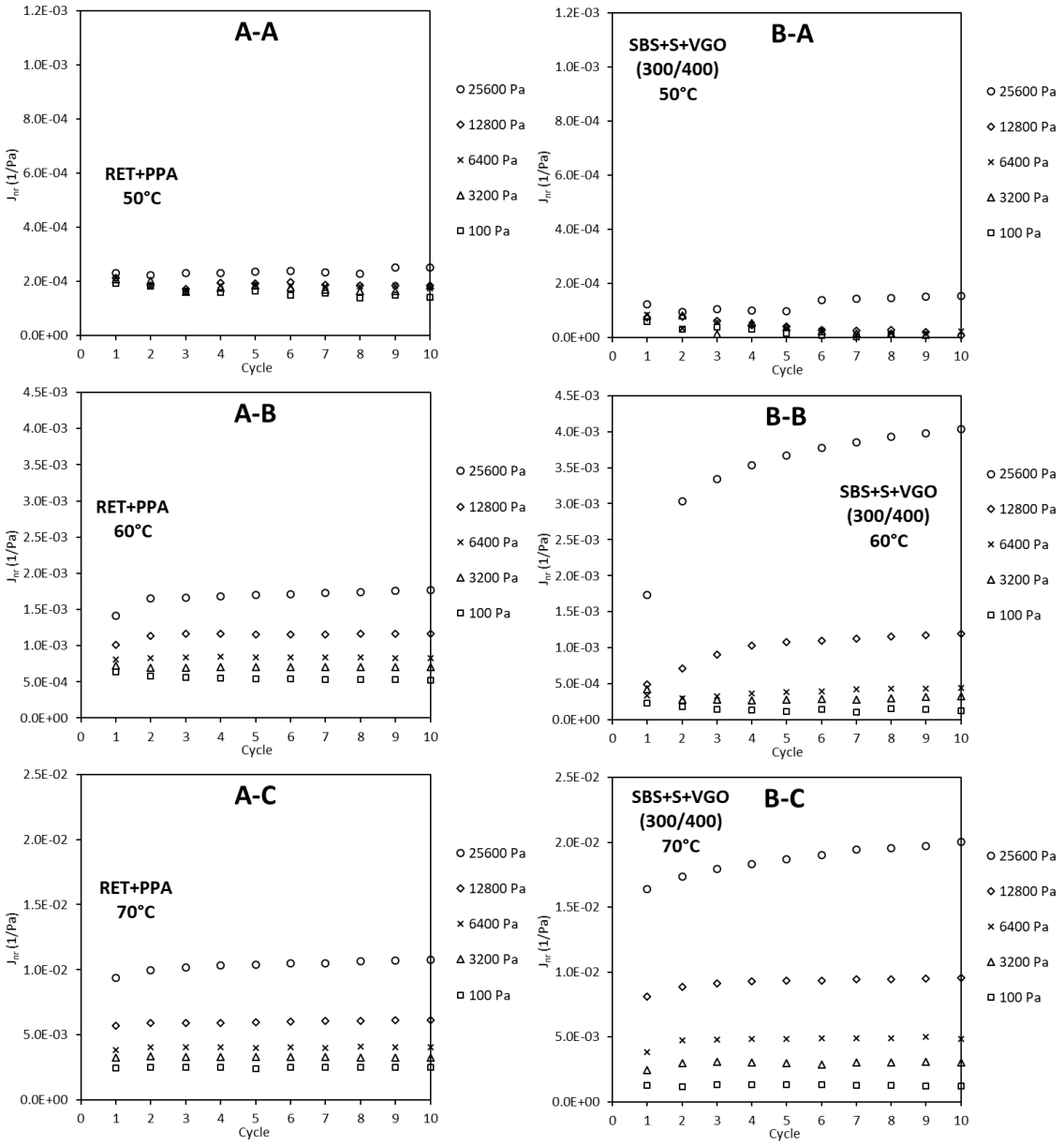

Figure 4.9 Non-recoverable creep compliance of RET+PPA-modified 200/300 Pen grade blend (left, A-) and SBS+S+VGO-modified 300/400 Pen grade blend (right, B-) at 50°C (-A), 60°C (-B), and 70°C (-C) at each MSCR cycle

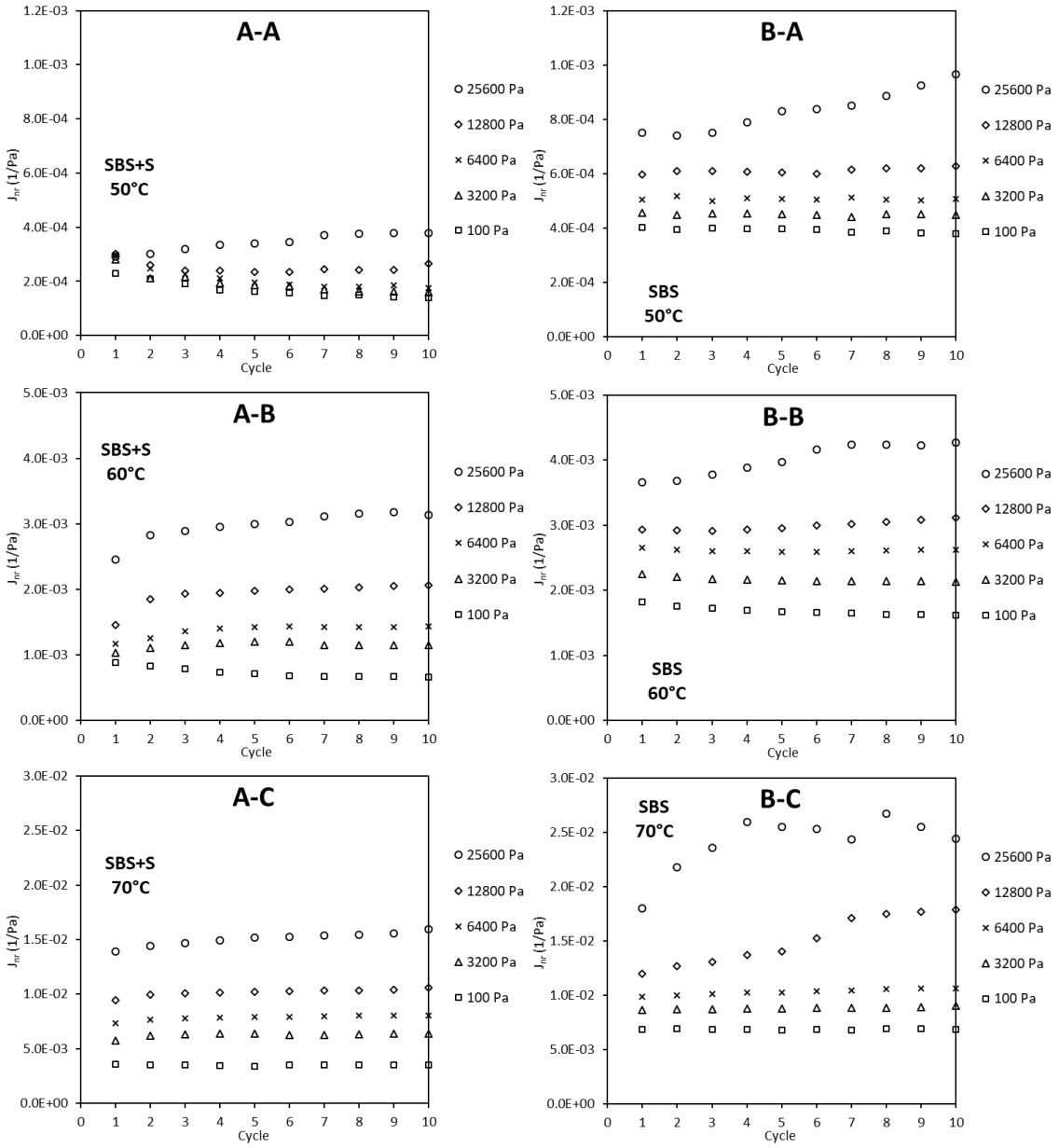

Figure 4.10 Non-recoverable creep compliance of SBS+S (left, A-) and SBS-modified 200/300 Pen grade blends (right, B-) at 50°C (-A), 60°C (-B), and 70°C (-C) at each MSCR cycle

4.1.4. Non-recoverable creep compliance, J_{nr}, and percent recovery, $\%R$, results of asphalt binders tested at five shear stress levels

The plot of the MSCR J_{nr} and $\%R$ values of all binders at five different stress levels and at three testing temperatures of 50, 60 and 70°C are presented in Figure 4.11, Figure 4.12, and Figure 4.13, respectively.

As the stress level increased, both values indicated shear thinning of the binders. However, the differences between the binders' susceptibility to the stress changes was more prominent between the highest two stress levels of 12.8 and 25.6 kPa than between the two standardized stress levels of 0.1 and 3.2 kPa.

Depending on the type and concentration of the polymer modifiers, the stress sensitivity of binders differed significantly at each temperature and stress level. This resulted in different relative rankings of binders for each stress/temperature combination. Thus, finding the most sufficient stress level which could successfully imitate the traffic related stresses and strains was the key objective of this study.

Note that the J_{nr} and $\%R$ results presented in this chapter are the average values after ten successive cycles measured at the same MSCR stress level.

According to the J_{nr} results presented in Figure 4.11, due to their outstanding elastic properties, the SBS+S+VGO and SBS+S-modified 300/400 Pen grade blends were the most rut resistant at 50°C. Both blends showed relatively constant J_{nr} and $\%R$ values up until the 12.8 kPa stress level and a somewhat higher stress sensitivity between the highest two stress levels. However, the SBS+S+VGO (300/400) blend indicated slightly higher sensitivity mainly at higher temperatures. The most likely reason for this was the softer consistency of the base binder and the higher concentration of the crosslinked thermoplastic elastomer. At lower stress levels the effect of the binders' elastic properties was more pronounced, hence the slightly better results at the lower stress levels. At higher stress levels the resistance of the blend was more influenced by the consistency of the asphalt base, which was, due to the presence of VGO, softer than the consistency of the SBS+S-modified 300/400 Pen grade binder. Moreover, at high stress levels the tangled polymer chains became completely extended and started to disentangle, resulting in slippage of the polymer chains. This phenomenon was more evident at 70°C (Figure 4.13), as the most rut resistant SBS+S+VGO (300/400) blend at 0.1 kPa became one of the least rut resistant at the highest shear stress level of 25.6 kPa.

From the modified 200/300 Pen grade asphalt blends the RET+PPA, the SBS+S, and the RET(EP)+PPA indicated the highest resistance to deformation, while the RET+PPA and RET-modified binders proved to be the least susceptible to the increase in stress level from all the tested binders at all testing temperatures.

On the other hand, the most susceptible binders to stress level change were the blends containing PPA, crumb rubber modifier (RET+PPA+CRM, SBS+S+CRM), or dispersed SBS. In all cases the higher stress sensitivity was the result of the complete or partial absence of strong polymer network within the binders. Nevertheless, the stress sensitivity of PPA-modified binder was the most prominent of all binders through all the test temperatures.

Even though, the 80/100 Pen grade straight-run asphalt yielded relatively "slowly" increasing J_{nr} and decreasing $\%R$ values at every successive stress level, it was raked by the MSCR test among the four least resistant binders. Generally, the MSCR test tended to favor soft asphalt binders with exceptionally good elastic properties, while overly underestimate stiffer binders with low elasticity.

Except the four susceptible blends, and most of all the PPA-modified binder, the bulk of the tested binders yielded "slowly" increasing J_{nr} values through the whole stress level range at 50°C.

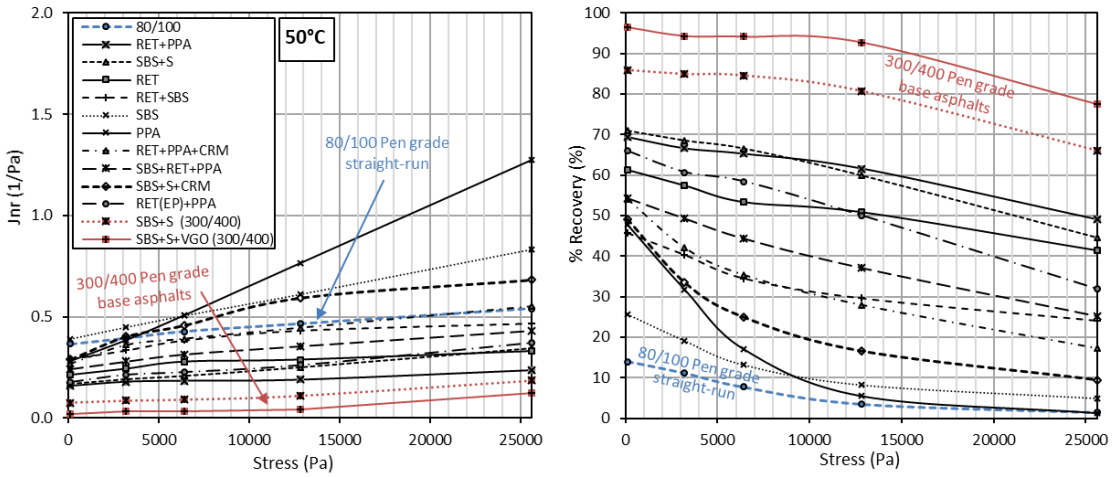

Figure 4.11 Plot of the average non-recoverable creep compliance, J_{nr}, (left) and percent recovery, $\%R$, (right) results of all tested binders at 50°C over multiple stress levels from the MSCR test

At testing temperature of 60°C, which was close to the binders' maximum service temperature and above their RTFO-aged softening point, they became more susceptible to change in stress, which was again more prominent between the two standard (i.e., 0.1, 3.2 kPa) and between the highest two shear stress levels (i.e., 12.8, 25.6 kPa).

The most susceptible to high stresses were the PPA-modified 200/300 Pen grade binder, the 80/100 Pen grade straight-run asphalt, and the binders blended from 300/400 Pen grade asphalt base (SBS+S, SBS+S+VGO), while the PPA-modified binder was the only binder that was completely damaged at 25.6 kPa shear stress level resulting in separation of the two spindles of the DSR.

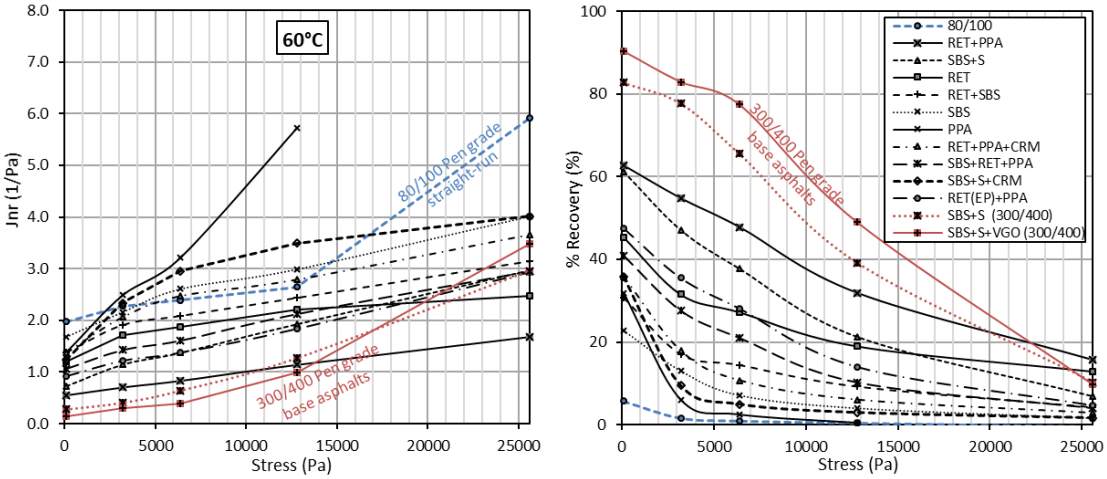

Figure 4.12 Plot of the average non-recoverable creep compliance, J_{nr}, (left) and percent recovery, $\%R$, (right) results of all tested binders at 60°C over multiple stress levels from the MSCR test

The almost linearly increasing relationship between most of the binders' J_{nr} results and the applied stress levels indicated that at 70°C, which was one PG grade higher than the binders' maximum service temperature, the only major factor that affected their resistance to rutting was the consistency or viscosity of the blends (Figure 4.13). This behavior was most evident at shear stress levels higher than 3.2 kPa.

The most likely reason for the good performance of the RET+PPA-modified binder was the creation of chemical bonds between the RET and asphaltene molecules that completely altered the structure of the whole binder making it more viscous, stiffer, and less sensitive to changes in temperature within the studied temperature range.

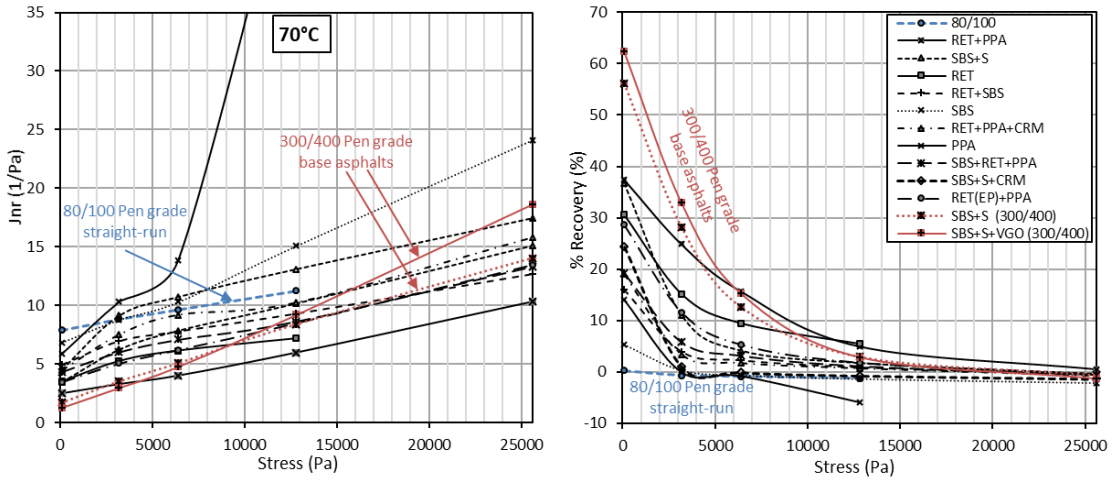

Figure 4.13 Plot of the average non-recoverable creep compliance, J_{nr}, (left) and percent recovery, $\%R$, (right) results of all tested binders at 70°C over multiple stress levels from the MSCR test

From the presented results it is evident that the highest shear stress level should be the function of the testing temperature. Thus, the use of 25.6 kPa is only justified at considerably low temperatures relative to the binders' maximum service temperature.

4.1.5. Creep compliance, J_c, and recovered compliance, J_{rec}, results of asphalt binders tested at five shear stress levels

The J_{nr} results discussed in the previous chapter indicated that the MSCR test favored soft binders with good elastic properties that might perform weakly at higher stress levels and temperatures and underestimated "hard" (more viscous) binders with negligible elastic properties that might be more resilient to deformation in the first place.

To determinate the separate contribution of viscosity and elasticity to the rut resistance, creep resistance and the magnitude of elastic recovery were calculated and compared with the actual rut resistance of all binders (results presented in Chapter 4.3.3). In this chapter the stress sensitivity of these two properties were expressed and presented in terms of compliance values.

Neither the J_{nr} nor the $\%R$ values were capable to express creep resistance and recovery elasticity separately, since both values were the combination or ratio of the two (Equations (3.2) and (3.5)). Therefore, by using the strain values that occurred during the

creep phase (creep strain, $\varepsilon_c^N - \varepsilon_0^N$) and during the recovery phase (recovered strain, $\varepsilon_c^N - \varepsilon_r^N$), both properties could be expressed separately (Figure 3.14).

For comparison the strain results had to be normalized by the applied creep stress. Thus, the average creep compliance, J_c, and the recovered compliance, J_{rec}, of each binder were calculated for ten successive cycles, by dividing the average strain results with the respective applied shear stress level. Both values were measured at testing temperatures 50, 60 and 70°C and were presented in Figure 4.14, Figure 4.15, and Figure 4.16, respectively.

As it was expected from the accumulated compliance results, the 80/100 Pen grade straight-run asphalt showed the highest resistance to deformation from all the tested binders at 50°C (Figure 4.14). Interestingly, the other binders indicated very similar resistance at the three lowest stress levels while their different stress sensitivity became clearly distinct only at the highest stress level of 25.8 kPa, with PPA and dispersed SBS-modified binders being the least resistant and the RET+PPA-modified the most resistant to high stresses.

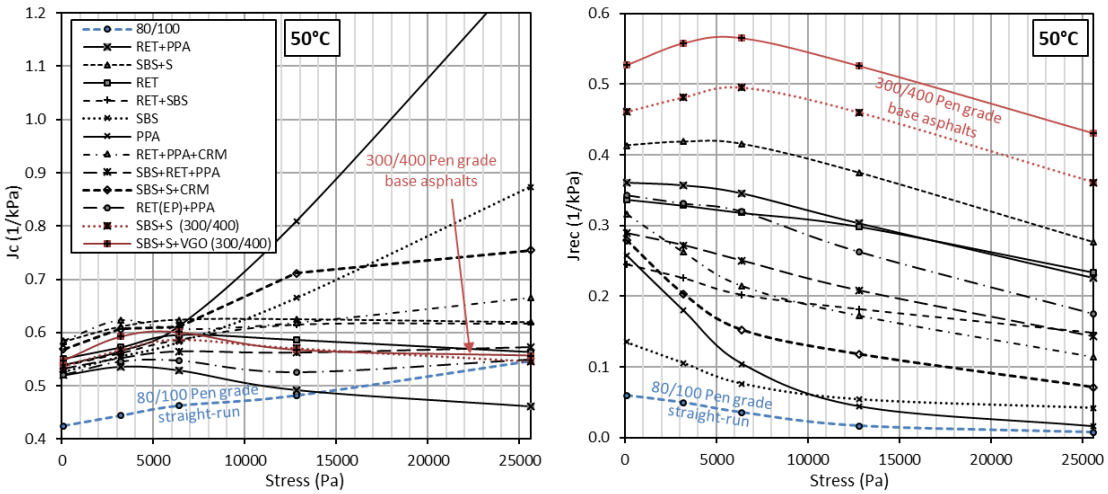

Figure 4.14 Plot of the average creep compliance, J_c, (left) and recoverable creep compliance, J_{rec}, (right) results of all tested binders at 50°C over multiple stress levels from the MSCR test

Both soft binders of SBS+S and SBS+S+VGO-modified 300/400 Pen grade asphalts showed increasing recovery compliance (right graph in Figure 4.14) at the first three creep stress levels, indicating that the entangled polymer chains could be further stretched and therefore store more energy up until 6.4 kPa stress level at 50°C.

Based on the J_{rec} results, the PPA-modified binder and the two CRM-modified binders showed the greatest reduction in their elastic behavior, making them the most susceptible to changes in stress levels.

Again, the creep compliance of RET and RET+PPA-modified binders were the most resistant to stress changes, while the PPA-modified the least resistant at 60°C temperature (Figure 4.15) which was approximately about the RTFO-aged binders' R&B softening point.

According to the J_c results at 60°C the 80/100 Pen grade asphalt became less stiff and was ranked among the weaker performing binders. Moreover, at the highest creep stress level of 25.6 kPa it became the second weakest binder and also showed the signs of material fatigue (see also Figure 4.8A-B). These results contradicted with the expectations that the main reason why MSCR J_{nr} parameter ranked this binder among the weaker performing ones at relatively low stress levels was mainly due to its low elasticity.

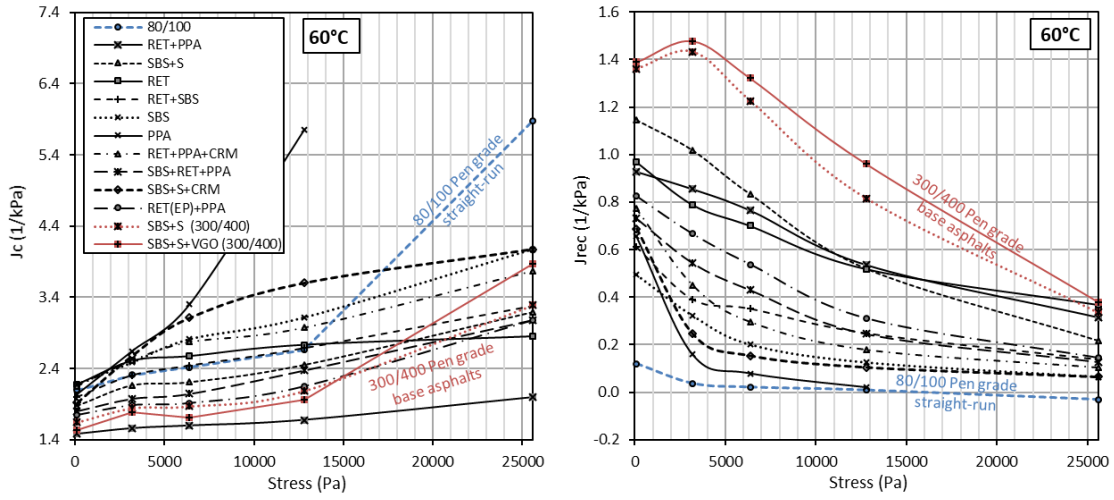

Figure 4.15 Plot of the average creep compliance, J_c, (left) and recoverable creep compliance, J_{rec}, (right) results of all tested binders at 60°C over multiple stress levels from the MSCR test

Nonetheless, most of the binders indicated relatively similar increase in creep compliance with higher increase between the lowest two and, in some cases, the highest two stress levels. As discussed above, depending on the polymer network, a considerable amount of the invested energy could be stored as elastic energy during the process of deformation. Thus, when tested in the linear viscoelastic (LVE) range polymer modified

asphalt binders appear much stiffer than at higher stress levels, such as those normally experienced by the binders in the pavements under heavy traffic loads.

With minor differences the J_c values at one grade higher temperature than the binders' maximum service temperature (Figure 4.16), showed very similar results to the J_{nr} values at the same temperature (Figure 4.13). This indicated that at such high temperatures the gained elasticity does not play a major role (if any) in the resistance to deformation and presumably only stiffens the material.

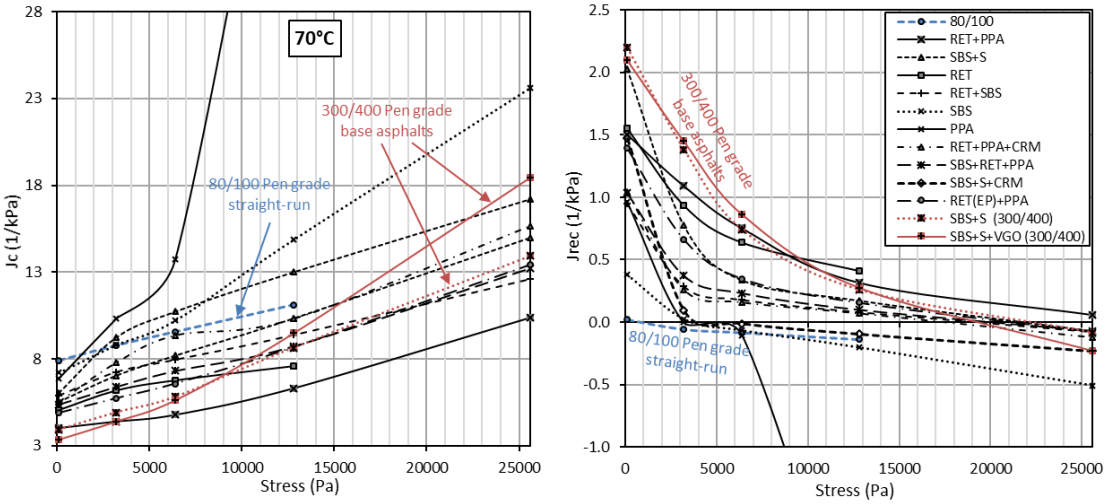

Figure 4.16 Plot of the average creep compliance, J_c, (left) and recoverable creep compliance, J_{rec}, (right) results of all tested binders at 70°C over multiple stress levels from the MSCR test

4.2. Asphalt mix results

In order to understand the relation between the performance of asphalts and asphalt mixes at high temperature where the rutting of asphalt mixes are most likely to occur, the dynamic modulus test results and the Hamburg wheel-tracking test results are assessed in this chapter.

4.2.1. Hamburg wheel-tracking test results

The Hamburg rutting resistance of asphalt mixes, prepared from all the used asphalt binders, was tested at 60°C temperature.

Generally, the rut resistance of the HMAs could be affected by a large number of variables, such as the combined aggregate gradation, the type and content of asphalt

binder in the mixture, and the volumetric properties of the compacted asphalt mixture specimens. For this reason the same mix design (e.g., aggregate gradation, asphalt content, volumetric properties, and percentage of air voids) was used, and the same short-term mixture conditioning procedure was conducted in the case of all mixes, to ensure that the only difference between the mixes was the type of the asphalt binder. The volume of asphalt binder in the mixes was set to 5.9 wt.%.

The most important volumetric properties of the compacted specimens, such as specific gravity (G_{mb}), air void (V_a), voids in the mineral aggregate (VMA), and voids filled with asphalt (VFA), along with the Hamburg wheel-tracking asphalt mix results, are summarized in Table 4.6. The HMA test specimens were compacted to 6.2 ± 0.9% air voids.

The mix properties presented in Table 4.6 showed negligible differences between the volumetric properties of asphalt mixes prepared with different asphalt binders. Therefore, any major difference between the rut resistance of asphalt mixes could be attributed to the differences between the asphalt binders they were prepared from.

Table 4.6 Hot mix asphalt specimen properties and the Hamburg wheel-tracking test results

		Superpave® Test Results				
Base Binder	Polymer Type Designation	G_{mb} (kg/m^3)	V_a (%)	VMA (%)	VFA (%)	HWTT (mm)
80/100	None	2.293	6.2	17.257	63.877	4.05
200/300	RET+PPA	2.284	6.6	17.589	62.364	3.93
	SBS+S	2.293	6.2	17.251	63.838	4.07
	RET	2.300	6.0	17.010	64.930	5.59
	RET+SBS	2.317	5.3	16.406	67.816	7.30
	SBS	2.296	6.1	17.173	64.189	8.11
	PPA	2.294	6.2	17.228	63.942	14.04
	RET+PPA+CRM	2.272	7.1	18.013	60.590	7.05
	SBS+RET+PPA	2.285	6.6	17.566	62.498	5.43
	SBS+S+CRM	2.282	6.7	17.670	62.112	8.10
	RET(EP)+PPA	2.289	6.4	17.419	63.101	4.27
300/400	SBS+S	2.294	6.2	17.222	63.984	5.41
	SBS+S+VGO	2.298	6.1	17.091	64.560	5.86

The Hamburg wheel-tracking test (HWTT) results from Table 4.6 are presented in increasing order in Figure 4.17. According to the HWTT results, almost all mixes, examined in this study, could be divided into three distinct groups of four binders with very similar results. The only asphalt mix that showed significantly different rut resistance, in compliance with the MSCR results measured at higher stresses, was the mix

prepared from the PPA-modified asphalt blend, which also proved to be the least rut resistant from all the tested binders.

The most resistant mixes were the ones prepared from the RET+PPA, the SBS+S, the RET(EP)+PPA-modified 200/300 Pen grade blends, and the 80/100 Pen grade straight-run asphalt. When considering only the blends prepared from the 200/300 Pen grade asphalt base, RET+PPA, SBS+S, and RET(EP)+PPA were among the best performing binders even according to their J_{nr} results at 50 and 60°C. However, when comparing all binders, the SBS+S and SBS+S+VGO-modified 300/400 Pen grade asphalt blends showed substantially better J_{nr} results at 50 and 60°C than all the remaining ones, mainly due to their very good elastic properties (as discussed in Chapter 4.1.4). Nevertheless, despite the promising MSCR results, the exceptional rut resistance of these binders was not confirmed by HWTT asphalt mix testing and ranked them, along with the SBS+RET+PPA and RET-modified 200/300 Pen grade blends, into the second most rut resistant group.

When compared to all binders, the 80/100 Pen grade straight-run asphalt also showed similar peculiarities as the 300/400 Pen grade blends, only in the opposite sense. Namely, the asphalt mix prepared from the stiffest and most viscous 80/100 Pen grade straight-run asphalt binder indicated significantly better rutting resistance than as it could have been assumed from the MSCR test results of the binder.

These findings also supported the hypothesis that the rut resistance strongly depended on the stiffness of the asphalt base, regardless of the entropic elasticity achieved through modification. Consequently, the MSCR test overestimated the effect of elasticity on the binders' rut resistance and underestimated the stiffness/viscosity of their respective asphalt base. Therefore, a higher accent should be given to the binder's ability to resist the applied stresses than to their gained elasticity.

Asphalt binders prepared by modification with non-crosslinked SBS and asphalt binders modified by both non-crosslinked SBS and CRM scored among the worst in rut resistance from the tested paving mixes. Compared to crosslinked modifiers, it appeared that when CRM and non-crosslinked SBS were used as asphalt modifiers they increased the binders' maximum service temperature and their standard MSCR test performances considerably more than they increased the rut resistance of their respective mixes.

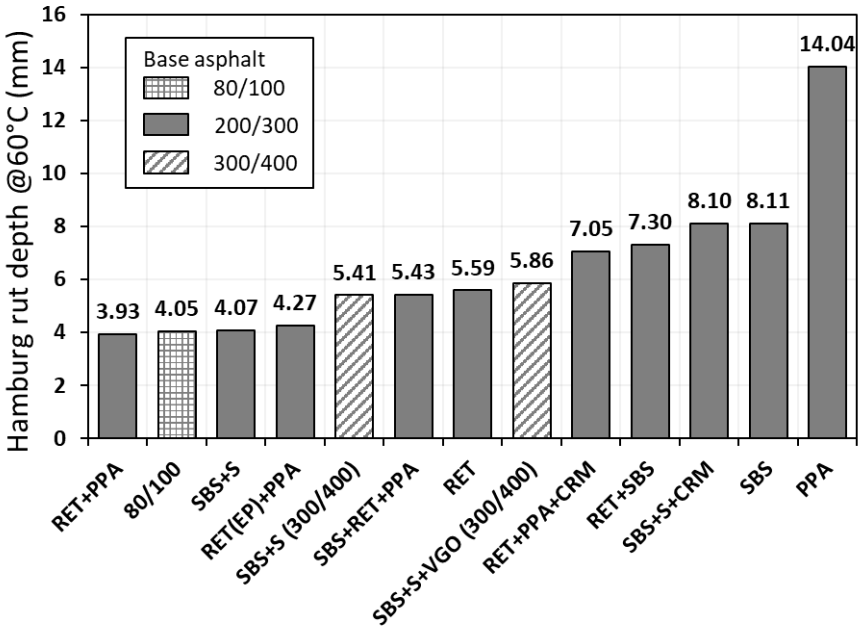

Figure 4.17 Rut depth after 10,000 cycles of all tested mixes at 60°C, sorted according to their rut resistance

As it was discussed in Chapter 2.6, the development of rut is the result of densification and shear deformation. Initially, during densification, the asphalt mix layers become load-compacted and stiffened due to the rearrangements of the aggregate particles and expelling of air voids. After the densification is complete, further deformations occur resulting in material displacement (without change in volume) beneath the wheel path. In the final stage (i.e., tertiary flow), when enough distortion has occurred, the rate of deformations rapidly increase resulting in partial or complete destruction of the asphalt mix layer.

Examples showing the development of rut in mix samples with six selected binders as the test progressed are depicted in Figure 4.18. Possibly due to densification (also consolidation or primary stage) of the mixes an initial sharp increase in the rut depth was typical for all binders. In most cases the increase (or rate of rutting) tended to stabilize with the application of more wheel passes (i.e., secondary stage). This general trend of changes in rutting with the number of wheel passes was observed in all Hamburg wheel-tracking tests conducted in this study. Note that under the same loading conditions at 60°C temperature and after 10,000 cycles none of the examined mixes exhibited tertiary flow.

After 10,000 cycles the paving mixes prepared with the RET+PPA, SBS+S, RET(EP)+PPA-modified 200/300 Pen grade asphalt blends, and the 80/100 Pen grade straight-run asphalt proved to be the most resistant to rutting, while with the PPA-modified binder the least resistant to rutting.

By comparing asphalt mixes prepared with RET+PPA and 80/100 (Figure 4.18), one could notice that initially during densification the RET+PPA mix indicated lower rate of deformation. However, once the densification was complete, the 80/100 mix became stiffer and exhibited lower rate of rutting.

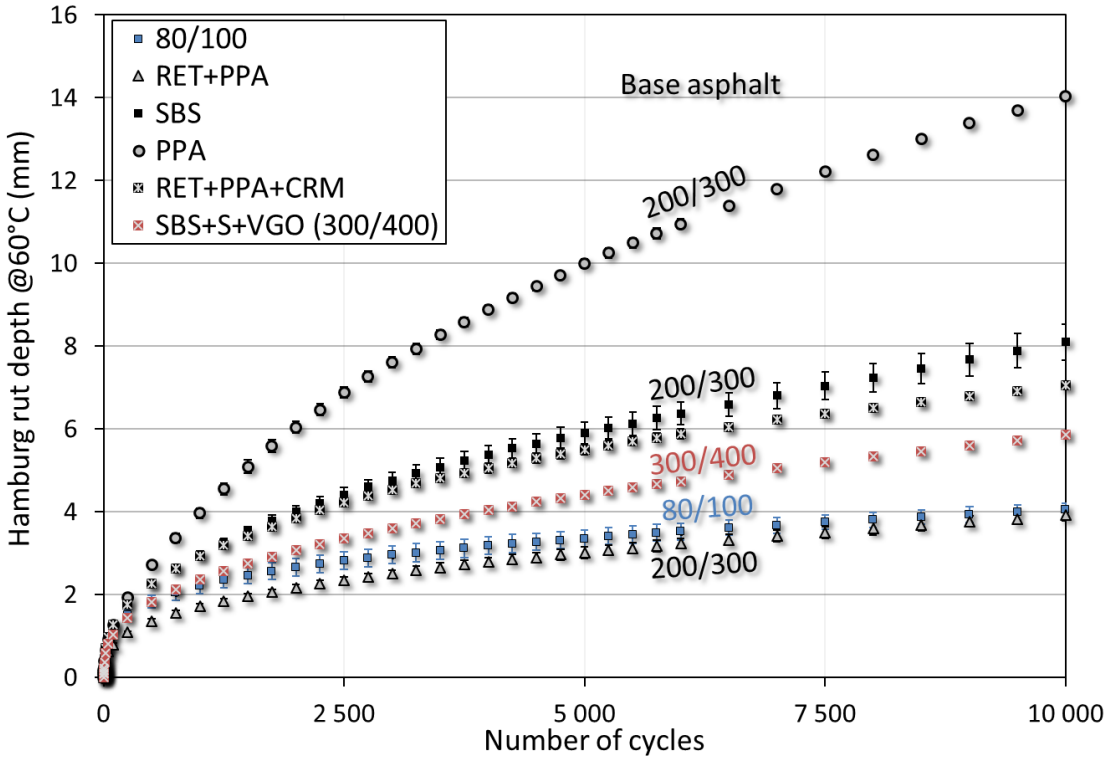

Figure 4.18 Rut development in mixes presented on an example of six selected asphalt binders

According to Kose *et al.* [217] the strain in the binder could range between an average of 7.8 times and a maximum of 510 times the bulk strain of the asphalt mix. He also reported that the directional film thickness (aggregate particles coated with thin film of asphalt) within a typical asphalt mix appeared to be varying between 13.5 and 600 μm, but film thickness of less than 5 μm was also reported [272].

Thus, during densification, when the rearrangement of aggregate particles was most pronounced, and the magnitude of bulk strain the highest, the thin films of asphalt binders had to endure much higher stress levels than during the secondary stage. After the

densification was complete, the mixes were already load-compacted and stiffened with minimal room for any particle rearrangements. Thus, most of the strains occurring within the mixture was due to material displacement and the rate of deformation was driven by the stiffness of the whole mixture, which was also why the rate of rutting stabilized.

Therefore, the conditions during densification, when the highest stresses and strains occurred, were more favorable for less stress sensitive asphalt binders, such as the RET+PPA-modified binder. However, stiffer base binders, such as the 80/100 Pen grade straight-run asphalt, were more successful in withstanding lower stress and strain levels that occurred during the secondary stage, than binders with less viscous asphalt base.

This phenomenon could be seen in Figure 4.14 at 50°C, where the 80/100 Pen grade straight-run asphalt at lower stress levels outperformed (lower creep compliance, J_c) the RET+PPA-modified 200/300 Pen grade asphalt blend, however, at higher stress levels, it showed inferior performance (higher creep compliance, J_c).

However, due to the high temperature susceptibility of 80/100 Pen grade binder, at higher temperatures (e.g., 60 and 70°C) than its RTFO-aged softening point (i.e., 56°C), this trend was no longer evident (Figure 4.15). In other words, the creep compliance, J_c, results better described this phenomenon when measured at 50°C than at 60 or 70°C.

One possible explanation for this was that the RTFO short-term ageing had different impact on the binders' chemical and rheological properties than what they experienced during mixing with aggregates. In addition, all binders had different aging properties and thus the change of their relative stiffness or viscosity (i.e., "hardness") could vary in magnitude.

Another explanation for this phenomenon was the selective nature of asphalt absorption, when lighter, less viscous, fractions of the asphalt (i.e., saturates, aromatics) might have been absorbed preferentially into the pores of aggregates while the heavier asphaltene rich fraction was left behind in the effective asphalt film. In turn, because of this selective absorption, the asphalt film became more viscous and stiffer than the original asphalt binder added during mix preparation, resulting in, that asphalt binder results, measured at lower than the HWTT temperature, better described the material behavior in asphalt mixes [273].

Both explanations lead to the conclusion that the creep compliance, J_c, results were more successful in predicting the binders' rutting development at lower temperatures than the HWTT testing temperature of the mixes.

Note that even though the non-recoverable creep compliance, J_{nr}, value, measured at higher shear stress levels, was able to detect the susceptibility to rutting of the worst performing PPA-modified binder, it failed to properly determine the exceptional rut resistance of the 80/100 Pen grade straight-run asphalt. Furthermore, J_{nr} consequently overestimated the effect of elasticity on the binders' rut resistance in the case of SBS+S and SBS+S+VGO-modified 300/400 Pen grade binders. On the other hand, J_{nr} value better estimated the relative rut resistance of SBS+S-modified 200/300 Pen grade blend when compared only to binders prepared from the same asphalt base, while the J_c value consistently underestimated its rut resistance and ranked it close to less rut resistant binders such as the RET+PPA+CRM-modified binder (Figure 4.14 and Figure 4.19).

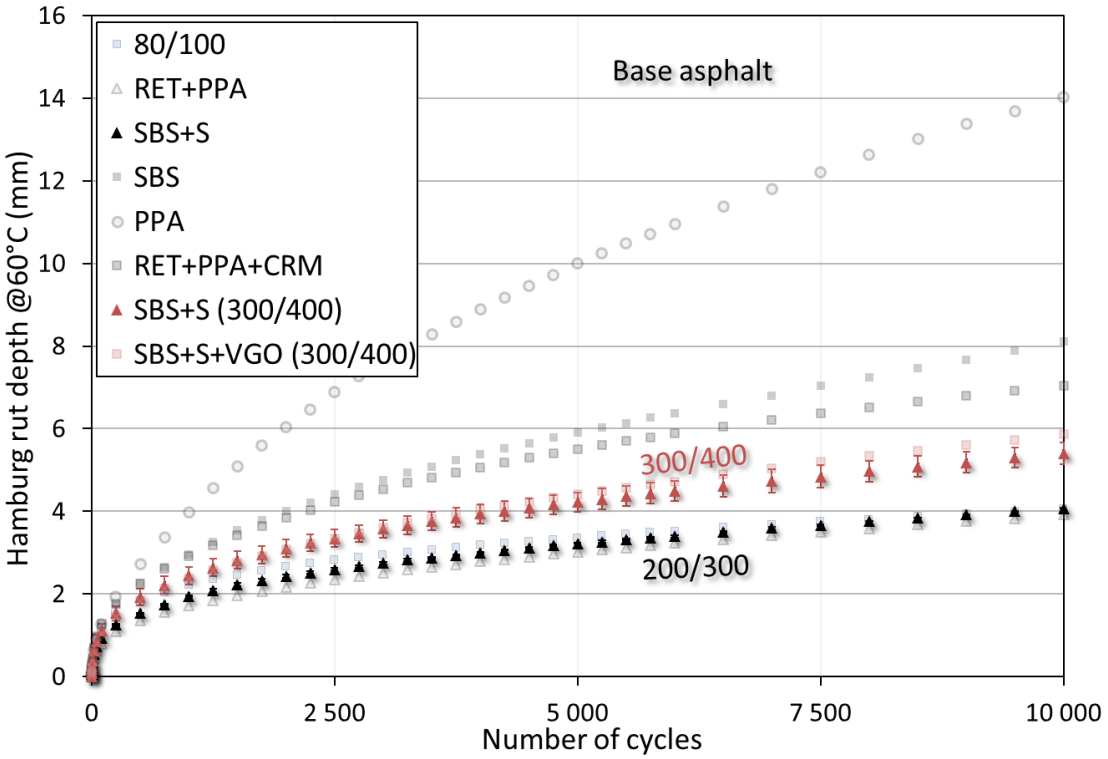

Figure 4.19 Rut development in mixes on an example of two additional asphalt binders indicating good performance

In the case of the 300/400 Pen grade blends, J_c, measured at 50°C, proved to be more successful in predicting the rut resistance of both blends relative to each other and to all binders tested. It is worth mentioning, that despite the higher amount of crosslinked SBS in the SBS+S+VGO-modified 300/400 Pen grade asphalt base, the addition of VGO to the asphalt base made the binder less resistant to rutting than the SBS+S-modified binder blended with the same 300/400 Pen grade base asphalt but with less amount of

crosslinked SBS. This further proved that by using less viscous base asphalts, the resulting modified binders became less resistant to deformation and more sensitive to stress changes, and all this despite the higher concentration of the modifiers in the asphalt base and thus their better elastic properties.

4.2.2. Dynamic modulus testing results

In accordance with AASHTO 342 [266], the dynamic modulus test was conducted in servo-hydraulic-controlled universal testing machine (UTM). During the test uniaxial sinusoidal compressive stress was applied to an unconfined test specimen, and the corresponding strain using three LVDTs mounted on the middle of the sample was monitored.

Three cylindrical specimens per mix were tested in order to obtain the rheological parameters and develop the dynamic modulus, $|E^*|$, master curves for each asphalt mix. The dynamic modulus test was conducted at testing temperatures of –15, 0, 15, 30, 45, and 60°C and at testing frequencies of 25, 10, 5, 1, 0.5, and 0.1 Hz.

Especially at the higher temperature ranges common problem of dynamic modulus testing is the loosening of the glued gauge points, resulting in inconsistent or high deviation results between each test specimen. Therefore, data from "problematic" experiments (e.g., unstable LVDT, slightly damaged sample due to the loading) were eliminated and as a result a substantial amount of data had to be omitted. The dynamic load was adjusted to comply with AASHTO 342 condition that recoverable axial microstrain should be within the range of 50–150 microstrains.

Black diagram, a rheological plot of the dynamic modulus, $|E^*|$, versus the phase angle, ϕ, was used to identify inconsistencies in rheological data in order to determine the reference temperature, T_r, for the construction of the master curves. Black diagram is a useful tool to eliminate frequency and temperature from the plot of dynamic data and enabled to assess how stiffness and elasticity of a material were related. This allowed for dynamic data to be presented in one plot without applying time temperature superposition (TTS).

According to Airey [274], a smooth curve in the Black diagram generally indicates time-temperature equivalency, while a disjointed curve indicates breakdown of the TTS. In Figure 4.20 the dynamic raw data of asphalt mixes prepared from 80/100 Pen grade straight-run and the SBS+RET+PPA-modified 200/300 Pen grade asphalt were plotted.

Based on the results, plotted in Black diagrams, all mixes indicated relatively consistent results at intermediate and low temperatures. Thus, to ensure the most accurate vertical position of the master curves in the plot, 15.0°C was chosen as the reference temperature, T_r, for the creation of the master curves. Note that the shapes of the master curves of the dynamic material functions would be identical at any chosen reference temperature, they would be only shifted on the ordinate (y-axis).

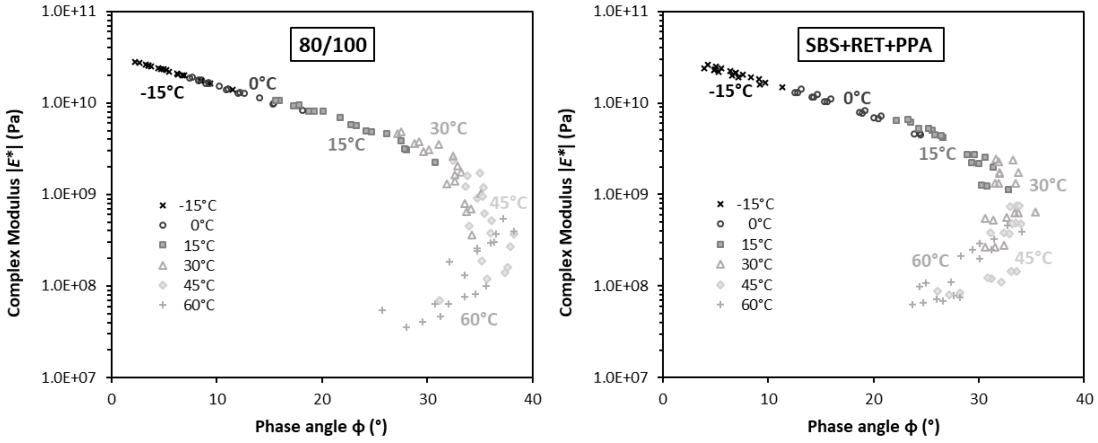

Figure 4.20 Black diagrams of the 80/100 (left) and the SBS+RET+PPA (right) asphalt mixes

Dynamic moduli values determined at various temperatures before and after shifting were presented in Figure 4.21 and in Figure 4.23, respectively.

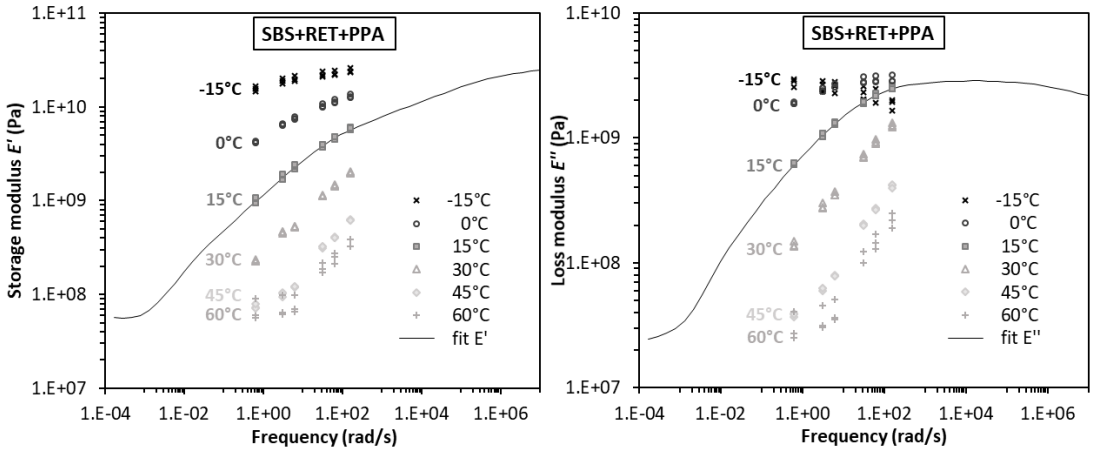

Figure 4.21 Storage modulus, E', and loss modulus, E'', curves of SBS+RET+PPA asphalt mix at different temperatures before shift, T_r=15°C, fit to the master curves, Equations (3.14) and (3.15)

In accordance with the TTS principle, by shifting each individual curve obtained at different temperatures, the dynamic moduli master curves at reference temperature of 15°C were prepared for all the tested materials in the IRIS platform [267].

According to Lou *et al.* [275] the master curve constructed by using the Williams-Landell-Ferry (WLF) equation should result in the most accurate predictions of dynamic modulus in a wide range of frequencies. Therefore, the reduced frequency, f_r, (Equation (2.50)) was calculated using the horizontal shift factor, a_T, which was fitted to the WLF relation (Equation (2.52)), presented in Figure 4.22 on an example of asphalt mix prepared from the SBS+RET+PPA-modified asphalt blend. No vertical shifting was needed to obtain the master curves of the dynamic material functions for all the materials used in this study.

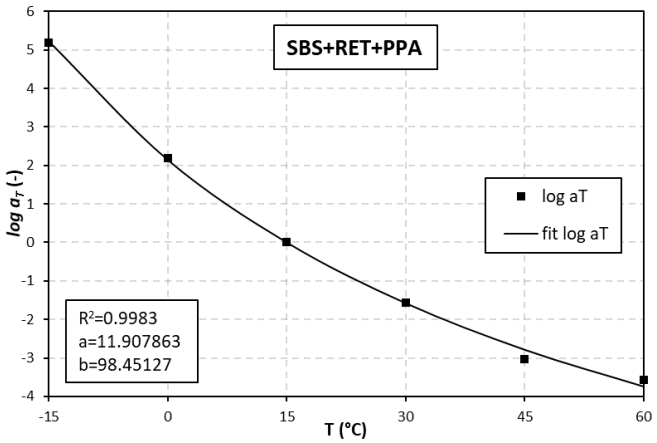

Figure 4.22 Horizontal shift factor for SBS+RET+PPA asphalt mix, T_r=15°C, fit to WLF relation, Equation (2.52)

Once the dynamic moduli were fitted to Equations (3.14) and (3.15), IRIS calculated the relaxation and retardation spectra for each HMA sample.

As an example, the master curves of the dynamic material functions (E', E'', $\tan\phi$) at reference temperature of 15°C were presented in Figure 4.23 and Figure 4.24 for HMA prepared from SBS+RET+PPA-modified 200/300 Pen grade asphalt blend. Typically, the storage modulus, E', increased with frequency and reached its plateau at high frequencies (low temperatures), while the loss modulus, E'', after reaching its maximum started to decrease at higher frequencies.

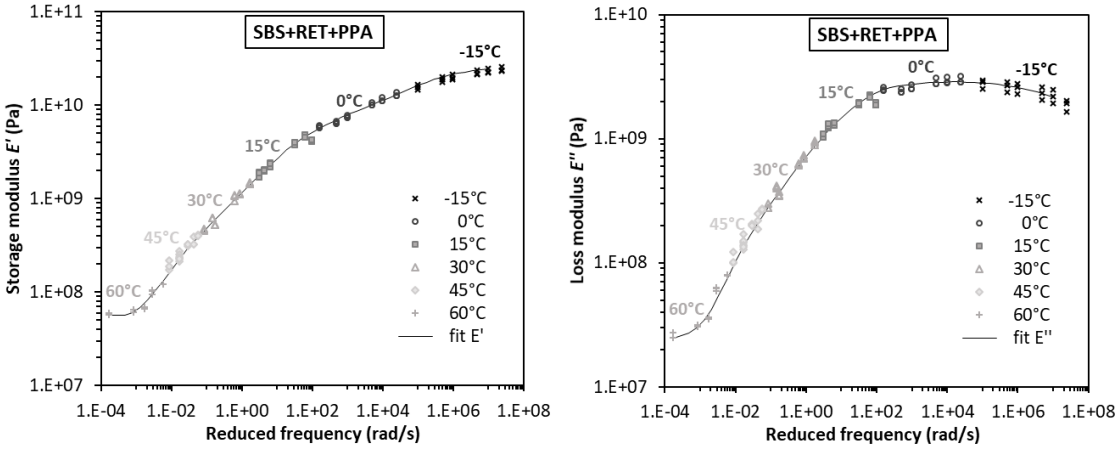

Figure 4.23 Storage modulus E' (left) and loss modulus E'' (right) curves of SBS+RET+PPA-modified asphalt at different temperatures after shift, T_r=15°C, fit to the master curves, Equations (3.14) and (3.15)

As for the loss tangent, $\tan\phi$, it reached its absolute maximum well before the loss moduli did, indicating that at low frequencies (high temperatures), due to the low stiffness and viscous flow of the asphalt binder, the aggregate structure dominated the behavior of the HMA specimens.

Usually, at lower frequencies (higher temperatures than ~60°C) asphalt binders show liquid-type behavior (Newtonian zone) and are greatly affected by their composition. Therefore, testing at such high temperatures was in many cases not possible and often resulted in unreliable data due to the loosening of the glued gauge points.

In contrary, at high frequencies (low temperatures) other factors, such as mix volumetrics and binder stiffness became dominant and controlled the dynamic material functions. Typically, at such low temperatures, the maximum of loss modulus, E'', could be associated with the glass transition temperature of the asphalt binder the HMA contained. After reaching the absolute maximum, the loss modulus, E'', started to decrease in the glassy region.

The presence of peak loss tangent suggested that at low frequencies the HMA specimen behaved as linear viscoelastic solid in the tested domain of reduced frequencies. For example, the Black curves presented in Figure 4.20 clearly indicated that the peak value of loss tangent was reached between the temperatures of 30 and 45°C, which was substantially lower than the maximum service temperature of the binder used in the mix.

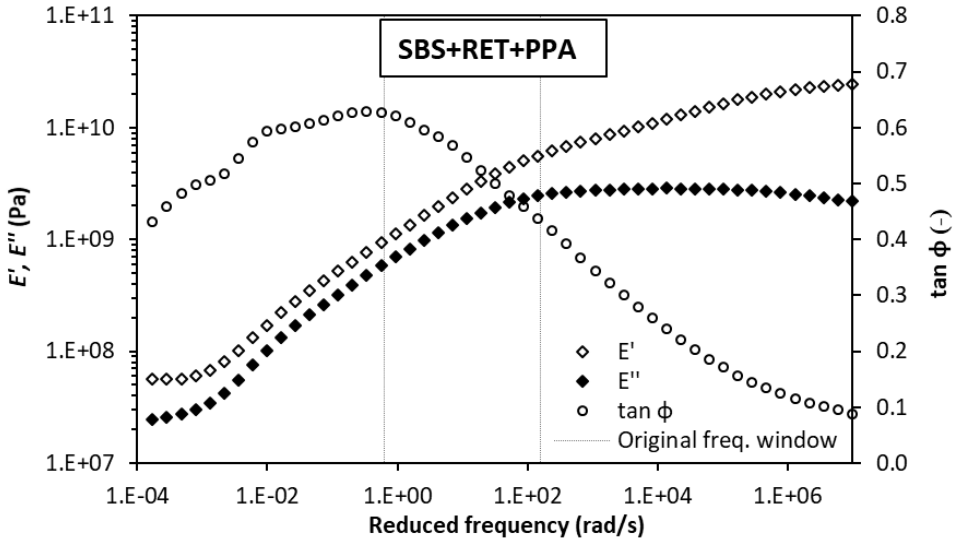

Figure 4.24 The master curves of the dynamic material functions (E', E'', $\tan\phi$) at the reference temperature of 15°C, the SBS+RET+PPA asphalt mix

All the tested samples indicated similar behavior as the SBS+RET+PPA asphalt mix discussed above. In Figure 4.25 the dynamic modulus, $|E^*|$, and the loss tangent, $\tan\phi$, of all HMAs were presented (for storage and loss moduli see Figure B.1 and Figure B.2 in Appendix-B). The HMA prepared with the 80/100 Pen grade straight-run asphalt indicated the highest dynamic modulus of all mixes in the tested domain of reduced frequencies.

The difference between the dynamic values of the 80/100 mix and the other HMAs was most pronounced at high temperatures, suggesting a stiff asphalt material that was the most resistant to permanent deformation under cyclic loading. In contrary, the lower dynamic modulus values of the HMA prepared with the SBS+S+VGO-modified 300/400 Pen grade asphalt base indicated a tendency towards permanent deformation mainly at higher temperature ranges. This was further supported by the loss tangent values of both mixes. They reached their maximum at substantially different frequencies, indicating that the mix prepared from the least viscous modified asphalt base, despite the high modification level, softened at much lower temperatures than the remaining twelve HMAs. According to these LVE results, the SBS+S+VGO (300/400) asphalt mix was the least resistant to rutting while the 80/100 mix was the most resistant. At lower temperatures (high frequencies), the dynamic modulus of all mixtures converged to the same magnitude, suggesting very similar material properties.

Asphalt mixes prepared with the 200/300 Pen grade modified blends indicated similar dynamic modulus through the whole tested domain of reduced frequencies. The differences between the individual asphalt mixes became more pronounced when the values of their loss tangent was examined at high temperature. Nonetheless, the significantly lower rut resistance of HMA containing PPA-modified 200/300 Pen grade base asphalt was not revealed by the mixture's LVE dynamic functions.

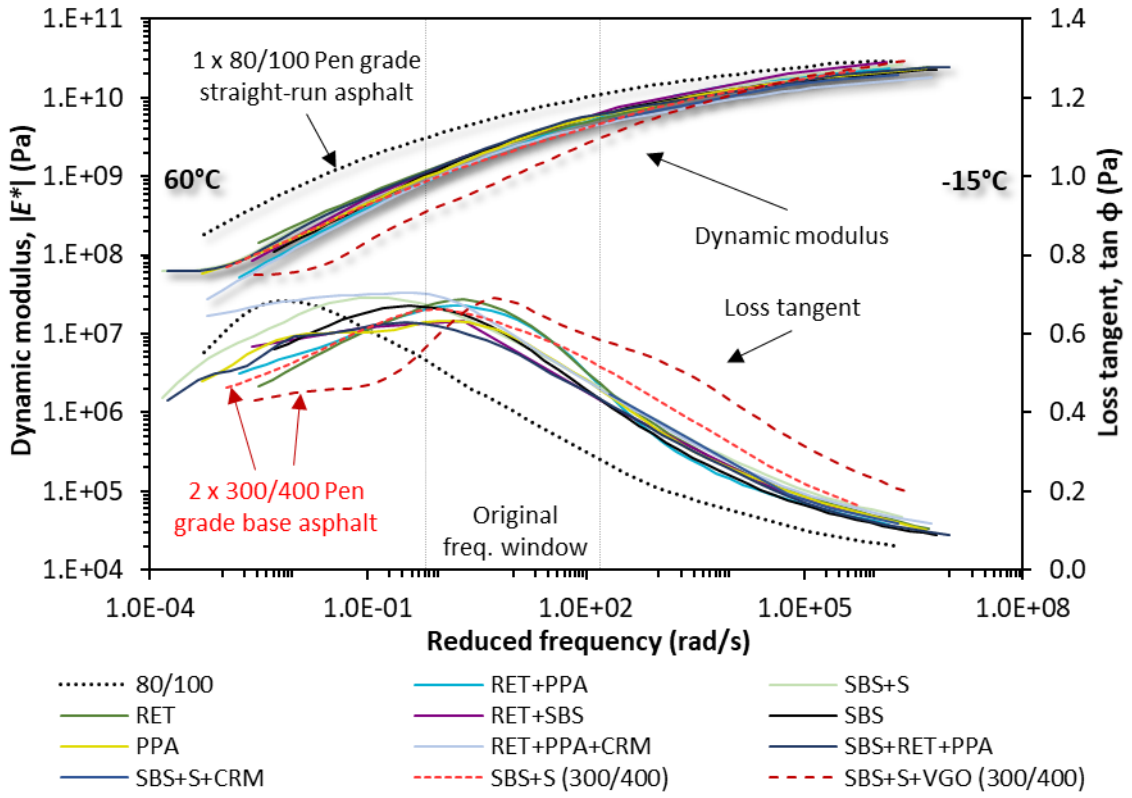

Figure 4.25 Magnitude of the dynamic modulus, $|E^*|$, and the loss tangent, $\tan\phi$, results at reference temperature of 15°C, comparison of all tested asphalt mixes

Due to the independency of time and temperature via the use of the WLF relation for the horizontal shift factor described in Equation (2.52), it was possible to transform the frequency domain to the temperature domain for the chosen test frequency as follows:

$$T = T_0 + \frac{B[\log(\omega_0) - \log(\omega)]}{[A - \log(\omega_0) + \log(\omega)]} \tag{4.1}$$

where $T_0 = T_r$ was the reference temperature, ω_0 was the fixed frequency and A and B were the parameters of the WLF equation for horizontal shift factor, a_T [196].

Dynamic moduli at fixed frequency of 1 Hz were selected for rutting susceptibility evaluation of asphalt mixes as it was the closest to the loading frequency of the Hamburg wheel-tracking test (52 wheel passes per minute ≈ 1 Hz).

The temperature dependency of dynamic modulus and loss tangent at fixed frequency of 1 Hz was presented in Figure 4.26 (for storage and loss moduli see Figure B.3 and Figure B.4 in Appendix-B). Most of the unreliable data from "problematic" experiments was eliminated at high temperatures. As a result of this and the different horizontal shift factors of each HMA, many of the dynamic functions presented in Figure 4.26 could not be estimated at high temperatures and were therefore missing from the plots.

According to the dynamic modulus results, the 80/100 asphalt mix was the most resistant to permanent deformation at 60°C. In contrary, asphalt mixes containing either RET+PPA+CRM or PPA-modified 200/300 Pen grade asphalt blends indicated the lowest stiffness at high testing temperatures.

None of the best performing asphalt mixes in HWTT showed significantly higher stiffness in dynamic measurements, nor the worst performing (PPA asphalt mix) showed significantly lower stiffness through the whole temperature range.

Generally, most of the HMAs' loss tangent functions reached their maximum between 30 and 45°C, marking the initial temperature at which the aggregate structure started (i.e., the binder softened) to dominate the behavior of the HMA specimens. This temperature was the highest for the 80/100 and the lowest for the SBS+S+VGO (300/400) asphalt mix.

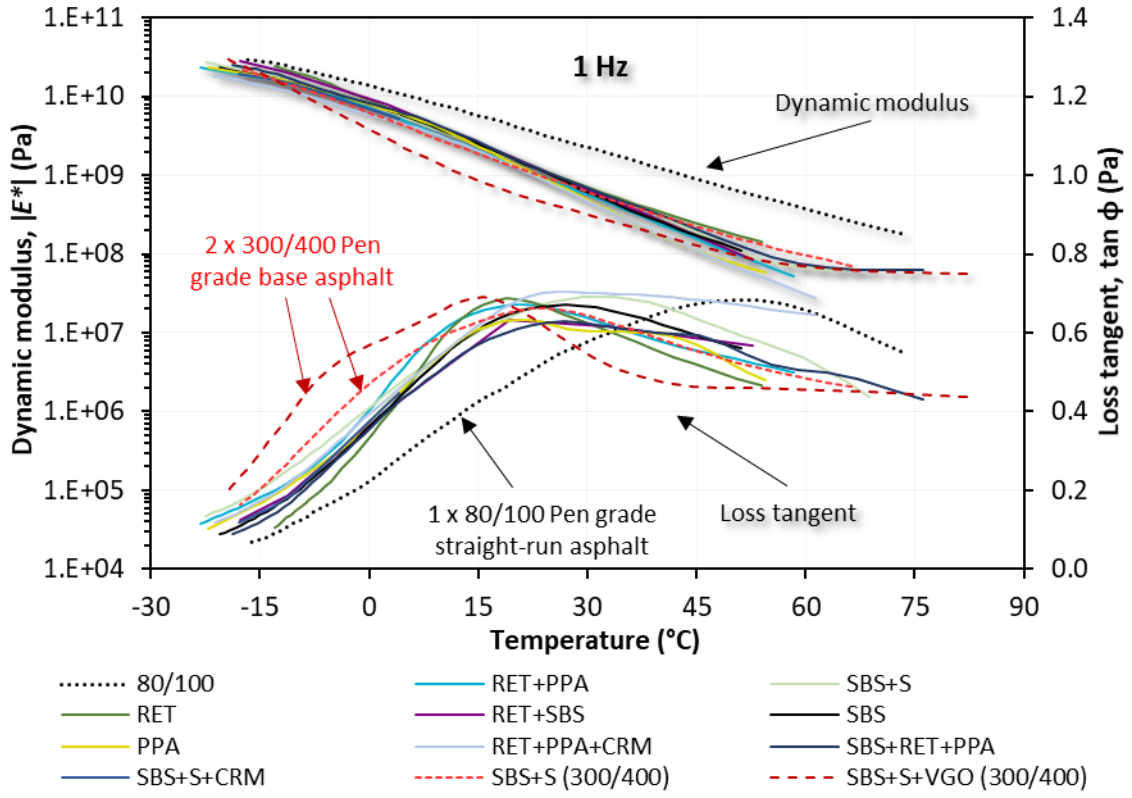

Figure 4.26 Dynamic modulus, $|E^*|$, and loss tangent, $\tan\phi$, results at fixed frequency of 1 Hz, all tested asphalt mixes

Analogously to the SHRP rutting parameter of $|G^*|/\sin\delta$ used as the specification parameter for asphalt binders at high temperatures, the National Cooperative Highway Research Program (NCHRP) proposed the parameter of $|E^*|/\sin\phi$ to indicate susceptibility to permanent deformation (rutting) of HMAs [265].

Due to the absence of several HMA results at 60°C and higher temperatures, 50°C was chosen for comparison of the $|E^*|/\sin\phi$ parameter with HWTT results measured at 60°C. As described and suggested by Witczak *et al.* [265], power law function was used to fit the data as presented in Figure 4.27. However, in contrast to the results reported by Witczak *et al.* [265], no strong correlation could be observed between the dynamic test results and the final HWTT rut depth results of HMAs. The possible reason may lie in the fact that all asphalt binders had similar dynamic test results within the LVE range and, therefore, their respective asphalt mixes also showed similar dynamic properties. Thus, the main cause of the differences between the dynamic properties of asphalt mixtures within LVE range was due to the possible differences occurring in their volumetric

properties. Nonetheless, the similarity of the dynamic properties in this case resulted in weak correlation with HWTT results, which, in contrary to the dynamic measurements, were evaluated in the non-linear viscoelastic region.

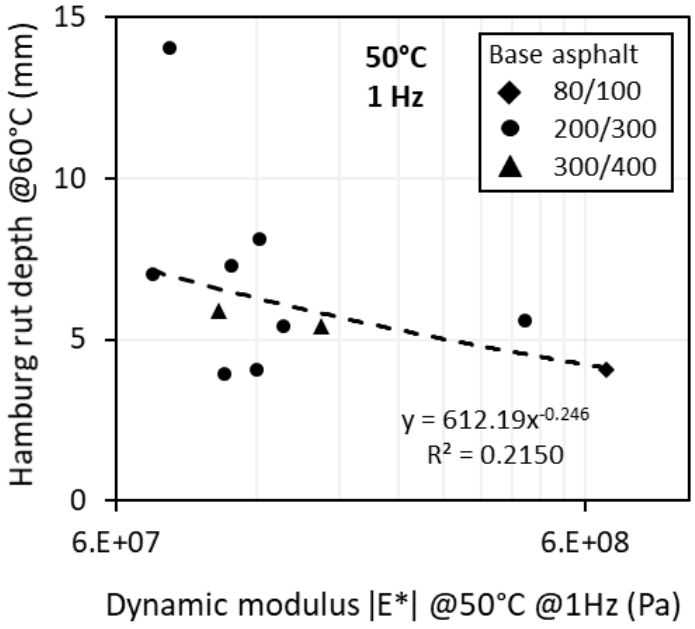

Figure 4.27 The relationship between the dynamic modulus, $|E^*|$, measured at 50°C and 1 Hz, and the final HWTT rut depth (10.000 cycles) of HMAs at 60°C

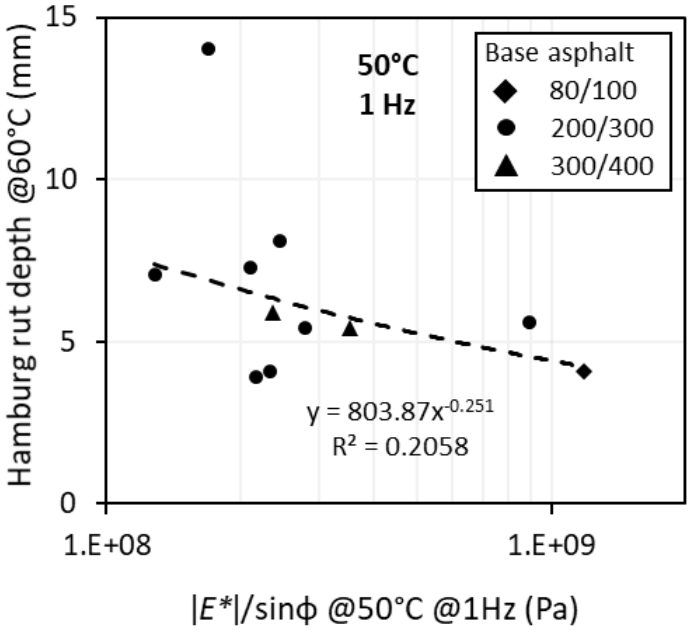

Figure 4.28 The relationship between the dynamic parameter of $|E^*|/\sin\phi$ measured at 50°C and 1 Hz, and the final HWTT rut depth (10.000 cycles) of HMAs at 60°C

4.3. Comparison of asphalt binder and mix results

4.3.1. The relationship between empirical test results and HWTT rut depth results of mixes

Empirical properties of penetration, R&B softening point, and elastic recovery were compared with HWTT rut depth results. Out of all the thirteen binders used in this study, three were blended from other than the 200/300 Pen grade asphalt base. Therefore, in addition to the comparison of all thirteen asphalt binders with Hamburg rut depth results, the regression function for only the 200/300 Pen grade blends (hereinafter referred to as "only 200/300") was also plotted in each graph. In such case, binders prepared from the 300/400 Pen grade base asphalt and the 80/100 Pen grade straight-run asphalt were omitted from the comparison.

In Figure 4.29 the relationship between the three empirical test results (i.e., softening point, penetration, elastic recovery) with the HWTT rut depth results were presented. The tested binders were either non-aged or experienced short-/long-term aging (i.e., RTFO, PAV). The penetration and the elastic recovery tests were conducted at 25°C.

It is apparent that no significant correlation could be found between the empirical test results and the asphalt mixes' rut depths. Furthermore, in the case of penetration, the correlation function showed the opposite trend than might have been expected, i.e., more viscous binders showed generally worse rut resistance in asphalt mixes.

Although the correlations were slightly higher in the case of binders prepared from the 200/300 Pen grade asphalt base ("only 200/300"), they still indicated negligible relationship between the binders' properties and their respective mixes' rut resistance. The elastic recovery of 200/300 Pen grade blends was the only empirical property that showed notable correlation with the HWTT mix results (Figure 4.29A). However, this relationship was no longer valid when all binders were included in the comparison.

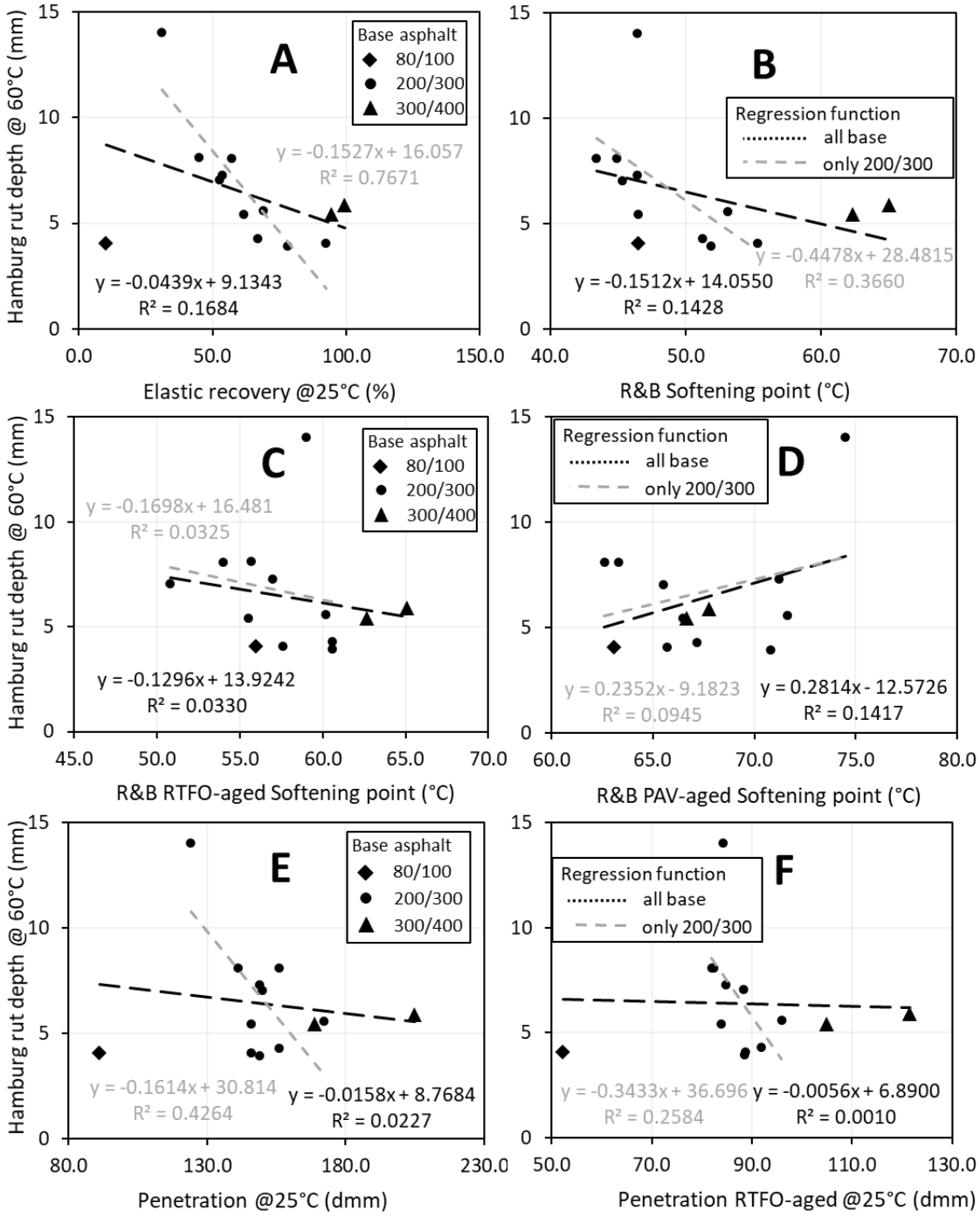

Figure 4.29 Selected empirical binder test results compared with Hamburg rut depth results of mixes

4.3.2. The relationship between the performance related non-recoverable creep compliance, J_{nr}, results of asphalt binders and the HWTT rut depth results of mixes

The values of non-recoverable creep compliance, J_{nr}, measured at 50, 60 and 70°C, against rut depth from HWTT testing conducted at 60°C are presented in Figure 4.30, Figure 4.31 and Figure 4.32, respectively. Charts designated as A, B, C, D and E represented the MSCR results evaluated at different shear stress levels.

Again, two linear correlations were calculated for each stress and temperature combination. The first correlation (symbolized with black dotted regression line) compared all the studied binders with HWTT mix results. The second correlation compared only the modified asphalt blends prepared from the 200/300 Pen grade asphalt base with HWTT mix results (grey dashed regression line).

The MSCR results evaluated at the standard stress levels of 0.1 and 3.2 kPa at 50°C, which was two grades lower than the binders' maximum service temperature and on average 8°C lower, than the RTFO-aged binders' softening point, showed negligible correlation between the asphalt mixes rut depths and the binders' non-recoverable creep compliance (Figure 4.30A and B). Measurements conducted at higher shear stress levels of 6.4 kPa (Figure 4.30C), 12.8 kPa (Figure 4.30D), and even 25.6 kPa (Figure 4.30E) resulted in better correlations. However, the results measured at the two highest shear stress levels showed significantly better correlation with the Hamburg rut depth results at 50°C than at any lower shear stress levels. Moreover, at the highest 25.6 kPa the PPA-modified blend already indicated signs of fatigue, which manifested itself in an increasing difference between the J_{nr} values of the cycles, discussed in Chapter 4.1.3 (Figure 4.8B-A).

Nonetheless, the MSCR test conducted at 50°C failed to point out the PPA-modified asphalt blend's stress sensitivity, $J_{nr,diff}$, (Table A.1) and its lower HWTT rut resistance at standard shear stress levels.

As it was expected from the compliance and the HWTT rutting results, discussed in the previous sections, the two blends prepared from the less viscous 300/400 Pen grade asphalt base (in figures denoted ▲) and the more viscous unmodified 80/100 Pen grade straight-run asphalt (denoted ♦) tended to deviate from the expected values. For example, asphalt mixes prepared form modified 300/400 Pen grade asphalt performed worse than

it could be assumed from the MSCR test results. Contrarily, the asphalt mix prepared from the more viscous non-modified 80/100 Pen grade asphalt proved to be more resistant than it could be assumed from the MSCR test results of the vacuum residue.

Consequently, when considered only the asphalt binders blended from 200/300 Pen grade asphalt base, the regression functions showed significant improvement at all stress levels. Nonetheless, measurements conducted at 12.8 and 25.6 kPa still yielded the best correlation with HWTT rut depth results at 50°C.

These findings also proved that the rut resistance of the binders in the paving mixes strongly depended on the consistency of the asphalt base, regardless of the maximum service temperature and even on the entropic elasticity of binders achieved through modification.

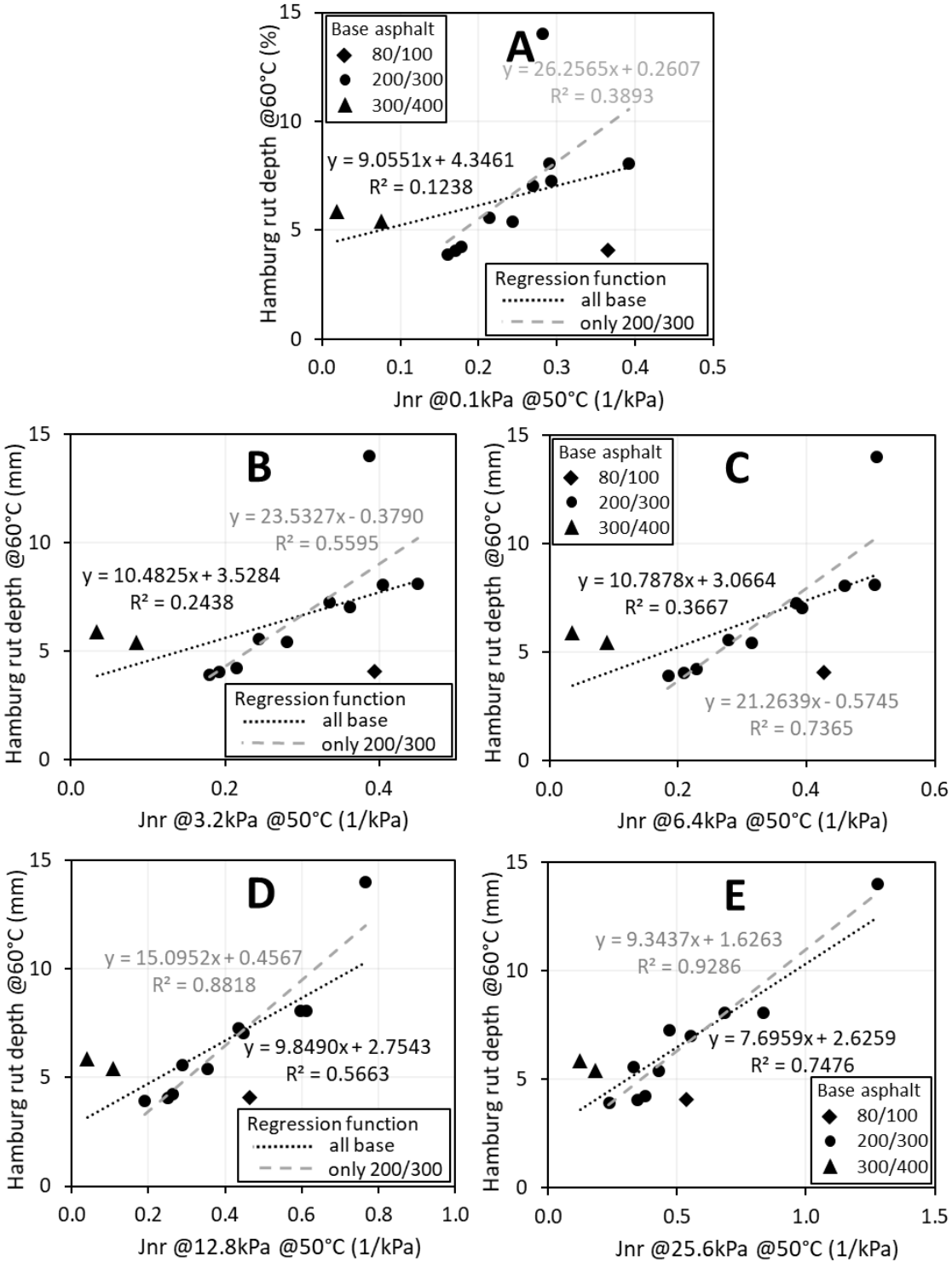

Figure 4.30 J_{nr} **at 50°C and at shear stress levels of 0.1 kPa (A), 3.2 kPa (B); 6.4 kPa (C); 12.8 kPa (D); 25.6 kPa (E) versus HWTT rut depth at 60°C**

In Figure 4.31 the MSCR results obtained at 60°C, the same temperature at which the Hamburg wheel-tracking test was conducted, are presented. When compared with results obtained at 50°C, they showed better correlation at almost every shear stress levels. The only exception was the 25.6 kPa stress level (Figure 4.31E), as the application of such high stress level resulted in complete damage of the PPA-modified sample, i.e., after five cycles, the upper and lower plates of the DSR rheometer were no longer connected. Furthermore, the 80/100 Pen grade straight-run asphalt also showed signs of fatigue in each successive cycle at 25.6 kPa shear stress level (Figure 4.8A-B).

Consequently, the absence (due to separation of the sample) of the PPA-modified binder's results and the unstable 80/100 Pen grade asphalt results, obtained at 60°C and at 25.6 kPa, resulted in low correlation between the HWTT mix and MSCR binder results. Based on these findings it was concluded that 25.6 kPa should not be applied in MSCR test close to the binders' maximum service temperature or higher.

According to the current MSCR standard specification criteria ($J_{nr,diff}$ < 75%) the PPA-modified binder's stress sensitivity was first revealed at 60°C (**Chyba! Nenalezen zdroj odkazů.**), although two other binders blended with crosslinked SBS (i.e., SBS+S+CRM and SBS+S+VGO) also indicated out-of-specification stress sensitivity at 60°C testing temperature. Therefore, none of the three binders mentioned above met the requirements defined in AASHTO T332 at 60°C. Based on these results, all of them would be considered as too stress sensitive, even though the SBS+S+VGO-modified 300/400 Pen grade blend showed relatively good rut resistance in asphalt mixes.

Despite its high stress sensitivity the PPA-modified binder, tested at 60°C, would have been identified as a binder with relatively good resistance to rutting according to its J_{nr} results, even at 6.4 kPa shear stress level. Its extremely low rut resistance was first revealed at the combination of 12.8 kPa shear stress level and 60°C testing temperature. Consequently, the application of 12.8 kPa stress level around the binder's maximum service temperature was recommended.

As far as the correlations of blends prepared from only 200/300 Pen grade asphalt base were concerned, similar conclusions could be drawn as from the MSCR results measured at 50°C, namely, that J_{nr} overestimated the rut resistance of 300/400 Pen grade asphalts blended with crosslinked SBS, but underestimated the rut resistance of the 80/100 Pen grade asphalt base.

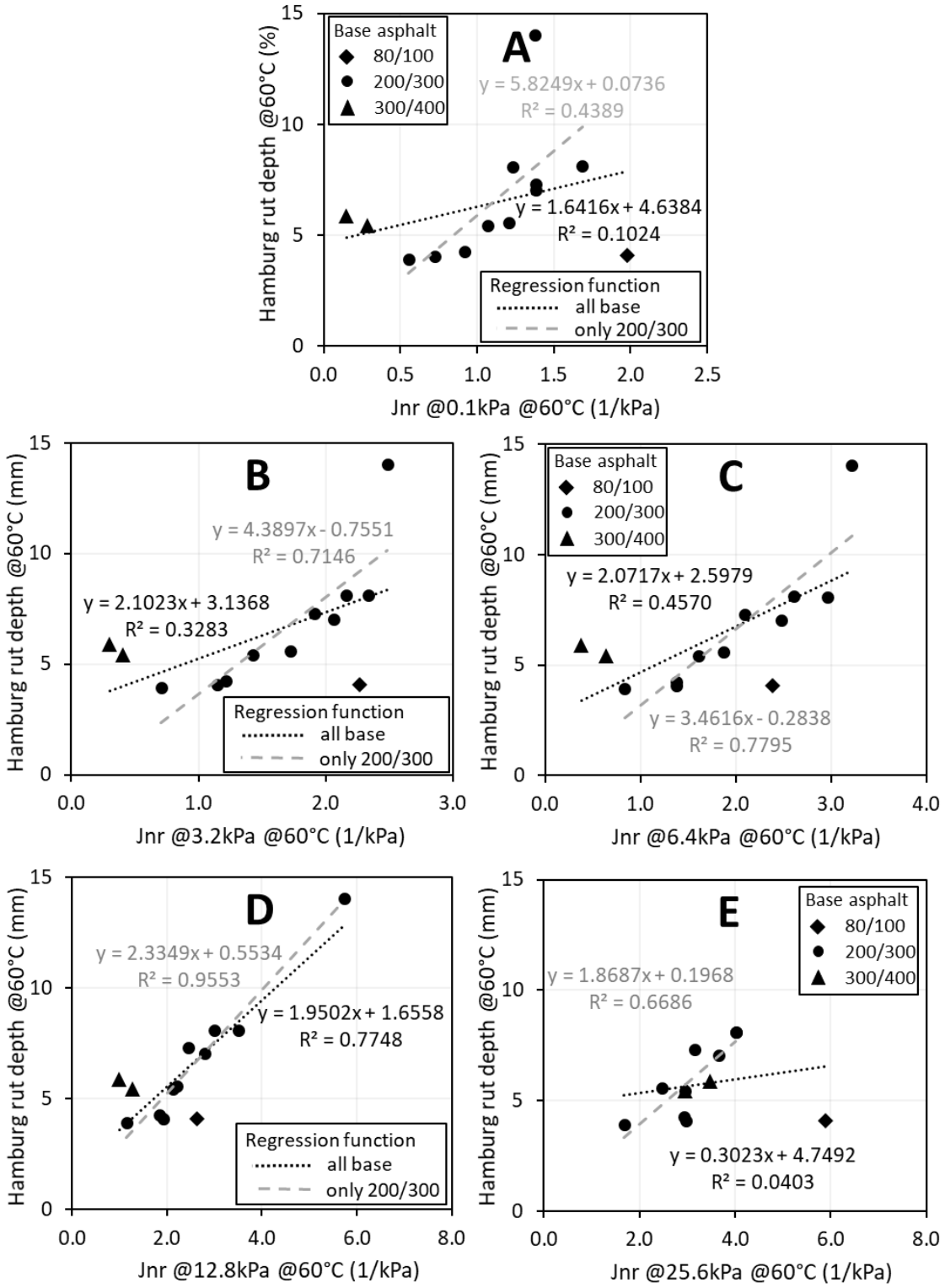

Figure 4.31 J_{nr} **at 60°C and at shear stress levels of 0.1 kPa (A), 3.2 kPa (B); 6.4 kPa (C); 12.8 kPa (D); 25.6 kPa (E) versus HWTT rut depth at 60°C**

The comparison of the binders' HWTT rut results and MSCR results measured at 70°C, which was on average one PG grade higher than the binders' maximum service temperature, are presented in Figure 4.32.

MSCR results obtained at 70°C also showed better correlations with HWTT results at almost all shear stress levels than at the two lower testing temperatures of 60 and 50°C. However, measurements conducted at 12.8 and 25.6 kPa indicated the same shortcomings, i.e., fatigue, unstable results and/or complete damage of the 80/100 Pen grade straight-run asphalt and the PPA-modified 200/300 Pen grade blend, as at 60°C testing temperature. Therefore, even though the MSCR results measured at 12.8 kPa shear stress yielded better correlation than at 6.4 kPa, stress levels higher than or equal to 12.8 kPa should not be applied at such high temperature.

When considering only the results of asphalt binders prepared from 200/300 Pen grade asphalt base, they once again yielded significantly better correlation with the HWTT rut depth results at almost all shear stress levels. The fact that MSCR overestimated the rut resistance of SBS+S+VGO and SBS+S-modified 300/400 Pen grade blends (denoted ▲) while underestimated the 80/100 Pen grade straight-run asphalt binder (denoted ♦) proved that the rut resistance generally strongly depends on the consistency of the asphalt base, regardless of the maximum service temperature and even on the entropic elasticity achieved through modification. All these results demonstrated that the MSCR test had difficulties in determining the binders' rut resistance in case they were prepared from different asphalt bases.

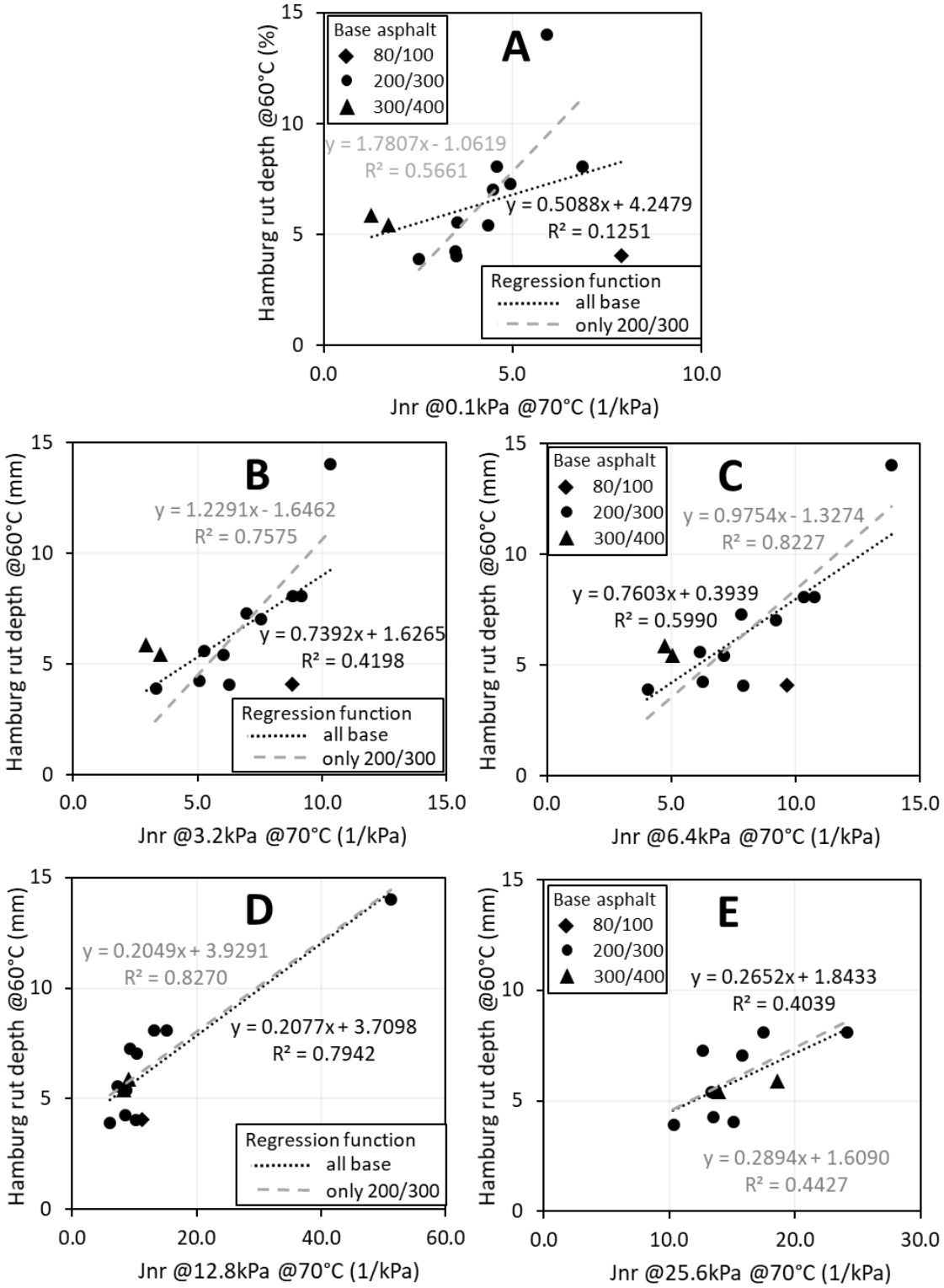

Figure 4.32 J_{nr} **at 70°C and at shear stress levels of 0.1 kPa (A), 3.2 kPa (B); 6.4 kPa (C); 12.8 kPa (D); 25.6 kPa (E) versus HWTT rut depth at 60°C**

4.3.3. The relationship between the creep compliance, J_c, results and the recovered compliance, J_{rec}, results of asphalt binders and the HWTT rut depth results of asphalt mixes

As it was discussed earlier in Chapter 3.4.3, one cycle of the MSCR test could be divided into two distinguishable phases of creep and recovery (viz. Figure 3.14). During creep phase, when the shear stress is applied, the resulting strain predominantly depends on the binder's viscosity, while during recovery phase the entropic elasticity prevails. Therefore, in order to determine the influence of each property (i.e., viscosity, elasticity) on the HMAs' rutting performance, in the following chapter the average creep compliance, J_c, representing viscous behavior, and the recovered compliance, J_{rec}, representing elastic behavior were compared with the rut depth results of HWTT mix testing.

In Figure 4.33, Figure 4.34, and Figure 4.35 are presented the creep compliance, J_c, results evaluated at 50, 60, and 70°C, respectively. Charts designated as A, B, C, D, E continue to represent the results measured at different shear stress levels.

The creep compliance results measured at the standard shear stress levels of 0.1 and 3.2 kPa and at 50°C showed only a marginal correlation with the asphalt mixes' rut depth results (Figure 4.33A and Figure 4.33B). Measurements conducted at the higher shear stress level of 6.4 kPa (Figure 4.33C) resulted in better but still low correlations.

However, at the highest two shear stress levels of 12.8 and 25.6 kPa (Figure 4.33D and Figure 4.33E), the creep compliance results indicated substantially better correlation with the rut resistance of the asphalt mixes, than at the three lower shear stress levels. Furthermore, no significant difference was observed between the correlations of all binders and mixes, and between the correlations of only the 200/300 Pen grade blends and their respective mixes. Therefore, the creep compliance did not distinguish between asphalt binders according to their base asphalts. Moreover, the relationship between the creep compliance, J_c, results and the rut depth of asphalt mixes was comparable to the correlations of the J_{nr} results of binders prepared with 200/300 Pen grade asphalt only. Thus, as far as all binders were concerned, at the combination of 50°C temperature and 12.8 or 25.6 kPa shear stress levels, J_c, showed substantially better correlations with the rut resistance of HMAs than the non-recoverable creep compliance, J_{nr}, at any of the applied shear stress levels.

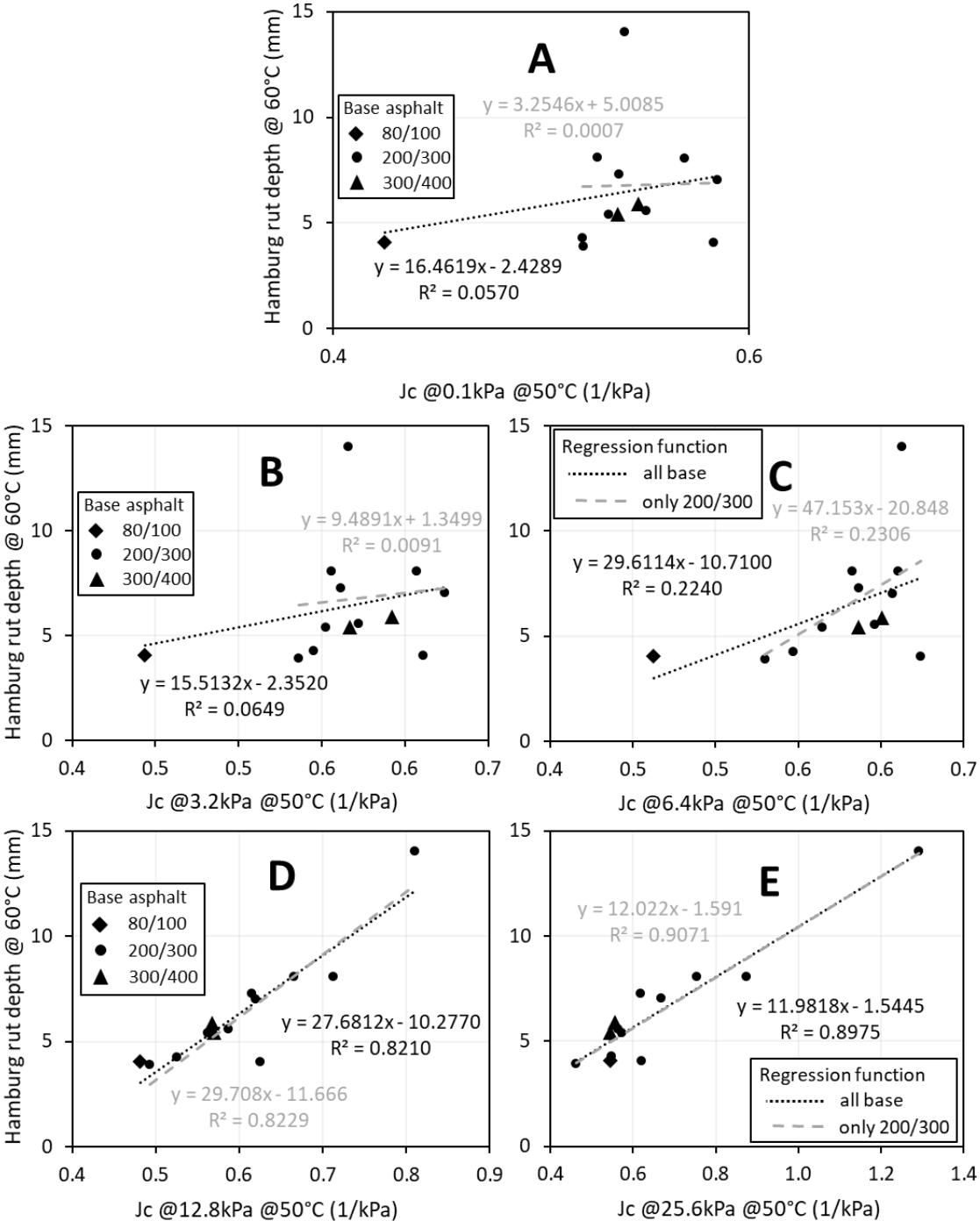

Figure 4.33 J_c at 50°C and at shear stress levels of 0.1 kPa (A), 3.2 kPa (B); 6.4 kPa (C); 12.8 kPa (D); 25.6 kPa (E) versus HWTT rut depth at 60°C

The comparison of creep compliance results obtained at 60°C and at the standard shear stress levels of 0.1 and 3.2 kPa (Figure 4.34A and Figure 4.34B) or at 6.4 kPa (Figure 4.34C) with HWTT test results showed distinctively improved correlations than at 50°C. Nevertheless, the best correlation was obtained at 12.8 kPa (Figure 4.34D). On the contrary, low correlation could be observed at 25.6 kPa (Figure 4.34E). This was mainly due to the inadequacy of the application of such high shear stress levels at the testing temperature close to the binders' maximum service temperatures. Such occurrence might cause unwanted damage or even disintegration of the samples that might falsely distort the testing results, as discussed in the previous chapters. This once again led to the conclusion that the use of 25.6 kPa should be completely avoided close to the binders' maximum service temperature.

A larger difference was observed between the correlation functions of all binders and their mixes, and between the correlation functions of the "only 200/300" Pen grade blends and their respective mixes at 60°C than at 50°C. Even though these differences were smaller, than in the case of the J_{nr} results at 60°C, the trend clearly indicated that the measurements conducted at lower temperatures yielded such results that could be generalized for all binders regardless of the asphalt base they were prepared from.

When compared to the non-recoverable creep compliance, J_{nr}, results obtained at 60°C, the J_c results indicated considerably better correlation with the rut resistance of the mixes. This further affirmed the hypothesis that the mixes' resistance to rutting was more dependent on the viscosity and stiffness of their respective binders than on the elasticity they gained through modification.

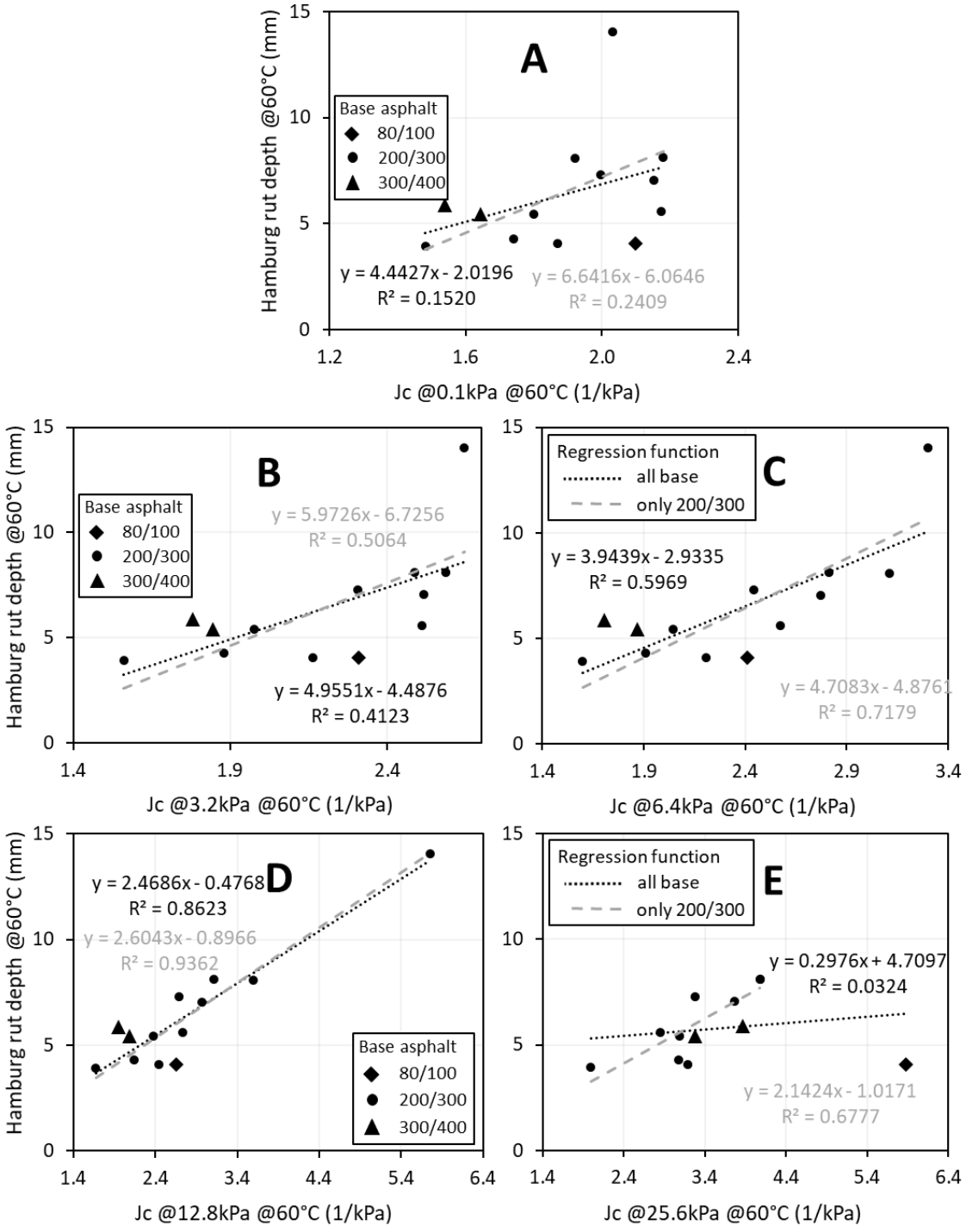

Figure 4.34 J_c **at 60°C and at shear stress levels of 0.1 kPa (A), 3.2 kPa (B); 6.4 kPa (C); 12.8 kPa (D); 25.6 kPa (E) versus HWTT rut depth at 60°C**

In Figure 4.35 the comparison of the HWTT test results with the creep compliance, J_c, results obtained at 70°C are presented. These results showed better correlation with the rut depth of HMAs at 12.8 kPa (Figure 4.35D) shear stress than with the results obtained at 6.4 kPa (Figure 4.35C). Nevertheless, as previously observed, the combination of 70°C and shear stress levels higher than or equal to 12.8 kPa resulted in inaccurate measurements and separation of several samples.

When compared with the correlations of J_{nr}, the creep compliance, J_c, results showed only slightly better correlations with the HWTT rut resistance of the mixes. Furthermore, a relatively large difference could be observed between the correlations of all binders and their mixes, and between the correlations of the "only 200/300" Pen grade blends and their respective mixes at 70°C. These findings suggested that the measurements conducted at a temperature one PG grade higher than the maximum service temperature of the binders yielded results that could no longer be generalized to all binders.

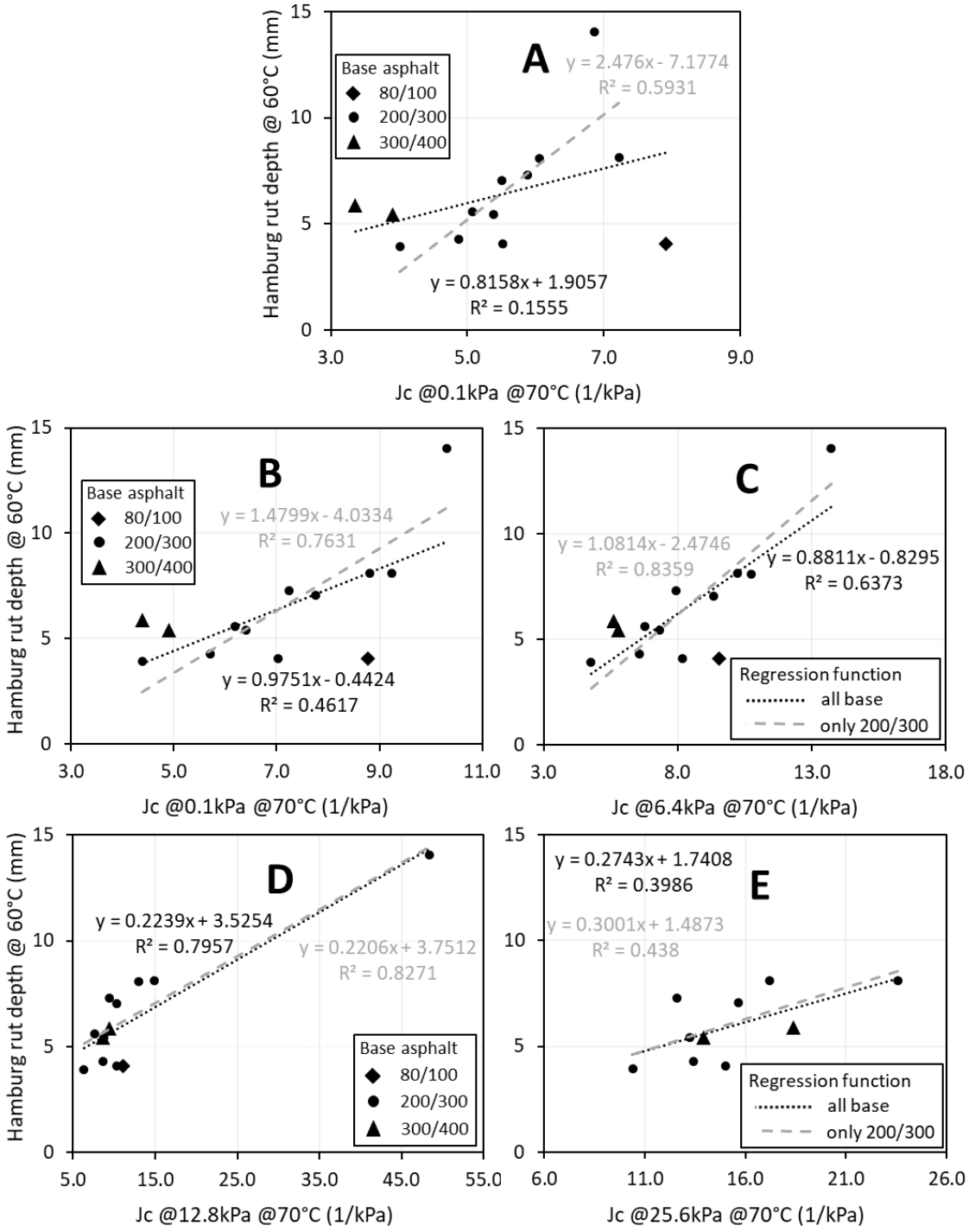

Figure 4.35 J_c at 70°C and at shear stress levels of 0.1 kPa (A), 3.2 kPa (B); 6.4 kPa (C); 12.8 kPa (D); 25.6 kPa (E) versus HWTT rut depth at 60°C

The relationship between the recovered compliance, J_{rec}, and the HWTT test results at 50, 60 and 70°C are presented in Figure 4.36, Figure 4.37, and Figure 4.38, respectively. Although, relatively high correlation was obtained between the recovered compliance and the HWTT results at 12.8 and 25.6 kPa at 70°C, it was obvious that such spurious correlations were only the results of outliers (e.g., the damaged PPA-modified binder and the 80/100 Pen grade straight-run asphalt) that were offsetting the actual trends. Except the abovementioned two cases, the recoverable compliance showed negligible correlation with the HWTT rut results of mixes through the whole studied shear stress and temperature range.

In addition, as a result of the delayed response of the DSR during stress unloading (discussed in Chapter 4.1.2), some binders under certain conditions had negative J_{rec} values, which further complicated and made impossible to relate the recovered compliance binder results to the HWTT mix results. Consequently, no direct correlation was observed between the elastic component of the J_{nr} value (i.e., the J_{rec} value) and the rut resistance of the asphalt mixes.

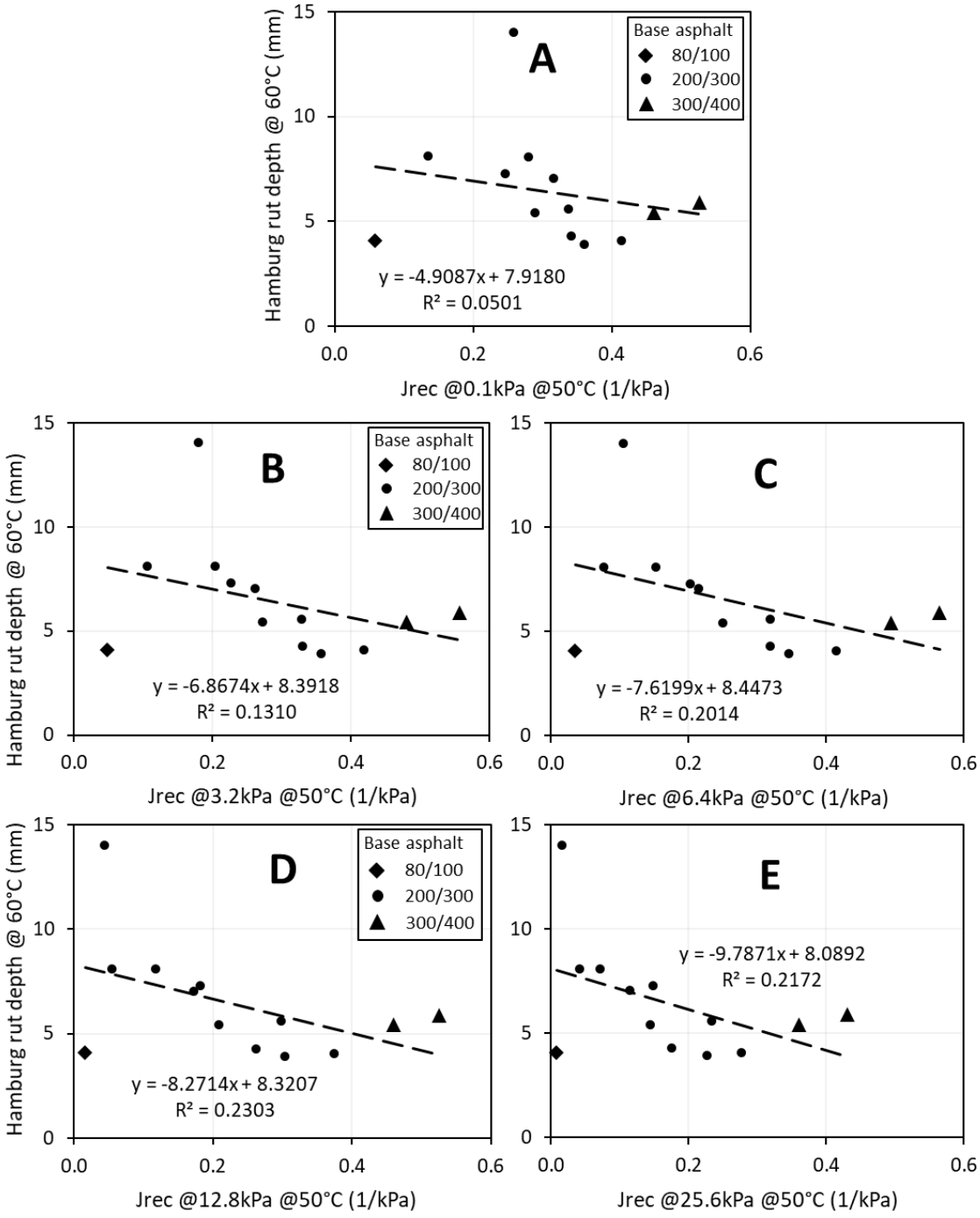

Figure 4.36 J_{rec} at 50°C and at shear stress levels of 0.1 kPa (A), 3.2 kPa (B); 6.4 kPa (C); 12.8 kPa (D); 25.6 kPa (E) versus HWTT rut depth at 60°C

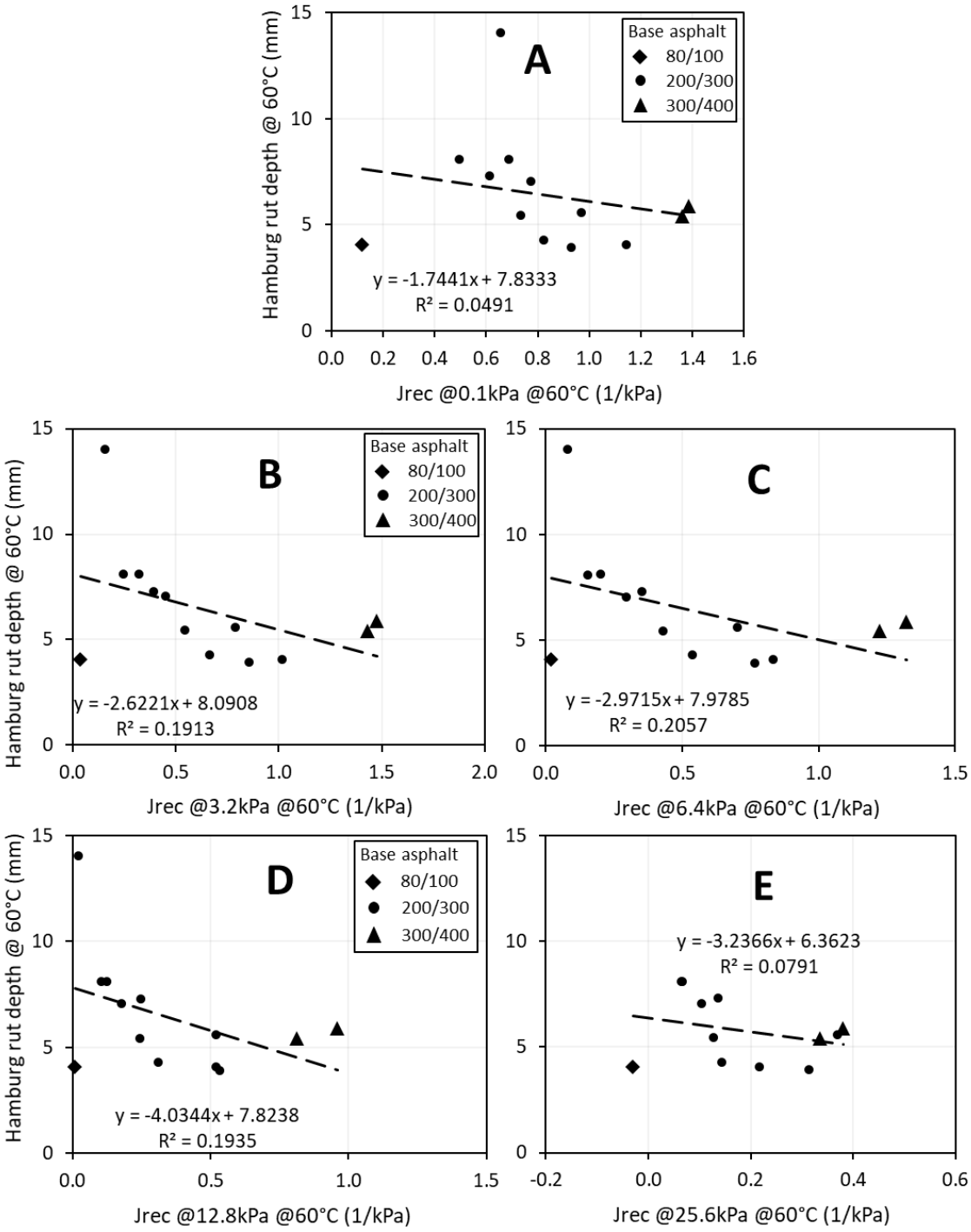

Figure 4.37 J_{rec} at 60°C and at shear stress levels of 0.1 kPa (A), 3.2 kPa (B); 6.4 kPa (C); 12.8 kPa (D); 25.6 kPa (E) versus HWTT rut depth at 60°C

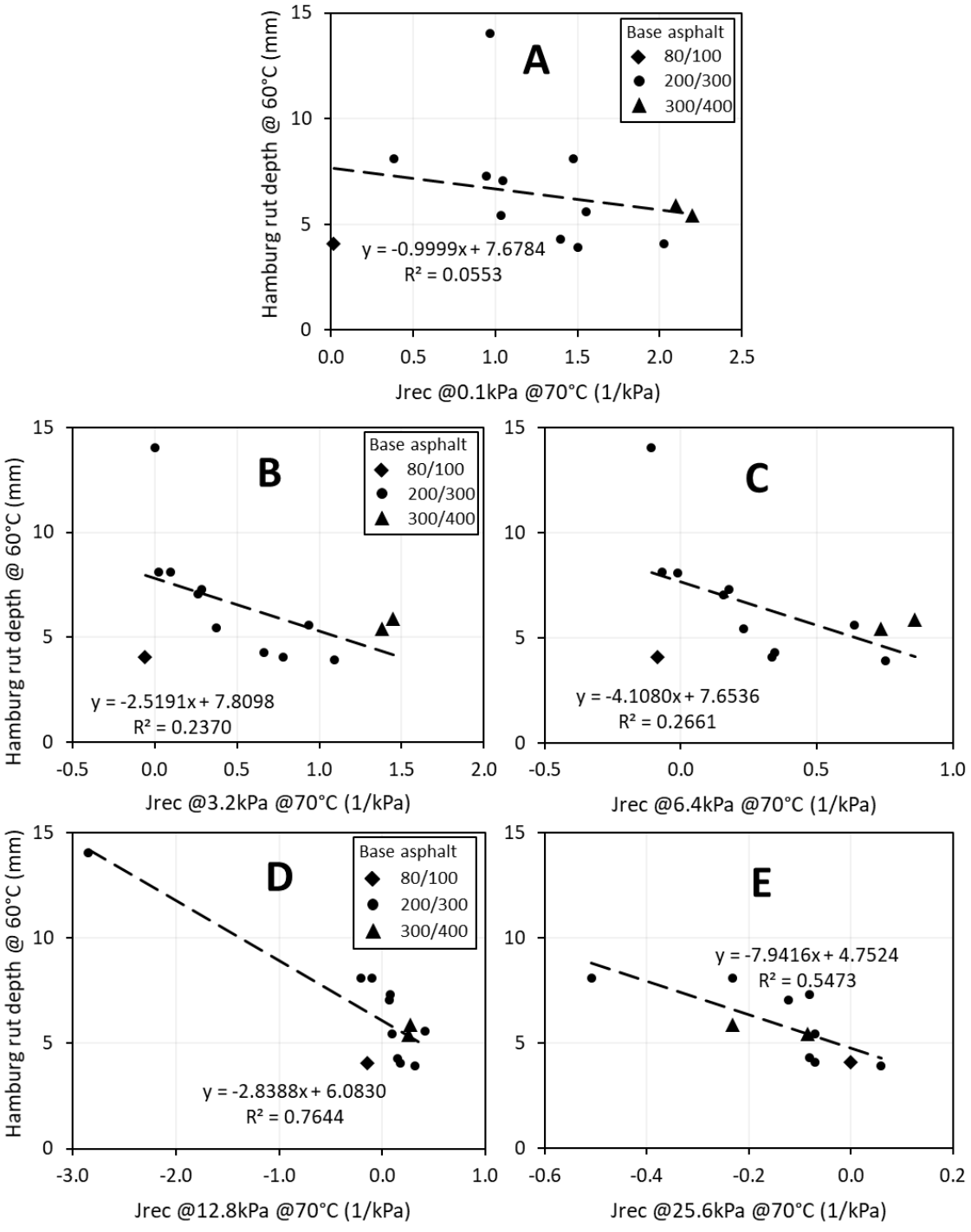

Figure 4.38 J_{rec} at 70°C and at shear stress levels of 0.1 kPa (A), 3.2 kPa (B); 6.4 kPa (C); 12.8 kPa (D); 25.6 kPa (E) versus HWTT rut depth at 60°C

According to the results it might be assumed that the MSCR test could successfully predict the binders' rut resistance, nonetheless, depending on the testing temperature, seemingly only at higher than the standard 0.1 and 3.2 kPa shear stress levels.

To determine the most promising combination of shear stress level and testing temperature from the results of the studied binders, the correlation coefficients between the different MSCR test results (i.e., J_{nr}, J_c, J_{rec}) at all testing temperatures and at all shear stress levels, and the HWTT rut results (conducted at 60°C) are summarized in Table 4.7. All coefficients with an R^2 value greater than 0.7 are emphasized.

Table 4.7 The correlation coefficients of the regression functions

	Shear Stress Level	Linear Correlation Coefficient R^2		
		50°C	60°C	70°C
Non-recoverable Creep Compliance J_{nr}	0.1 kPa	0.1238	0.1024	0.1251
	3.2 kPa	0.2438	0.3283	0.4198
	6.4 kPa	0.3667	0.4570	0.5990
	12.8 kPa	0.5663	**0.7748**	**0.7942**[2]
	25.6 kPa	**0.7476**	0.0403[1]	0.4039[1]
Creep Compliance J_c	0.1 kPa	0.0570	0.1520	0.1555
	3.2 kPa	0.0649	0.4123	0.4617
	6.4 kPa	0.2240	0.5969	0.6373
	12.8 kPa	**0.8229**	**0.8623**	**0.7957**[2]
	25.6 kPa	**0.8975**	0.0324[1]	0.3986[1]
Recovered Compliance J_{rec}	0.1 kPa	0.0501	0.0491	0.0553
	3.2 kPa	0.1310	0.1913	0.2370
	6.4 kPa	0.2014	0.2057	0.2661
	12.8 kPa	0.2303	0.1935	**0.7644**[2]
	25.6 kPa	0.2172	0.0791[1]	0.5473[1]

[1] Not all binders could be evaluated, separation of samples
[2] Extreme load vs temperature, possible outliers

From the correlations of J_{nr} results of all studied binders with the HWTT rut depth results, it might been assumed that the highest applied shear stress of 25.6 kPa during the MSCR testing would be justified only for testing temperatures two PG grades below the maximum service temperature of the prepared asphalt blends. At such temperature, lower shear stresses resulted in weak correlations. However, at the testing temperature close to the binders' maximum service temperature, the best correlation was obtained at 12.8 kPa.

When compared to the non-recoverable creep compliance, J_{nr}, the creep compliance, J_c, results indicated relatively good correlations at shear stress levels of 6.4 kPa at 70°C, 6.4 and 12.8 kPa at 60°C, and 12.8 and 25.6 kPa at 50°C.

The binders' recovered compliance results, however, showed insignificant correlation with HWTT rut depth results through the whole studied temperature and shear

stress range. The substantially better correlation of creep compliance results, J_c, with HWTT rut results proved that MSCR test overestimated the effect of entropic elasticity on the binders' rut resistance and, as such, a higher accent should be given to the binder's ability to resist to the applied stresses than to their elasticity. Furthermore, since the goodness-of-fit was highly dependent on the combination of shear stress level and the testing temperature, both parameters should be chosen according to the binders' PG grade one wants to examine.

The reason behind these findings might lie in the differences between the way how MSCR evaluates the rutting potential and the way how rutting truly develops in the pavement mixes. During MSCR testing, the only resistance that occur to the applied shear stress is the binder's own viscoelastic material properties. The same applies to the recovery phase, where the entropic component of the elasticity of a polymer chain tries to recover the deformed sample to its original shape.

However, asphalt mixes show much higher resistance to the applied loads. The aggregate skeleton helps the mix resist permanent deformation during the loading phase, but it also resists the binder's attempt to restore the HMA's original micro- and macrostructure once a deformation occurred. However, the stresses resulting from the traffic load that originally caused the deformation, and the stresses exerted by the stretched polymer chains attempting to regain their original shape and structure may vary substantially. Hence, the weaker correlation between the rut resistance of HMAs and the binders' elastic response expressed in recovered compliance, J_{rec}, and the higher correlation of their viscosity expressed in creep compliance, J_c, than with the combination of the two behaviors expressed as non-recoverable creep compliance, J_{nr}.

These results lead to the conclusion that the MSCR test either overestimated (e.g., less viscous binder with high elastic response) or underestimated (e.g., more viscous binder with no or low elastic response) the resistance of asphalt binders to rutting. This limitation of the MSCR test can be partially addressed by applying higher shear stresses and by giving a higher accent to the evaluation of creep strain. The level of shear stress should depend on the temperature at which the test is conducted.

It should be also pointed out that the non-recoverable creep compliance, J_{nr}, overestimated the rutting resistance of some modified asphalt binders (including those that have been modified by PPA) regardless of the testing temperature and/or applied standard shear stress (i.e., 0.1, 3.2 kPa). It could be assumed that the MSCR test may have similar shortcomings when applied to other modified asphalt binders.

CONCLUSIONS AND RECOMMENDATIONS FOR FUTURE WORK

5.1. Summary and conclusions

Aiming to improve the now most promising test for the evaluation of binder rutting susceptibility, namely the multiple stress creep recovery (MSCR) test, several binder and mix performance properties were studied.

The magnitude of stresses that asphalt mixes experience vary depending on the applied load, the contact area, the type of the tire, the temperature, and the time of loading. It was discussed that neither empirical properties nor linear viscoelastic properties, such as the Superpave® PG rutting parameter of $|G^*|/\sin\delta$, cannot directly relate to asphalt mixture rutting potential. This is due to the fact that the strains in the binder of asphalt mixes loaded at high temperatures could be several hundred times greater than the bulk strain of the mixture. Therefore, the binder rutting parameter should capture the materials' non-linear response to stresses occurring in the paving mixes during normal traffic circumstances.

The adequacy of multiple stress creep recovery test conducted at standardized shear stress levels (i.e., 0.1 kPa, 3.2 kPa) was investigated in this study. Thirteen asphalt binders, prepared from three vacuum distillation residues of different viscosity (80/100 Pen grade, 200/300 Pen grade, and 300/400 Pen grade) and their high temperature behavior was studied under different thermal and mechanical conditions. The two softer vacuum residues were used as base for modification by different polymers and their combinations, producing in total twelve polymer modified asphalt binders. The 80/100 Pen grade base asphalt was studied without modification.

In total, six different modifiers and additives were used to alter the physical properties of the 200/300 and the 300/400 Pen grade base asphalt. The base asphalts were blended with styrene-*b*-butadiene-*b*-styrene (SBS), reactive elastomeric terpolymer (RET), polyphosphoric acid (PPA), and crumb rubber modifier (CRM). Four of the SBS-modified blends were crosslinked with sulfur, and to one of them vacuum gas oil (VGO) was added. The content and combination of modifiers and additives was chosen and adjusted in a way that the Superpave® performance grade temperature of the modified blends was similar to true performance grade PG 64-yy, before and after RTFO short-term aging.

The multiple stress creep recovery test was conducted on all binders at five different shear stress levels: two standard levels of 0.1 and 3.2 kPa, and three additional stress levels of 6.4, 12.8, and 25.6 kPa. Asphalt mixes were prepared from the analyzed asphalt binders using the same job mix formula.

The goal was to evaluate the MSCR rutting potential (i.e., non-recoverable creep compliance, J_{nr}) of the asphalt binders at different shear stress levels and to compare the results with the actual rutting results of the mixes determined by HWTT. To determinate the contribution of viscosity and elasticity to the rut resistance separately, the creep compliance, J_c, and the recoverable compliance, J_{rec}, results were calculated and compared with the actual HWTT rut resistance of mixes. All studied binders were tested at three different testing temperatures of 50, 60 and 70°C. The Hamburg wheel-tracking test performed at 60°C was conducted on each paving mix prepared by adding different asphalt binders. The results helped to evaluate the contribution of different asphalt binders to the rut resistance of a standard asphalt mix. In addition, dynamic modulus test was conducted in order to evaluate the performance potentials of asphalt mixes and to develop their dynamic modulus, $|E^*|$, master curves.

From the binder and mix results presented in this research, the following conclusions could be made:

- By increasing the stress levels in MSCR test, a great stress dependency variation could be observed depending on the temperature and the internal structure of the binder.

- Based on the J_{nr} values measured at the maximum service temperature of the binders, the MSCR test may classify poor performing asphalt binders as adequately rut resistant. On the other hand, $J_{nr,diff}$ values may disqualify asphalt binders with good or relatively good performance.

- At two PG grade lower than the maximum service temperature of the binders, the most susceptible to stress level change were the blends containing PPA, crumb rubber modifier (RET+PPA+CRM, SBS+S+CRM) or dispersed SBS. This was also supported by the HWTT results of their respective asphalt mixes.

- Except the four susceptible blends, and most of all the PPA-modified binder, the bulk of the tested binders indicated almost identical J_{nr} values through the whole stress level range at 50°C.

- The non-recoverable creep compliance, J_{nr}, values indicated that standard stress levels of 0.1 kPa and 3.2 kPa do not always satisfactory correlate with the rut resistance of asphalt mixes. Furthermore, MSCR generally tend to favor soft asphalt binders with exceptionally good elastic properties, while overly underestimate stiffer binders with low entropic elasticity.

- The parameter of $|E^*|/\sin\phi$, proposed to indicate susceptibility to permanent deformation (rutting) of HMAs, could not satisfactorily be correlated to the actual HWTT rutting resistance of asphalt mixes. Analogously to the testing of asphalt binders using rutting parameter of $|G^*|/\sin\delta$, asphalt mixes were also tested within the linear viscoelastic range. However, the fact that all asphalt binders had similar rutting parameters of $|G^*|/\sin\delta$ resulted in that their respective asphalt mixes also showed similar dynamic properties. This in turn resulted in weak correlation with the rutting results of asphalt mixes. Nonetheless, neither the parameter of $|E^*|/\sin\phi$ or the dynamic modulus, $|E^*|$, master curves could be directly related to the rutting susceptibility of asphalt mixes evaluated by HWTT.

- Empirical properties such as penetration, softening point, and elastic recovery could not satisfactorily correlate with the rut resistance of the asphalt mixes.

- MSCR measurements conducted at 12.8 kPa shear stress and around (or below) the maximum service temperature of the binders could provide the best correlation between the J_{nr} and HWTT rutting results. However, if the MSCR test was performed at temperatures two PG grades below the binder's maximum service temperature, even higher shear stress levels could be applied without damaging the samples and proved to have a strong MSCR/HWTT correlation.

- At high service temperatures, current standards and binder specifications favor materials with high entropic elasticity. The results of the MSCR and HWTT tests point to the fact that asphalt binders that have similar maximum service temperatures and J_{nr} values at standard shear stress levels but are prepared from asphalts bases of

different viscoelastic properties (i.e., viscosity, elasticity) exhibit different resistance to rutting in asphalt mixes. It appears that the "harder", the base asphalt the better the rut resistance of the paving mix regardless of the binder's elasticity. This is an extremely important finding that begs to rethink and re-evaluate high temperature binder performance parameters (including MSCR) and their validity over a wide range of modified binders produced from different base asphalts, different polymers, additives, and their combinations.

- The creep compliance, J_c, results were the most successful in predicting the binders' rutting resistance at temperatures two PG grades lower as well as around the binders' maximum service temperature. Furthermore, J_c values evaluated at 50°C temperatures yielded such results that could be generalized for all binders regardless of the asphalt base they were prepared from.

5.2. Recommendations for future work

Based on the results of this study, the following recommendations are suggested for future research:

- To validate the adequacy of the suggested changes to the MSCR test in this study, the current research should be expanded by using conventional asphalt binders of different sources of origin, different viscosity, and different modification types and levels.

- The suitability of the proposed changes could also be extended by the use of a wider range of polymer modifiers and additives.

- In order to assure the repeatability and reproducibility of MSCR measurements at higher stress levels, comparative tests should be conducted between several laboratories at two PG grade lower temperatures than the binders' maximum service temperature.

- The MSCR test should be evaluated at a higher number of cycles in order to assure more consistent compliance results.

- HWTT rut resistance should be evaluated at least at two more temperature sets.

REFERENCES

1. Connan J. Use and trade of bitumen in antiquity and prehistory: molecular archaeology reveals secrets of past civilizations. Philos Trans R Soc London Ser B Biol Sci. 1999;354(1379):33–50.
2. Marschner RF, Duffy LJ, Wright H. Asphalts from ancient town sites in southwestern Iran. Paleorient. 1978;4:97–112.
3. Böeda E, Connan J, Muhesen S. Bitumen as hafting material on middle paleolithic artifacts from the El Kowm Basin, Syria. In: Neandertals and Modern Humans in Western Asia. Plenum New York; 1998. p. 181–204.
4. Boëda E, Connan J, Dessort D, Muhesen S, Mercier N, Valladas H, et al. Bitumen as a hafting material on Middle Palaeolithic artefacts. Nature. 1996;380(6572):336–8.
5. Connan J, Deschesne O. Archaeological bitumen: indentification, origins and uses of an ancient near eastern material. Mater Res Soc Simp Proc. 1995;267:683–720.
6. Lay MG. Ways of the world. 1st ed. Rutgers University Press; 1992. 203–240 p.
7. Lesueur D. The colloidal structure of bitumen: consequences on the rheology and on the mechanisms. Adv Colloid Interface Sci. 2009;145(1–2):42–82.
8. Murali Krishnan J, Rajagopal K. Review of the uses and modeling of bitumen from ancient to modern times. Appl Mech Rev. 2003;56(2):149–214.
9. Barakat AO, Mostafa A, Qian Y, Kennicutt IC. Organic geochemistry indicates Gebel El Zeit, Gulf of Suez, is a source of bitumen used in some Egyptian mummies. Geoarchaeology. 2005;20(3):211–28.
10. Bilkadi Z, Grimsdale M. Bitumen–A history. Vol. 35, Saudi Aramco World. 1984.
11. Wisniak J. The Dead Sea–A live pool of chemicals. Indian J Chem Technol. 2002;9:79–87.
12. Nissenbaum A, Aizenshtat Z, Goldberg M. The floating asphalt blocks of the Dead Sea. Phys Chem Earth. 1980;12:157–61.
13. Nissenbaum A. Ancient and modern medicinal applications of Dead Sea asphalt (bitumen). Isr J Earth Sci. 1999;48(3–4):301–8.
14. Encyclopædia Britannica [Internet]. 1999 [cited 2019 Jul 3]. Available from: https://www.britannica.com/biography/John-Loudon-McAdam/media/1/353599/19288
15. Lay MG. Handbook of road technology [Internet]. CRC Press; 2009. 11–39 p. Available from: https://books.google.cz/books?id=YkNY6gjxnMIC&pg=P
16. Hooley EP. Apparatus for the preparation of tar macadam [Internet]. United States; 765975, 1904. p. 3. Available from: https://patentimages.storage.googleapis.com/23/d9/3e/9a6a47453514b6/US765975.pdf

17. Robertson WA. Nothing new under the Sun. In: The Mechanics' Magazine, Museum, Register, Journal, and Gazette [Internet]. 29th ed. London: Salmon, M.; 1838. p. 176. Available from: https://books.google.cz/books?id=ygoAAAAAMAAJ&pg=P

18. American Society for Testing and Materials. ASTM D 8-18. Standard terminology relating to materials for roads and pavements. West Conshohocken (PA): ASTM International; 2018.

19. European Committee for Standardization. EN 12597. Bitumen and bituminous binder–Terminology. Brussels: CEN; 2014.

20. European Committee for Standardization. EN 12591. Bitumen and bituminous binders–Specifications for paving grade bitumens. Brussels: CEN; 2009.

21. Abraham H. Asphalts and allied substances: their ocourrence, modes of production, uses in the arts and methods of testing [Internet]. 6th ed. New York: D. Van Nostrand Company; 1960. Available from: https://archive.org/details/asphaltsandallie031010

22. Kayukova GP, Uspensky BV, Abdrafikova IM, Musin RZ. Characteristic features of the hydrocarbon composition of Spiridonovskoe (Tatarstan) and Pitch Lake (Trinidad and Tobago) asphaltites. Pet Chem. 2016;56(7):572–9.

23. Lake Asphalt of Trinidad and Tobago (1978) Limited [Internet]. 2020 [cited 2020 Jan 23]. Available from: http://trinidadlakeasphalt.com/products/trinidad-lake-asphalt-tla/

24. Wood W. Lake Asphalt: paving the world. In: Official publication of the commonwealth heads of government meeting 2009. 2009. p. 36–7.

25. Renwick D. From Raleigh to runways: a brief history of Trinidad Lake asphalt. In: Trinidad and Tobago: Celebrating a century of commercial oil production. 2009. p. 144.

26. Jackson M. Pitch Lake [Internet]. 2011 [cited 2020 Jan 23]. Available from: https://upload.wikimedia.https//www.atlasobscura.com/places/pitch-lake

27. Speight JG, Özüm B. Petroleum refining processes. Marcel Dekker, Inc.; 2002.

28. Jinsheng G. Coal, oil shale, natural bitumen, heavy oil and peat–Volume I. EOLSS Publications; 2009.

29. Zhang JH, Feng ZH, Fang W, Huo QL, Zhang K, Li JK, et al. Crude-oil hydrocarbon composition characteristics and oil viscosity prediction in the northern Songliao Basin. Sci China Earth Sci. 2014;57(2):297–312.

30. Keesom W, Blieszner J, Unnasch S. EU pathway study: life cycle assessment of crude oils in a European context [Internet]. 2012. Available from: http://www.assembly.ab.ca/lao/library/egovdocs/2011/alpmc/161480_app1.pdf

31. Nimana B, Canter C, Kumar A. Energy consumption and greenhouse gas emissions in the recovery and extraction of crude bitumen from Canada's oil sands. Appl Energy. 2015;143:189–99.

32. Charpentier AD, Bergerson JA, MacLean HL. Understanding the Canadian oil sands industry's greenhouse gas emissions. Environ Res Lett. 2009;4(1).

33. Oil sands 101 [Internet]. [cited 2020 Jan 25]. Available from: https://www.alberta.ca/oil-sands-101.aspx#toc-1

34. Brownie J, Gale MJ, Moran LE. Asphalt production from oil sand bitumen [Internet]. Canada; CA2878172A1, 2012. Available from: https://patents.google.com/patent/CA2878172A1

35. Spencer D. BP statistical review of world energy 2019 [Internet]. 2019 [cited 2020 Jan 30]. p. 1–69. Available from: https://www.bp.com/en/global/corporate/energy-economics/statistical-review-of-world-energy.html

36. Paliukaitė M, Vaitkus A, Zofka A. Evaluation of bitumen fractional composition depending on the crude oil type and production technology. In: Proceedings of the international conference on environmental engineering. 2014.

37. Coufalík P. Reologické vlastnosti asfaltových pojiv. PhD [dissertation]. Brno: Brno University of Technology; 2017.

38. Hunter RN, Self A, Read J. The Shell bitumen handbook. 6th ed. London: ICE Publishing; 2015.

39. Corbett LW. Refinery processing of asphalt cement. Transp Res Rec 999. 1984;1–6.

40. Lavin PG. Asphalt pavements–A practical guide to design, production, and maintenance for engineers and architects. Taylor & Francis; 2003.

41. Blažek J, Rábl V. Základy zpracování a využití ropy. VSCHT; 2006.

42. Speight JG. Asphalt materials science and technology. Elsevier Science & Technology; 2015.

43. Speight JG. The chemistry and technology of petroleum. 5th ed. CRC Press. CRC Press; 2014.

44. Gray MR. Upgrading oilsands bitumen and heavy oil. 1st ed. University of Alberta Press; 2015.

45. Robertson RE. Chemical properties of asphalts and their relationship to pavement performance. Washington, DC: Strategic Highway Research Program; 1991. Report No.: SHRP-A/UWP-91-510.

46. Jasso M. The mechanism of modification and properties of polymer modified asphalts. PhD [dissertation]. Calgary (AB): University of Calgary; 2016.

47. The bitumen industry–A global perspective. 3rd ed. Asphalt Institute Inc. European Bitumen Association - Eurobitume; 2015. Report No.: IS-230.

48. Český normalizační institut. ČSN 65 6073. Petroleum product–Determination of asphaltenes–Precipitation with heptane. Prague: ČNI; 2008.

49. American Society for Testing and Materials. ASTM D 4124-9. Standard test method for separation of asphalt into four fractions. West Conshohocken (PA): ASTM International; 2018.

50. Jennings PW, Pribanic JAS, Dawson KR, Bricca CE. Use of HPLC and NMR spectroscopy to characterize asphaltic materials. American Chemical Society, Division of Petroleum Chemistry, Preprints. 1981. Report No.: CONF-810813-(Vol.2).

51. Corbett LW. Composition of asphalt based on generic fractionation, using solvent deasphaltening, elution-adsorption chromatography, and densimetric characterization. Anal Chem. 1969;41(4):576–9.

52. Remišová E, Holý M. Impact of bitumen composition on empirical properties. MATEC Web Conf. 2018;196:1–8.

53. Petersen JC, Plancher H. Model studies and interpretive review of the competitive adsorption and water dispacement of petroleum asphalt chemical functionalities on mineral aggregate surfaces. Pet Sci Technol. 1998;16(1–2):89–131.

54. Pernyeszi T, Patzkó Á, Berkesi O, Dékány I. Asphaltene adsorption on clays and crude oil reservoir rocks. Colloids Surfaces A Physicochem Eng Asp. 1998;137(1):373–84.

55. Nellensteyn FJ. Bereiding en constitutie van asphalt. PhD [dissertation]. Delft: Delft University of Technology; 1923.

56. Rosinger A. Beiträge zur kolloidchemie des asphalts. Kolloid-Zeitschrift. 1914;15(5):177–9.

57. Le Guern M, Chailleux E, Farcas F, Dreessen S, Mabille I. Physico-chemical analysis of five hard bitumens: identification of chemical species and molecular organization before and after artificial aging. Fuel. 2010;89(11):3330–9.

58. Li J, Huang X, Zhang Y, Xu M. Bitumen colloidal and structural stability characterization. Road Mater Pavement Des. 2009;10(sup1):45–59.

59. Andersen SI, Birdi KS. Aggregation of asphaltenes as determined by calorimetry. J Colloid Interface Sci. 1991;142(2):497–502.

60. Park SJ, Mansoori GA. Aggregation and deposition of heavy organics in petroleum crudes. Energy Sources. 1988;10(2):109–25.

61. Gaestel C, Smadja R, Lamminan KA. Contribution à la connaissance des propriétés des bitumes routiers. Rev Générale des Routes Aérodrômes. 1971;466:85–94.

62. Oyekunle LO. Certain relationships between chemical composition and properties of petroleum asphalts from different origin. Oil Gas Sci Technol. 2006;61(3):433–41.

63. Siddiqui MN, Ali MF. Studies on the aging behavior of the Arabian asphalts. Fuel. 1999;78(9):1005–15.

64. Pfeiffer JP, Saal RN. Asphaltic bitumen as colloid systems. J Phys Chem. 1940;44(2):139–49.

65. Dickie JP, Yen TF. Macrostructure of the asphaltic fractions by various instrumental methods. Anal Chem. 1967;39(14):1847–52.

66. Rogel E. Studies on asphaltene aggregation via computational chemistry. Colloids Surfaces A Physicochem Eng Asp. 1995;104(1):85–93.

67. Petersen JC, Robertson RE, Branthaver JF, Harnsberger PM, Duvall JJ, Kim SS, et al. Binder characterization and evaluation. Volume 1. Washington, DC; 1994. Report No.: SHRP-A-367.

68. Anderson DA, Christensen DW, Bahia HU, Dongre R, Sharma MGG, Antle CE, et al. Binder characterization and evaluation. Volume 3: physical characterization. Washington, DC; 1994. Report No.: SHRP-A-369.

69. Duvall JJ, Miyake G, Catalfomo MW, Kim SS, Colgin DC, Branthaver JF. Size exclusion chromatography and ion exchange chromatography separations of asphalts. Washington, DC; 1993. Report No.: SHRP-A-663.

70. Polacco G, Stastna J, Biondi D, Zanzotto L. Relation between polymer architecture and nonlinear viscoelastic behavior of modified asphalts. Curr Opin Colloid Interface Sci. 2006;11(4):230–45.

71. Mallick RB, El-Korchi T. Pavement engineering: principles and practice. 2nd ed. CRC Press; 2013.

72. The Local Government and Municipal Knowledge Base. Rutting [Internet]. [cited 2020 Mar 24]. Available from: http://www.lgam.info/rutting

73. Hajj R, Bhasin A. The search for a measure of fatigue cracking in asphalt binders–A review of different approaches. Int J Pavement Eng. 2018;19(3):205–19.

74. Frost L. Alligator cracking & severity [Internet]. 2020 [cited 2020 Mar 24]. Available from: https://alphapavingtexas.com/alligator-cracking-severity/

75. Teltayev B, Radovskiy B. Predicting thermal cracking of asphalt pavements from bitumen and mix properties. Road Mater Pavement Des. 2018;19(8):1832–47.

76. Liu J. Cutting down [Internet]. 2018 [cited 2020 Mar 25]. Available from: https://www.roadsbridges.com/cutting-down

77. Bardesi A, Brûlé B, Corte JF, Diani E, Gerritsen A, Lefebvre G, et al. Use of modified bituminous binders, special bitumens and bitumens with additives in road pavements. World Road Association. 1999. Report No.: PIARC 303.

78. Siegmann MC. Manufacture of asphaltic bitumen. In: Pfeiffer JP, editor. The Properties of Asphaltic Bitumen. Amsterdam: Elsevier; 1950. p. 121–54.

79. De Carcer ÍA, Masegosa RM, Teresa Viñas M, Sanchez-Cabezudo M, Salom C, Prolongo MG, et al. Storage stability of SBS/sulfur modified bitumens at high temperature: influence of bitumen composition and structure. Constr Build Mater. 2014;52:245–52.

80. Brûlé B. Polymer-modified asphalt cements used in the road construction industry: basic principles. Transp Res Rec. 1996;1535(1):48–53.

81. Carreaul PJ, Bousmina M, Bonniotl F. The viscoelastic properties of polymer-modified asphalts. Can Jaournal Chem Eng. 2000;78(3):495–503.

82. Becker YM, Müller AJ, Rodriguez Y. Use of rheological compatibility criteria to study SBS modified asphalts. J Appl Polym Sci. 2003;90(7):1772–82.

83. European Asphalt Pavement Association. Asphalt in figures 2018 [Internet]. 2018 [cited 2020 Mar 27]. Available from: https://eapa.org/asphalt-in-figures

84. Drobny JG. Styrenic block copolymers. In: Handbook of thermoplastic elastomers. Elsevier Science & Technology Books; 2007. p. 161–77.

85. Jouenne S, González-León JA, Ruzette AV, Lodefier P, Tencé-Girault S, Leibler L. Styrene/butadiene gradient block copolymers: molecular and mesoscopic structures. Macromolecules. 2007;40(7):2432–42.

86. Grady BP, Cooper SL, Robertson CG. Thermoplastic elastomers. In: Mark JE, Erman B, Roland M, editors. The science and technology of rubber. 4th ed. Elsevier Science & Technology; 2013. p. 591–652.

87. Polymer Properties Database [Internet]. [cited 2020 Mar 23]. Available from: http://polymerdatabase.com/Elastomers/TPEs.html

88. Brûlé B, Ramond G, Such C. Relationships between composition, structure, and properties of road asphalts: state of research at the French Public Works Central Laboratory. Transp Res Rec. 1986;1096:22–34.

89. Adedeji A, Grunfelder T, Bates FS, Macosko CW, Stroup-Gardiner M, Newcomb DE. Asphalt modified by SBS triblock copolymer: structures and properties. Polym Eng Sci. 1996;36(12):1707–23.

90. Zhang Q, Wang T, Fan W, Ying Y, Wu Y. Evaluation of the properties of bitumen modified by SBS copolymers with different styrene–butadiene structure. J Appl Polym Sci. 2014;131(12):1–7.

91. Vonk W, Hartemink R. SBS-modified binders, also cost effective in hot climates! In: Proceedings of the 8th Conference on Asphalt Pavements for Southern Africa (CAPSA'04). Sun City; 2004.

92. Zanzotto L, Stastna J, Vacin O. Thermomechanical properties of several polymer modified asphalts. Appl Rheol. 2000;10(4):185–91.

93. Zhu J, Birgisson B, Kringos N. Polymer modification of bitumen: advances and challenges. Eur Polym J. 2014;54:18–38.

94. Airey GD, Singleton TM, Collop AC. Properties of polymer modified bitumen after rubber-bitumen interaction. J Mater Civ Eng. 2002;14(4):344–54.

95. Airey GD. Styrene butadiene styrene polymer modification of road bitumens. J Mater Sci. 2004;39(3):951–9.

96. Airey GD. Rheological properties of styrene butadiene styrene polymer modified road bitumens. Fuel. 2003;82(14):1709–19.

97. Fawcett AH, McNally T. Polystyrene and asphaltene micelles within blends with a bitumen of an SBS block copolymer and styrene and butadiene homopolymers. Colloid Polym Sci. 2003;281(3):203–13.

98. Fawcett AH, McNally T. Blends of bitumen with polymers having a styrene component. Polym Eng Sci. 2001;41(7):1251–64.

99. Polacco G, Stastna J, Vlachovicova Z, Biondi D, Zanzotto L. Temporary networks in polymer-modified asphalts. Polym Eng Sci. 2004;44(12):2185–93.

100. Polacco G, Biondi D, Stastna J, Vlachovicova Z, Zanzotto L. Effect of SBS on rheological properties of different base asphalts. Macromol Symp. 2004;218(1):333–42.

101. Elseifi MA, Flintsch GW, Al-Qadi IL. Quantitative effect of elastomeric modification on binder performance at intermediate and high temperatures. J Mater Civ Eng. 2003;15(1):32–40.

102. Xiaohu L, Isacsson U. Chemical and rheological evaluation of ageing properties of sbs polymer modified bitumens. Fuel. 1998;77(9–10):961–72.

103. Wloczysiak P, Vidal A, Papirer E, Gauvin P. Relationships between rheological properties, morphological characteristics, and composition of bitumen-styrene butadiene styrene copolymers mixes. I. A three-phase system. J Appl Polym Sci. 1997;65(8):1595–607.

104. Wloczysiak P, Vidal A, Papirer E, Gauvin P. Relationships between rheological properties, morphological characteristics, and composition of bitumen–styrene butadiene styrene copolymers mixes. II. A thermodinamical interpretation. J Appl Polym Sci. 1997;65(8):1609–18.

105. Chen JS, Liao MC, Shiah MS. Asphalt modified by styrene-butadiene-styrene triblock copolymer: morphology and model. J Mater Civ Eng. 2002;14(3):224–9.

106. Lundström R, Isacsson U. Linear viscoelastic and fatigue characteristics of styrene–butadiene–styrene modified asphalt mixtures. J Mater Civ Eng. 2004;16(6):629–38.

107. Geyer R, Jambeck JR, Law KL. Production, use, and fate of all plastics ever made. Sci Adv. 2017;3(7):e1700782.

108. Okhotnikova ES, Ganeeva YM, Frolov IN, Yusupova TN, Firsin AA. Plastic properties and structure of bitumen modified by recycled polyethylene. Pet Sci Technol. 2018;36(5):356–60.

109. Panda M, Mazumdar M. Utilization of reclaimed polyethylene in bituminous paving mixes. J Mater Civ Eng. 2002;14(6):527–30.

110. García-Morales M, Partal P, Navarro FJ, Gallegos C. Effect of waste polymer addition on the rheology of modified bitumen. Fuel. 2006;85(7–8):936–43.

111. Costa LMB, Silva HMRD, Peralta J, Oliveira JRM. Using waste polymers as a reliable alternative for asphalt binder modification–Performance and morphological assessment. Constr Build Mater. 2019;198:237–44.

112. Okhotnikova ES, Frolov IN, Ganeeva YM, Firsin AA, Yusupova TN. Rheological behavior of recycled polyethylene modified bitumens. Pet Sci Technol. 2019;37(10):1136–42.

113. Hınıslıoğlu S, Ağar E. Use of waste high density polyethylene as bitumen modifier in asphalt concrete mix. Mater Lett. 2004;58(3–4):267–71.

114. Carraher CE. Seymour/Carraher's polymer chemistry. 6th ed. Vol. 27. Ringgold, Inc; 2003. 39–60 p.

115. Roman C, García-Morales M. Linear rheology of bituminous mastics modified with various polyolefins: a comparative study with their source binders. Mater Struct. 2017;50(1):1–12.

116. Zhang XM, Elkoun S, Ajji A, Huneault MA. Oriented structure and anisotropy properties of polymer blown films: HDPE, LLDPE and LDPE. Polym. 2004;45(1):217–29.

117. Maier C, Calafut T. Morphology and commercial forms. In: Polypropylene: The definitive user's guide and databook. Plastics Design Library; 1998. p. 1–16.

118. Fawcett AH, McNally T. Blends of bitumen with various polyolefins. Polym. 2000;41(14):5315–26.

119. Upadhyay S, Mallikarjunan V, Subbaraj VK, Varughese S. Swelling and diffusion characteristics of polar and nonpolar polymers in asphalt. J Appl Polym Sci. 2008;109(1):135–43.

120. Spadaro C, Plummer CJG, Manson JAE. Thermal and dynamic mechanical properties of blends of bitumen with metallocene catalyzed polyolefins. J Mater Sci. 2011;46(23):7449–58.

121. Polacco G, Berlincioni S, Biondi D, Stastna J, Zanzotto L. Asphalt modification with different polyethylene-based polymers. Eur Polym J. 2005;41(12):2831–44.

122. Awwad MT, Shbeeb L. The use of polyethylene in hot asphalt mixtures. Am J Appl Sci. 2007;4(6):390–6.

123. Vargas MA, Vargas MA, Sánchez-Sólis A, Manero O. Asphalt/polyethylene blends: rheological properties, microstructure and viscosity modeling. Constr Build Mater. 2013;45:243–50.

124. Ait-Kadi A, Brahimi B, Bousmina M. Polymer blends for enhanced asphalt binders. Polym Eng Sci. 1996;36(12):1724–33.

125. Giavarini C, De Filippis P, Santarelli ML, Scarsella M. Production of stable polypropylene-modified bitumens. Fuel. 1996;75(6):681–6.

126. Pérez-Lepe A, Martínez-Boza FJ, Attané P, Gallegos C. Destabilization mechanism of polyethylene-modified bitumen. J Appl Polym Sci. 2006;100(1):260–7.

127. Yousefi AA. Polyethylene dispersions in bitumen: the effects of the polymer structural parameters. J Appl Polym Sci. 2003;90(12):3183–90.

128. Giuliani F, Merusi F, Filippi S, Biondi D, Finocchiaro ML, Polacco G. Effects of polymer modification on the fuel resistance of asphalt binders. Fuel. 2009;88(9):1539–46.

129. Yuliestyan A, Cuadri AA, García-Morales M, Partal P. Influence of polymer melting point and Melt Flow Index on the performance of ethylene-vinyl-acetate modified bitumen for reduced-temperature application. Mater Des. 2016;96:180–8.

130. Airey GD. Rheological evaluation of ethylene vinyl acetate polymer modified bitumens. Constr Build Mater. 2002;16(8):473–87.

131. García-Morales M, Partal P, Navarro FJ, Martínez-Boza F, Gallegos C, González N, et al. Viscous properties and microstructure of recycled eva modified bitumen. Fuel. 2004;83(1):31–8.

132. García-Morales M, Partal P, Navarro FJ, Martínez-Boza F, Mackley MR, Gallegos C. The rheology of recycled EVA/LDPE modified bitumen. Rheol Acta. 2004;43(5):482–90.

133. González O, Muñoz ME, Santamaría A, García-Morales M, Navarro FJ, Partal P. Rheology and stability of bitumen/EVA blends. Eur Polym J. 2004;40(10):2365–72.

134. González E, Costa LMB, Silva HMRD, Hilliou L. Rheological characterization of EVA and HDPE polymer modified bitumens under large deformation at 20°C. Constr Build Mater. 2016;112:756–64.

135. Saboo N, Kumar R, Kumar P, Gupta A. Ranking the rheological response of SBS- and EVA-modified bitumen using MSCR and LAS tests. J Mater Civ Eng. 2018;30(8):4018165.

136. Yuliestyan A, Cuadri AA, García-Morales M, Partal P. Binder design for asphalt mixes with reduced temperature: EVA modified bitumen and its emulsions. Transp Res Procedia. 2016;14:3512–8.

137. Padhan RK, Gupta AA, Sreeram A. Effect of cross-linking agent on ethylene vinyl acetate/polyoctenamer modified bitumen. Road Mater Pavement Des. 2019;20(7):1615–23.

138. Bulatović VO, Rek V, Marković KJ. Rheological properties and stability of ethylene vinyl acetate polymer-modified bitumen. Polym Eng Sci. 2013;53(11):2276–83.

139. Polacco G, Stastna J, Biondi D, Antonelli F, Vlachovicova Z, Zanzotto L. Rheology of asphalts modified with glycidylmethacrylate functionalized polymers. J Colloid Interface Sci. 2004;280(2):366–73.

140. Ahmedzade P. The investigation and comparison effects of SBS and SBS with new reactive terpolymer on the rheological properties of bitumen. Constr Build Mater. 2013;38:285–91.

141. Polacco G, Filippi S, Merusi F, Stastna G. A review of the fundamentals of polymer-modified asphalts: Asphalt/polymer interactions and principles of compatibility. Adv Colloid Interface Sci. 2015;224:72–112.

142. Jasso M, Hampl R, Vacin O, Bakos D, Stastna J, Zanzotto L. Rheology of conventional asphalt modified with SBS, Elvaloy and polyphosphoric acid. Fuel Process Technol. 2015;140:172–9.

143. Selvavathi V, Sekar VA, Sriram V, Sairam B. Modifications of bitumen by elastomer and reactive polymer–A comparative study. Pet Sci Technol. 2002;20(5–6):535–47.

144. Keyf S. The modification of bitumen with reactive ethylene terpolymer, styrene butadiene styrene and variable amounts of ethylene vinyl acetate. Res Chem Intermadiates. 2015;41(3):1485–97.

145. Geckil T, Seloglu M. Performance properties of asphalt modified with reactive terpolymer. Constr Build Mater. 2018;173:262–71.

146. Keyf S, Ismail O, Corbacıoglu BD, Ozen H. The modification of bitumen with synthetic reactive ethylene terpolymer and ethylene terpolymer. Pet Sci Technol. 2007;25(5):561–8.

147. Bulatović VO, Rek V, Marković J. Rheological properties of bitumen modified with ethylene butylacrylate glycidylmethacrylate. Polym Eng Sci. 2014;54(5):1056–65.

148. Lo Presti D. Recycled tyre rubber modified bitumens for road asphalt mixtures: a literature review. Constr Build Mater. 2013;49:863–81.

149. Behnood A, Olek J. Rheological properties of asphalt binders modified with styrene-butadiene-styrene (SBS), ground tire rubber (GTR), or polyphosphoric acid (PPA). Constr Build Mater. 2017;151:464–78.

150. Cong P, Xun P, Xing M, Chen S. Investigation of asphalt binder containing various crumb rubbers and asphalts. Constr Build Mater. 2013;40:632–41.

151. Bahia HU, Davies R. Effect of crumb rubber modifiers (CRM) on performance related properties of asphalt binders. Asph Paving Technol. 1994;63:414–38.

152. Navarro FJ, Partal P, Martinez-Boza FJ, Gallegos C. Influence of processing conditions on the rheological behavior of crumb tire rubber-modified bitumen. J Appl Polym Sci. 2007;104(3):1683–91.

153. Wong CC, Wong W. Effect of crumb rubber modifiers on high temperature susceptibility of wearing course mixtures. Constr Build Mater. 2007;21(8):1741–5.

154. Thodesen C, Shatanawi K, Amirkhanian S. Effect of crumb rubber characteristics on crumb rubber modified (CRM) binder viscosity. Constr Build Mater. 2009;23(1):295–303.

155. Roberts FL, Kandhal PS, Brown ER, Dunning RL. Investigation and evaluation of ground tire rubber in hot mix asphalt. National Center for Asphalt Technology. Auburn, AL; 1989. Report No.: NCAT 89-03.

156. Lee SJ, Akisetty CK, Amirkhanian SN. The effect of crumb rubber modifier (CRM) on the performance properties of rubberized binders in HMA pavements. Constr Build Mater. 2008;22(7):1368–76.

157. Wang S, Cheng D, Xiao F. Recent developments in the application of chemical approaches to rubberized asphalt. Constr Build Mater. 2017;131:101–13.

158. Toth C, Petho L, Geiger A, Soos Z. Performance assessment of hot mix asphalt with chemically stabilized rubber bitumen. In: Proceedings of the 6th Euroasphalt & Eurobitume Congress. Prague; 2016.

159. Kisgyörgy L, Tóth C, Geiger A. Elastic modulus of asphalt with chemically stabilized rubber bitumen. Građevinar. 2016;68(7):533–41.

160. Geiger A, Hollo A, Thernesz A, Durgo R, Czibor S, Bartha L, et al. Chemically stabilized rubber bitumen. In: Turkey, editor. Proceedings of the 5th Eurasphalt & Eurobitume Congress. Istanbul; 2012.

161. Heitzmann M. Design and construction of asphalt paving materials with crumb rubber modifier. In: Transportation Research Record. 1992. p. 1–8.

162. Ghavibazoo A, Abdelrahman M. Effect of crumb rubber modification on short term aging susceptibility of asphalt binder. Int J Pavement Res Technol. 2014;7(4):297–304.

163. Huang S-C, Pauli AT. Particle size effect of crumb rubber on rheology and morphology of asphalt binders with long-term aging. Road Mater Pavement Des. 2008;9(1):73–95.

164. Wang S, Wang Q, Li S. Thermooxidative aging mechanism of crumb-rubber-modified asphalt. J Appl Polym Sci. 2016;133(16).

165. Wang S, Yuan C, Jiaxi D. Crumb tire rubber and polyethylene mutually stabilized in asphalt by screw extrusion. J Appl Polym Sci. 2014;131(23).

166. Liang M, Xin X, Fan W, Luo H, Wang X, Xing B. Investigation of the rheological properties and storage stability of CR/SBS modified asphalt. Constr Build Mater. 2015;74:235–40.

167. Lo Presti D, Izquierdo MA, Jiménez del Barco Carrión A. Towards storage-stable high-content recycled tyre rubber modified bitumen. Constr Build Mater. 2018;172:106–11.

168. Dašek O. Uplatnění pryžového granulátu v asfaltových pojivech a hutněných asfaltových směsích. PhD [dissertation]. Brno: Brno University of Technology; 2013.

169. Brno University of Technology. TP 148:2009. Hutněné asfaltové vrstvy s asfaltem modifikovaným pryžovým granulátem z pneumatik. Ministerstvo dopravy ČR; 2009.

170. Yao H, Zhou S, Wang S. Structural evolution of recycled tire rubber in asphalt. J Appl Polym Sci. 2016;133(6).

171. Ghavibazoo A, Abdelrahman M. Composition analysis of crumb rubber during interaction with asphalt and effect on properties of binder. Int J Pavement Eng. 2013;14(5):517–30.

172. Glover CJ, Davison RR, Bullin JA, Estakhri CK, Williamson SA, Billiter TC, et al. A comprehensive laboratory and field study of high-cure crumb-rubber modified asphalt materials. Texas Department of Transportation and the U.S. Department of Transportation, Federal Highway Administration. 2000. Report No.: FHWA/TX-01/1460-1.

173. Alexander SH. Method of treating asphalt. United States; US3751278, 1973.

174. Baumgardner GL. Why and how of polyphosphoric acid modification–An industry perspective. In: Transportation Research Circular E-C160, Polyphosphoric Acid Modification of Asphalt Binders. Minneapolis (MN): Transportation Research Board; 2012. p. 14–26.

175. Masson JF. Brief review of the chemistry of polyphosphoric acid (PPA) and bitumen. Energy and Fuels. 2008;22(4):2637–40.

176. Fort J. Blown bitumens and a process for making them. United States; US3126329A, 1964.

177. Baldino N, Gabriele D, Lupi FR, Oliviero C, Caputo P, Falvo T. Rheological effects on bitumen of polyphosphoric acid (PPA) addition. Constr Build Mater. 2013;40:397–404.

178. Arnold TS, Youtcheff J, Needham SP. Use of phosphoric acid as modifier for hot-mix asphalt. In: Transportation Research Circular E-C160, Polyphosphoric Acid Modification of Asphalt Binders. Minneapolis (MN): Transportation Research Board; 2012. p. 40–51.

179. Domingos MDI, Faxina AL. Creep-recovery behavior of asphalt binders modified with SBS and PPA. J Mater Civ Eng. 2014;26(4):781–3.

180. Li X, Clyne T, Reinke G, Johnson EN, Gibson N, Kutay ME. Laboratory evaluation of asphalt binders and mixtures containing polyphosphoric acid. In: Proceedings of the 90th Annual Meeting of the Transportation Research Board. 2011. p. 47–56.

181. Domingos MDI, Faxina AL, Bernucci LLB. Characterization of the rutting potential of modified asphalt binders and its correlation with the mixture's rut resistance. Constr Build Mater. 2017;144:207–13.

182. Gama DA, Rosa Júnior JM, de Melo TJA, Rodrigues JKG. Rheological studies of asphalt modified with elastomeric polymer. Constr Build Mater. 2016;106:290–5.

183. Cao W. Experimental research on crumb rubber and polyphosphoric acid composite modified asphalt binders. Appl Mech Mater. 2012;174–177:1579–83.

184. Dupuis D, Lesueur D, Potti JJ, Orange G, Godber J. Bituminous binder and method for the production thereof. United States; US8114926B2, 2012.

185. Wen G, Zhang Y, Zhang Y, Sun K, Fan Y. Rheological characterization of storage-stable SBS-modified asphalts. Polym Test. 2002;21(3):295–302.

186. Chen JS, Huang CC. Fundamental characterization of SBS-modified asphalt mixed with sulfur. J Appl Polym Sci. 2007;103(5):2817–25.

187. Wen G, Zhang Y, Zhang Y, Sun K, Fan Y. Improved properties of SBS-modified asphalt with dynamic vulcanization. Polym Eng Sci. 2002;42(5):1070–81.

188. Zhang F, Yu J, Han J. Effects of thermal oxidative ageing on dynamic viscosity, TG/DTG, DTA and FTIR of SBS- and SBS/sulfur-modified asphalts. Constr Build Mater. 2011;25(1):129–37.

189. Zhang F, Yu J, Wu S. Effect of ageing on rheological properties of storage-stable SBS/sulfur-modified asphalts. J Hazard Mater. 2010;182(1):507–17.

190. Barnes HA, Hutton JF, Walters K. An introduction to rheology. Vol. 3. Amsterdam: Elsevier; 1989.

191. Tia M, Ruth BE. Basic rheology and rheological concepts established by HE Schweyer. In: Briscoe OE, editor. Asphalt Rheology: Relationship to Mixture. ASTM International; 1987. p. 118–45.

192. Kelly PA. Mechanics lecture notes: an introduction to solid mechanics [Internet]. Available from: http://homepages.engineering.auckland.ac.nz/~pkel015/SolidMechanicsBooks/index.html

193. Menard KP. Dynamic mechanical analysis: a practical introduction. CRC Press; 1999.

194. Tschoegl NW. The phenomenological theory of linear viscoelastic behavior: an introduction. Springer Science & Business Media, 2012; 1989.

195. Roscoe R. Mechanical models for the representation of visco-elastic properties. Br J Appl Phys. 1950;1(7):171–3.

196. Ferry JD. Viscoelastic properties of polymers. 3rd ed. John Wiley & Sons; 1980.

197. Mezger TG. The rheology handbook: for users of rotational and oscillatory rheometers. Hannover, Germany: Vincentz Network; 2006.

198. Murayama T. Dynamic mechanical analysis application to dynamic thermo-mechanometry. In: Johnson JF, Gill PS, editors. Analytical Calorimetry. 5th ed. Boston, MA: Springer; 1984. p. 81–93.

199. Baumgaertel M, Winter HH. Determination of discrete relaxation and retardation time spectra from dynamic mechanical data. Rheol Acta. 1989;28:511–9.

200. Dealy JM, Wissbrun KF. Rotational and sliding surface rheometers. In: Melt Rheology and Its Role in Plastics Processing. 1999. p. 269–97.

201. Bonaquist RF, Mogawer WS. Analysis of pavement rutting data from FHWA pavement testing facility superpave validation study. Transp Res Rec. 1997;1590(1):80–8.

202. White TD, Haddock JE, Hand AJT, Fang H. Contributions of pavement structural layers to rutting of hot mix asphalt pavements. National Cooperative Highway Research Program. Washington, DC; 2002. Report No.: NCHRP 468.

203. Faruk ANM, Lee SI, Zhang J, Naik B, Walubita LF. Measurement of HMA shear resistance potential in the lab: The simple punching shear test. Constr Build Mater. 2015;99:62–72.

204. Sousa JB, Craus J, Monismith CL. Summary report on permanent deformation in asphalt concrete. Strategic Highway Research Program. Washington, DC; 1991. Report No.: SHRP-A/IR-91-104.

205. Zhang J, Zhu C, Li X, Pei J, Chen J. Characterizing the three-stage rutting behavior of asphalt pavement with semi-rigid base by using UMAT in ABAQUS. Constr Build Mater. 2017;140:496–507.

206. Carvalho RLE. Prediction of permanent deformation in asphalt concrete. PhD [dissertation]. College Park: University of Maryland; 2012.

207. American Association of State and Highway Transportation Officials. AASHTO M320-16. Standard specification for performance-graded asphalt binder. Washington, DC: AASHTO; 2016.

208. American Association of State and Highway Transportation Officials. AASHTO T 315-12. Standard method of test for determining the rheological properties of asphalt binder using a dynamic shear rheometer (DSR). Washington, DC: AASHTO; 2012.

209. D'Angelo JA. New high-temperature binder specification using multistress creep and recovery. In: Transportation Research Circular E-C147, Development in Asphalt Binder Specifications. Washington, DC: Transportation Research Board; 2010. p. 1–13.

210. Zhang X, Huber G. Effect of asphalt binder on pavement performance: an investigation using the superpave mix design system. J Assoc Asph Paving Technol. 1996;65:449–90.

211. Sherwood JA, Thomas NL, Qi X. Correlation of Superpave G*/Sin δ with Rutting Test Results from Accelerated Loading Facility. Transp Res Rec. 1998;1630(1):53–61.

212. Bahia HU, Hanson DI, Zeng M, Zhai H, Khatri MA, Anderson RM, et al. Characterization of modified asphalt binders in Superpave mix design. National Cooperative Highway Research Program. Washington, DC; 2001. Report No.: NCHRP 459.

213. Hossain Z, Zaman M, Ghosh D. Creep compliance and percent recovery of Oklahoma certified binder using the multiple stress recovery (MSCR) method. Federal Highway Administration. Oklahoma Department of Transportation. Oklahoma City (OK): FHWA. ODOT; 2015. Report No.: FHWA-OK-14-19.

214. Delgadillo R, Cho DW, Bahia H. Nonlinearity of repeated creep and recovery binder test and relationship with mixture permanent deformation. Transp Res Rec. 2006;1962(1):2–11.

215. Shenoy A. Refinement of the Superpave specification parameter for performance grading of asphalt. J Transp Eng. 2001;127(5):357–62.

216. Masad E, Somadevan N. Microstructural finite-element analysis of influence of localized strain distribution on asphalt mix properties. J Eng Mech. 2002;128(10):1105–14.

217. Kose S, Guler M, Bahia HU, Masad E. Distribution of strains within hot-mix asphalt binders: applying imaging and finite-element techniques. Transp Res Rec. 2000;1728(1):21–7.

218. Airey GD, Rahimzadeh B, Collop AC. Linear rheological behavior of bituminous paving materials. J Mater Civ Eng. 2004;16(3):212–20.

219. Collop AC, Airey GD, Khanzada S. Creep testing of bitumens using the dynamic shear rheometer. Int J Pavement Eng. 2002;3(2):107–16.

220. D'Angelo JA, Kluttz RQ, Dongre R, Stephens K, Zanzotto L. Revision of the Superpave high temperature binder specification: the multiple stress creep recovery test. J Assoc Asph Paving Technol. 2007;76:123–62.

221. Robertus C, Rooijen R Van, Thimm L. A comparison of binder tess that relate to asphalt mixture deformation. In: Proceedings of the 5th Eurasphalt & Eurobitume Congress. Istanbul; 2012.

222. Li X, Zofka A, Li X, Marasteanu M, Clyne TR. Investigation of the low-temperature fracture properties of three MnROAD asphalt mixtures. Minnesota Department of Transportation. Department of Civil Engineering. Minneapolis (MN): MnDOT; 2006. Report No.: MN/RC-2006-15.

223. D'Angelo JA. The relationship of the MSCR test to rutting. Road Mater Pavement Des. 2009;10(sup1):61–80.

224. Qi X, Al-khateeb G, Shenoy A, Mitchell T, Gibson N, Youtcheff J, et al. Performance of the FHWA's ALF Modified-Binder Pavements. In: Proceedings of the 10th International Conference on Asphalt Pavements. Quebec; 2006.

225. Al-khateeb G, Gibson N, Qi X. Mechanistic analyses of FHWA's accelerated loading facility pavements: primary response. Transp Res Rec. 2007;1990(1):150–61.

226. Al-Khateeb G, Shenoy A, Gibson N. Mechanistic performance analyses of the FHWA's accelerated loading facility pavements. J Assoc Asph Paving Technol. 2007;76:737–70.

227. Albritton GE, Barstis WF, Crawley AB. Polymer modified hot mix asphalt field trial. Federal Highway Administration. Mississippi Department of Transportation. FHWA. MDOT; 1999. Report No.: FHWA/MS-DOT-RD-99-111.

228. Reinke G. Use of Hamburg rut testing data to validate the use of Jnr as a performance parameter for high-temperature permanent deformation. In: Transportation Research Circular E-C147, Development in Asphalt Binder Specifications. Washington, DC: Transportation Research Board; 2010. p. 14–24.

229. Wasage TLJ, Stastna J, Zanzotto L. Rheological analysis of multi-stress creep recovery (MSCR) test. Int J Pavement Eng. 2011;12(6):561–8.

230. Anderson M, D'Angelo JA, Walker D. MSCR: A better tool for characterizing high temperature performance properties. Asph Mag Asph Inst. 2010;25(2).

231. Plitz J. Zpráva o činnosti TNK 134 "ASFALTY" a spolupráci s TC 336 v roce 2015. Technická normalizační komise 134. Prague: TNK 134; 2015.

232. Bureš P, Fiedler J, Komínek Z. Reologické vlastnosti asfaltových pojiv a směsí za středních a vysokých teplot. In: Proceedings of the Conference Asfaltové Vozovky 2011. České Budějovice, Czech Republic; 2011.

233. Benešová L, Valentin J. Influence of selected test parameters on measured values during the MSCR test. IOP Conf Ser Mater Sci Eng. 2017;236.

234. De Beer M, Fisher C, Jooste FJ. Determination of pneumatic tyre/pavement interface contact stresses under moving loads and some effects on pavements with thin asphalt surfacing layers. In: Proceedings of the 8th International Conference on Asphalt Pavements. Seattle (WA); 1997. p. 179–227.

235. De Beer M, Fisher C, Kannemeyer L. Towards the application of Stress-In-Motion (SIM) results in pavement design and infrastructure protection. In: Proceedings of the 8th International Symposium on Heavy Vehicle Weights and Dimensions. Johannesburg; 2004.

236. Tielking JT, Roberts FL. Tire contact pressure and its effect on pavement strain. J Transp Eng. 1987;113(1):56–71.

237. Yoo PJ, Al-Qadi IL, Elseifi MA, Janajreh I. Flexible pavement responses to different loading amplitudes considering layer interface condition and lateral shear forces. Int J Pavement Eng. 2006;7(1):73–86.

238. El-Kholy SA, Galal SA. A study on the effects of non-uniform tyre inflation pressure distribution on rigid pavement responses. Int J Pavement Eng. 2012;13(3):244–58.

239. De Beer M, Maina JW, Van Rensburg Y, Greben JM. Toward using tire-road contact stresses in pavement design and analysis. Tire Sci Technol. 2012;40(4):246–71.

240. Hu X, Zhong S, Walubita LF. Three-dimensional modelling of multilayered asphalt concrete pavement structures: strain responses and permanent deformation. Road Mater Pavement Des. 2015;16(3):727–40.

241. Jiang X, Zeng C, Gao X, Liu Z, Qiu Y. 3D FEM analysis of flexible base asphalt pavement structure under non-uniform tyre contact pressure. Int J Pavement Eng. 2019;20(9):999–1011.

242. Bai T, Cheng Z, Hu X, Fuentes L, Walubita LF. Viscoelastic modelling of an asphalt pavement based on actual tire-pavement contact pressure. Road Mater Pavement Des [Internet]. 2020;1–20. Available from: https://doi.org/14680629.2020.1766545

243. Žák J, Vavřička J. Load distribution in Hamburg wheel tracking test. In: Proceedings of the 9th European Conference of Young Research and Scientific Workers (Transcom 2011). Žilina; 2011. p. 129–34.

244. Chaturabong P, Bahia HU. Mechanisms of asphalt mixture rutting in the dry Hamburg Wheel Tracking test and the potential to be alternative test in measuring rutting resistance. Constr Build Mater. 2017;146:175–82.

245. Tsai B-W, Coleri E, Harvey JT, Monismith CL. Evaluation of AASHTO T 324 hamburg-wheel track device test. Constr Build Mater. 2016;114:248–60.

246. Ředitelství silnic a dálnic ČR. Celostátní sčítání dopravy [Internet]. [cited 2020 Jun 23]. Available from: https://www.rsd.cz/wps/portal/web/Silnice-a-dalnice/Scitani-dopravy

247. Elvaloy™ 5160 copolymer technical data sheet [Internet]. 2019 [cited 2020 Mar 6]. Available from: https://www.dow.com/en-us/document-viewer.html?ramdomVar=4068393990281677173&docPath=/content/dam/dcc/documents/en-us/productdatasheet/914/914-13601-01-elvaloy-5160-copolymer-tds.pdf

248. Polyphosphoric Acid 115%; 116% PPA 115 ; PPA 116 [Internet]. 2015 [cited 2020 Mar 6]. Available from: https://add.lanxess.com/fileadmin/product-import/polyphosphoric_acid_115116_ppa_115_ppa_116_en_rcr.pdf

249. Kraton® D1101 K Polymer [Internet]. 2009 [cited 2020 Mar 6]. Available from: https://cdn.thomasnet.com/ccp/01308444/107551.pdf

250. American Association of State and Highway Transportation Officials. AASHTO R35-12. Standard practice for Superpave volumetric design for hot-mix asphalt (HMA). Washington, DC, USA: AASHTO; 2012.

251. American Association of State and Highway Transportation Officials. AASHTO M323-12. Standard specification for Superpave volumetric mix design. Washington, DC, USA: AASHTO; 2012.

252. American Association of State and Highway Transportation Officials. AASHTO R30-02. Standard practice for mixture conditioning of hot-mix asphalt (HMA). Washington, DC, USA: AASHTO; 2015.

253. American Association of State and Highway Transportation Officials. AASHTO T316-13. Standard method of test for viscosity determination of asphalt binder using rotational viscometer. Washington, DC, USA: AASHTO; 2013.

254. American Association of State and Highway Transportation Officials. AASHTO T240-13. Standard method of test for effect of heat and air on a moving film of asphalt binder (rolling thin-film oven test). Washington, DC: AASHTO; 2013.

255. American Association of State and Highway Transportation Officials. AASHTO R28-12. Standard practice for accelerated aging of asphalt binder using a pressurized aging vessel (PAV). Washington, DC: AASHTO; 2012.

256. American Association of State and Highway Transportation Officials. AASHTO T315-12. Standard method of test for determining the rheological properties of asphalt binder using a dynamic shear rheometer (DSR). Washington, DC: AASHTO; 2012.

257. American Association of State and Highway Transportation Officials. AASHTO T313-12. Standard method of test for determining the flexural creep stiffness of asphalt binder using the bending beam rheometer (BBR). Washington, DC: AASHTO; 2012.

258. American Association of State and Highway Transportation Officials. AASHTO T350-14. Standard method of test for multiple stress creep recovery (MSCR) test of asphalt binder using a dynamic shear rheometer (DSR). Washington, DC, USA: AASHTO; 2014.

259. D'Angelo JA. Development of a performance based binder specification for rutting using creep and recovery testing. PhD [dissertation]. Calgary (AB): University of Calgary; 2009.

260. American Association of State and Highway Transportation Officials. AASHTO M332-14. Standard specification for performance-graded asphalt binder using multiple stress creep recovery (MSCR) test. Washington, DC: AASHTO; 2014.

261. Walubita LF, Fuentes L, Prakoso A, Rico Pianeta LM, Komba JJ, Naik B. Correlating the HWTT laboratory test data to field rutting performance of in-service highway sections. Constr Build Mater. 2020;236:117552.

262. Zhang W, Chen X, Shen S, Mohammad LN, Cui B, Wu S, et al. Investigation of field rut depth of asphalt pavements using Hamburg wheel tracking test. J Transp Eng Part B Pavements. 2021;147(1):04020091.

263. Yildirim Y, Stokoe II KH. Project summary report O-4185-S. Analysis of Hamburg wheel tracking device results in relation to field performance. Center for Transportation Research. Austin (TX); 2006. Report No.: O-4185.

264. European Committee for Standardization. EN 12697-22+A1. Bituminous mixtures–Test methods for hot mix asphalt–Part 22: wheel tracking. CEN; 2007.

265. Witczak MW, Kaloush K, Pellinen T, El-Basyouny M, Quintus H Von. Simple performance test for Superpave mix design. National Cooperative Highway Research Program. Washington, DC; 2002. Report No.: NCHRP 465.

266. American Association of State and Highway Transportation Officials. AASHTO T342-11. Standard method of test for determining dynamic modulus of hot mix asphalt (HMA). Washington, DC: AASHTO; 2011.

267. IRIS. Amherst (MA): IRIS Development LLC.; 2007.

268. Jafari M, Babazadeh A, Aflaki S. Effects of stress levels on creep and recovery behavior of modified asphalt binders with the same continuous performance grades. Transp Res Rec. 2015;2505(1):15–23.

269. Jafari M, Babazadeh A. Evaluation of polyphosphoric acid-modified binders using multiple stress creep and recovery and linear amplitude sweep tests. Road Mater Pavement Des. 2016;17(4):859–76.

270. Soenen H, Blomberg T, Pellinen T, Laukkanen OV. The multiple stress creep-recovery test: A detailed analysis of repeatability and reproducibility. Road Mater Pavement Des. 2013;14(sup1):2–11.

271. Visscher J De, Paez-dueñas A, Cabanillas P, Carrera V, Cerny R. European round robin tests for the multiple stress creep recovery test and contribution to the development of the European standard test method. In: Proceedings of the 6th Eurasphalt & Eurobitume Congress. Prague; 2016.

272. Remišová E. Effect of film thickness on resistance to permanent deformation in asphalt mixtures. Balt J Road Bridg Eng. 2015;10(4):333–9.

273. Lee D-Y, Guinn JA, Khandhal PS, Dunning RL. Absorption of asphalt into porous aggregate. American Chemical Society, Division of Petroleum Chemistry, Preprints. Washington, DC; 1990. Report No.: SHRP-A/UIR-90-009.

274. Airey GD. Use of black diagrams to identify inconsistencies in rheological data. Road Mater Pavement Des. 2002;3(4):403–24.

275. Luo R, Liu H. Improving the accuracy of dynamic modulus master curves of asphalt mixtures constructed using uniaxial compressive creep tests. J Mater Civ Eng. 2017;29(7):04017032.

APPENDIX-A: EFFECT OF STRESS LEVEL AND TEMPERATURE CHANGE ON VARIOUS PROPERTIES OF ASPHALT BINDERS

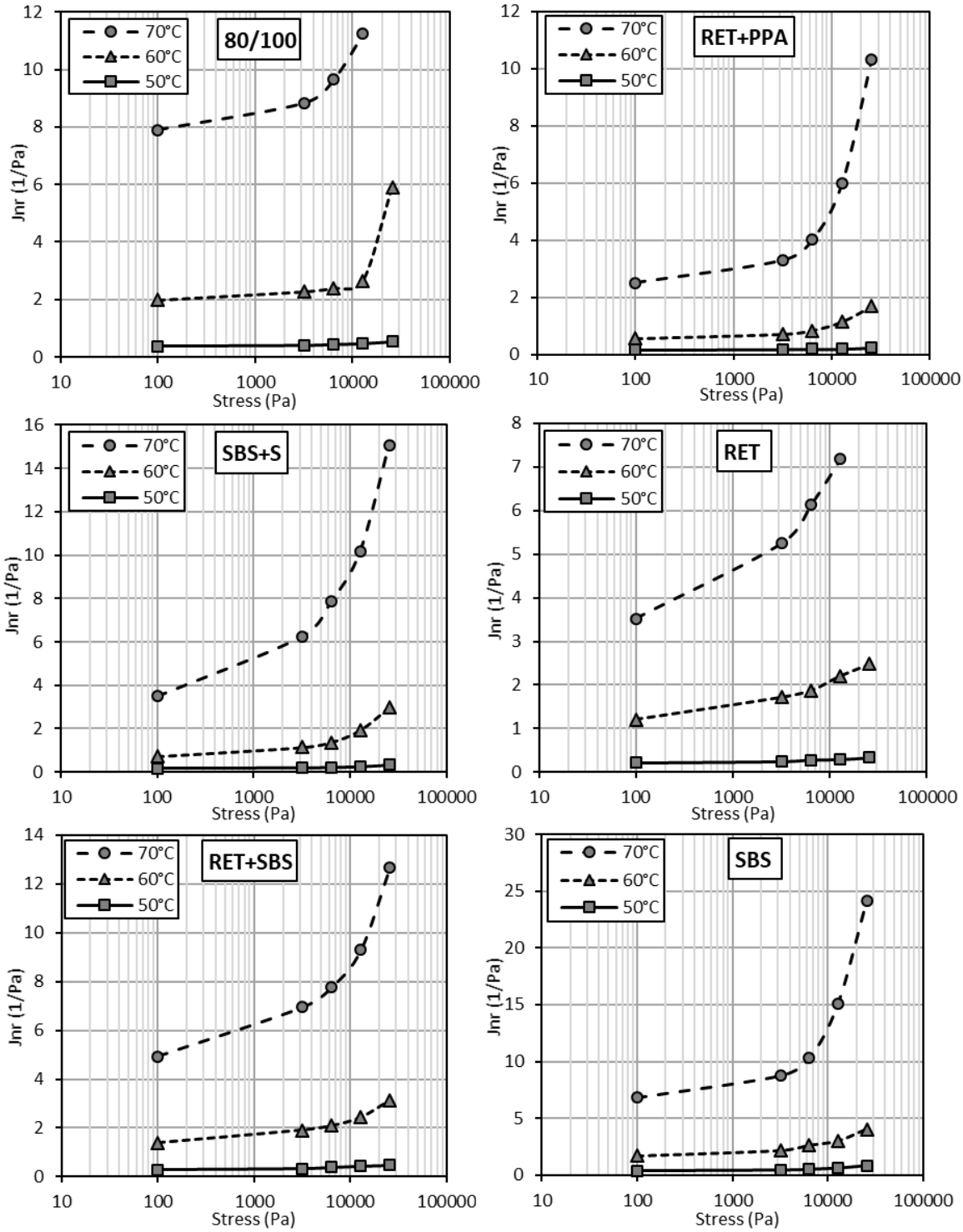

Figure A.1 Change of the non-recoverable creep compliance, J_{nr}, results of the asphalt binders with stress level at temperatures 50, 60, 70°C for asphalt binders: 80/100, RET+PPA, SBS+S, RET, RET+SBS, and SBS

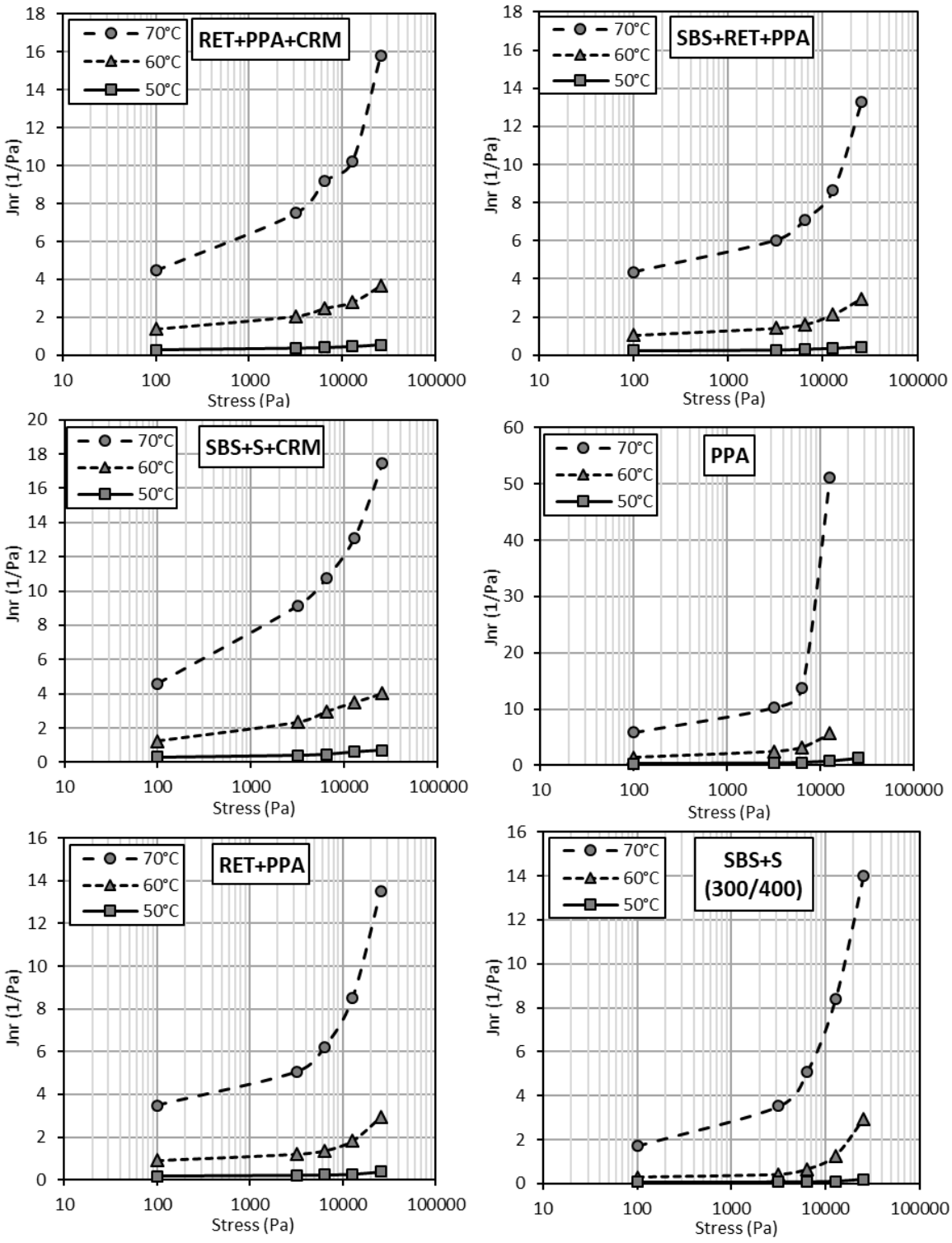

Figure A.2 Change of the non-recoverable creep compliance, J_{nr}, results of the asphalt binders with stress level at temperatures 50, 60, 70°C for asphalt binders: RET+PPA+CRM, SBS+RET+PPA, SBS+S+CRM, PPA, RET+PPA, and SBS+S (300/400)

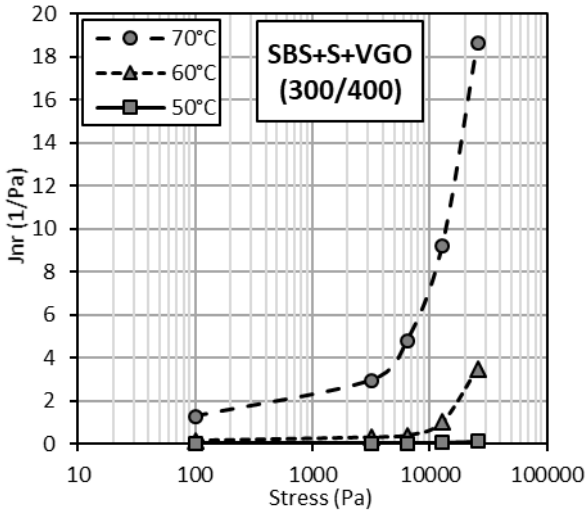

Figure A.3 Change of the non-recoverable creep compliance, J_{nr}, results with stress level at temperatures 50, 60, 70°C for the SBS+S+VGO (300/400)-modified asphalt blend

Table A.1 The non-recoverable creep compliance, J_{nr}, and the stress sensitivity, $J_{nr,diff}$, results of the asphalt binders at 50°C over multiple stress levels

Base Binder	Polymer Type Designation	J_{nr} (kPa^{-1}) at 50°C					$J_{nr,diff}$ (%) at 50°C			
		0.1 kPa	3.2 kPa	6.4 kPa	12.8 kPa	25.6 kPa	0.1–3.2 kPa	3.2–6.4 kPa	6.4–12.8 kPa	12.8–25.6 kPa
80/100	None	0.366	0.395	0.427	0.465	0.539	8.0	8.3	8.9	15.9
200/300	RET+PPA	0.159	0.179	0.184	0.189	0.235	12.5	2.7	2.8	24.4
	SBS+S	0.169	0.192	0.209	0.250	0.343	13.5	8.5	19.9	37.1
	RET	0.213	0.244	0.278	0.288	0.330	14.2	14.2	3.6	14.4
	RET+SBS	0.292	0.335	0.384	0.433	0.468	14.8	14.7	12.6	8.2
	SBS	0.392	0.450	0.506	0.611	0.832	14.8	12.6	20.7	36.2
	PPA	0.282	0.386	0.508	0.765	1.276	37.0	31.7	50.6	66.7
	RET+PPA+CRM	0.269	0.362	0.392	0.446	0.552	34.6	8.5	13.7	23.7
	SBS+RET+PPA	0.243	0.280	0.314	0.354	0.429	15.1	12.3	12.6	21.2
	SBS+S+CRM	0.289	0.404	0.458	0.594	0.683	39.5	13.6	29.6	15.0
	RET(EP)+PPA	0.177	0.214	0.228	0.263	0.374	20.9	6.2	15.3	42.5
300/400	SBS+S	0.076	0.086	0.091	0.110	0.185	13.0	5.9	21.1	68.4
	SBS+S+VGO	0.020	0.034	0.035	0.042	0.126	72.3	4.4	17.1	202.6

Table A.2 The non-recoverable creep compliance, J_{nr}, and the stress sensitivity, $J_{nr,diff}$, results of the asphalt binders at 60°C over multiple stress levels

Base Binder	Polymer Type Designation	J_{nr} (kPa^{-1}) at 60°C					$J_{nr,diff}$ (%) at 60°C			
		0.1 kPa	3.2 kPa	6.4 kPa	12.8 kPa	25.6 kPa	0.1-3.2 kPa	3.2-6.4 kPa	6.4-12.8 kPa	12.8-25.6 kPa
80/100	None	1.979	2.272	2.393	2.650	5.910	14.8	5.3	10.7	123.0
200/300	RET+PPA	0.553	0.706	0.834	1.143	1.683	27.7	18.3	37.0	47.2
	SBS+S	0.726	1.144	1.374	1.928	2.972	57.6	20.1	40.3	54.1
	RET	1.205	1.720	1.874	2.212	2.480	42.7	9.0	18.0	12.1
	RET+SBS	1.382	1.913	2.090	2.439	3.146	38.4	9.3	16.7	29.0
	SBS	1.685	2.163	2.612	2.991	4.011	28.4	20.8	14.5	34.1
	PPA	1.377	2.486	3.219	5.728	–	79.5	29.5	77.9	–
	RET+PPA+CRM	1.382	2.065	2.476	2.794	3.661	49.4	19.9	12.8	31.0
	SBS+RET+PPA	1.066	1.430	1.614	2.128	2.957	34.1	12.9	31.8	39.0
	SBS+S+CRM	1.234	2.339	2.958	3.495	4.010	89.5	26.5	18.2	14.7
	RET(EP)+PPA	0.915	1.214	1.373	1.895	2.937	32.7	13.1	38.0	55.0
300/400	SBS+S	0.284	0.412	0.646	1.272	2.954	44.9	56.7	97.0	132.2
	SBS+S+VGO	0.150	0.305	0.385	0.998	3.488	103.3	26.2	159.4	249.5

Table A.3 The non-recoverable creep compliance, J_{nr}, and the stress sensitivity, $J_{nr,diff}$, results of the asphalt binders at 70°C over multiple stress levels

Base Binder	Polymer Type Designation	J_{nr} (kPa^{-1}) at 70°C					$J_{nr,diff}$ (%) at 70°C			
		0.1 kPa	3.2 kPa	6.4 kPa	12.8 kPa	25.6 kPa	0.1-3.2 kPa	3.2-6.4 kPa	6.4-12.8 kPa	12.8-25.6 kPa
80/100	None	7.895	8.835	9.648	11.250	–	11.9	9.2	16.6	–
200/300	RET+PPA	2.508	3.297	4.025	5.992	10.330	31.5	22.1	48.9	72.4
	SBS+S	3.492	6.257	7.859	10.170	15.070	79.2	25.6	29.4	48.2
	RET	3.524	5.259	6.140	7.180	–	49.2	16.8	16.9	–
	RET+SBS	4.934	6.952	7.774	9.293	12.660	40.9	11.8	19.5	36.2
	SBS	6.844	8.785	10.300	15.080	24.110	28.4	17.2	46.4	59.9
	PPA	5.899	10.320	13.830	51.190	–	74.9	34.0	270.1	–
	RET+PPA+CRM	4.460	7.506	9.193	10.240	15.790	68.3	22.5	11.4	54.2
	SBS+RET+PPA	4.352	6.028	7.091	8.645	13.310	38.5	17.6	21.9	54.0
	SBS+S+CRM	4.577	9.145	10.740	13.100	17.440	99.8	17.4	22.0	33.1
	RET(EP)+PPA	3.483	5.059	6.228	8.521	13.500	45.2	23.1	36.8	58.4
300/400	SBS+S	1.718	3.529	5.078	8.383	14.010	105.4	43.9	65.1	67.1
	SBS+S+VGO	1.264	2.953	4.767	9.203	18.650	133.6	61.4	93.1	102.7

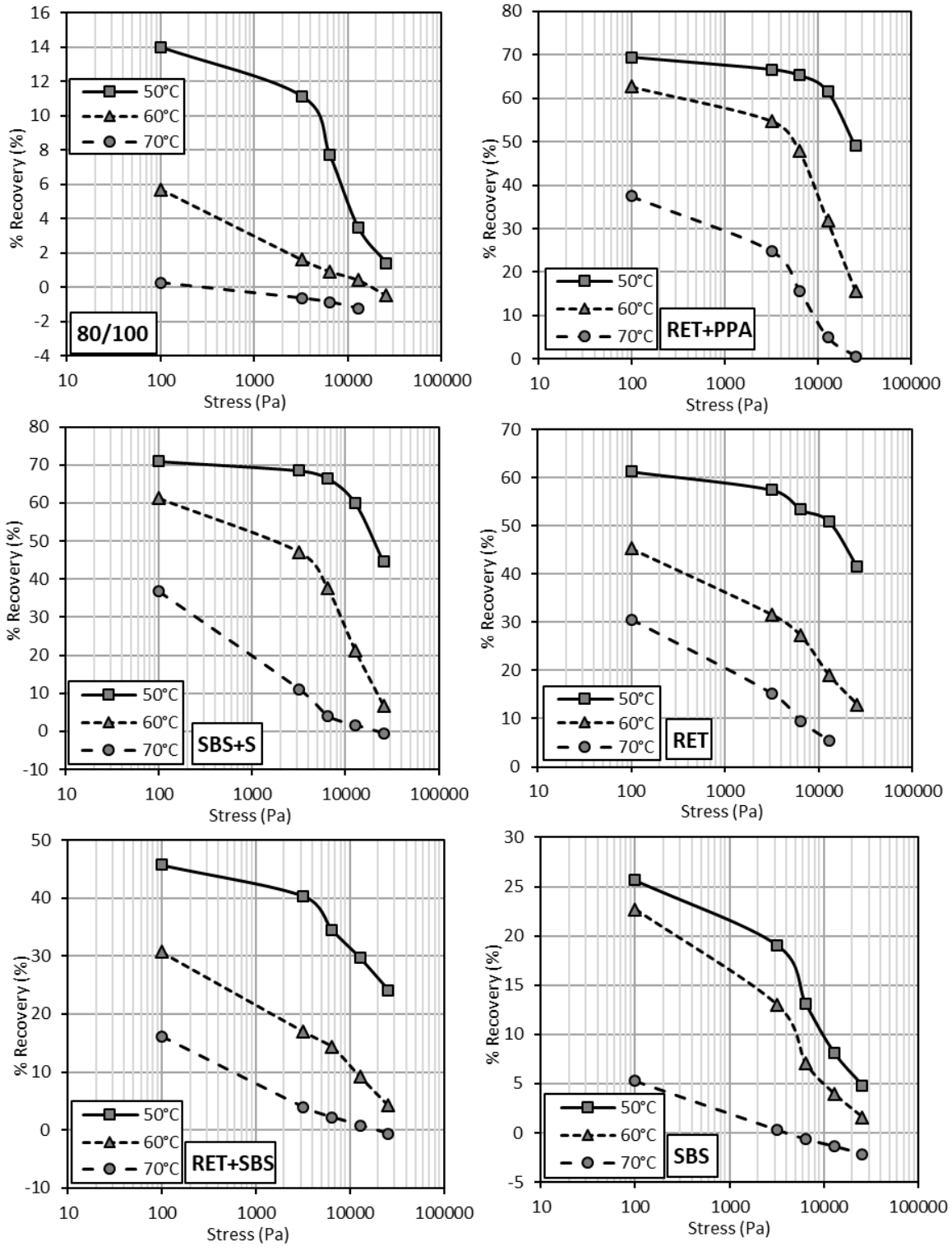

Figure A.4 Change of the percent recovery, %*R*, results of the asphalt binders with stress level at temperatures 50, 60, 70°C for asphalt binders: 80/100, RET+PPA, SBS+S, RET, RET+SBS and SBS

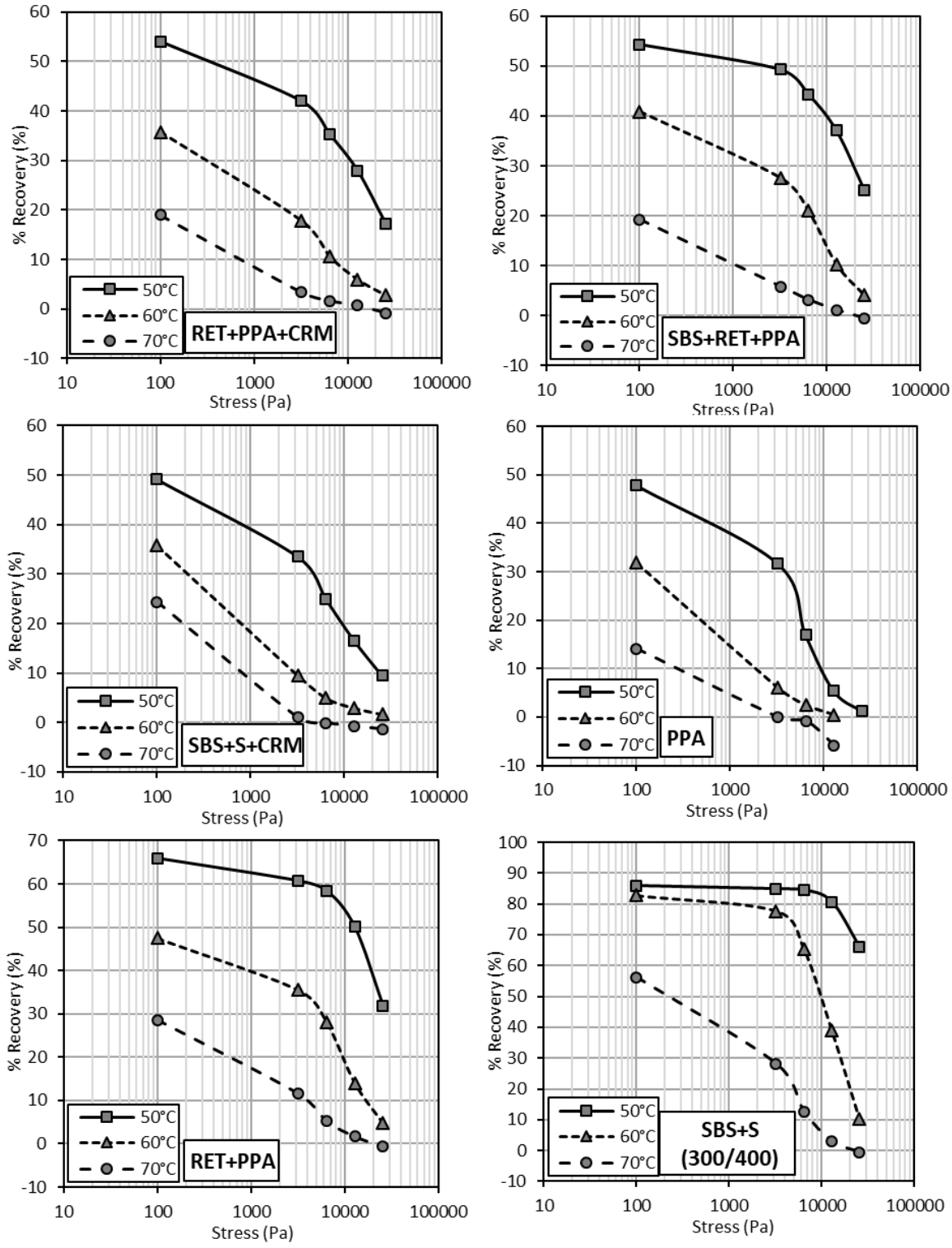

Figure A.5 Change of the percent recovery, %*R*, results of the asphalt binders with stress level at temperatures 50, 60, 70°C for asphalt binders: RET+PPA+CRM, SBS+RET+PPA, SBS+S+CRM, PPA, RET+PPA, SBS+S (300/400)

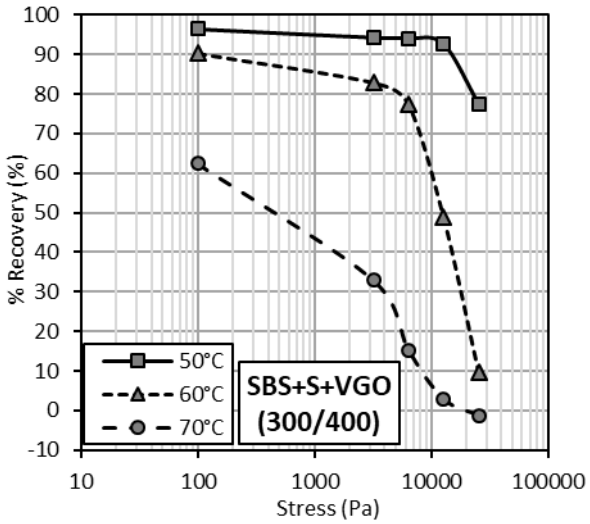

Figure A.6 Change of the percent recovery, %R, results with stress level at temperatures 50, 60, 70°C for the SBS+S+VGO (300/400)-modified asphalt blend

Table A.4 The percent recovery, $\%R$, and the stress sensitivity ($\%R_{diff}$) results of the asphalt binders at 50°C over multiple stress levels from the MSCR test

Base Binder	Polymer Type Designation	$\%R$ (%) at 50°C					$\%R_{diff}$ (%) at 50°C			
		0.1 kPa	3.2 kPa	6.4 kPa	12.8 kPa	25.6 kPa	0.1-3.2 kPa	3.2-6.4 kPa	6.4-12.8 kPa	12.8-25.6 kPa
80/100	None	14.0	11.1	7.7	3.5	1.4	20.4	31.0	54.7	59.6
200/300	RET+PPA	69.3	66.6	65.2	61.6	49.0	4.0	2.0	5.6	20.4
	SBS+S	70.9	68.5	66.6	59.9	44.6	3.4	2.9	9.9	25.6
	RET	61.3	57.4	53.4	50.9	41.5	6.2	7.1	4.6	18.5
	RET+SBS	45.7	40.3	34.5	29.6	24.1	11.8	14.4	14.2	18.8
	SBS	25.6	19.0	13.1	8.1	4.8	25.7	31.1	38.0	41.1
	PPA	47.8	31.8	17.1	5.4	1.2	33.5	46.3	68.1	77.6
	RET+PPA+CRM	54.1	42.0	35.4	27.9	17.2	22.2	15.9	21.1	38.5
	SBS+RET+PPA	54.3	49.3	44.3	37.1	25.1	9.2	10.1	16.4	32.3
	SBS+S+CRM	49.2	33.5	24.9	16.6	9.4	31.8	25.6	33.6	43.1
	RET(EP)+PPA	65.9	60.7	58.4	50.0	31.9	7.9	3.8	14.3	36.2
300/400	SBS+S	85.9	84.9	84.5	80.7	66.1	1.2	0.4	4.5	18.1
	SBS+S+VGO	96.4	94.3	94.1	92.7	77.4	2.2	0.2	1.5	16.5

Table A.5 The percent recovery, $\%R$, and the stress sensitivity ($\%R_{diff}$) results of the asphalt binders at 60°C over multiple stress levels from the MSCR test

Base Binder	Polymer Type Designation	$\%R$ (%) at 60°C					$\%R_{diff}$ (%) at 60°C			
		0.1 kPa	3.2 kPa	6.4 kPa	12.8 kPa	25.6 kPa	0.1-3.2 kPa	3.2-6.4 kPa	6.4-12.8 kPa	12.8-25.6 kPa
80/100	None	5.7	1.6	0.9	0.4	-0.5	71.9	43.8	55.6	225.0
200/300	RET+PPA	62.7	54.8	47.8	31.9	15.7	12.6	12.8	33.3	50.8
	SBS+S	61.2	47.1	37.7	21.2	6.8	23.0	20.0	43.8	67.9
	RET	45.3	31.5	27.2	19.0	12.9	30.5	13.7	30.1	32.1
	RET+SBS	30.7	17.0	14.4	9.2	4.2	44.6	15.3	36.1	54.3
	SBS	22.7	13.0	7.1	4.0	1.6	42.7	45.4	43.7	60.0
	PPA	31.8	6.0	2.4	0.4	–	81.1	60.0	83.3	–
	RET+PPA+CRM	35.8	17.9	10.7	6.0	2.8	50.0	40.2	43.9	53.3
	SBS+RET+PPA	40.8	27.6	21.0	10.3	4.1	32.4	23.9	51.0	60.2
	SBS+S+CRM	35.8	9.5	4.9	2.9	1.6	73.5	48.4	40.8	44.8
	RET(EP)+PPA	47.5	35.5	28.1	14.0	4.7	25.3	20.8	50.2	66.4
300/400	SBS+S	82.7	77.7	65.5	39.1	10.2	6.0	15.7	40.3	73.9
	SBS+S+VGO	90.3	82.9	77.4	49.0	9.8	8.2	6.6	36.7	80.0

Table A.6 The percent recovery, $\%R$, and the stress sensitivity ($\%R_{diff}$) results of the asphalt binders at 70°C over multiple stress levels from the MSCR test

Base Binder	Polymer Type Designation	$\%R$ (%) at 70°C					$\%R_{diff}$ (%) at 70°C			
		0.1 kPa	3.2 kPa	6.4 kPa	12.8 kPa	25.6 kPa	0.1-3.2 kPa	3.2-6.4 kPa	6.4-12.8 kPa	12.8-25.6 kPa
80/100	None	0.2	-0.7	-0.9	-1.2	–	365.6	34.5	41.3	–
200/300	RET+PPA	37.5	24.9	15.7	5.0	0.6	33.6	36.7	68.1	88.7
	SBS+S	36.7	11.1	4.1	1.7	-0.5	69.9	63.0	59.1	128.0
	RET	30.6	15.1	9.4	5.4	–	50.6	37.6	42.4	–
	RET+SBS	16.1	3.9	2.2	0.8	-0.6	75.5	43.7	62.3	176.4
	SBS	5.3	0.3	-0.7	-1.4	-2.2	94.6	330.4	108.8	58.3
	PPA	14.1	0.0	-0.8	-5.9	–	100.1	5379.4	649.7	–
	RET+PPA+CRM	19.0	3.4	1.7	0.7	-0.8	82.2	49.8	60.2	216.5
	SBS+RET+PPA	19.2	5.8	3.2	1.1	-0.5	69.6	45.7	64.1	146.9
	SBS+S+CRM	24.3	1.0	-0.1	-0.7	-1.4	95.9	110.1	624.5	84.7
	RET(EP)+PPA	28.6	11.6	5.3	1.8	-0.6	59.4	54.5	66.3	133.5
300/400	SBS+S	56.1	28.2	12.7	3.0	-0.6	49.8	54.9	76.2	119.7
	SBS+S+VGO	62.4	32.9	15.3	2.9	-1.2	47.2	53.5	81.0	142.9

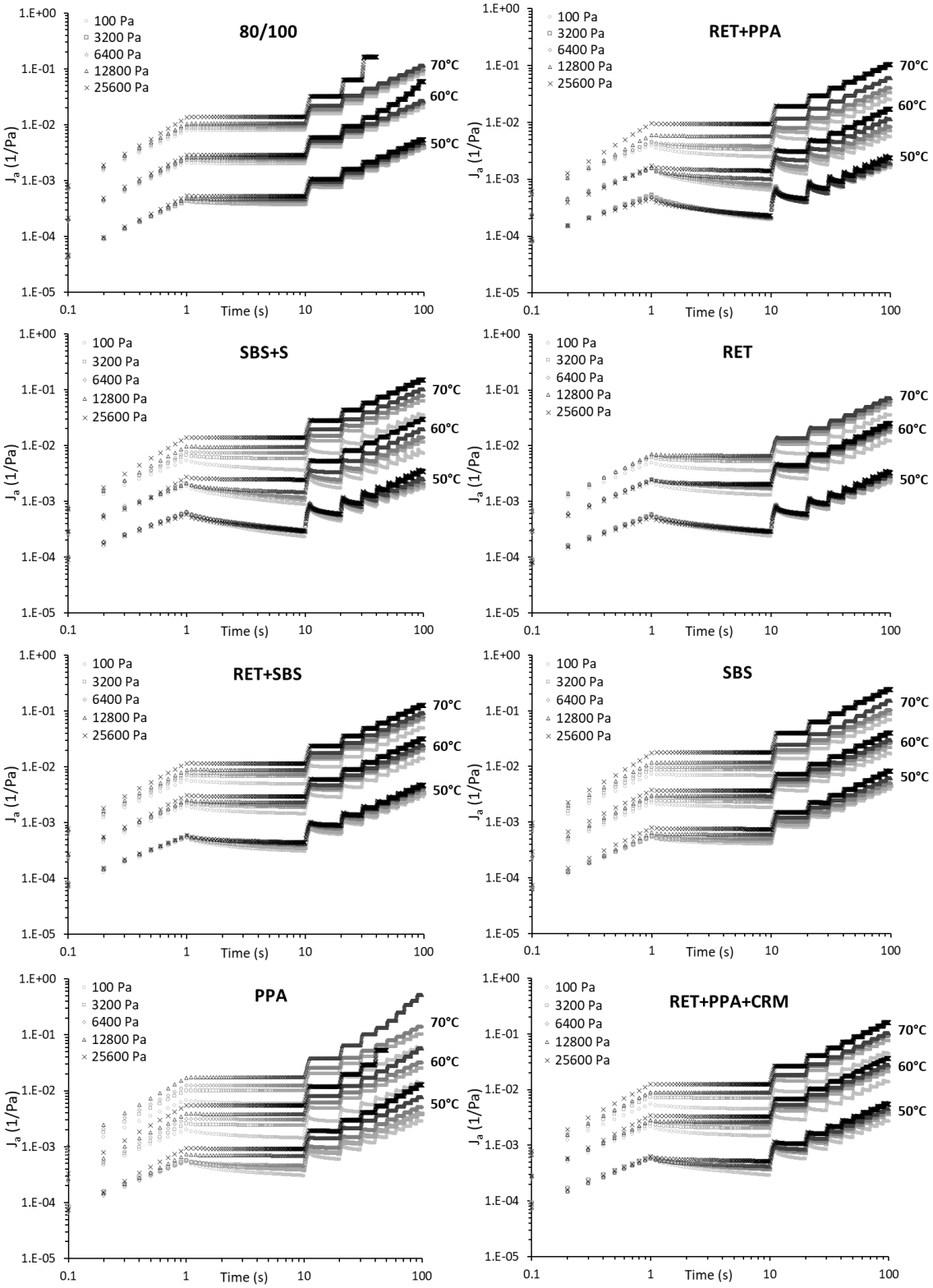

Figure A.7 Plot of the accumulated creep compliance, J_a, of eight tested binders at five different stress levels and three different testing temperatures

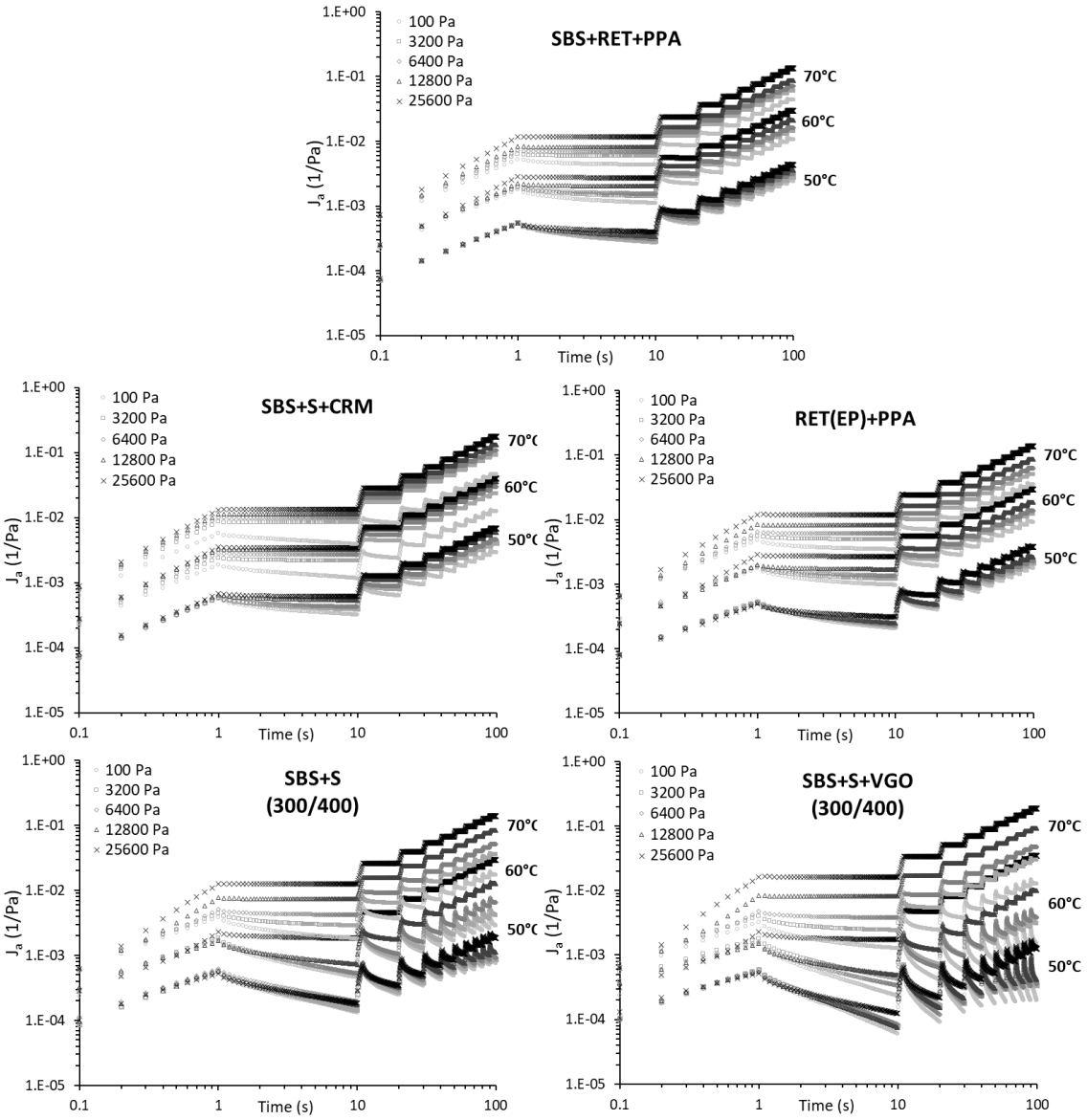

Figure A.8 Plot of the accumulated creep compliance, J_a, of five tested binders at five different stress levels and three different testing temperatures

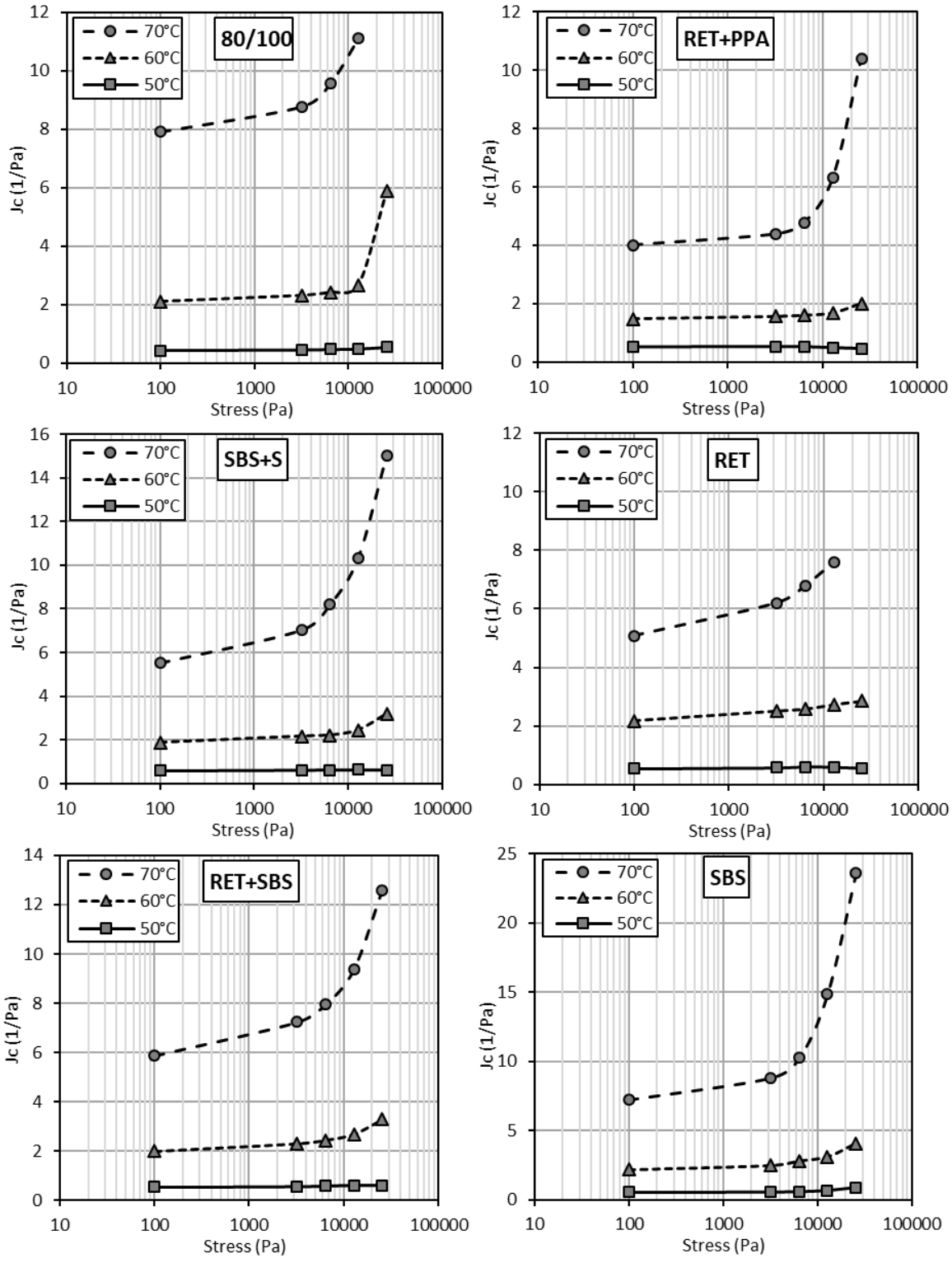

Figure A.9 Change of the average creep compliance, J_c, results (end of the creep phase) with stress level at temperatures 50, 60, 70°C for asphalt binders: 80/100, RET+PPA, SBS+S, RET, RET+SBS, and SBS

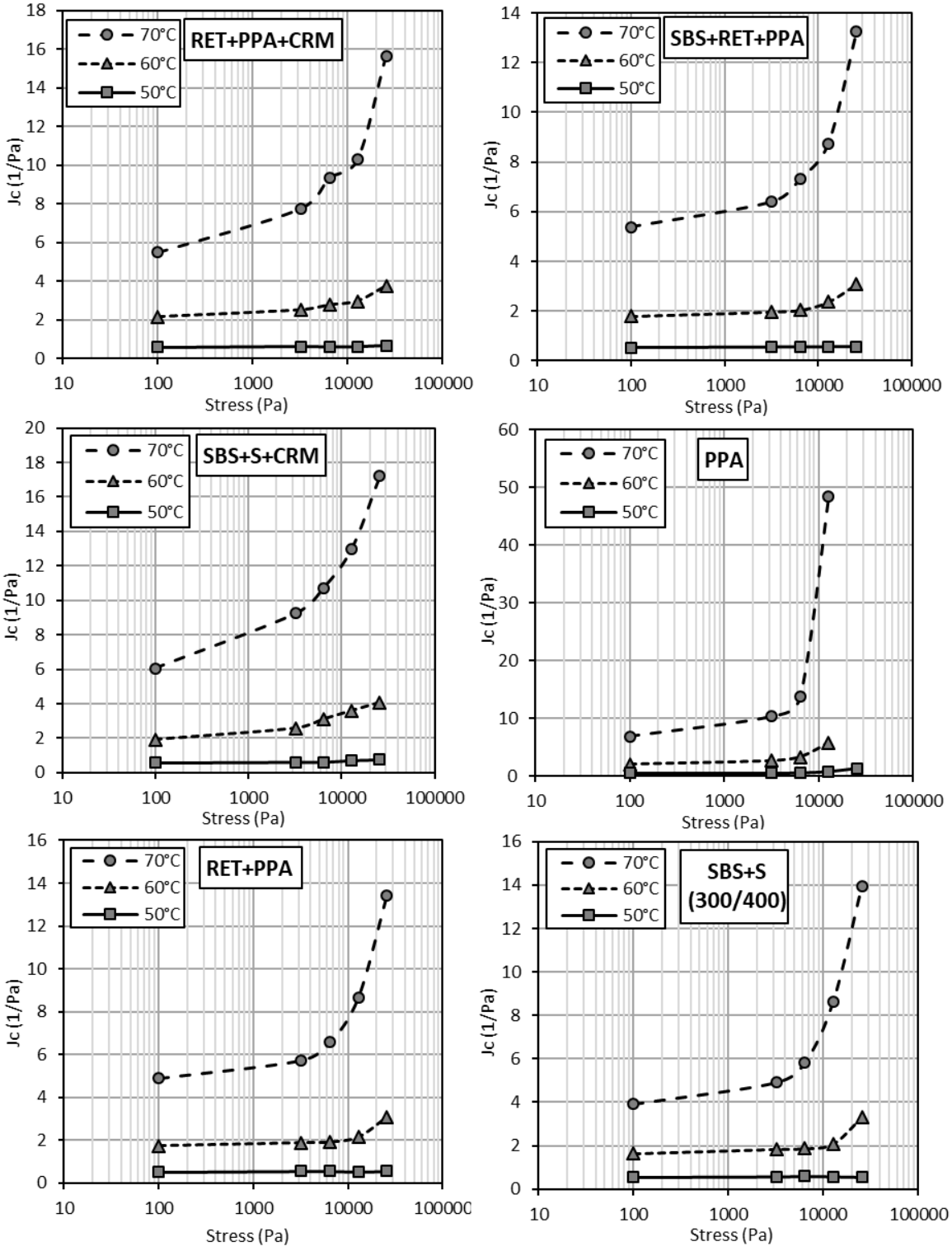

Figure A.10 Change of the average creep compliance, J_c, results (end of the creep phase) with stress level at temperatures 50, 60, 70°C for asphalt binders: RET+PPA+CRM, SBS+RET+PPA, SBS+S+CRM, PPA, RET+PPA, SBS+S (300/400)

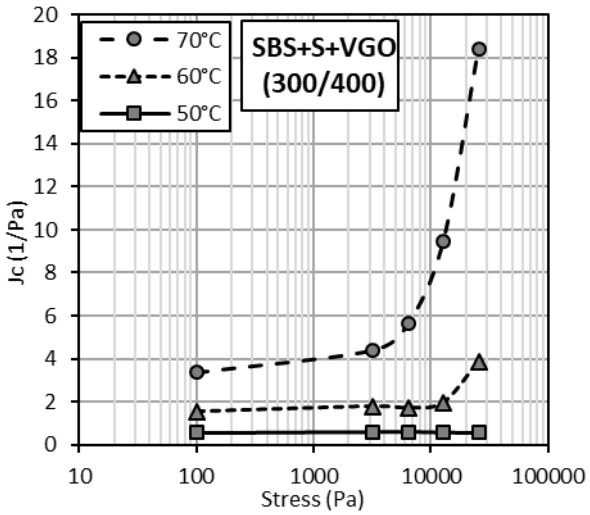

Figure A.12 Change of the average creep compliance, J_c, results (end of the creep phase) with stress level at temperatures 50, 60, 70°C for asphalt binder SBS+S+VGO (300/400)

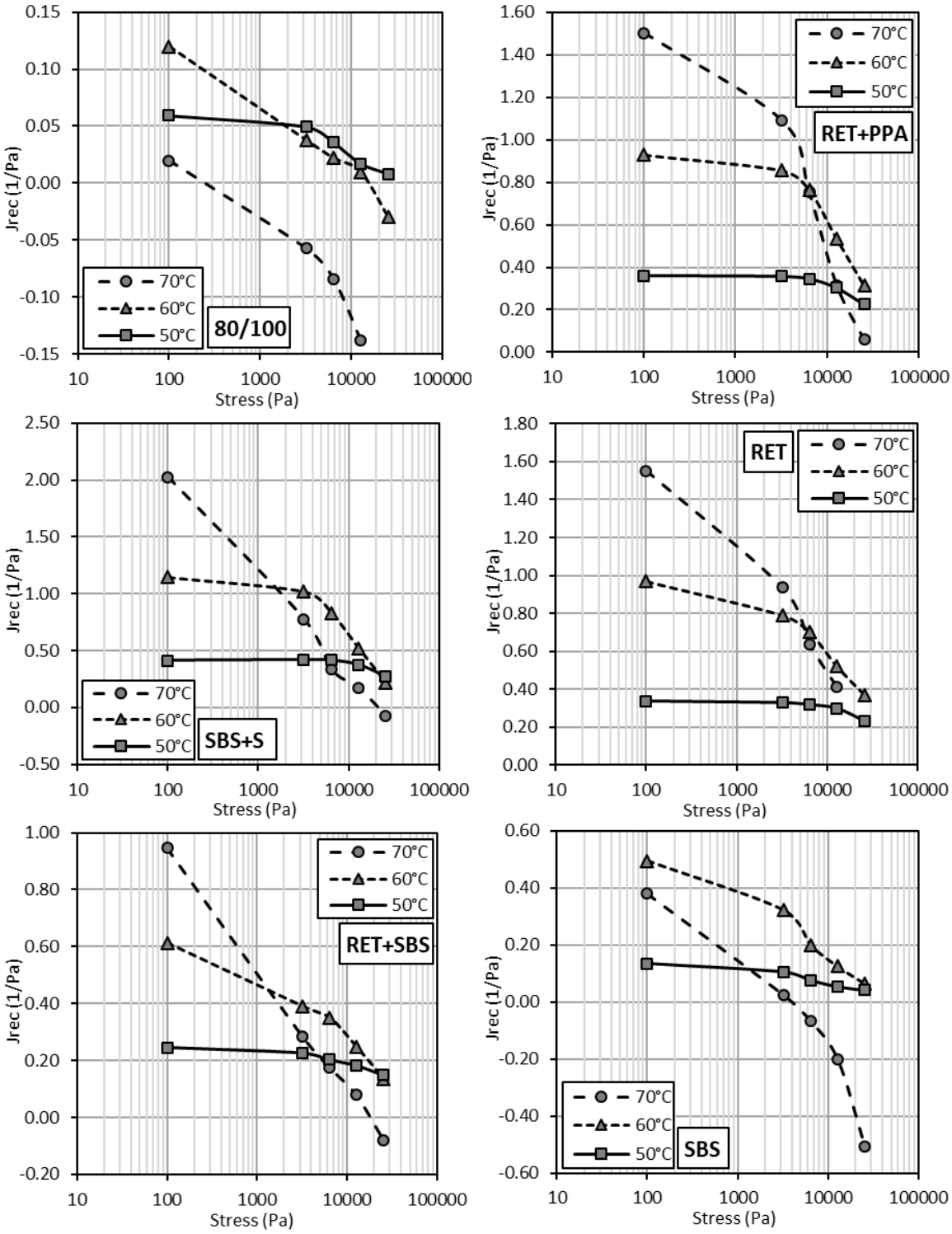

Figure A.13 Change of the average recoverable compliance, J_{rec}, results (end of the recovery phase) with stress level at temperatures 50, 60, 70°C for asphalt binders: 80/100, RET+PPA, SBS+S, RET, RET+SBS and SBS

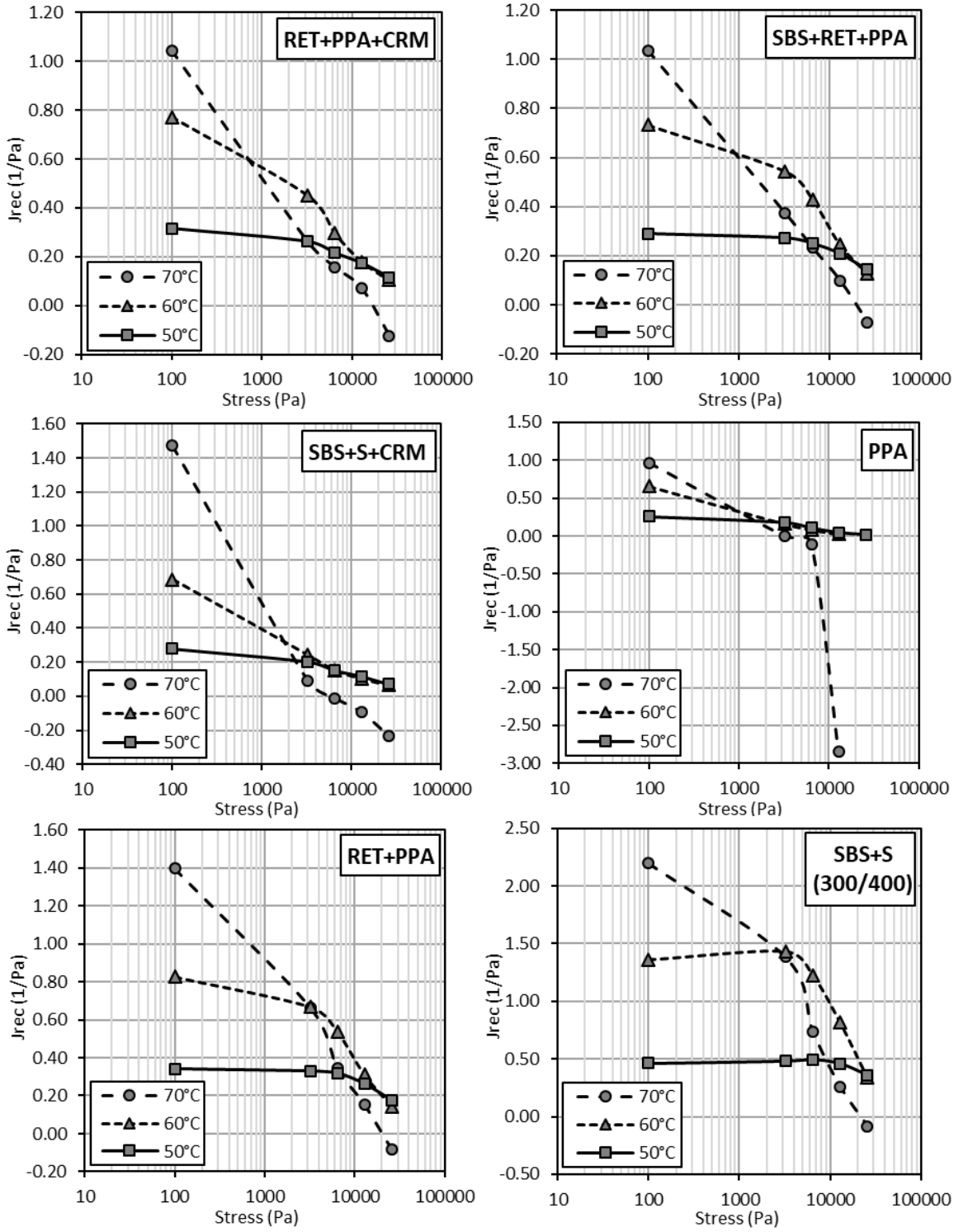

Figure A.14 Change of the average recoverable compliance, J_{rec}, results (end of the recovery phase) with stress level at temperatures 50, 60, 70°C for asphalt binders: RET+PPA+CRM, SBS+RET+PPA, SBS+S+CRM, PPA, RET+PPA, SBS+S (300/400)

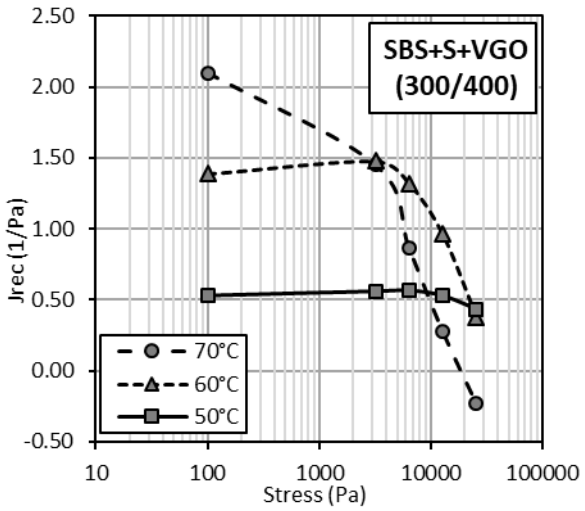

Figure A.15 Change of the average recoverable compliance, J_{rec}, results (end of the recovery phase) with stress level at temperatures 50, 60, 70°C for asphalt binder SBS+S+VGO (300/400)

APPENDIX-B: DYNAMIC TEST RESULTS

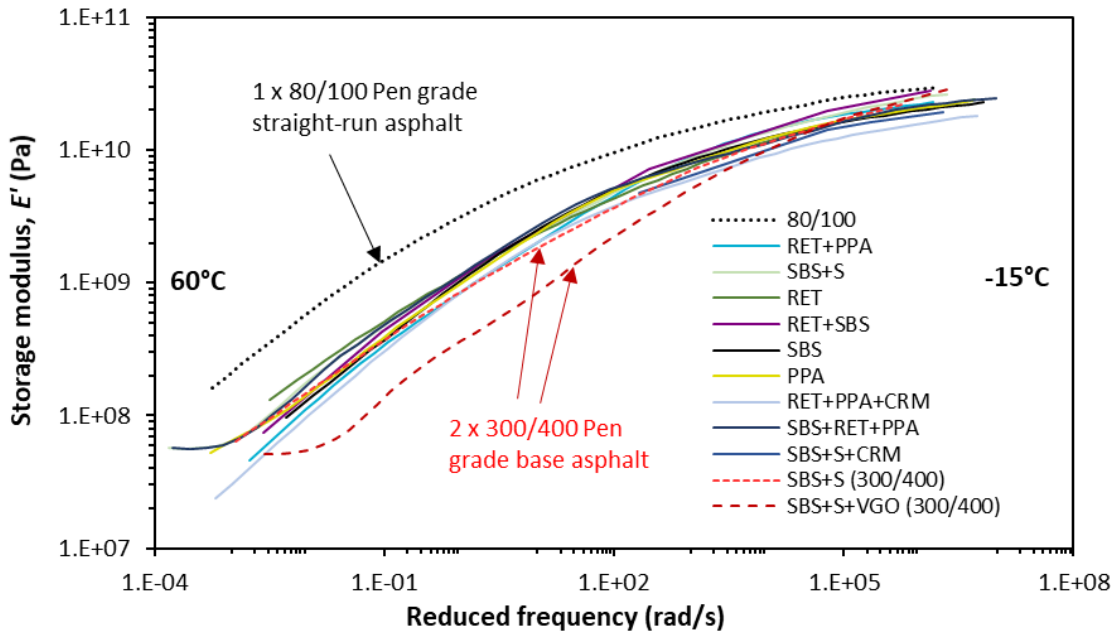

Figure B.1 Master curves of storage modulus, E', for all tested asphalt mixes, T_r=15°C

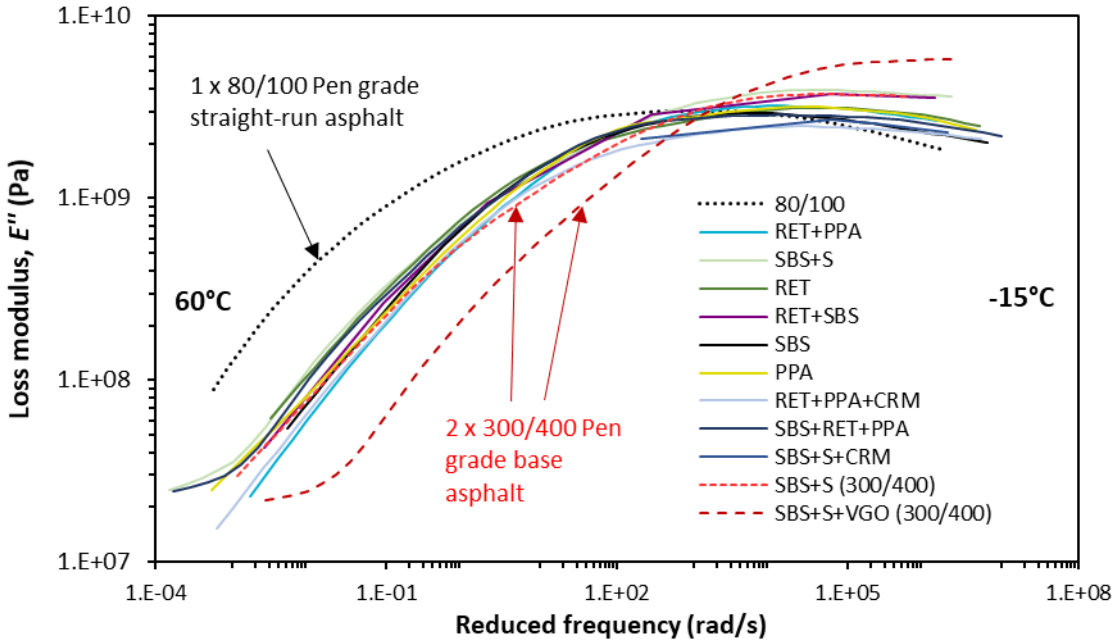

Figure B.2 Master curves of loss modulus, E'', for all tested asphalt mixes, T_r=15°C

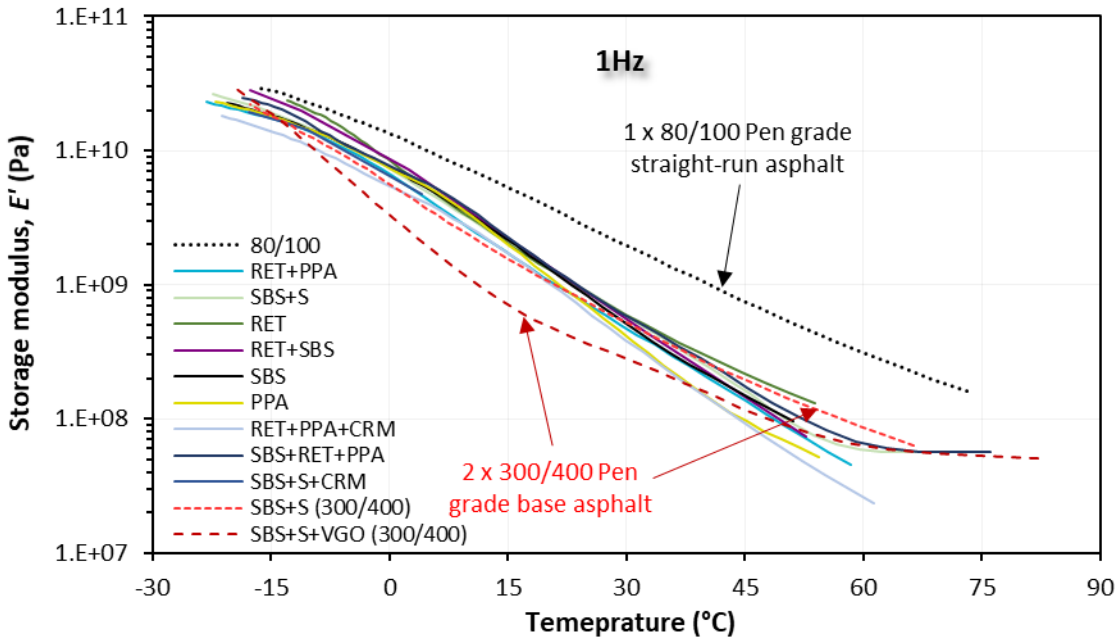

Figure B.3 Storage modulus, $|E'|$, functions at fixed frequency of 1 Hz, all tested asphalt mixes

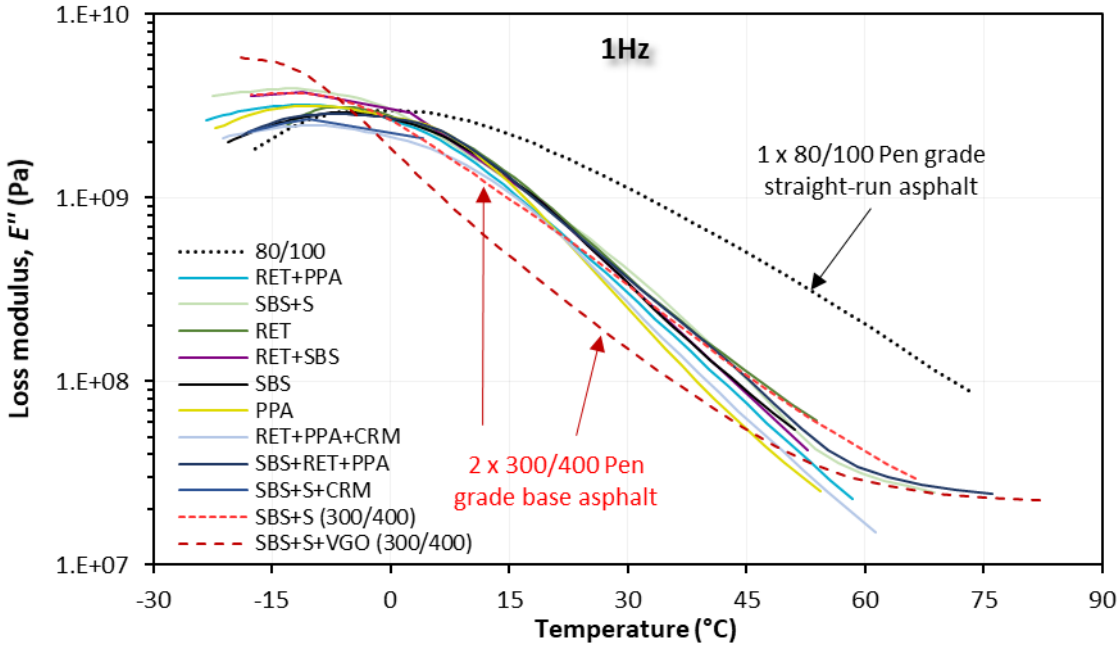

Figure B.4 Loss modulus, $|E''|$, functions at fixed frequency of 1 Hz, all tested asphalt mixes